Sensitivity Analysis of Mountain Hydrology to Changing Climate

A Thesis Submitted to the
College of Graduate Studies and Research
in Partial Fulfillment of the Requirements
for the degree of Doctor of Philosophy
in the Department of Geography and Planning
University of Saskatchewan
Saskatoon

By
Kabir Rasouli

Permission to Use

In presenting this thesis in partial fulfilment of the requirements for a Postgraduate degree from the University of Saskatchewan, I agree that the Libraries of this University may make it freely available for inspection. I further agree that permission for copying of this thesis in any manner, in whole or in part, for scholarly purposes may be granted by the professor or professors who supervised my thesis work or, in their absence, by the Head of the Department or the Dean of the College in which my thesis work was done. It is understood that any copying or publication or use of this thesis or parts thereof for financial gain shall not be allowed without my written permission. It is also understood that due recognition shall be given to me and to the University of Saskatchewan in any scholarly use which may be made of any material in my thesis.

Requests for permission to copy or to make other use of material in this thesis in whole or part should be addressed to:

Head of the Department of Geography and Planning
125 Kirk Hall Building
117 Science Place
University of Saskatchewan
Saskatoon, Saskatchewan
Canada
S7N 5C8

Abstract

Understanding the sensitivity of hydrological processes to climate change in snow–covered mountains is important for water and energy security. The objectives of this study are: (i) to quantify the sensitivity of simulated mountain hydrological processes to changes in air temperature and precipitation; (ii) to document the uncertainty in estimations of future mountain hydrological processes due to uncertainty in climate models; and (iii) to quantify the response of simulated mountain hydrology to climate change when there are transient changes in vegetation and soils. Three basins are selected for this research: Wolf Creek Research Basin (WCRB), Canada; Marmot Creek Research Basin (MCRB), Canada; and Reynolds Mountain East (RME) catchment, USA. A hydrological model for each basin was set up in the Cold Regions Hydrological Modelling platform (CRHM) and a climate perturbation sensitivity (CPS) analysis was conducted based on a series of annually perturbed climate (APC), monthly perturbed climate (MPC), and transient vegetation changes. Peak snow water equivalent (SWE), evapotranspiration, and annual runoff have a pronounced sensitivity to both warming and precipitation change in all three basins. The timing of snow regime is most sensitive to changes in temperature. The impacts of warming on alpine snow in WCRB and to lesser extent in MCRB can be offset by increases in precipitation. In response to MPC, modelled peak SWE decreases while evapotranspiration and total annual runoff increase. Annual runoff responds very strongly to precipitation increases in MCRB, to warming in RME, and to both precipitation increase and warming in WCRB. Warming increases rainfall fraction of precipitation, as all three snow–dominated basins become more rain–dominated and precipitation phase becomes latitudinally more similar. The impact of climate change is moderated by the impact of vegetation change on peak SWE timing, snow transport, evapotranspiration, and annual runoff. The hydrological uncertainty due to uncertainty in climate models is greater than the range of hydrological changes due to climate change for streamflow regimes in the three basins and snow regimes at high elevations and latitudes. The results of this research can be used to anticipate the hydrological impacts of climate and vegetation changes on uncertain future mountain environments.

Acknowledgements

The guidance and commitment of Prof. John Pomeroy as a supervisor is gratefully acknowledged. This research could not have been completed without his coordination. His excellent knowledge of hydrology made it possible for me to enjoy my time at the Centre for Hydrology in the University of Saskatchewan as a PhD student. His constant support and nice attitude allowed completion of this research without external pressure or tension. As my committee members, Dr. Paul Whitfield for his invaluable discussions and his excellence in statistics, Dr. Lawrence Martz for his great guidance on transient vegetation and soil changes in the mountain basins, and Dr. Andrew Ireson for his insightful comments and advice on model performance assessment, permafrost, frozen ground, and subsurface flows in each phase of the research deserved thanks for approving my research and for inspiring me through their passion for hydrology. I also would like to thank my warmhearted friends at Centre for Hydrology for their help and support. I wish to acknowledge over two decades of Reynolds Creek Experimental Watershed, Marmot Creek Research Basin, and Wolf Creek Research Basin operation with substantial staff and grad student contributions to installation, maintenance and operation of the core snow surveys, meteorological stations and hydrometric stations under inclement conditions. Modelling support from Tom Brown and Xing Fang is greatly appreciated. Funding for the basin has come from Alexander Graham Bell Canada graduate scholarship–Doctoral NSERC, Yukon Environment, Environment Canada, DIAND, NSERC, CFCAS, NERC, NOAA and other sources. Funding for this study came from AAND Canada, Yukon Environment and NSERC. Thanks to my family, Neda and Ayla. I could not complete this without your patience and support. Thanks to my parents Sabileh and Manouchehr for their love and encouragement every time I phoned them, even though we were separated by the oceans.

Contents

List of Tables

List of Figures

List of Abbreviations

AO	Arctic Oscillation
APC	Annually Perturbed Climate
AOGCM	Atmosphere–Ocean General Circulation Model
CI	Confidence Interval
CRCM5	Canadian Regional Climate Model– version five
CRHM	Cold Regions Hydrological Model
CV	Coefficient of Variation
DDS	Dynamically Dimensioned Search
DEM	Digital Elevation Model
ET	Evapotranspiration
GCM	General Circulation Model
GHG	Greenhouse Gas
GLUE	Generalised Likelihood Uncertainty Estimation
HRU	Hydrological Response Unit
ICAR	Intermediate Complexity Atmospheric Research
IPCC	Intergovernmental Panel on Climate Change
MCRB	Marmot Creek Research Basin
MPB	Mountain Pine Beetle
MPC	Monthly Perturbed Climate
MSC	Meteorological Service of Canada
NAC	North American Cordillera
NARCCAP	North American Regional Climate Change Assessment Program
NDVI	Normalised Difference Vegetation Index
NSE	Nash-Sutcliffe Efficiency
NSRP	Neyman-Scott Rectangular Pulses
PDF	Probability Density Function
PDO	Pacific Decadal Oscillation
CPS	Climate Perturbation Sensitivity
RCM	Regional Climate Model
RCP	Representative Concentration Pathways
RME	Reynolds Mountain East
SWE	Snow Water Equivalent
WCRB	Wolf Creek Research Basin
WRF	Weather Research and Forecasting model

Chapter 1
INTRODUCTION

1.1 General

Snow and its seasonal dynamics are key components of mountain hydrological systems that supply water to downstream communities and ecosystems. Investigation of climate change impacts on snow processes along with other hydrological mechanisms in cold regions that are sensitive to warming and precipitation changes is of great interest to water resources stakeholders and the climate change research community. Snowmelt amount and timing in the spring play a key role in fresh water availability, flood control, and ecological sustainability of mountainous regions with near-freezing temperatures and cold climates (Stewart et al., 2004; Semmens and Ramage, 2013). The contribution of mountainous regions to the total discharge of watersheds ranges from 35% in cold and humid basins to 90% in hot and arid watersheds (Viviroli and Weingartner, 2004). Mountains cover 25% of the Earth's land surface (Diaz et al., 2003) and 26% of the world's population live in high-elevation areas (Meybeck et al., 2001). The origin of discharges from 50% of the world's rivers are mountains (Beniston, 2003). Mountains are also ecologically important for biodiversity due to strong elevation and temperature gradients (Beniston, 2003; Diaz et al., 2003).

Modelling mountain hydrology is challenging as there are sparse monitoring networks at high elevations and, hence, high uncertainties in forcing data (Klemeš, 1990). High spatial variability of soil type and depth, vegetation cover, and meteorological variables in mountains makes modelling and representation of the hydrological processes in these regions difficult (Klemeš, 1990). The range of hydrological modelling uncertainties due to the uncertainties in climate models and transient vegetation changes in mountainous basins has not been

adequately quantified in the literature.

A common approach for investigating hydrological response to climate change is to apply climate model projections under different GHG emission scenarios and to downscale large-scale atmospheric circulations obtained from the climate models to local-scale variables using statistical or dynamical methods (Fowler et al., 2007). There are some issues in direct application of climate model outputs in the projection of future hydrological processes in mountains, including:

- different hydrological responses with different sets of forcing data from gauge, radar, and reanalysis sources (Elsner et al., 2014);
- uncertain precipitation due to coarse simulation of synoptic dynamics (Addor et al., 2016);
- orographic complexity in mountainous terrain (Barry, 1992);
- large biases when comparing observations with climate simulations for the control period (Fowler et al., 2007); and
- change in large-scale climate signals including El Niño-like conditions and strong cold events under increased greenhouse gas (GHG) concentrations (Timmermann et al., 1999).

Large biases between simulated current climate by climate models and observed current climate necessitate the application of an ensemble of climate models (e.g., regional climate models, RCMs) (Hsieh, 2009) to study the uncertainty of the future hydrology. Application of the ensemble of RCM outputs in hydrological modelling and improving the resolution and physics representation of the climate models are the main strategies that are needed in climate change impact studies rather than solely climate model output bias correction, which is sensitive to uncertainties associated with the lack of proper representation of synoptic circulation in climate models (Addor et al., 2016).

Bias correction of climate model outputs and statistical downscaling approaches are widely used for reducing uncertainty in the atmospheric products (Bourdin and Stull, 2013; Addor et al., 2016). One of the major assumptions in statistical downscaling is that the predictor–predictand relationship is stationary and that future relationships will be the same as past ones (Wilby and Wigley, 1997). Duan et al. (2012) downscaled five slices of 150-year observed time series of atmospheric variables to monthly precipitation to assess the predictor–predictand stationary and to evaluate the uncertainties associated with selection of different GCMs. They found that there is a significant change from one time slice of 30 years to another and between GCMs. Some of the assumptions in downscaling are that: (i) there is a strong relationship between large-scale circulations and local-scale processes; (ii) the feedback from local-scale phenomena is not important in large-scale climate models; and (iii) statistical relationships between atmospheric variables and locally observed variables under current and future climates are stationary (Wilby and Wigley, 1997; Maraun et al., 2010).

The uncertainties related to forcing data, model structure and parameters, and calibrating and downscaling methods in mountain hydrology shows that modelling is challenging in mountains. Bennett et al. (2012) quantified uncertainties from GCMs, emissions scenarios, and hydrological parametrisation and found that uncertainties from all sources for winter in the 2050s were from 31% to 84% in different headwater basins in British Columbia. Other than the study by Bennett et al. (2012), the range of hydrological uncertainty from different sources has not been adequately compared with the range of hydrological changes due to climate change reported in the literature. In addition to the large uncertainties in precipitation and air temperature changes projected by GCM models under different scenarios, orographic complexity in mountainous terrain adds more uncertainty to alpine precipitation and temperature simulations. Elsner et al. (2014) found that the temperature uncertainty in different datasets obtained from different gauge, radar, and reanalysis sources are large in mountains (e.g., Rocky Mountains), which might be related to the high spatial variability of temperature in mountains and the use of fixed lapse rates with elevation for extrapolation of point temperature measurements. The extrapolation of forcing data in a

complex orographic terrain where the observing network is sparse is challenging because of high temporal and spatial variability (Klemeš, 1990). Precipitation generally increases with elevation, especially on windward steep slopes where the mountain blocks the moisture movements, leading to uplift and condensation of vapour (Sevruk, 1997). With the absence of sufficient winds to mix atmospheric moisture in valleys, layers become dense and stratified above which inversions can occur (Daly et al., 2008). Temperature normally decreases with elevation if the atmosphere is well-mixed. In stratified layers, particularly during inversions, maximum temperatures may increase with elevation above the layers (Daly et al., 2008). Both fixed and varying lapse rates for temperature and fixed gradients for precipitation have been widely used in the literature (e.g., Crochet et al., 2007).

To assess climate change impacts on hydrological processes in mountains, high resolution climate and weather prediction model outputs (e.g., Weather Research and Forecasting model, WRF) can be used (Hijmans et al., 2005; Skamarock et al., 2005). The common approaches that are widely used to downscale large-scale atmospheric circulations to high resolution variables at local-scaleto are: (1) statistical downscaling approaches that link the atmospheric circulation, precipitation and air temperature fields obtained from RCM and GCM (Cannon, 2008; Maraun et al., 2010; Gaitan et al., 2014; Gutmann et al., 2014); (2) reanalysis products (Gutmann et al., 2014); and (3) dynamical downscaling approaches (Mearns et al., 2007). Dynamical downscaling approaches include using GCMs output to set the boundary conditions of RCMs to provide regional scale circulation fields consistent with those obtained from GCMs (e.g., Mearns et al., 2007; Maples et al., 2014). Dynamical downscaling approaches, however, are computationally expensive (Gutmann et al., 2016). Computational cost is important in climate change impact studies as high resolution climate models (Hijmans et al., 2005) are needed to run current and future climates with sufficient resolution to adequately represent alpine terrain and with sufficient ensemble members to represent the uncertainty in climate models. The GCM/RCMs need also to capture the important climate processes i.e., El Niño. Alternatively, one can apply the delta change (also called the perturbation) method (Fowler et al., 2007). The commonly used approach for delta change method is applying change factors to baseline observations on an annual scale. Nayak

(2008) perturbed the current climate with $\Delta T = \pm 2°C$ change factor for air temperatures and studied the response of snow regime to temperature perturbations in dry and wet snowcover seasons in Reynolds Mountain East (RME), Idaho, USA. The cold scenario used in Nayak (2008) is unlikely to occur in the future with current rate of warming.

Climate warming effects have been studied in some mountain catchments (e.g., Stewart et al., 2004; Bales et al., 2006; López-Moreno et al., 2016). The high sensitivity to warming of snow- dominated mountain basins with air temperatures near to zero (Nayak, 2008) and with seasonally frozen ground or permafrost (Hayashi et al., 2004) makes mountain basins appropriate study areas for investigating climate change impacts on the hydrological cycle (Bunbury and Gajewski, 2012). Snow regime and snowmelt runoff timing in low elevation basins with near-freezing air temperatures are more sensitive to warming than high elevation basins with winters well below the freezing point (Stewart et al., 2004; McCabe and Clark, 2005; Nayak, 2008). The snow fraction of precipitation is also sensitive to warming in basins with winter temperatures warmer than $-5°C$ (Knowles et al., 2006) and a considerable fraction of snow converts to rain as climate warms. Hydrological sensitivity of mountain basins to a warming climate depends on elevation and consequently to winter temperatures (Stewart et al., 2004) and, hence, low elevation basins are more susceptible to climatic changes. There are limited studies that have compared both elevational and latitudinal hydrological sensitivities to a warming climate (e.g., Knowles and Cayan, 2004; McCabe and Clark, 2005).

Transient vegetation and soil changes under climatic changes also alter hydrological mechanisms (DeFries and Eshleman, 2004). Studies indicate that the forest composition in the Pacific Northwest has changed (Dale and Franklin, 1989), the growth rates of trees has increased (Innes, 1991) and tree-line (Hansell et al., 1971) has heterogeneously moved vertically and latitudinally within the last century. These are most likely linked to increases in air temperature, carbon dioxide, and nitrogen (Innes, 1991). Neilson and Marks (1994) applied a biogeographic model to simulate changes in vegetation leaf area index (LAI) in association to changes in hydrological variables under climate changes and found that there is

a consistent regional pattern between vegetation and annual runoff changes. This is however, region-specific and it cannot be generalised to other regions. In general, knowledge on the interaction between vegetation and climate changes in relation to hydrological processes over mountain basins is limited. Hydrological responses to different types of vegetation change including afforestation, deforestation, regrowth, and forest conversion (Brown et al., 2005) with regard to soil changes can provide a basis to compare the climate change impacts to transient vegetation change impacts on hydrology.

1.2 Research Gaps

Statistical and dynamical downscaling methods have limitations in application to mountain hydrometeorology: (i) the assumption in statistical downscaling that the predictor–predictand relationship is stationary and future relationships will be the same as past ones (Wilby and Wigley, 1997) does not guarantee that statistical downscaling approaches would perform better than the delta change method (Hay et al., 2000; Fowler et al., 2007; Kay et al., 2009; Sunyer et al., 2012); and (ii) dynamical models driven by an ensemble of multiple boundary conditions have high computational cost. These limitations make consideration of an alternative solution necessary. There is a need for methods that are appropriate for mountainous regions and can avoid the limitations of the available downscaling methods. The delta change method, as an alternative approach to dynamical and statistical methods, can represent the main hydrometeorological processes analogous to historical measurements, while minimizing computational resources. The delta method method has been widely used in the literature, however, its application has been limited to air temperature changes factors (e.g., $\Delta T = \pm 2^{\circ}$C in Nayak, 2008) or precipitation change factors (e.g., $\Delta P = \pm 25\%$ in López-Moreno et al., 2016) and concomitant changes in precipitation and air temperature have not been investigated. To improve understanding of the snow and other hydrological processes in mountain basins with cold and near freezing air temperatures, a wide range of annual or monthly change factors for air temperatures and precipitation is needed in the delta method. Since changes in simulated future climate have strong seasonal variability,

change factors on a monthly basis can be used as approximations of this variability. The first research gap therefore is whether warming impact on mountain hydrology can be offset by precipitation increases under climate changes. This has not been resolved in the literature.

Many studies have assessed uncertainties from different sources in future hydrological processes (e.g., Binley et al., 1991; Wilby, 2005; Wilby and Harris, 2006; Minville et al., 2008; Bennett et al., 2012). Some hydroclimatological studies have reported large uncertainties in mountainous regions (e.g., Viviroli et al., 2011; Bennett et al., 2012). This is because of the high heterogeneity of alpine environments and the sparse monitoring networks in mountains. Assessing the uncertainties from different sources and comparing with the range of projected changes in the future has not been done for mountain regions. There is limited knowledge about impacts of transient climate and vegetation changes (e.g., afforestation, deforestation, regrowth, forest expansion into tundra, shrub expansion or growth) on hydrological processes in cold or even mild climates. The hydrological uncertainty due to uncertainty in transient changes in vegetation and associated soils has not been well understood as there is a complex relation between vegetation, climate, and soils (Rodriguez-Iturbe, 2000). The second gap is the limited knowledge on how transient climate, vegetation, and soil changes can transfer into hydrological changes.

1.3 Research Objectives, Scope, and Importance

There is no unique definition for sensitivity in the literature and, depending on the theory and mathematics behind each approach, it can be interpreted differently (Razavi and Gupta, 2016). Sensitivity analysis in hydrology is usually used to (i) test and diagnose model fidelity (Spear and Hornberger, 1980), (ii) find important and unimportant parameters (Muleta and Nicklow, 2005), (iii) calibrate uncertain parameters (Rakovec et al., 2014), and (iv) obtain interdependency between model parameters (Nossent et al., 2011). In this study, the response to different forcing factors (inputs to the model) was characterised instead of the commonly used approach of response to parameter factors. The hydrological model inputs are the

forcing factors and output hydrological variables form the response surfaces. Therefore, sensitivity analysis in this research is a simple case of variability of hydrological responses being attributed to differences in the inputs.

In this study, hydrological sensitivity analyses were conducted in an uncertainty framework based on current climate conditions and the transient impact of (i) warming air temperatures and changing precipitation and (ii) changing vegetation and soils. Specific objectives for sensitivity analyses are defined as the following:

- To quantify the sensitivity of simulated mountain hydrological processes to changes in air temperature and precipitation associated with climate change;
- To document the uncertainty in estimations of future hydrological processes and mountain basin hydrology due to uncertainty in climate models; and
- To quantify the response of simulated mountain hydrology to climate change when there are transient changes in vegetation and soils.

The scope of this research is limited to three highly instrumented and well studied mountain basins that are partially covered by forest or shrubs and have seasonal snowmelt as a major component of their runoff. The results can be interpreted more broadly within mountainous regions. This study makes several important contributions to understanding of how mountain basins will respond to climate warming. Whereas other studies demonstrated the potential impact of changes in single variables such as precipitation or air temperature on mountain hydrology, this study investigates the combined impact of changes in multiple variables including transient vegetation and soil changes on hydrology.

1.4 Thesis Structure

This chapter provides the research gaps and objectives. A literature review on climate and transient vegetation change impacts on mountain hydrology, uncertainty of hydrological models, and cold regions hydrological processes is presented in Chapter 2. In Chapter 3,

study sites and methodology are explained; physically based modelling of the hydrological processes is introduced; and approaches for the sensitivity analysis are explained. The performance of the developed models in capturing measured streamflow and snowpack and calibration of the uncertain parameters are discussed in Chapter 4. Chapter 5, Chapter 6, and Chapter 7 are core parts of this research with Chapter 5 focusing on climate change impacts on hydrological processes based on air temperature perturbations up to 5°C and precipitation perturbations up to ±20%. Results from Chapter 5 have been published (Rasouli et al., 2014, 2015b). Rasouli et al. (2014) examined the hydrological sensitivity of a northern Canadian mountain basin (Wolf Creek Research Basin) to perturbations in temperature and precipitation. Rasouli et al. (2015b) studied the sensitivity of snowpack to similar perturbed climate in a mountain basin in the US northwestern interior. In Chapter 6, first-order impacts of changing climate on mountain hydrology are investigated using a perturbation of high elevation weather data adapted from RCM–GCM combinations. In Chapter 7, transient changes in vegetation and soils as second-order impacts of changing climate on mountain hydrology are investigated using ecological estimation of vegetation and soils change due to climate change. Finally, a summary and then conclusions are described in Chapter 8.

1.5 Definition of Some Terms

- **Mean annual** (used for peak snow water equivalent, peak runoff, total runoff): average of the variable in water year starting 1 October and ending 31 September over n number of years;
- **Climatological value**: average of a variable over a long period of time (e.g., 30 years);
- **Julian day of the water year**: day of the water year starting from 1 October instead of 1 January.
- **Sensitivity analysis**: is defined as as "the study of how changes in the input of a hydrological model can affect the output of the model. In this study, the changes are associated with the modelled changes in climate."

Chapter 2
LITERATURE SURVEY

2.1 Hydrological Processes Under Climate Change

The hydrological impacts of global climate changes have been studied with different approaches. Studies on climate change impact assessments can be categorized into two main groups: (1) observed changes in water balance components; and (2) hydrological modelling using general circulation models (GCMs) under different scenarios of greenhouse gas (GHG) emissions. This category forms the framework for the literature review of the climate change impacts on hydrology in general and mountain hydrology in particular in this study.

2.1.1 Observed Changes in Hydrological Processes Due to Climate Change

Studying observed hydrological trends and regime shifts associated with climate changes is important to understand potential future changes. Air temperatures in northern latitudes (Jorgenson et al., 2010) e.g., the Yukon Territory, Canada (Janowicz, 2010) have increased in recent decades; changes in precipitation have been more variable. These temperature and precipitation changes are associated with changes in the hydrological cycle (Bunbury and Gajewski, 2012), such as the river ice cover period shortening due to later freeze-up in the fall, and earlier ice break-ups in the spring and a greater frequency of midwinter break-up events with subsequent flooding (Janowicz, 2008, 2010). Warming in northern latitudes is amplified by sea ice decline (Chapman and Walsh, 1993; Johannessen et al., 2004), ice albedo feedback (Perovich et al., 2007), and changes in atmospheric and oceanic heat and moisture

fluxes (Vihma, 2014; Bintanja and Van der Linden, 2013).

Studies show that snow processes have altered (Pomeroy et al., 2006; Déry and Brown, 2007). Snowcover extent in the northern hemisphere decreased 5.4% over the period from 1972 to 2006 (Déry and Brown, 2007), especially in March (7%) and April (11%) when loss of snowcover is associated mainly with warming (Brown and Robinson, 2011). Permafrost has degraded (Jorgenson et al., 2001) and shrub tundra has expanded (Tape et al., 2006) with a rapid warming in the northern latitudes. Snow and terrestrial changes under warming climate have affected streamflow (St Jacques and Sauchyn, 2009). Studies show that river flow in winter and April has increased in the Yukon Territory and regions of significant permafrost with ground thaw (Walvoord and Striegl, 2007). In April, the transition period between streamflow dominated by baseflow and snowmelt runoff, groundwater contributions to streamflow have increased (Brabets and Walvoord, 2009). Leith and Whitfield (1998) examined observed hydrological changes in western Canada and found statistically significant changes in streamflows that might be caused by climate change. Rasouli et al. (2013) studied hydrological variability and regime shifts in observed streamflows feeding Lake Athabasca in Canada and found significant hydrological changes in streamflows in the headwater basins of the Athabasca River as well as lake water levels, which may link to climatic changes. Headwater basins of the Athabasca River drain meltwater from Colombia Icefield (Schindler and Donahue, 2006; Rasouli et al., 2013, 2015a) and melting rates are expected to intensify under warm conditions.

To assess actual (observed) climate change impacts on the hydrology of a basin, water balance methods (Thornthwaite and Mather, 1957) were widely applied (e.g., Gleick, 1986; Gibson and Edwards, 2002). Observed water balance methods are one way to study the hydrological impacts of the global climate changes. These methods show flexibility and are useful for studying climate change impacts on regional hydrological processes (Gleick, 1986). Gibson and Edwards (2002) investigated water balance trends and variations in evaporation losses using isotopic data in northern Canada. They showed that estimated evaporation losses typically range from 10–15% in tundra biomes to 60% in forested sub-Arctic biomes and

evaporation from open water bodies, which accounts for 5–50% of total evapotranspiration, decreases with increasing latitude (Gibson and Edwards, 2002). The water balance methods can propagate seasonal variability and change of the climatological fields to snowfall and snowmelt mechanisms, groundwater recharge, evapotranspiration, and soil moisture characteristics. These methods can be applied along with the general circulation model outputs and expert opinions on climate change scenarios (Gleick, 1986). Gibson and Edwards (2002) coupled meteorological and isotropic measurements to partition regional evaporation – transpiration fluxes and to study variations in evaporation losses. Stable isotopes can be employed to identify potential changes in water balance components due to climate changes (Gibson and Edwards, 2002). Global-scale climatic changes affect local-scale meteorological fields, which consequently affect snowpack, snowcover, snowmelt, soil moisture, infiltration, evapotranspiration, and streamflows. The response of each water balance component of a hydrological system to climate change needs to be studied in order to detect streamflow trends and regime shifts.

2.1.2 Hydrological Modelling and Climate Change Studies

Hydrological models are widely used to simulate, predict, and diagnose processes that are difficult to measure in wide ranges of time, space, and scale (Pechlivanidis et al., 2011). There are different hydrological models with varying structures, which are grouped into (1) metric models based on events and observations; (2) conceptual models based on hypotheses and not necessarily direct physical interpretations; (3) physically based (distributed) models representing processes that are solved by partial differential equations; and (4) hybrid models based on a combination of two or three model types (Pechlivanidis et al., 2011). Hydrological models such as SLURP, HBV (Bergstrom, 1995), Snowmelt Runoff Model (SRM) (Martinec et al., 2008), and Soil and Water Assessment Tool (SWAT; Arnold et al., 1998) do not represent the important cold regions processes, such as direct and diffuse radiation to slopes, long-wave radiation in complex terrains, intercepted snow, blowing snow, sub-canopy turbulent and radiative transfer, sublimation, energy balance snowmelt, and infiltration to frozen and unfrozen soils. Therefore, these models may not be appropriate for simulating cold

regions processes. To capture the cold regions processes and to understand the role of topography and aspect/slope (López-Moreno et al., 2014) and the impacts of warming and precipitation phase change on snow (Knowles et al., 2006; MacDonald et al., 2012) and streamflow (Stewart et al., 2004; McCabe and Clark, 2005) regimes in mountainous regions, a distributed model based on cold regions physics needs to be chosen. As spatial variability of topography and meteorology in mountainous regions is high, a hydrological model with an appropriate scale representation is required. A physically based distributed model, which captures the hydrological mechanism across scales, is likely to perform well in environments with rapidly changing weather (Patil et al., 2014). Woo and Thorne (2006) studied large-scale streamflow generation due to snowmelt in a mountain basin in sub-Arctic Canada by applying a semi-distributed land-use based runoff processes (SLURP) model (Kite et al., 1994). They showed that the combination of snow accumulation in winter and snowmelt rates in spring controls the interannual streamflow variability. Understanding the energetics of snow and frozen ground as well as the timing and magnitude of vertical and horizontal water fluxes in alpine environments is challenging as the spatial variability of meteorological variables (precipitation, wind) and snow redistribution (drifts, wind blowing snow source/sinks, canopy sublimation) is large. With improved understanding of the physical processes in mountain basins, predictability of future hydrology still remains uncertain due to unpredictable natural variability of future climates (Deser et al., 2012).

The Cold Regions Hydrological Model (CRHM) (Pomeroy et al., 2007), an objective oriented and partially physically based platform, represents major cold region hydrological processes. The CRHM has been widely applied to studies in the continental climates of western Canada (in Yukon Territory (Dornes et al., 2008), the Canadian Rockies (Ellis and Pomeroy, 2007; Ellis et al., 2010; Fang et al., 2013), the Canadian Prairies (Mahmood et al., 2016), and the Northwest Territories (Dornes et al., 2008)) and other cold regions such as the Tibetan–Qinghai Plateau (Zhou et al., 2014), Patagonia (Krogh et al., 2015), the Pyrenees (López-Moreno et al., 2013), and the Alps (Weber et al., 2016). CRHM was evaluated in the SnoMIP2 snow model intercomparison and it performed very well in modelling forest snowmelt at sites in Switzerland, the USA, Finland, and Japan (Rutter et al., 2009).

High surface runoff derives from spring snowmelt and occurs as a result of limited infiltration into frozen soils at the time of melt and a relatively rapid release of water from melting snowpacks (Janowicz et al., 2003). Meltwater infiltration into frozen soils can be restricted, limited, or unlimited depending on the degree of soil saturation by liquid water and ice and the overwinter development of ice layers on top of the soil (Granger et al., 1984). Infiltration into frozen mineral soils is usually limited. Substantial midwinter melts can create ice layers, which restrict infiltration such that most snowmelt forms overland flow (Gray et al., 2001). Snowmelt timing and melt rate are primarily controlled by the net inputs of solar radiation, long-wave radiation, energy advected from rainfall, and turbulent transfer of sensible and latent heat (Pomeroy et al., 2003). The impact of these inputs on snowmelt are moderated by the storage of internal energy in the initially cold snowpacks and the snow surface albedo, both of which change rapidly in the pre-melt and melt period. The degree of saturation can be estimated from soil porosity and the volumetric moisture content measured the preceding fall if overwinter soil moisture changes are minimal. During summer, rainfall infiltrates the porous soils and then is withdrawn by plant roots for evapotranspiration associated with the growth of mountain tundra and forests (Granger, 1999). Evapotranspiration occurs quickly from wet surfaces such as water bodies, wetted plant canopies, and wet soil surfaces and relatively slowly from unsaturated surfaces such as bare soils and plant stomata (Granger and Gray, 1989). Any hydrological model to be used for climate change assessment in this region must correctly represent these hydrological processes.

Application of Climate Models in Hydrological Modelling

The United Nations Intergovernmental Panel on Climate Change (IPCC), which has issued assessment reports on global climate change since 1990, reported that the atmosphere and ocean have warmed and the snowpack and Greenland/Antarctic ice mass have decreased since 1950s (Barros et al., 2014; Pachauri et al., 2015). Air temperature warming is predicted to exceed 2°C by 2040 in regions such as Canada and Eurasia and by 2100 over the globe, compared to air temperatures during the period from 1850 to 1900 (Joshi et al., 2011).

The warming rates are heterogeneous in different regions, latitudes, atmospheric layers, and seasons of the year, which is associated with snow and ice feedbacks, and the stability of atmospheric stratification. The highest warming rates are expected to occur in the winter season in cold regions (Balling Jr et al., 1998).

Global climate changes cause local changes that, in turn, lead to global changes (Wilbanks and Kates, 1999). MacDonald et al. (2012) assessed local-scale climate change effects on the zero degree isotherm, precipitation phase, snowpack, and snowmelt period for the North Saskatchewan River watershed using a range of GCMs. With the emergence of supercomputers in recent decades, climate models with sufficient resolution and complexity have become possible and assessment of climate change impacts under different scenarios of greenhouse gas (GHG) emissions has been widely practiced. With improvements in computational cost in recent years, the interaction of changes at both global and local scales can be more appropriately investigated. Hydrological changes in mountains can contribute to global and local climate changes (Barnett et al., 1989). A common approach for investigating hydrological response to climate change is to apply climate model projections under different GHG emission scenarios and to downscale large-scale atmospheric circulations obtained from the climate models to local-scale variables using statistical or dynamical methods (Fowler et al., 2007).

Statistical downscaling approaches are categorised into three main groups: regression based, weather-type, and weather generators. Advantages of the statistical downscaling methods are that they have the ability to present a full distribution (moderate and extreme values) and have higher computational efficiency. The regression based methods represent a linear or nonlinear relationship between local-scale variables and large-scale atmospheric circulations (Fowler et al., 2007). The weather-type methods find the observed event in the past when the situation is most closely analogous to the event for which the simulation is made (Benestad et al., 2008; Gaitan et al., 2014). Weather generators are able to produce unlimited length time series; they can keep spatial correlation of the atmospheric fields when multi-station weather generators are applied. In general, the statistical downscaling methods

can be used to randomise the downscaled results in order to obtain the local variability and extremes (Maraun et al., 2010). The statistical downscaling methods, however, have some limitations. There is no feedback between larger and finer scales of atmospheric circulations. At least 10 years of data are needed for calibration to simulate the hourly extreme precipitation with downscaling methods (Maraun et al., 2010). The statistical relationships for current and future climates are also assumed to be stationary.

The dynamical downscaling approach with high resolution outputs provides a representation of (1) grid-based features such as orography and land characteristics; (2) finer-scale physical processes; and (3) sub-grid features in complex terrain when compared with GCM. These methods also have some limitations: (1) the dynamical downscaling approaches propagate climate model biases from synoptic-scale to regional-scale atmospheric fields (Addor et al., 2016); (2) at the grid scale, they show considerable noise; (3) there is usually a relative disagreement between precipitation fields produced from dynamical downscaling approaches and those measured in local point-scale stations, especially at sub-daily scales; (4) they are deficient with respect to convective parametrisation especially in summer and sub-daily scales; (5) they overestimate the occurrence of wet days and underestimate extreme precipitation; and (6) energy balance closure is not always correct (Ehret et al., 2012). There is a trade-off between the resolution of the climate model outputs and their application in hydrological impact studies (Seyyedi et al., 2014; Gutmann et al., 2016). The limitations of both statistical and dynamical downscaling approaches necessitate the consideration of an alternative solution that considers the main physical processes while minimizing computational resources.

As biases due to scale and parametrisation issues have not yet resolved by statistical and dynamical downscaling methods, the delta change factor method (e.g., Stockton and Boggess, 1979; Semadeni-Davies et al., 2008; Kawase et al., 2009), an an alternative, can produce plausible hydroclimatological changes in the future. The delta change factor method usually represents the changes in monthly climatology between current and future climates for variables such as precipitation and air temperature (Stockton and Boggess, 1979).

2.2 Hydrological Processes in Mountains Under Climate Change

High elevations are ecologically (Beniston, 2003) important as they are key zones for biodiversity due to steep gradients of temperature, precipitation, and topography and also hydrologically important (Bales et al., 2006) as they store water in the form of snowpack in winter and release it in spring and summer. Water contribution from alpine snow to river flows is high in much of Europe and North America (Fang et al., 2013; López-Moreno et al., 2013). The distinct cold season nature of alpine climates means that processes of blowing snow redistribution, sublimation, melt, infiltration, evaporation, and runoff over and through frozen and unfrozen soils govern the generation of spring and summer flows from non-glaciated high mountain catchments (Pomeroy et al., 2012).

2.2.1 Observed Changes in Mountain Hydrological Processes Due to Climate Change

The higher sensitivity of snow and frozen soils to warming makes mountain basins with air temperatures near zero degree suitable study areas for investigating climate change impacts on the hydrological cycle (Bunbury and Gajewski, 2012). Climate warming effects were studied in some mountain catchments (e.g., Stewart et al., 2004; Bales et al., 2006), and is expected to proceed further and threaten the ecological and hydrological integrity of these regions (Malmqvist and Rundle, 2002). Rapid weather changes over short distances in mountains (Beniston, 2003) can lead to rapid runoff generation and soil erosion (Zuazo et al., 2006). Mountain-Research-Initiative-EDW-Working-Group (2015) studied warming rates with elevation and suggested that warming depends on elevation. The effect of elevation dependent warming (EDW) on snowmelt runoff timing was studied by Stewart et al. (2004) and McCabe and Clark (2005). Fyfe and Flato (1999) showed that temperature increase over the Rocky Mountains in winter and spring is elevation dependent with higher warming at high elevations, which is due to an upslope movement of the snow line (MacDonald et al., 2012) and the snow-albedo feedback. Fyfe and Flato (1999) showed that the role of elevation becomes

more effective on the pattern of climate change over western North America only when a significant continental-scale warming dominates and it is not detectable in the early stages of climate change. Winter temperatures have a key role in insensitivity of a mountain basin to a warming climate and snowmelt runoff timing in regions with near-freezing air temperatures (Stewart et al., 2004; McCabe and Clark, 2005). Nayak (2008) found significant trends of rise in temperature, especially in minimum temperature, a reduction in number of soil freeze days, earlier occurrence of plant-water stress, and a strong seasonal shift in streamflow over the period of 1962–2006 at high elevations of Reynolds Creek Experimental Watershed (RCEW), USA.

Siemens (2016) studied variability of the main hydrological processes in Marmot Creek Research Basin located in the Canadian Rocky Mountains over the period from 1962 to 2013 and reported an increasing trend in mean annual air temperature and precipitation. Over the same period, snowpack has become deeper and runoff volumes have increased at high elevations in this basin (Siemens, 2016). The basin discharge was not affected by increased temperature and precipitation due to increased sublimation and evapotranspiration losses (Siemens, 2016). Air temperature, precipitation, and rainfall fraction of precipitation have also increased at all elevations of a research mountain basin in northwestern USA, resulting in decreases in snowpack (Nayak et al., 2010). Bonsal and Prowse (2003) detected temporal trends in the 0°C isotherm across Canada and reported that spring freshets have become earlier in the last decades in mountainous regions in western Canada. Changes in meteorological variables have been shown to affect snow processes, soil moisture, evepotranspiration, and streamflows in mountains.

2.2.2 Application of Climate Models in Mountain Hydrological Modelling

Climate warming projections show that mountain systems are expected to warm even more than other systems, by about 2.8°C in temperate areas and 5.3°C in northern latitudes by the

end of the 21st century (Nogués-Bravo et al., 2007). High rates of warming at high latitudes and high elevations will alter snow dynamics, hydrological mass balance, and water fluxes in mountainous regions. Climate models with sufficient resolution and complexity are useful tools that can be used to study the hydrological mechanisms under climate and vegetation changes (Abramopoulos et al., 1988). The difference between the spatial scales of climatic and hydrological models makes coupling the two sets of models for climate change analyses very challenging (Kite and Haberlandt, 1999). Hydrological modelling generally requires a spatial resolution of 0.1° (≈10 km) latitude and longitude or smaller (Salathé, 2003). The resolution of a General Circulation Model (GCM), for instance the T63 version of the Environment Canada CGCM3.1 model, is 2.8°, which is much coarser resolution than needed for direct application in a semi-distributed hydrological model such as CRHM without downscaling and bias adjustment. The GCM outputs are not entirely credible in capturing the effects of sub-grid features, such as orography, cloud, convection, and vegetation (Ban et al., 2014). Biases in synoptic-scale atmospheric circulations can transfer to regional-scale atmospheric fields even with bias corrections (Addor et al., 2016). The GCMs need to capture key climate processes i.e., El Niño.

Application of the climate model output is challenging in mountainous regions for the following reasons: (1) uncertainty in climate model outputs and gridded observational products are high in mountain basins, which propagates to hydrological responses when different sets of gridded atmospheric products in a given mountain catchment are applied (e.g., Eum et al., 2014); (2) because of the coarse spatial resolution of atmospheric circulations in climate models, projected changes in mountain precipitation are very uncertain (Shepherd, 2014; Addor et al., 2016); (3) steep precipitation and temperature gradients and orographic complexity over mountainous terrain make spatial simulation of the alpine precipitation and temperature uncertain (Klemeš, 1990; Barry, 1992); and (4) most of the climate model outputs used for future projections, even those that are dynamically downscaled by regional climate models (RCMs) (Fowler et al., 2007), show large simulation biases when compared to current conditions (Maraun et al., 2010). Regional-scale biases are due to scale inconsistency between coarse spatial resolution of the atmospheric circulations and local-scale processes

and parametrisation biases in representing soil moisture depletion (Bellprat et al., 2013), surface albedo and cloud cover (Maraun, 2012), or convective precipitation (Ban et al., 2014).

To improve these issues in climate change impact studies, downscaling the atmospheric variables (Cannon, 2008; Kawase et al., 2009; Seyyedi et al., 2014), bias correction (Bourdin and Stull, 2013; Vrac and Friederichs, 2015; Addor et al., 2016), ensemble based approaches (Hunt, 2005; Wilby and Harris, 2006; Bennett et al., 2012), application of upper-air precipitation and temperatures (Jarosch et al., 2012), weather generators (Wilks and Wilby, 1999; Kuchment and Gelfan, 2002; Fowler et al., 2005; Kilsby et al., 2007; Burton et al., 2008; Forsythe et al., 2014), and high resolution climate model outputs (Rasmussen et al., 2011) have been introduced in the literature. Direct application of a single RCM in hydrological studies needs bias correction approaches, which may impair the spatio-temporal fields of meteorological variables (Ehret et al., 2012) and propagate the biases in climate models from the synoptic-scale to the regional-scale (Addor et al., 2016). A multivariate bias correction of air temperature, precipitation, and humidity in mountain basins is challenging due to high interdependency among these variables (Vrac and Friederichs, 2015). Despite its limitations, the delta change method is widely used in hydrological sensitivity analysis (e.g., Hay et al., 2000; Nayak, 2008; Kay et al., 2009; Wang et al., 2012; López-Moreno et al., 2013, 2016) because of its simplicity and the fact that uncertainty introduced by the delta change method has not been shown to be higher than other statistical downscaling methods (Fowler et al., 2007; Kay et al., 2009; Sunyer et al., 2012).

2.2.3 Hydrological Sensitivity Analysis

A sensitivity analysis can be conducted on different modeling components, including observed model inputs, parameters, and structures, to either identify and quantify the sources of model uncertainties or investigate the response of hydrological processes to the changes. There are two categories for hydrological sensitivity analysis: (1) methods in which sensitivity of a hydrological model output or performance measure (response) is characterised across the mutli-dimensional space of the factors (parameters or forcings) by attributing the variability

of the response to the factors (Morris, 1991; Sobol, 1993; Razavi and Gupta, 2016); and (2) methods in which sensitivity of a model response is characterised in relation to changes in model inputs (e.g., Jones et al., 2006). One method for doing the sensitivity analysis is the delta change factor method (also known as the perturbation method; Stockton and Boggess, 1979; Gleick, 1986; Fowler et al., 2007), which examines the change in an output variable for a change in air temperature due to global warming (Fowler et al., 2007). Saltelli et al. (2008) defined sensitivity as "the study of how uncertainty in the output of a model (numerical or otherwise) can be apportioned to different sources of uncertainty in the model input." Wilby (2005) showed that a sensitivity analysis can quantify the hydrological uncertainty due to parameter selection in climate change impact studies.

Uncertainty is ubiquitous in hydrological modelling and so there are several methods for evaluating the performance of hydrological models, including (i) parameter estimation for assessing uncertain parameters and (ii) uncertainty analysis for tracking sources of modelling uncertainty (Matott et al., 2009). Razavi and Gupta (2016) presented a general sensitivity analysis tool, based on an analogy to "variogram analysis", that attributes variability of the response (model output or performance measure) space to the factor (e.g., model parameters, forcings) space. The Variogram Analysis of Response Surfaces (VARS) method, which is introduced by Razavi and Gupta (2016), is a general method linking the commonly used "derivative-based" Morris (Morris, 1991) and "variance-based" Sobol (Sobol, 1993) approaches. For problems with single point solutions, parameter estimation is considered as optimisation problem, e.g., a dynamically dimensioned search (DDS) (Tolson and Shoemaker, 2007). For multiple solution problems, parameter estimation is conducted based on either importance sampling (e.g., generalised likelihood uncertainty estimation method (GLUE) introduced by Beven and Binley, 1992) or Markov Chain Monte Carlo sampling. The importance sampling method, which distinguishes the plausible or behavioural ranges of the parameters from non-behavioural configurations, is usually applied to uncertainty analysis to ensure that all ranges of the parameters are assessed. Because the sampling is computationally expensive, alternative methods such as the stochastic response surface method (Isukapalli et al., 1998) and deterministic preemption technique (Razavi et al., 2010) have been introduced

in order to reduce the computational cost.

Bennett et al. (2012) assessed hydroclimatological modelling uncertainties in northwestern Canada and estimated that uncertainties from GCMs, emissions scenarios, and hydrological parametrisation were 84% for the Peace River, 58% for the Fraser River, and 31% for the Campbell River (coastal basin) in British Columbia for winter in the 2050s. The smaller uncertainty in the coastal basin relative to the other two basins is due to its insensitivity to changes in hydrological parameters, which might be linked to high soil moisture conditions and high precipitation in winter (Bennett et al., 2012). Wilby and Harris (2006) found that simulations of low streamflows are very sensitive to uncertainties in GCMs. Wilby (2005) indicated that a sensitivity analysis can quantify the hydrological uncertainty from various sources in climate change impact studies. Simulation of future mountain hydrology has large uncertainties even with application of sophisticated dynamical downscaling methods. This is because of the scale mismatch between hydrological and climate models and uncertainty of the projected changes in regional precipitation and air temperatures in future climate scenarios due to coarse simulation of the synoptic dynamics in GCMs (Kite and Haberlandt, 1999).

2.2.4 Application of the Delta Change Factor Method in Hydrological Modelling

Higher uncertainties in capturing current climate reduce the credibility of the climate models, suggesting that climate projection by RCMs/GCMs is one way of producing plausible changes in the future (Beven, 2011). The delta change factor method is another way of producing plausible hydroclimatological changes in the future. The delta change factor method usually represents the changes in monthly climatology between current and future climates for variables such as precipitation and air temperature (Stockton and Boggess, 1979). The delta change method (Semadeni-Davies et al., 2008) was widely used in hydrological sensitivity analysis as uncertainty due to application of the change factors has not been shown to be

higher than other statistical downscaling methods (Fowler et al., 2007; Kay et al., 2009; Sunyer et al., 2012). Kawase et al. (2009) used the delta change factor method in the form of a pseudo-global warming downscaling method with multiple CMIP3 atmosphere–ocean coupled general circulation models (AOCGCMs) to investigate the variability of East Asian Monsoon rainfall. They used the Weather Research and Forecast model (WRF) (Skamarock et al., 2005) forced by ERA–40 reanalysis outputs (Uppala et al., 2005). The change factors in monthly climatology between current and future climate variables, along with the 6-hourly reanalysis products, were used as initial and boundary conditions of the WRF runs to obtain the pseudo-future ERA–40 data (Kawase et al., 2009; Rasmussen et al., 2011). Running long-term ensembles of weather prediction models such as WRF with high temporal and spatial resolutions to study climate change is computationally expensive and extremely challenging in complex terrain. Mahat and Anderson (2013) studied the streamflow change in the Crowsnest Creek catchment in the Canadian Rockies under climate and vegetation changes using a weather generator model, the HBV-EC hydrological model (Hydrologiska Byråns attenbalansavdelning, Environment Canada), and a GCM to obtain changes factors in monthly climatology between present and future climates. As applying one or two climate models is not enough to show the full range of climate uncertainty in hydrological response – application of the delta change factor method with a range of GCMs and forcing meteorological data provides an estimation of the uncertainties, which should be addressed in hydrological studies (Bennett et al., 2012; Elsner et al., 2014).

2.3 Hydrological Processes under Transient Vegetation and Soil Changes

Interaction between climate, vegetation, soil, snow, and ecosystem leads to changes in ice/ snowcover, permafrost, streamflow, soil moisture, vegetation, and other defining properties of ecosystems (Osterkamp et al., 2009). These changes provide important local-scale feedbacks from ecology, surface energy balance, and hydrological cycle of northern latitudes to global scale (Osterkamp et al., 2009; Rawlins et al., 2009). Transient vegetation changes can be grouped into four categories (Brown et al., 2005): afforestation, deforestation, regrowth, and

forest conversion. Brown et al. (2005) reported that the time taken to reach a new equilibrium in terms of water yield under deforestation is more quickly than afforestation.

2.3.1 Climate and Vegetation Interactions

The response of vegetation communities to warming varies from one climate to another (Stow et al., 2004). In northern latitudes, where air temperature is low, growing season is short, cloud cover is persistent, and solar angle is small, the vegetation composition responds quickly to changes in climate and nutrient transport; therefore, rapid changes in hydrological processes are expected (Hope and Stow, 1995). In contrast, the growing season in moderate climates is longer and snow depth and snowmelt rates affect vegetation composition (Billings and Bliss, 1959; Stanton et al., 1994). Many mountain plants begin growth at near freezing temperatures, when snowpacks start to melt (Billings and Bliss, 1959).

In northern latitudes, small changes in temperature and precipitation affect thawing and freezing (Zhang et al., 2008; Walvoord and Kurylyk, 2016) and snowmelt rates and associated soil moisture (Bales et al., 2011), all of which affect the vegetation growth season (Denmead and Shaw, 1960). The impacts of climate change, wildfires, logging, and mountain pine beetle (MPB) on vegetation dynamics are important from a hydrological perspective. The growing season lengthened by 3 day/decade (Euskirchen et al., 2010) and the ground temperature at northern latitudes increased by 0.7°C/decade over the last four decades (Jorgenson et al., 2010). If these conditions continue, an ecological regime shift in Interior Alaska is expected and white spruce forests, which are very susceptible to warming, will convert to aspen parkland or grassland with 2°C of warming (Chapin III et al., 2004). Warming in winter is also an important factor in vegetation change. For instance, winter rate of warming in the Arctic is 0.19°C/year, which is four times greater than summer warming (0.05°C/year) (Bintanja and Van der Linden, 2013). Greenness in the Arctic provides a positive warming feedback by reducing the surface albedo. Vegetation enhancement, however, decreases the warming in mid-latitudes as evapotranspiration increases (Chae et al., 2015).

In a modelling experiment, Chae et al. (2015) applied three scenarios to differentiate the impacts of doubling CO_2 concentration and vegetation change above 60° latitude. Those scenarios were: i) current CO_2 concentration and altered vegetation, ii) doubled CO_2 and no change in vegetation, and iii) doubled CO_2 and conversion of all grassland and shrublands to boreal forests. When only the vegetation was altered, the Arctic warmed by 3.5°C, which was 20% greater than when CO_2 was doubled and vegetation not changed. This suggests that Arctic warming will be enhanced by vegetation shifts. The peak warming would be expected to shift from November to August under combination of both doubled CO_2 and changed vegetation (Chae et al., 2015).

To study vegetation dynamics, ground level and remotely sensed measurements have been widely applied in the literature. For small-scale studies, "plot measurements" are used to monitor the vegetation growth in a controlled area. For this purpose, the height of the plants or shrubs is measured during the growing season and changes in vegetation phenology (e.g., start and end dates of the growing season) are determined over a few years or decades. The other method is "repeat photography" in which images from the same location are taken repeatedly over time and changes detected. The repeated photography approach has the advantage that it dates back to before remote sensing imagery era and it does not require radiometric corrections (Stow et al., 2004). For instance, Clark and Hardegree (2005) examined photographs taken over 145 years at Whiskey Mountain within Reynolds Creek Experimental Watershed in Idaho, USA. Sampled images in 1917 and 2000 for vegetation cover showed that mountain big sagebrush and bare ground/rock, which were respectively about 40% and 35% in 1917 dropped to $\approx$ 35% and 14% of the total vegetation cover in 2000. Mountain mahogany and antelope bitterbrush coverages increased from 10% and 0.7% to 31% and 4%, respectively, over the same period. Over 7% of the lands covered with mountain big sagebrush and rock have converted to mountain mahogany (Clark and Hardegree, 2005). Bare ground also converted to big sagebrush and mahogany over the period 1917–2000 (Clark and Hardegree, 2005). Clark et al. (2001) used remote sensing images to classify the mountain plant communities in Reynolds Creek Experimental Watershed (RCEW), Idaho, USA and suggested that images taken during the dry season (early August) are less uncertain for

classifying vegetation types. Monitoring changes in vegetation dynamics with a combination of ground based and remotely sensed measurements (Stow et al., 2004) can help to delineate catchment land cover and appropriately model the changes in hydrological processes under transient vegetation changes.

An ecological regime shift is expected to happen in northern latitudes under rapid warming, in which the currently spruce-dominated vegetation will likely convert to its early Holocene state, which is similar to the present-climate boreal mixedwoods in southern Alberta, Canada (Mann et al., 2012). This would increase the albedo and latent heat flux in summer months. In contrast, when the snow-free season extends into the winter months under a warmer climate, the albedo will decrease, which will also alter the energy balance. Increase in the deciduous to coniferous stands ratio would increase the ground heat flux in summer by 3–6% (Mann et al., 2012). The expanding shrub extent, which might enhance or delay melting of permafrost in tundra regions (Sturm et al., 2005), and its relation to the surface energy balance alters albedo feedbacks to the climate system (Pomeroy et al., 2006).

2.3.2 Snow and Vegetation Interactions

In cold regions, interaction between snow and vegetation plays an important role in altering hydrological processes. Snow depth in forests is usually lower than that in open areas because of the sublimation of snow intercepted on the canopies (Pomeroy et al., 1998). Snow is intercepted in needle-leaf forest canopies, that large proportions of winter snowfall sublimate instead of unloading from the canopy to the ground (Pomeroy et al., 1999). Forest cover increases long-wave radiation and reduces incoming shortwave radiation, which results in reduction in the total energy to melt the snowpack (Essery et al., 2008). Musselman et al. (2008) investigated the effects of forest vegetation on snow accumulation and ablation in New Mexico and showed that snow depth and peak snow water equivalent (SWE) were 25% higher and 21 days later on a north facing slope relative to a south facing slope. Canopy interception reduced peak SWE under the canopy by 47%, while snow ablation rates were 54% greater in open areas compared to under the canopy (Musselman et al., 2008). The

impacts of the extensive changes in forest cover by anthropogenic activities (e.g., forest clearcutting), wildfires, and insect disturbance (e.g., Mountain Pine Beetle) might offset the impact of snowpack loss due to sublimation (Pomeroy et al., 1998). Forest removal, however, can cause early and faster melts, with the potential to increase the magnitude and frequency of floods (Alila et al., 2009). Varhola et al. (2010) in a review paper complied and listed the previous works and reported that forest cover change explains 57% of the variance in snow accumulation change and 72% of the variance in snow ablation change. The extension of the clearings (gaps) in forests plays an important role in snow accumulation and melt and flow can increase through this type of forest manipulation (Troendle, 1983; Pomeroy et al., 2002, 2012; Ellis et al., 2013). Small forest gaps are wind sheltered and, as the gap area increases, the snowpack is exposed to wind erosion and sublimation from blowing snow (Pomeroy et al., 2002; Ellis et al., 2013). Landscape vegetation cover and local topography affect snow redistribution and sublimation from blowing snow (Pomeroy et al., 1999; MacDonald et al., 2009).

In mountains, change in snow regimes affect moisture availability and consequently vegetation composition (Billings and Bliss, 1959; Stanton et al., 1994). If snowmelt is slow in summer in the central Rocky Mountains (Wyoming), the ecological gradient is usually steep over a short distance; however, if snowmelt releases water after late July, plant growth becomes negligible because of a short and dry growing season (Billings and Bliss, 1959).

In windy areas with thin snowcover, alpine plants emerge early and become mature early and tolerate to mild droughts. Plants in deep snow-covered areas have short growing seasons and sometimes cannot complete the full annual growth cycle (Billings and Bliss, 1959). Walker et al. (1993) investigated the primary role of elevation gradients and the secondary role of wind-driven snow redistribution in vegetation productivity in the Front Range of Colorado, USA. A strong relationship between greenness represented by the normalised difference vegetation index (NDVI) and soil moisture supplied by snowmelt was found in the City of Boulder watershed with vegetation areas classified as barren, fellfield, meadow, and shrub (Walker et al., 1993). They suggested that elevation gradients control biomass production

because of the long and cold snow-covered periods and shallow soils in mountainous regions. Walker et al. (1993) classified optimal snow depths (up to 5 m) suitable for growth of 50 plant species. Some plants are never seen in areas with higher than 50 cm of snow while others occur where there is a deep snowpack. Extending this study to regions and landscapes covered with different shrub and forest types would add more knowledge about snow–vegetation interactions. Stow et al. (2004) showed that there is a strong relationship between NDVI values and air temperature anomalies, suggesting that warming during the growing season is important factor in vegetation productivity.

In alpine areas and tundra shrub biomes, snow is redistributed by wind; the blowing snow transport and sublimation processes are affected by the interaction of local topography and landscape vegetation cover with regional wind flow patterns (Pomeroy et al., 1999; MacDonald et al., 2009). Snow is also intercepted on the needle-leaf forest canopies from which large proportions of winter snowfall sublimate rather than unload to the surface (Pomeroy et al., 1999). Snowmelt in shrub tundra is complicated by the emergence and spring-up of tall tundra shrubs, which form a canopy over the snowpack and change the energy inputs to the underlying snow (Pomeroy et al., 2006; Bewley et al., 2010; Ménard et al., 2014a).

The amount and timing of snowmelt affects soil moisture, nutrient transport, soil and leaf temperature, surface microclimate, and growing season (Billings and Bliss, 1959; Walker et al., 1993; Stanton et al., 1994). Changes in climatic conditions that alter snowmelt will affect vegetation composition. Anthropogenic changes and natural variability in vegetation cover are two important sources of uncertainty in climate models that are regarded as cross-cutting issues in climate change studies (Deser et al., 2012; Brown et al., 2014). In assessment of vegetation–climate feedback exchanges, Loveland and Mahmood (2014) suggested the following steps should be considered: establishing possible trends of vegetation changes, identifying sensitive vegetation types and regions, and strategic planning for adaptation to climate changes. Vegetation and climate interactions and feedbacks from vegetation changes to climate are important as ecosystem dynamics have a significant influence on atmospheric

processes (Pielke et al., 1998). Both climate and transient vegetation changes are also important to understand changes in hydrological processes. To understand vegetation–climate interactions, the following questions need to be considered (Loveland and Mahmood, 2014): how will vegetation change with climate changes over time and how will feedback from vegetation change affect climate and weather systems? Understanding the interactive dynamics of climate and vegetation and careful assessment of the uncertainties in future climate and vegetation are important in climate change studies (Pielke et al., 1998).

2.3.3 Soil and Vegetation Interactions

Transient vegetation change can also alter soil properties or be affected by changes in soil over long time periods. Therefore climate changes indirectly can change soil properties. Interactions between climate, vegetation, and soils, however are complex (Rodriguez-Iturbe, 2000) and time lag between vegetation response to climate changes and soil response to vegetation changes is unclear (Innes, 1991). Deforestation, for instance, can change soil properties. Removal of organic materials from soil due to wildfires can lead to soil erosion (Imeson and Vis, 1984) and reduced infiltration rates (DeBano, 1991), and consequent increased overland flows, which enhance the soil loss (Imeson et al., 1992). Thermokarst, which is an alteration of topography due to thawing processes, happens when the forest is burned and organic materials are removed from the soil. This is another factor that can change the soil properties, radiation and heat fluxes, and hydrological streamflow networks in forested areas (Schuur et al., 2009). Regrowth of pine forest after a wildfire (Shakesby et al., 1996) and vegetation restoration (Zheng, 2006) can reduce the soil loss. Conversion of forest to pasture can increase the soil bulk density and decrease the soil porosity, both of which distort infiltration, percolation, aeration, and erodibility (Reiners et al., 1994). Transient changes in vegetation composition on a snowmelt slope in Mosquito Ranges, Colorado were shown to be linked to snowmelt timing, rock cover, soil disturbance, and soil organic materials (Stanton et al., 1994).

While vegetation removal can affect soil properties, so too can afforestation (Ritter

et al., 2003). Afforestation slowly modifies soil properties including soil acidity and nitrogen storage (Ritter et al., 2003). Soil properties including bulk density, reaction, organic carbon, calcium carbonate, and nitrogen storage vary during vegetation change phases from the initial colonization of the bare surface to the establishment of a forest (Crocker and Major, 1955). Roots can grow onto newly-exposed rock and facilitate weathering, both of which accelerate soil formation in early stages of forest establishment (5 to 10 mm per year in Ouachita Mountains, Arkansas, Phillips et al., 2008). From a hydrological perspective, the interaction between climate, soil, and vegetation depends mainly on scale of the problem, physiological characteristics of the vegetation, pedology of the soil, and type of climate (Rodriguez-Iturbe, 2000).

2.3.4 Driving Factors on Transient Vegetation Changes

Main driving factors that affect vegetation communities in mountains include (1) climate changes, (2) mountain pine beetle (MPB, in western Canada), (3) logging, and (4) wildfires. Some of these factors might be consequences of climate change. An example of how interaction between climate and vegetation can change ecosystems is the expansion of shrubs in northern latitudes. Change in active layer thickness, as a result of warming climate, allows more subsurface water storage, higher nutrient transport, and a deeper root zone leading to the expansion of shrubs (Sturm et al., 2005). Mountain pine beetle has changed a considerable portion of the coniferous forests in western Canada (Bewley et al., 2010). MPB is a destructive insect that first attacks stressed trees and, in the second phase, healthy and old pine stands (Borden, 1982). Extreme cold events (e.g., $\leq -40°C$) control the MPB population (Safranyik et al., 1975). MPB destroyed 16.8 million ha of pine forest over 1960–2004 in western Canada (Taylor et al., 2006). Winter mortality, availability of hosting trees, warmer growing season, precipitation variability, spring droughts, and aridity are factors that control the growth and reproduction of the beetles (Moore et al., 2005). Macias Fauria and Johnson (2009) investigated the spatiotemporal expansion of MPB-affected forests in British Columbia in association with climate teleconnections and variables. They found that the Pacific Decadal Oscillation (PDO) change to the warm phase in 1976 and periods of positive Arctic Oscillation

(AO) in the late 1980s and 1990s have limited the number of extreme cold winters in the Canadian Rockies. Periods without cold winter minimum temperatures reduce the winter die off and enhance the spread of MPB and destruction of vast parts of Canadian forests. MPB has already spread to the boreal forest in Northern Alberta despite the fact that the Rocky Mountains act as a barrier that often prevents Arctic cold weather systems from drifting toward British Columbia but not strong enough to prevent beetles migrating to boreal forests (Macias Fauria and Johnson, 2009).

Logging has also changed the shape of landscapes and the hydrology in forested regions. Bosch and Hewlett (1982) reviewed results from 94 experiments across the world on the impacts of deforestation and afforestation on water yield in forested landscapes with 600–2600 mm mean annual precipitation. They concluded that, on average, coniferous forests (e.g., pine), deciduous hardwood forests, and scrubs increases water yield by 40, 25, and 10 mm, respectively, per each 10% reduction in cover; maximum increases occur during the first five years following forest cover removal. Higher values in water yield are expected for areas with higher precipitation, however, higher annual precipitation accelerates regrowth of the forest. The maximum decline in water yield following afforestation is equivalent to the maximum increase in water yield one year after logging (Bosch and Hewlett, 1982). At local and regional scales for instance, converting vegetated areas to irrigated agricultural lands, or urbanisation, can change near-surface micrometeorology (Fall et al., 2010), regional precipitation (DeAngelis et al., 2010), and greenhouse gas production (Burney et al., 2010).

Warmer and drier summers and more frequent fires can cause a vegetation change and an increase in deciduous trees at the expense of the white spruce and shrub tundra (Mann et al., 2012). Vegetation composition can change with a shift in snowmelt regime, changes in the nutrient fluxes, increases in the length of the growing season, and, in colder areas, with changes in permafrost depth (Jorgenson et al., 2001) and water storage. In a modelling experiment, Retana et al. (2002) showed that a Mediterranean pine forest became dominated by oaks 30 years after fire. Shakesby et al. (1996) designed an experiment to study pre- and post-fire overland flows in a burnt plot and a control plot in a pine forest and found that

post-fire overland flow was higher than pre-fire. Pine needles are important for reducing soil losses as they can bind the soil particles together within a year after the fire (Shakesby et al., 1996).

Under a longer snow-free season and increased precipitation in northern latitudes, abundant vegetation is expected in valley bottoms where adequate soil moisture and nutrients are available. Therefore, synchronous increases in precipitation and air temperature would enhance vegetation cover in the North. Plausible scenarios of transient changes in vegetation based on trends from historical high resolution remote sensing images considering wildfire, mountain pine beetle, and other natural changes as a result of climate regime shifts, along with terrestrial changes caused by anthropogenic activities or by climate changes, should be considered in hydrological modelling. Most future projections for changes in vegetation cover are not dynamically coupled with climate projections (Loveland and Mahmood, 2014). Coupling climate and weather systems with vegetation change models would provide the feedbacks that must be considered in climate change assessments. A plausible way to evaluate the projected vegetation changes in northern latitudes under warmer climates is, for instance, to compare them with current vegetation composition in warmer and drier boreal mixedwood forests of southern and central Canada than to Alaska (Schneider et al., 2009; Alberta-Natural-Regions-Committee, 2006; Mann et al., 2012). An assumption of no change in vegetation when modelling hydrological processes under both present and future climates could introduce uncertainty in climate change assessment. Therefore, a detailed hydrological model with and without vegetation change can help to evaluate hydrological uncertainties due to climate and vegetation changes in mountainous watersheds.

2.4 Summary

Previous studies diagnosing the changes in hydrometeorology and vegetation of mountains are presented in this chapter and mountain hydrological modelling and downscaling approaches applied in the literature are reviewed. The higher sensitivity of alpine snow regimes to

warming makes mountain basins with annual mean air temperatures near zero suitable case studies for sensitivity to climatic changes. Studies showed that warming at high latitudes and high elevations was amplified, which caused large changes in hydrological processes.

A common approach for investigating hydrological response to climate change is to apply climate model projections or their changes under different GHG emission scenarios using statistical or dynamical downscaling methods. This is challenging in mountainous regions, as projected changes in regional precipitation are very uncertain and the monitoring network is sparse. A large bias between observations and climate model outputs is due to: (1) scale issue and coarse spatial resolution of the atmospheric circulations that do not adequately capture processes; and (2) parametrisation issues in simulating processes such as soil moisture, surface albedo, cloud cover, and convective precipitation. Most of the climate models used for future projections, even those that their outputs are dynamically downscaled by regional climate models (RCMs), showed large simulation biases when compared to current conditions. An ensemble of delta change factors obtained from a group of climate models can be applied to observations to assess the climate change impact on mountain hydrology. Models require a full representation of hydrological processes in cold regions to assess the impact of climate change and variability.

Plausible scenarios of transient changes in vegetation and soils for different natural and anthropogenic disturbances should be considered in hydrological modelling. Trends of vegetation changes and conversions within a vegetation community can be estimated from historical high resolution remote sensing images and aerial photos. Wildfire, logging, mountain pine beetle, transient soil development, and other natural changes as a result of climate regime shifts, along with terrestrial changes caused by anthropogenic activities or by climate changes, can be potential drivers for transient vegetation changes (e.g., afforestation, regrowth, deforestation, forest conversion). Studies show that time taken to reach a new equilibrium in terms of water yield under deforestation is more quickly than afforestation.

Chapter 3

METHODOLOGY

3.1 Study Sites and Data Sources

Potential hydrological responses to warming, precipitation changes, and transient vegetation changes in three headwater basins along a north–south transect through the North American Cordillera (NAC) are examined: Wolf Creek Research Basin ($\approx 61^\circ$ N), Yukon Territory, Canada, a sub-Arctic basin; Marmot Creek Research Basin ($\approx 51^\circ$ N), Alberta, Canada, a headwater basin of the Bow River in the Front Ranges of the Canadian Rocky Mountains; and Reynolds Mountain East catchment ($\approx 43^\circ$ N), Idaho, USA, a seasonally cool montane headwater basin. These three mountain basins are chosen for this detailed modelling study as they have been densely monitored, have sufficiently long observation records and parameter measurements. Comparing these will help to understand climate change impacts on mountain hydrology of different climates across the NAC. High quality measurements of hourly air temperature, relative humidity, wind speed, incoming shortwave radiation, daily precipitation observations, and streamflow data for each basin are used in this study. The availability of long-term data from high elevation stations representing multiple biomes in each basin makes them suitable case studies for comparing and contrasting the hydrological processes under climate and vegetation changes.

3.1.1 Wolf Creek Research Basin (WCRB)

Wolf Creek Research Basin (WCRB) is a headwater basin in the Yukon River in Canada (Figure 3.1). WCRB is divided into five subbasins (Figure A.2): Upper Wolf Creek, Coal

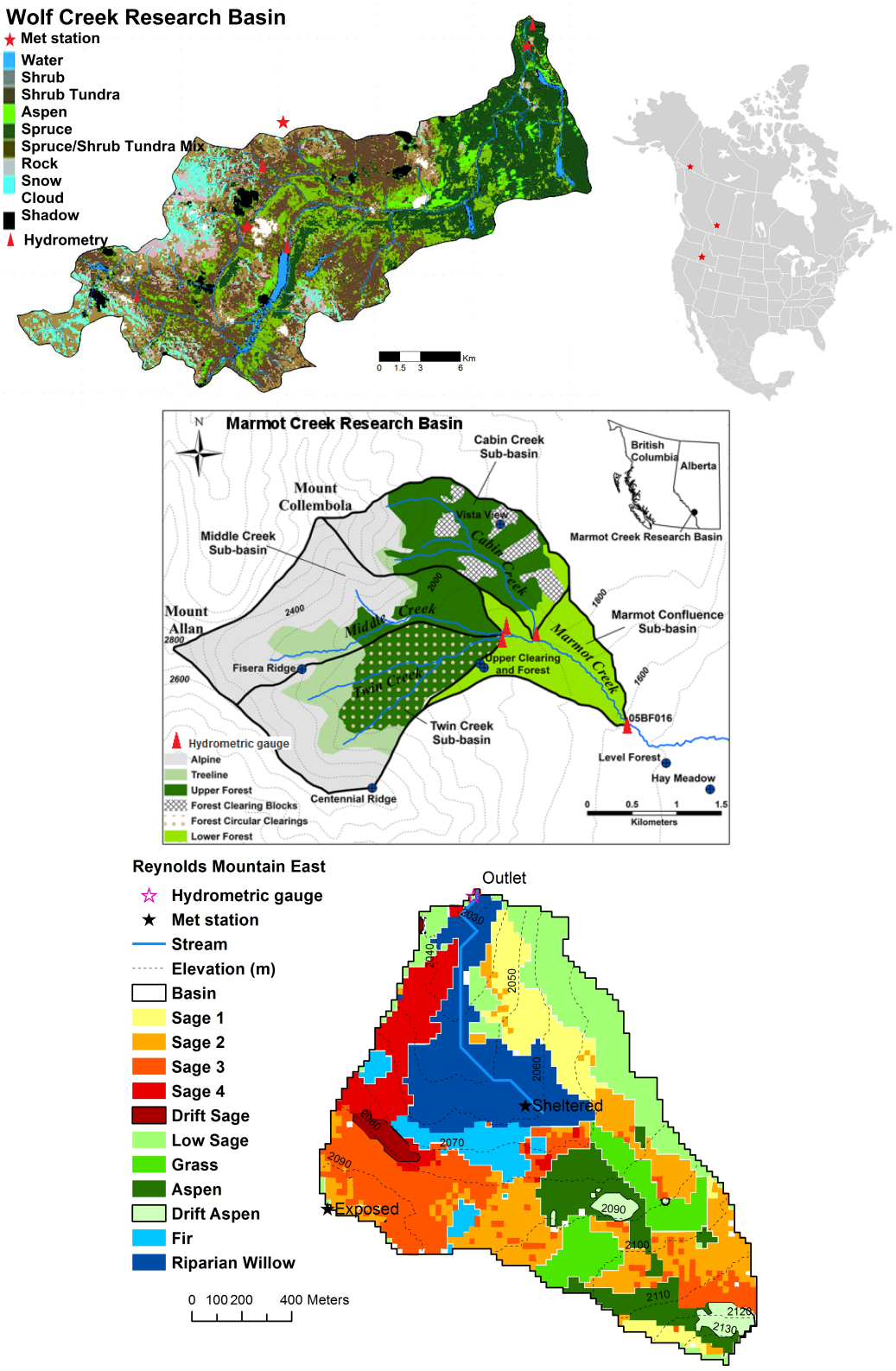

Figure 3.1: Three headwater basins across the Western North American Cordillera: Wolf Creek Research Basin, Yukon Territory; Marmot Creek Research Basin (MCRB); and Reynolds Mountain East (RME) catchment within Reynolds Creek Experimental Watershed, Idaho, USA.

Table 3.1: Description of the main meteorological and hydrometric stations within or near three headwater basins across the North American Cordillera (El: Elevation).

Station	El [m]	Lat [N], Long [W]	Site Details
(1) Wolf Creek Research Basin (WCRB)			
Shrub tundra	1250	60°31.34′, 135°11.84′	East facing moderate slope
Alpine	1615	60°34.04′, 135°08.98′	Windswept ridge top plateau
Forest	750	60°35.76′, 134°57.17′	Gently undulating terrain
Whitehorse WSO	706	60°44.00′, 135°05.00′	Located at Environment Canada site
Upper Wolf Creek	1295	60°29.45′, 135°17.50′	Hydrometry, drainage area: 14.4 km^2
Coal Lake Outlet	1190	60°30.61′, 135°09.74′	Hydrometry, drainage area: 70.5 km^2
Granger Creek	1312	60°32.79′, 135°11.08′	Hydrometry, drainage area: 7.6 km^2
Alaska Highway	703	60°36.00′, 134°57.00′	Hydrometry, drainage area: 179 km^2
(2) Marmot Creek Research Basin (MCRB)			
Centennial Ridge	2470	50°56.68′, 115°11.62′	Alpine rocks and talus
Fisera Ridge	2325	50°57.42′, 115°12.27′	Treeline
Vista View	1956	50°58.25′, 115°10.33′	Spruce, fir, lodgepole pine
Upper Clearing	1845	50°57.40′, 115°10.52′	High elevation forest clearing
Upper Forest	1845	50°57.42′, 115°10.57′	Spruce, fir, lodgepole pine
Hay Meadow	1436	50°56.63′, 115°08.38′	East facing moderate slope
Level Forest	1600	50°56.78′, 115°08.80′	Lodgepole pine forest
Water Survey	1600	50°57.03′, 115°09.17′	Hydrometry, drainage area: 9.4 km^2
Cabin Creek	1710	50°57.57′, 115°10.03′	Hydrometry, drainage area: 2.35 km^2
Middle Creek	1760	50°57.36′, 115°10.25′	Hydrometry, drainage area: 2.94 km^2
Twin Creek	1790	50°57.58′, 115°10.27′	Hydrometry, drainage area: 2.79 km^2
(3) Reynolds Mountain East (RME)			
Exposed	2094	43°11.15′, 116°47.01′	dominated by mixed sagebrush
Sheltered	2049	43°11.16′, 116°46.98′	in an aspen/fir grove
Outlet	2020	43°11.17′, 116°46.98′	Hydrometry, drainage area: 0.38 km^2

Lake, Granger, Mid Wolf Creek, and Lower Wolf Creek. Along the main branch of Wolf Creek is Coal Lake (area 1 km^2). At low elevations are jack pine, white and black spruce, and trembling aspen forest stands (Francis et al., 1998). Above the treeline, shrub tundra with birch and willow shrub heights from 30 cm to 2 m occupies the majority of the basin (65%). At the highest elevations is an alpine tundra biome of bare rock and short tundra moss and grass vegetation. Estimates by Lewkowicz and Ednie (2004) suggest that 43% of the basin contains permafrost, which restricts the movement of water beneath the surface, particularly in the case of saturated frozen soils (Carey and Woo, 2001; Quinton et al., 2009). The general aspect of WCRB is north–easterly. Studies have shown slope aspect to be an important control on runoff processes (Woo and Carey, 1998; Pomeroy et al., 2003).

Data sources and basin physiography are described in detail by Rasouli et al. (2014). Hydrometeorological data are available for WCRB for water years from 1993–1994 to 2010–2011 for the three main meteorological stations, one in each primary biome, and four streamflow gauges (Figure 3.1; Table 3.1). Measurements of snow depth and density along snow survey transects were collected at least monthly by Yukon Environment and university researchers at each of the three meteorological stations. These measurements and snow water equivalent (SWE) measured at a snow pillow located at the subalpine site provide model diagnostic information in each biome (Pomeroy and Granger, 1999). Hourly air temperature, relative humidity, wind speed, incoming shortwave radiation, and daily precipitation observations from above-canopy meteorological stations and streamflow data from the hydrometric stations are used in this study. Precipitation was measured by tipping bucket rain gauges, unshielded "BC style standpipe" precipitation gauges, and Nipher-shielded Meteorological Service of Canada (MSC) snowfall gauges. Nipher gauge solid precipitation measurements were corrected using a wind undercatch correction equation (Goodison et al., 1998) with wind speeds measured from nearby gauge-height anemometers. Gaps in data were infilled by establishing regression equations for meteorological variables between each of the three meteorological stations and the Whitehorse WSO station, which is located 13 km from WCRB. Changes in elevation rather than distance between stations are assumed to be responsible for the meteorological variation in this study basin.

3.1.2 Marmot Creek Research Basin (MCRB)

Marmot Creek Research Basin (MCRB) is a headwater basin of the Bow River in the Front Ranges of the Canadian Rocky Mountains. The MCRB (Figure 3.1) includes four subbasins: Cabin Creek, Middle Creek, Twin Creek, and the lower drainage area of the main stream. The general aspect of MCRB is easterly. Vegetation in MCRB is mainly Engelmann spruce and subalpine fir at the higher elevations and lodgepole pine at the lower elevations (Kirby and Ogilvie, 1969). Short shrubs and alpine larch are found adjacent to the treeline. Above 2250 m elevation, only exposed rocks and talus are present. Soils freeze seasonally in MCRB, which limits the infiltration and percolation of snowmelt water in the early melt season. Except for higher elevation parts of the basin that feature exposed bedrocks, the basin is covered by a deep layer of coarse and permeable soil allowing for rapid rainfall infiltration to subsurface layers overlying relatively impermeable shale. Westerly warm and dry Chinook (foehn) winds in winter months occasionally shift up the air temperature above 0°C. Approximately 70 to 75% of annual precipitation in MCRB occurs as snowfall.

Observations of air temperature, relative humidity, wind speed, precipitation, and incoming shortwave radiation were collected from meteorological stations. Precipitation data were measured with an Alter-shielded Geonor weighing precipitation gauge and corrected for wind-induced undercatch. Snow depth and density measurements were collected with a ruler and an ESC–30 snow tube to estimate snow water equivalent (SWE) in MCRB (Fang et al., 2013). Streamflow is measured by a gauge at the basin outlet, which is maintained by Environment Canada's Water Survey of Canada.

3.1.3 Reynolds Mountain East (RME)

The third basin in this research is Reynolds Mountain East (RME) catchment, which is located in the Owyhee Mountains and is one of the headwater catchments in Reynolds Creek

Experimental Watershed (RCEW), located approximately 80 km southwest of Boise, Idaho, USA (Figure 3.1). RME is not divided into subbasins as it is a relatively small basin. The general aspect of RME is westerly. Distributions of vegetation, soils, and SWE within RME vary greatly. (Seyfried et al., 2009; Kumar et al., 2013; Winstral and Marks, 2014). Six main vegetation types are present, ranging from grass to mountain sagebrush through riparian willow, aspen, and coniferous trees. Unlike the other two basins, soil in RME does not freeze during the year.

RME basin has two primary meteorological stations (Table 3.1) representing a wind/ topographically sheltered area and an open area (Reba et al., 2011a). 70% of annual precipitation falls as snow. This catchment is chosen for detailed modeling as it is densely monitored and has well-studied parameters that can be applied to develop a physically based snow model (Hanson, 2001; Hanson et al., 2001; Marks et al., 2001; Seyfried et al., 2001; Slaughter et al., 2001). It is also described in detail and has a published and freely available 25-year modeling data set (Reba et al., 2011a). It was selected to investigate climate change impacts on hydrological processes in mountain watersheds. The collected data include hourly air temperature, relative humidity, wind speed, precipitation (corrected), shortwave radiation, and long-wave radiation. SWE was measured at a snow pillow near the sheltered site, with data available for diagnostic purposes. Snow accumulation is thought to be enhanced at this site due to the impact of topographic and vegetation sheltering on wind redistribution (Reba et al., 2011b). Winstral and Marks (2014) showed that, over recent snow seasons (2001–2012), detailed ground measurements indicate that the snow pillow has adequately represented the basin-wide SWE. Nayak (2008) showed that maximum SWE decreased at all elevations in RCEW, including the RME subbasin, and that the length of the snow season decreased by nearly a month over the period 1962–2006.

3.1.4 Similarities and Differences Between the Basins

Comparing similarities and differences between the three basins helps to understand the hydrological differences and climatic differences amongst the basins. Table 3.2 compares and

contrasts the main characteristics of the three study basins. Comparison of the physiographic features including elevation bands, vegetation, distance to ocean, latitude, and climatological variables such as annual mean temperature and precipitation and number of freezing days in a year, will provide a strong explanation for potential hydrological changes due to climate and vegetation changes within a basin and amongst the basins. Table 3.2 also contains some information about hydrological response units (HRUs) used in models. WCRB has the largest drainage area, shortest distance to the Pacific Ocean (Figure 3.1), highest latitude, greatest elevation range, lowest average elevation, coldest climate, highest humidity, and lowest annual precipitation amongst the three basins. MCRB has the highest elevation, highest annual precipitation and wind speed, and shortest data record period. RME has the smallest drainage area, highest average elevation, smallest elevation range, lowest latitude, lowest humidity, lowest wind speed, and longest data record period.

Despite differences amongst the basins, there are some similarities. For instance, all three basins are partly covered by a coniferous forest and are snow-dominated under current climate: WCRB and MCRB both have spruce trees; MCRB and RME both have fir trees. Similar to all elevations in WCRB, high elevations in MCRB are very cold. A cold snow season with high precipitation (Figure 3.2) leads to a long winter at high elevations in MCRB with a snow regime resistant to climatic changes. In contrast, RME and low elevations in MCRB have warmer air temperatures with fewer freezing days. This makes these areas more sensitive to warming. Air temperatures of the forest biome in WCRB are lower than for the alpine biome in winter, even though it is located at low elevations (Figure 3.2). High wind speed in MCRB can transport snow from high elevations to the treeline.

3.1.5 Modelling Strategy

Basic characteristics of the study area, including dominant land-cover, elevation of representative stations, and soil type, are defined in the hydrological models. Three elevation bands (high, mid, and low elevation, respectively) are covered by three biomes in WCRB (alpine tundra, shrub tundra, and forest) and in MCRB (alpine, treeline/sink for blowing snow, and

Table 3.2: Comparison of physiography and climatology amongst the three basins across the North American Cordillera. UC denotes Upper Clearing meteorological station in Marmot Creek Research Basin (MCRB). All three basins are located in transition climate zones based on Köppen (1936) climate classification.

Characteristics	**WCRB**	**MCRB**	**RME**
Drainage area [km^2]	179	9.4	0.38
Elevation range [m]	660–2080	1600–2825	2028–2137
Latitude	60°36′N	50°57′N	43°11′N
Longitude	134°57′W	115°09′W	116°47′W
Record period [–]	1993–2011	2005–2014	1983–2008
Dominant vegetation cover			
high elevation	tundra moss, grass	Rock, grass	grass, sage
middle elevation	shrub tundra	spruce, fir	fir
low elevation	spruce	lodgepole pine	aspen, willow
Climate zone	Cordillera & sub-Arctic	Cordillera & Prairie & Boreal	Cordillera & Continental & Mediterranean
Elevation bands [–]	3	3	1
Temperature [°C]			
high elevation	–3.4	–1.8	5.0
middle elevation	–2.0	1.0 (UC)	–
low elevation	–1.5	2.9	–
Number of Freezing days [day]			
high elevation	224	217	120
middle elevation	203	166 (UC)	–
low elevation	179	128	–
Precipitation [mm]	380	1011	858
Wind speed [ms^{-1}]	3.7	5.8	1.9
Relative humidity [%]	74	69	61
Number of subbasin & HRUs [–]	5 & 29	4 & 36	1 &12
HRU area range [km^2]	0.92–25.4	0.01–1.37	0.01–0.07

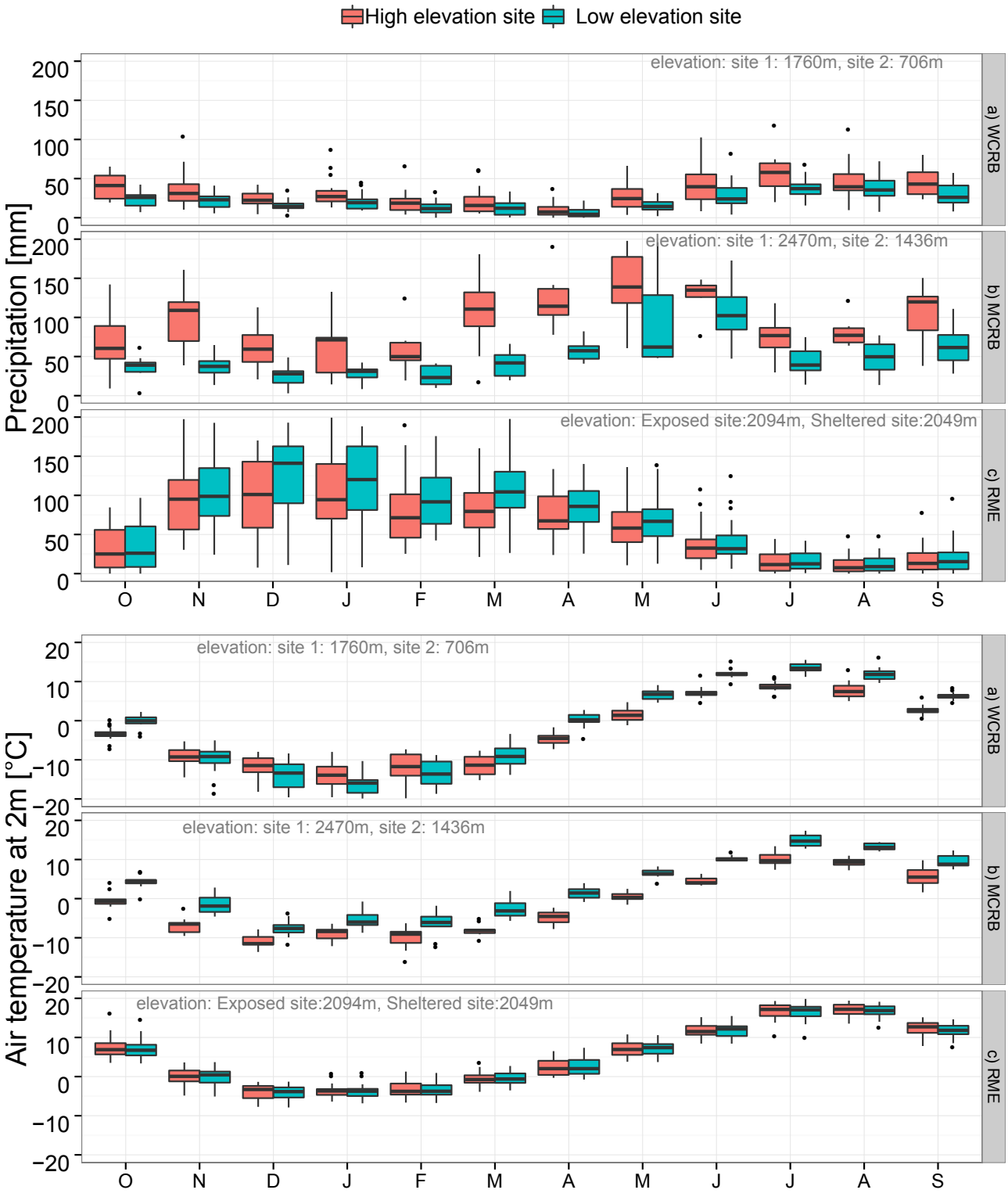

Figure 3.2: Monthly precipitation and air temperature measured at two meteorological stations in each of the three headwater basins across the North American Cordillera. The elevation difference between sites in RME is not large, so two sites represent HRUs that have different wind sheltering but small elevation differences. Black dots denote outliers (outliers were not statistically tested).

forest). Because RME has the highest average elevation but smallest elevation range, it is comparable to high elevation bands and alpine biomes in the other two basins. Therefore, RME is considered to have only a high elevation band and four blowing snow regimes (source, sink, sheltered (from wind), and forest with intercepted snow on the canopy). A spatially distributed modeling structure (Figure A.1) is developed with five subbasins and 29 HRUs in WCRB, based on three elevation bands, four classes of slope and aspect, and three biomes (Figure A.2). All the HRUs are categorised into one of the three biome groups (Janowicz, 1999); alpine tundra, shrub tundra, or forest for parsimonious parametrisation. Four streamflow gauges along Wolf Creek serve as the outlet of subbasins or the whole basin. Another subbasin is Mid-Wolf Creek between Coal Lake and the forest in the lower basin. CRHM modelling structures are replicated by biome to simulate hydrological processes in the five subbasins.

MCRB is segregated into four subbasins and 36 HRUs, based on variability of Marmot Creek attributes, vegetation type and cover, slope/ aspect/ elevation, and experimental anthropogenic deforestation. All of the HRUs are categorised into one of four biomes: alpine, treeline with blowing snow sink, forest, and forest clearings. Seven hydrometeorological stations are located inside and around the basin and four streamflow gauge stations serve as the outlets of subbasins or the whole basin.

HRU configuration in RME is adapted from (Newman et al., 2014) and developed from a multivariate *a priori* classification, an approach for capturing the variability of snowcover and snow depth within the catchment. This method is found by Newman et al. (2014) to be superior to approaches in which grids are segregated based on elevation bands and vegetation types without considering sub-grid variability. Mountain sage is the dominant vegetation in RME and due to its higher variability is disaggregated into five HRUs based on a wind-sheltering index. Drift HRUs in aspen and sage vegetation are in topographic depressions downwind of slope breaks where deep snow accumulates (Newman et al., 2014). As this research basin is located at high elevation, snow is likely to be redistributed by blowing winds. Therefore, for evaluating snow accumulation, ablation, and redistribution by wind,

12 HRUs in RME are categorised into four groups to analyse different snow regimes: blowing snow sink and source, snow regime intercepted on the canopy, and wind sheltered snow regime. The division of a catchment into source and sink areas for blowing snow based on topographic exposure and vegetation height was proposed by Pomeroy et al. (1997) as a way to implement a distributed blowing snow model in a shrub-covered Arctic catchment. Blowing snow sink HRUs include drift HRUs but also riparian and tall sage HRUs. Therefore, the drift aspen, drift sage, willow, and sage 4 are considered sink HRUs and other short vegetation HRUs are grouped as source HRUs. Pomeroy et al. (2002) proposed that forested landscapes could be divided into two areas, one where interception and subsequent sublimation occur and one that is cleared or have minimal winter interception capacity. The fir forest has substantial canopy interception capacity in winter and so is considered a forest HRU with interception, and the aspen forest and gap HRUs have neither blowing snow nor intercepted snow fluxes and so are considered sheltered HRUs.

3.2 Methods and Research Workflow

In this study, components of the hydrological water balance are estimated using a partially physically based model created on the CRHM platform. The model is developed with real data and then used to assess the sensitivity of the hydrological response to climate change in each of the three mountain basins. The sensitivity experiments performed here used different inputs to these models to simulate outputs such as snow dynamics and timing and magnitude of runoff to capture the uncertainties and to some extent disagreement between the climate model outputs for the future. This research examines the sensitivity of hydrological responses to changes in air temperature and precipitation by perturbing an observed time series of air temperature and precipitation data with a range of changes that are predicted by most climate models under late 21st century scenarios of global change for those basins. This linear sensitivity analysis is a step in understanding the possible alteration of the hydrological cycle of cold regions in mountain basins by climate change. The main purpose of this study is to highlight the combination of changes in temperature and precipitation that will

induce important changes in basin hydrology. Knowing which combinations of warming and precipitation changes can induce hydrological change in mountain basins from northern to mid-latitudes can help in assessing how climate change might impact future hydrology. The methodological steps to achieve the research objectives are:

- Set up and test hydrological models in the Cold Regions Hydrological Modelling (CRHM) platform (Pomeroy et al., 2007), implementing cold regions hydrological processes and observed data in the alpine mountain basins across the NAC;
- Conduct climate perturbation sensitivity (CPS) analysis for the mountain basins using observed data as input and applying delta changes in annual and monthly climatology obtained by subtracting the modelled current climate from the modelled future climate and adding to observed time series;
- Compare the water balance and hydrological regime responses to climate change in the context of the range of modelling uncertainties introduced by different climate models and a number of discrete scenarios of possible change in vegetation composition; and
- Compare the changes in processes such as runoff over and infiltration to frozen and unfrozen soils, evapotranspiration, groundwater percolation, and streamflow generation with varying frost table depth due to warming and changes in precipitation.

3.2.1 Modelling Hydrological Processes

Models created using CRHM can have a wide variety of structures with differing levels of process detail and representation, including structures that are suitable for northern basins (Pomeroy et al., 2007) such as WCRB and mountain basins such as MCRB and RME. The CRHM system is very flexible and creates 'objected-oriented' models for particular basins, environments, and predictive needs. Options for redistribution of alpine blowing snow (MacDonald, 2010), a physical basis to soil moisture accounting, fill-and-spill depressional storage (Fang et al., 2010), and forest canopy interception and radiation modules (Ellis et al., 2010) are available in the CRHM platform. For this study, a CRHM model for each basin (WCRB, MCRB, and RME) that accurately characterised the surface and near-surface cold

regions hydrological processes was developed.

A set of physically based process modules describing the major processes can be combined into a model informed by results from previous modelling experiments in research basins such as WCRB (Pomeroy et al., 1999; McCartney et al., 2006; Pomeroy et al., 2003, 2006; Carey et al., 2007; Dornes et al., 2008; Quinton and Carey, 2008; MacDonald et al., 2009). Modules are selected that could be run to robustly simulate the hydrological cycle of the region in a primarily physically based manner. Figure 3.3 shows the schematic setup of these modules, which includes the following:

1. Observation module: reads the forcing meteorological data including air temperature, precipitation, wind speed, relative humidity, and incoming shortwave radiation. This module adjusts the meteorological data, e.g., hydrological lapse rate using elevation and wind-induced undercatch.

2. Radiation module: computes the theoretical global radiation, direct and diffuse solar radiation, and maximum sunshine hours based on latitude, elevation, ground slope, and azimuth (Garnier and Ohmura, 1970).

3. Sunshine hour module: estimates sunshine hours from incoming short-wave radiation and maximum sunshine hours.

4. Slope radiation module: adjusts the short-wave radiation on the slope with incoming short-wave radiation on a level surface.

5. Long-wave radiation module: calculates incoming long-wave radiation using short-wave radiation (Sicart et al., 2006).

6. Albedo module: estimates snow albedo throughout the winter and into the melt period and also indicates the beginning of melt (Verseghy, 1991).

7. Canopy module: estimates the snowfall and rainfall intercepted by and sublimated or evaporated from the forest canopy and unloaded or dripped from the canopy, updates sub-canopy snowfall and rainfall, and calculates short-wave and long-wave sub-canopy

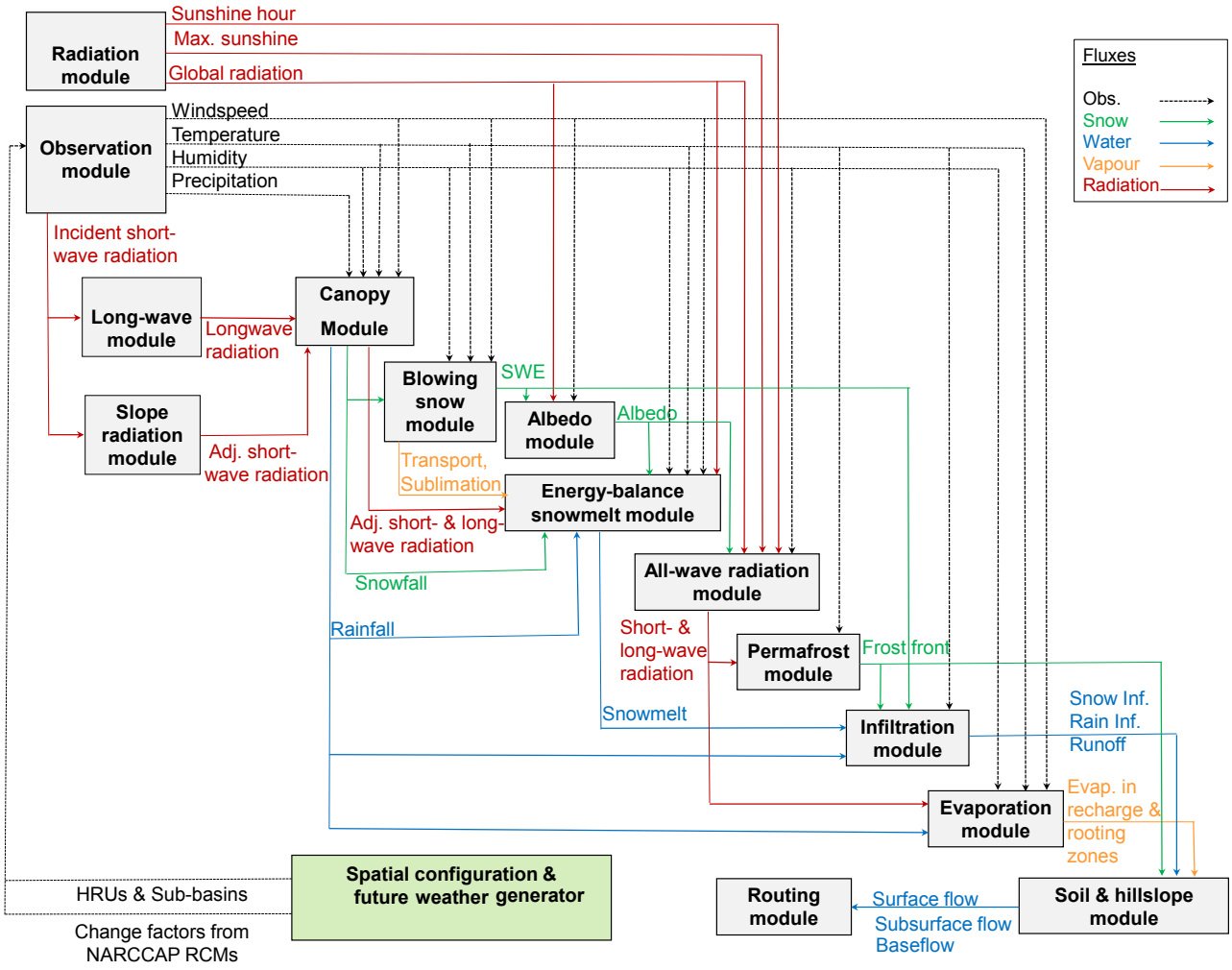

Figure 3.3: Flowchart of physically based hydrological modules used in the CRHM model. The model structure is the same for each of the three basins, except for Wolf Creek Research Basin in which a permafrost module is also used. A full list of field measurements for each basin, used as model parameters, is given in Chapter 4. (abbreviations: Adj.: Adjusted; Inf.: Infiltration; Evap.: Evapotranspiration; Obs.,: Observation)

radiation and turbulent transfer to snow. This module has options for open, small forest clearings, and forested environments (Ellis et al., 2010 and Ellis et al., 2013).

8. Blowing snow module: simulates the wind redistribution of snow transport between the HRUs and blowing snow sublimation losses throughout the winter period (Pomeroy and Li, 2000).

9. Energy balance snowmelt module: estimates snowmelt by calculating the energy balance of radiation, sensible heat, latent heat, ground heat, advection from rainfall, and change in internal energy (see Marks et al., 1998 and Appendix B for details).

10. All-wave radiation module: calculates the net all-wave radiation from short-wave radiation for snow-free conditions (Granger and Gray, 1990).

11. Snowmelt infiltration module: This module has two algorithms for infiltration into frozen and unfrozen soils. One estimates snowmelt infiltration into frozen soils using a parametric equation describing the results of a finite difference heat and mass transfer model (Gray et al., 2001) and the other estimates rainfall infiltration into unfrozen soils with macropores using a soil classification (Ayers, 1959). Surface runoff forms when snowmelt or rainfall exceeds the infiltration rate.

12. Evaporation module: Granger's evapotranspiration expression (Granger and Gray, 1989; Granger and Pomeroy, 1997) estimates actual evapotranspiration from unsaturated surfaces using an energy balance and extension of Penman's equation to unsaturated conditions; the Priestley and Taylor evaporation expression (Priestley and Taylor, 1972) estimates evaporation from saturated surfaces such as stream channels and lakes. Both evaporation algorithms modify moisture content in the canopy interception store, ponded surface water store, and soil column and by linking to the soil module are restricted by a soil water withdrawal relationship to ensure continuity of mass. The Priestley and Taylor evaporation method also updates moisture content for saturated surfaces.

13. Soil and hillslope module: estimates soil moisture balance, depressional storage, surface/ sub-surface flows in two soil layers and groundwater discharge in a groundwater layer,

and interactions between surface flow and groundwater (Leavesley et al., 1984; Pomeroy et al., 2007; Dornes et al., 2008; Fang et al., 2010, 2013). The top layer is the recharge layer, which receives infiltration from depressional storage, snowmelt, and rainfall. Evaporation takes water first from canopy interception and depressional storage and then from the recharge layer or from both soil column layers via transpiration based on the plant available soil moisture and the rooting depth (Armstrong et al., 2010). Aquifer recharge occurs via percolation from the lower soil layer or directly from the surface through macropores. Horizontal and vertical drainage from the soil and groundwater layers is regulated by Darcy's flux, parameterised using Brooks and Corey (1964)'s relationship to estimate the actual hydraulic conductivity in unsaturated zone.

14. Routing module: Clark's lag and route timing estimation method is used to route runoff (Clark, 1945).

15. Permafrost module: used only in WCRB. The module estimates the ground surface temperature from the air temperature, net radiation, and antecedent frost table depth (Williams et al., 2015) and tracks the evolution of thawing and freezing fronts (Xie and Gough, 2013) based on the modified Stefan's equation, which can calculate the freezing/thawing depth no matter how many layers it has or how thick they are. The deep frost table, which separates the subsurface flows from groundwater, controls the groundwater contribution to the baseflow. The XG algorithm proposed by Xie and Gough (2013) is applied to estimate the thawing processes and deep frost table fluctuations in WCRB.

The models for MCRB and RME did not contain the permafrost module but incorporated the same structure as developed for WCRB. The proposed physically based model operates on the spatially distributed control volumes of the HRU, which are found useful for modelling in basins where there is a good understanding of hydrological behaviour, but incomplete detailed sub-surface information to permit a fully distributed fine-scale modelling approach (Dornes et al., 2008). HRUs in a given basin are segregated based on the vegetation, slope, aspect, and elevation utilising a digital elevation model (DEM). The proposed models for

the WCRM, MCRB, and RME operate on the relatively homogeneous HRUs. HRUs are spatially segregated based on surface physiographic information relevant for hydrological model parametrisation including vegetation cover, topography, soil depth, layers, variability of basin attributes, and the level of model complexity. The temporal resolution of this CRHM model is hourly, while the spatial resolution is that of the HRU (see Table 3.2).

3.2.2 Climate Perturbation Sensitivity (CPS)

A climate perturbation sensitivity (CPS) method is introduced here in which current climate is perturbed based on projected future climatological changes. In the CPS methodology, a climate perturbation signal of the future atmosphere is added to high-resolution baseline hourly observations. Perturbation of climate, however, does not consider the changes in frequency and intensity of weather patterns. There are two main assumptions in the general delta change approach and the CPS method applied in this study: (i) GCM outputs for current and future climates show relative changes rather than absolute changes in climate; and (ii) the number of precipitation events is constant in current and future climates (Semadeni-Davies et al., 2008). The assumption of linear scaling of impact with temperature in the delta method for non-linear variables such as precipitation and for extremes introduces uncertainties (Kay et al., 2009). A detailed sensitivity assessment of hydrological responses to climate warming for a given basin is conducted with modelling experiments of climate change impacts assessing the effect of temperature and/or precipitation forcing change on hydrological responses. It is assumed that the basin vegetation and in the case of WCRB permafrost will remain unchanged. The purpose of CPS methodology is to look at first-order impacts of climate change on hydrological processes including snow regime and runoff magnitude and timing. Ménard et al. (2014b) showed for snowmelt in a small portion of a catchment that mountain topography can reduce the impact of changing shrubs on snow redistribution, spring energy balance, and meltwater generation. Second-order impacts of changing climate such as transient changes in vegetation and soils on mountain hydrology are investigated in Chapter 7.

In the CPS approach, change factors are applied to baseline observations on an annual

or a monthly basis. The first approach in this study, which is called "Annually perturbed climate" (APC), is constructed with ΔT from +0°C to +5°C for air temperatures, along with the ΔP from −20% to +20% for precipitation, to improve understating of the hydrological sensitivity to a wide spectrum of the climatic changes.

The second approach is called "monthly perturbed climate" (MPC), which takes into account the monthly variability of the change deltas. MPC is constructed from the dynamical downscaling method applying delta changes in monthly climatology to baseline hourly observations. Changes in monthly climatology give an estimate of the potential climate change impacts on hydrological processes that are consistent with the large-scale atmospheric circulations of the RCM–GCMs, described later. The MPC is developed based on the perturbed climatic fields obtained from current (1970–2000) monthly 30-year climatology subtracted from future (2041–2070) monthly 30-year climatology.

Annually Perturbed Climate (APC)

The range of annual perturbations in precipitation and warming considered for this study is partly based on the changes estimated by Representative Concentration Pathways (RCPs), which are an alternative to the special report on emission scenarios (SRES) (Moss et al., 2010) and were used in the recent Fifth Assessment Report (AR5) of the Inter-governmental Panel on Climate Change (IPCC, Barros et al., 2014). Four new atmospheric composition pathways corresponding to specific radiative forcing values of 2.6 to 8.5 W/m^2 are used as a basis for long-term and near-term modeling experiments in climate change studies. Based on RCP2.6 and RCP8.5 pathways, respectively, a warming of up to 2°C with an increase in the annual precipitation of less than 10% and a warming of up to 5°C with a 20% increase in annual precipitation are expected for the southern Yukon region (WCRB). Similar warming with lower precipitation increases are expected in MCRB and RME. Most modelled scenarios project the future climate to be wetter but some SRES scenarios used in AR5 show regional decreases in precipitation up to 15% for the 2080s. Based on the range of climate scenarios reviewed, APC for the sensitivity analysis is reconstructed by perturbing

observed air temperatures from 0°C to 5°C and observed precipitation from –20% to +20% for each of the three basins (Figure 3.4). Shape and slope of contours in plots under APC in schematic Figure 3.4 and also in Chapter 5 represent the degree of hydrological sensitivity to climatic changes. When one variable is more sensitive to air temperature increase or precipitation change, the lines will be parallel to that axis and when the variable is sensitive to an interaction of air temperature and precipitation changes, there will be a slope in the contour lines if interaction is simple and a slope and a curvature if the interaction is complex (Figure 3.4). Using the same ranges in the sensitivity analysis for all three basins helps to compare the hydrological impact of the climate changes of the temperature and precipitation in different mountain basins across the NAC.

Monthly Perturbed Climate (MPC)

It is unlikely that the seasonal patterns of temperature and precipitation will change in the single direction used in the APC. To capture the variability that might occur, monthly perturbed climates (MPC) were developed. Simulations of the hydroclimatic conditions in mountains are challenging because of the large biases between climate model outputs or reanalysis products and locally observed hydroclimatic conditions and the seasonal nature of snow accumulation and depletion. Most of the climate model outputs used for future projections, even those that are dynamically downscaled by the regional scale models (Fowler et al., 2007; Bennett et al., 2012), show large simulation biases when compared to local observations. This is also true to some extent when climate models are driven with reanalysis products (Wilby and Harris, 2006; Thorne, 2011; Eum et al., 2014; Seyyedi et al., 2014). Approaches that are used for correcting biases in regional climate simulations usually do not account for the origins of biases in synoptic signals simulated by general circulation models (GCMs) and instead apply empirical corrections (Addor et al., 2016). Biases in the synoptic circulation can propagate to regional-scale precipitation and temperature. Addor et al. (2016) used a quantile mapping bias correction method to study the origin of the biases in regional-scale atmospheric fields and reported that a systematic overestimation of the frequency of westerly flow in winter is responsible for overestimation of winter precipitation

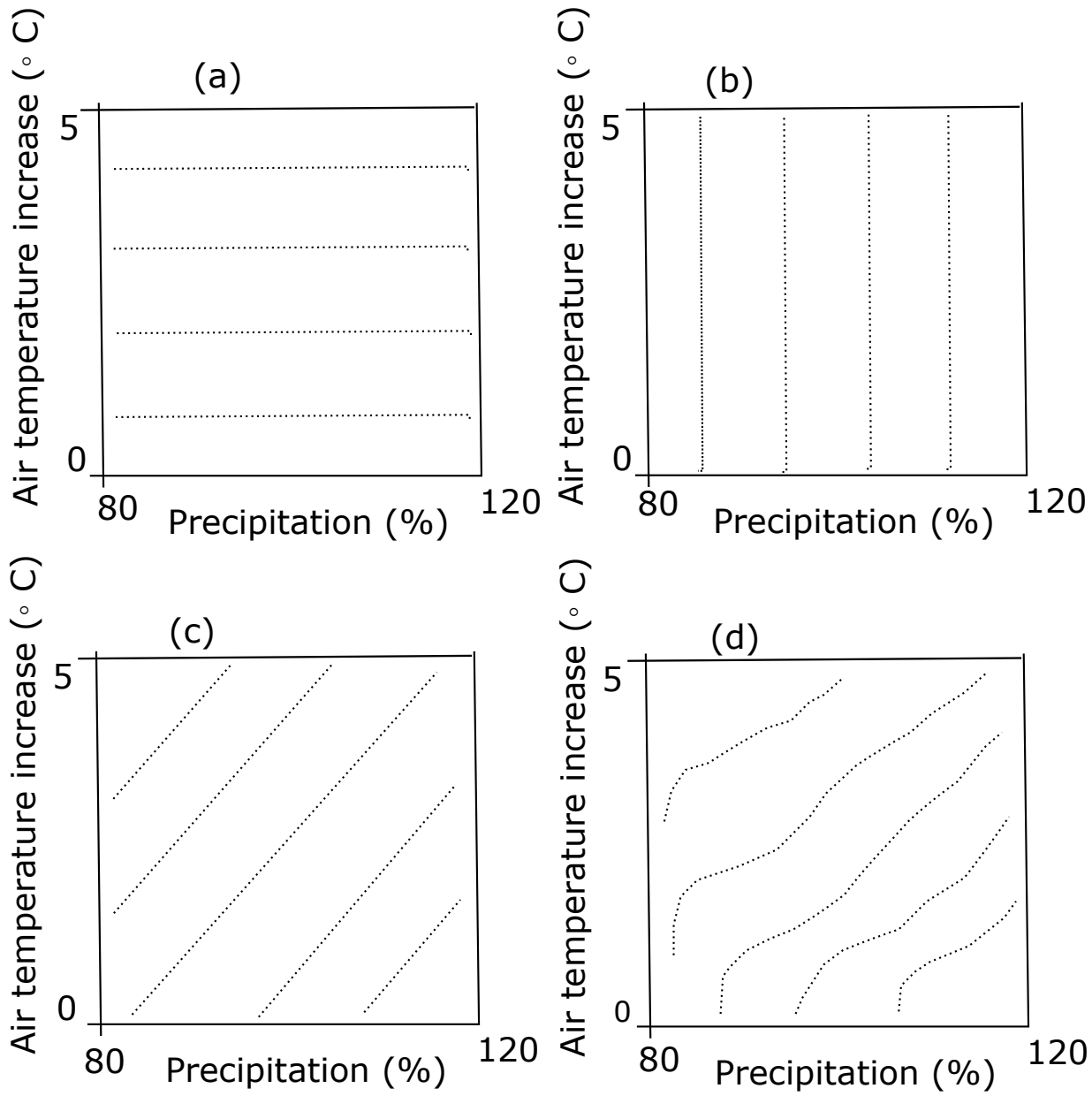

Figure 3.4: Schematic view of hydrological sensitivity to air temperature increase (0°C to 5°C) and changes in precipitation (-20% to +20%). Shape and slope of contours represent the sensitivity of a variable to climatic changes. When one variable is more sensitive to (a) air temperature increase, the lines will be parallel to the x-axis; (b) when one variable is more sensitive to precipitation change, the lines will be parallel to the y-axis; (c) when one variable is sensitive to a simple interaction of air temperature and precipitation changes, the contours will slope based on the interaction; and (d) when one variable is sensitive to a complex interaction of air temperature and precipitation changes, there will be slope and curvature in the contour lines.

over Switzerland. This suggests that bias correction of regional climate models (RCMs) without understanding the inadequate representation of the atmospheric circulations in GCMs does not improve modelling uncertainties in climate change impact studies. Hay et al. (2000) showed that the Hadley Centre for Climate Prediction and Research (HadCM2) GCM cannot produce accurate estimates of the meteorological variables needed for simulating runoff in mountainous basins in the USA. MacDonald et al. (2016) compared outputs from the Global Environment Multiscale (GEM) model driven by Canadian Precipitation Analysis (CaPA) against field observations in MCRB and found an overestimation of the snowcover season duration and large differences in simulated snow depth, soil moisture, and evapotranspiration when both forcing sets were applied to the Canadian Land Surface Scheme (CLASS). The main reasons were that observed precipitation at the higher elevations in MCRB was greater than GEM/CaPA precipitation and GEM/CaPA atmospheric pressure was not similar to the estimated pressure in MCRB (MacDonald et al., 2016). This shows the difficulties of atmospheric models in capturing hydrometeorological processes in cold regions and mountain basins.

In this study, a series of monthly perturbed climates (MPC) is reconstructed based on 11 North American Regional Climate Change Assessment Program (NARCCAP) RCMs (Mearns et al., 2007), which are driven by outputs from multiple atmosphere–ocean general circulation models (AOGCMs, Table 3.3). The reason that 11 ensemble members of RCMs are chosen is that numerical/dynamical cores, physics, dynamics-physics coupling approaches, and resolution of climate models are different, which leads to different simulations of climatic conditions. In order to capture full range of the variability of climate models, an ensemble of climate models are usually recommended. The MPC was developed based on projected climate in the 2041–2070 period.

The monthly CPS approach is chosen to investigate the climate change impacts on mountain hydrology and specifically to examine the variability of the hydrological processes in the basins across the NAC. Each month in the CPS method is considered 30 days and climatological change factors or monthly biases, which are presented in this research, are

Table 3.3: The 11 RCM–GCM models used from the NARCCAP project (Mearns et al., 2007), along with their driving GCMs. The RCM–GCM combinations, which cover a wide range of the climate model uncertainty, are not completely independent from each other as similar or slightly different physical schemes are applied in some of the GCMs.

RCM	Driving GCM – Institution	RCM–GCM
Weather Research and Forecasting model updated Grell configuration	Community Climate System Model	WRFG–CCSM
Weather Research and Forecasting model updated Grell configuration	Canadian Global Climate Model 3	WRFG–CGCM3
Canadian Regional Climate Model	Community Climate System Model	CRCM–CCSM
Canadian Regional Climate Model	Canadian Global Climate Model 3	CRCM–CGCM3
Regional Climate Model version 3	Geophysical Fluid Dynamics Lab.	RCM3–GFDL
Regional Climate Model version 3	Canadian Global Climate Model 3	RCM3–CGCM3
PSU/NCAR mesoscale model	Community Climate System Model	MM5I–CCSM
PSU/NCAR mesoscale model	Hadley Centre Coupled Model 3	MM5I–HadCM3
Hadley Regional Model 3	Hadley Centre Coupled Model 3	HRM3–HadCM3
Hadley Regional Model 3	Geophysical Fluid Dynamics Lab.	HRM3–GFDL
Experimental Climate Prediction–2	Geophysical Fluid Dynamics Lab.	ECP2–GFDL

based on 30-day intervals. Even though only four out of 23 AOGCMs used for the Fourth Assessment Report of the IPCC are selected in the NARCCAP, they are able to span almost the full range of uncertainty of the global climate models (Mearns et al., 2007; Tebaldi et al., 2005). The 11 RCM–AOGCM combinations in the NARCCAP program produce atmospheric data with a resolution of 50 km for both current (1971–2000) and future (2041–2070) periods under the SRES A2 emissions scenario (Mearns et al., 2007). The A2 scenario, as one of the higher GHG emission scenarios of the SRES, is widely used for impact studies. This scenario was also chosen by NARCCAP and regional climate research community in North America even though it is as likely as other 40 scenarios of SRES. The A2 scenario family describes a heterogeneous world with "business as usual", with more rapid global population growth but less rapid economic growth, technological changes, and regional difference than A1 scenario family. The expected global mean temperature increase is 2.0°C to 5.4°C by 2100 under A2 scenario (Meehl et al., 2007) and the expected CO_2 concentrations for the middle and end of the 21st century are about 575 and 870 parts per million, respectively (Nakicenovic et al., 2000).

To develop a monthly (30-day) perturbed climatic field, the modelled current (1970–2000) monthly 30-year climatology average is first subtracted from the modelled future (2041–2070) monthly 30-year climatology average from each of the 11 NARCCAP RCMs (Table 3.3). Then, these delta change factors are added to the locally observed values of precipitation, air temperature, humidity, and wind to represent the future climatic conditions in a given basin. Because climatological values shorter than a month are quite noisy, monthly climatological changes are used in this study. Refer to Appendix C and Figure C.14 for 10-day climatological changes for precipitation and air temperature. The monthly CPS method, is similar to the pseudo-global warming approach (Kawase et al., 2009; Rasmussen et al., 2011) that uses the change factors in monthly climatology obtained from global climate models. Synoptic dynamics of the atmosphere, however, cannot be captured by the CPS method due to the lack of dynamical core, which is an essential component of any climate and weather model and dynamical downscaling method (Staniforth and Wood, 2008).

Importance of Monthly Climate Perturbation Sensitivity

The RCM–GCM models are responding to the projected changes in CO_2 and other forcings. Regional climate model outputs both for current and future climate periods were compared with observations for two sites in each basin (see Appendix C). Distribution of the regional climate model outputs for the current climate period shows large biases when compared with observations. For example, comparison between observations and HRM3–HadCM3 outputs shows that precipitation is overestimated by this RCM in winter in WCRB, in all of the seasons in MCRB, and in summer in RME (Figure 3.5). Similar to precipitation, air temperature is also overestimated in winter and spring and underestimated in summer in all of the three basins. Distributions of observed and simulated precipitation and air temperature show that RCM biases are greater than the projected changes under future climate (Figure 3.5).

In addition to wet biases of the RCM outputs, probability of a dry day (PDD) is also overestimated by RCMs (Table 3.4). The monthly PDD estimated by WRFG–CCSM shows a systematic bias in the number of dry days in each month and especially in spring in WCRB (Figure 3.6). None of the 11 NARCCAP RCMs captures the local processes with sufficient accuracy and most of these models simulate more intense and clustered precipitation events in winter and spring and more frequent dry days than the actual measurements from the stations. The evidence described here suggests that even regional climate models are not yet sufficient to capture the local-scale processes such as convectional storms and the length of wet or dry spans in mountains. Therefore, the direct application, or even bias correction of the RCM outputs would misrepresent the hydrometeorological processes. Such unrealistic relationships would introduce more uncertainty in hydrological modelling than the MPC. Despite the temporal-scale limitations of the monthly CPS method, consistency between the measured atmospheric fields makes this method more physically meaningful and reliable than empirical methods and more computationally efficient than dynamical methods.

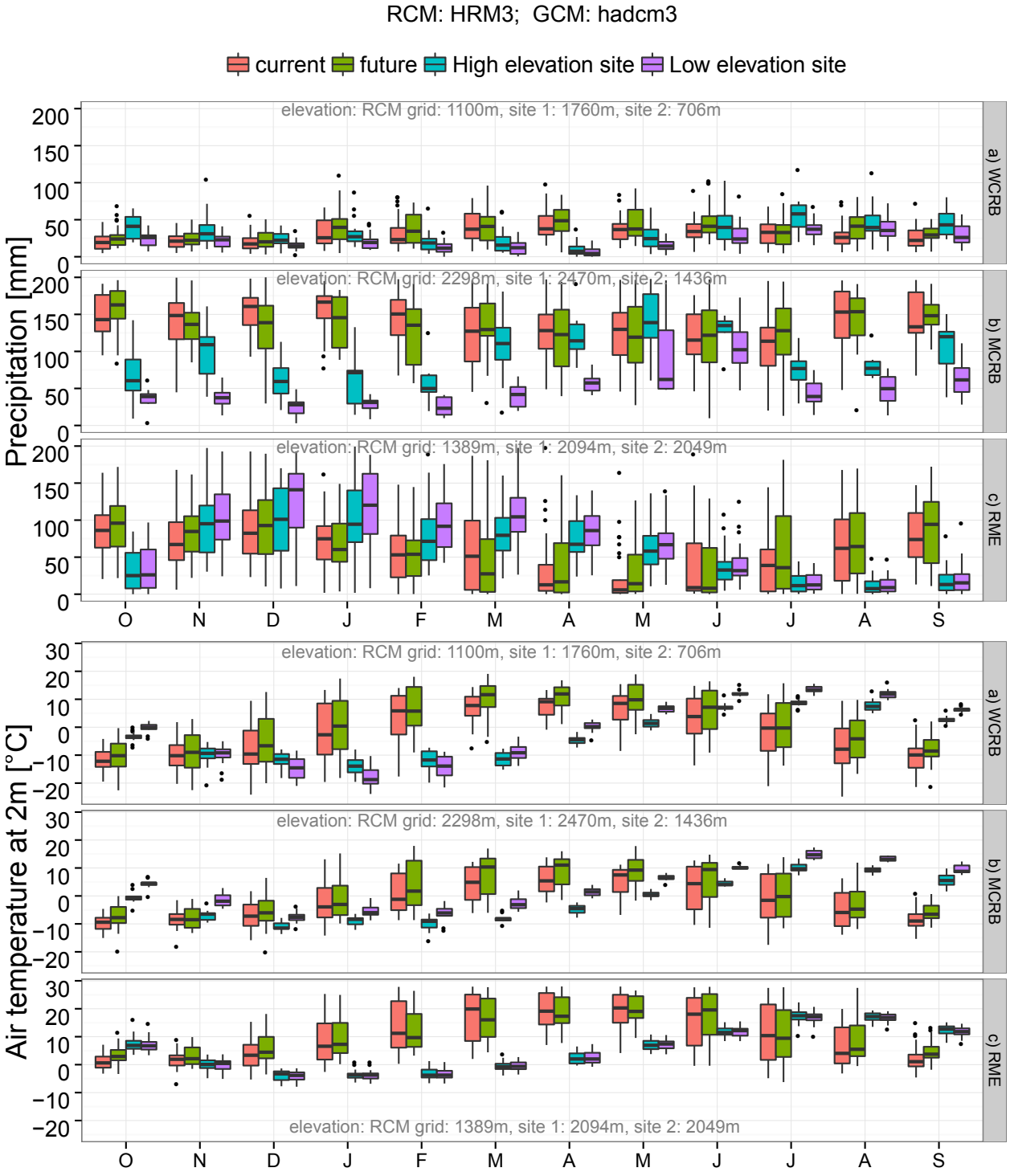

Figure 3.5: Comparison of precipitation and air temperature observed in two high elevation and low elevation stations in each basin and simulated by HRM3 regional climate model driven by HadCM3 GCM. The elevation difference between sites in RME is not large, so two sites represent HRUs that have different wind sheltering but small elevation differences. Black dots denote outliers (outliers were not statistically tested).

Table 3.4: Biases in the probability of dry day between 11 RCM outputs and measurements in the three basins. The positive biases denote more frequent dry days with no precipitation (< 0.5 mm) than the actually recorded dry days.

RCM–GCM	WCRB	MCRB	RME
WRFG–CCSM	0.11	–0.19	–0.02
WRFG–CGCM3	0.17	–0.12	–0.01
CRCM–CCSM	0.29	–0.12	0.28
CRCM–CGCM3	0.32	–0.08	0.27
RCM3–GFDL	0.34	0.13	0.23
RCM3–CGCM3	0.44	0.08	0.18
MM5I–CCSM	0.39	0.08	0.5
MM5I–HADCM3	0.37	0.1	0.51
HRM3–HADCM3	0.08	0.26	0.08
HRM3–GFDL	0.07	0.29	0.16
ECP2–GFDL	0.15	–0.05	0.09

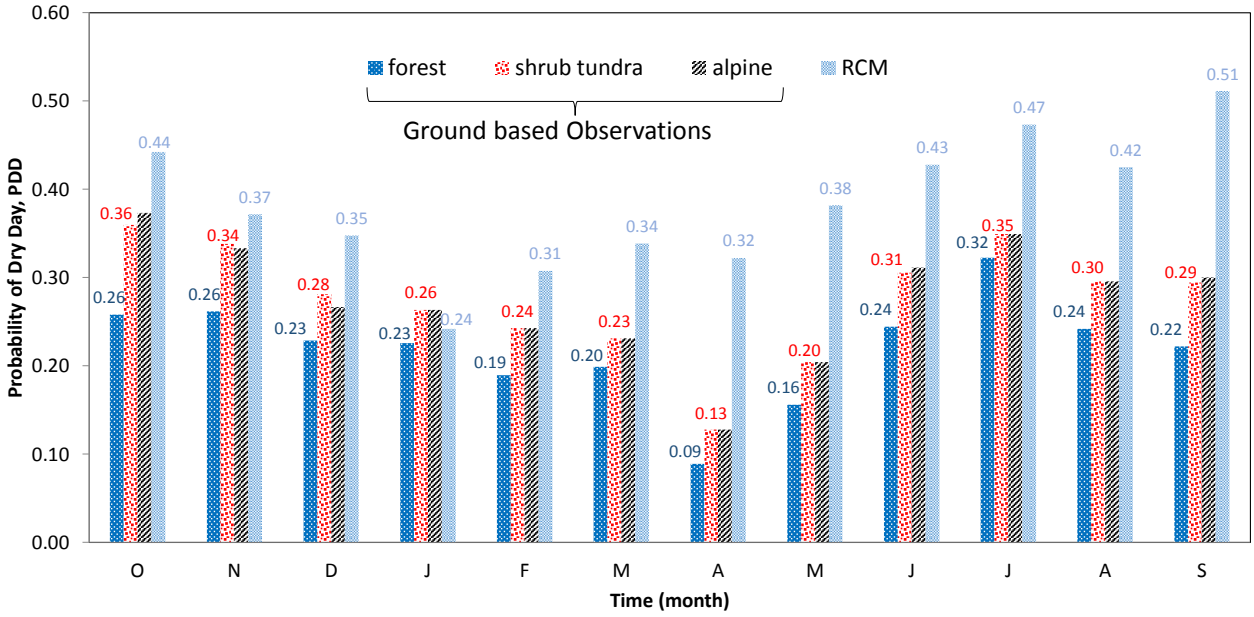

Figure 3.6: Probability of dry day (PDD) recorded in different elevation bands and estimated by the WRFG–CCSM regional climate model in Wolf Creek Research Basin for 1993–1999.

Advantages and Limitations of the CPS Approach

Monthly perturbed climate avoids the computational cost of the dynamical downscaling and maintains consistency in relationships of the atmospheric fields, which may be distorted in statistical methods if interaction of the variables are not considered. Sub-monthly and daily values obtained from RCMs are highly uncertain and contain a large amount of noise. The number of dry days simulated by RCMs for the control period is also higher than those actually observed in the basins. Unlike using the RCM outputs directly, the change factor based CPS approach produces spatial and seasonal precipitation based on observations and changes based on simulated differences. This represents weather with reasonable accuracy and also represents observed extreme dry periods and observed extreme storms. Limitations of applying change factors of the monthly climatological values to perturbed climate are that any future changes in weather patterns, extremes, sequences of wet or dry spans, and droughts or floods are not adequately represented. This is similar to assumption of the stationary relationships between large-scale circulations and locally observed data in statistical downscaling. Changes in synoptic dynamics of the atmosphere cannot be captured by the CPS method, nor can RCM capture local-scale processes in mountainous regions.

3.2.3 Simulation of Transient Vegetation and Soil Changes

Under warmer and drier conditions, vegetation is expected to change in temperate mountain climates such as French Alps, which will result in evapotranspiration increases (Beniston, 2003). In sub-Arctic mountains, warming can result in permafrost degradation and expansion of shrub tundra (Tape et al., 2006; Hallinger et al., 2010). The changing shrub extent traps windblown snow, increases snowmelt volumes, lowers spring albedo, and alters melt rates (Pomeroy et al., 2006). The changes in ice/snowcover, streamflow, soil moisture, vegetation, soils, and other defining properties of an ecosystem lead to important feedbacks in the ecology, surface energy balance, and hydrological cycle at local to global scales (Osterkamp et al., 2009; Rawlins et al., 2009). Climate change effects on hydrological mechanisms were examined in Chapter 6 assuming no changes in future vegetation will occur. In Chapter 7, the effect of vegetation changes on snow regimes and hydrological variables were evaluated

under conditions in which: (1) no changes in future climate but transient vegetation/soil changes will occur and (2) changes in future climate will be accompanied by transient vegetation/soil changes. Potential changes in soil properties including porosity and depth as a result of transient vegetation change were also examined. Two scenarios are applied to identify whether changes in vegetation, or combination of soil and vegetation is important in affecting hydrological processes. These scenarios are: (1) only vegetation changes and soils remain unchanged; and (2) both vegetation and soils change. In reality, soil properties vary during vegetation change phases from the initial colonisation of the bare surface to the establishment of a forest (Crocker and Major, 1955) and soil development may not be as quick as vegetation change. Potential changes in soil, especially changes in organic matter content under transient vegetation changes can be important and might affect infiltration, groundwater recharge, and runoff (DeBano, 1991). Therefore, transient soil changes also need to be considered in hydrological modelling along with the transient climate and vegetation changes.

3.2.4 Statistical Significance Test of Hydrological Changes

In this research, distributions of the simulated hydrological variables (e.g., annual peak SWE/runoff, timing of peak SWE/runoff, annual total runoff, annual rainfall/snowfall, annual sublimation, annual evapotranspiration) were obtained over 18 years for WCRB, 9 years for MCRB, and 25 years for RME and under monthly perturbed climate for 11 RCM–GCM combinations. The observed time series have many gaps that restrict the direct comparison of the observations and differences due to perturbations of the climate or vegetation changes. For instance, SWE data were collected once a month, which may not capture peak SWEs each year. The Mann–Whitney U-test (Wilcoxon, 1945; Mann and Whitney, 1947, *ranksum* function in Matlab) was used to test the significance of the changes in distribution of the variables under climate change and combined climate and vegetation change scenarios. The Mann–Whitney U-test is a nonparametric test for equality of distributions of two independent samples. Simulated distributions with n years in the control period for each hydrological variable ($x^c_{1:11\times \mathrm{n}}$, $11\times n$ values) are compared with the simulated future distributions obtained

for 11 RCM-GCMs ($x^f_{1:11\times n}$, $11 \times n$ values). The null hypothesis is that the distribution of $x^c_{1:11\times n}$ is equal to the distribution of $x^f_{1:11\times n}$. The alternative hypothesis is that the distribution under climate and vegetation change is not the same as in the control period. The statistic U in the Mann–Whitney U-test is the number of times an $x^f_{1:11\times n}$ precedes $x^c_{1:11\times n}$ in an ordered arrangement of the elements in the two independent samples ($P(x > y) > P(y > x)$) for current and future climates.

For assessing the significance of the hourly SWE distribution changes due to climate and vegetation changes, the two-sample Kolmogorov-Smirnov (K–S) test (Massey Jr., 1951, *kstest2* function in Matlab) was used. The K–S test is a nonparametric hypothesis test that evaluates the difference between the distributions of the hourly SWE in the control period and under climate or vegetation change over the range of x in each time series. The null hypothesis in the K–S test is that the time series in control (x_1) and future (x_2) periods are from the same continuous distribution. The alternative hypothesis is that x_1 and x_2 are from different continuous distributions. The two-sided test uses the maximum absolute difference between the cumulative density functions (cdfs) of the two time series. The test statistic D^* is:

$$D^* = max_x(\left|\hat{F}_1(x) - \hat{F}_2(x)\right|) \tag{3.1}$$

where $\hat{F}_1(x)$ is the proportion of x_1 values less than or equal to x. The decision to reject the null hypothesis is based on comparing the p-value with the significance level of 0.05, not by comparing the test statistic with a critical value.

3.3 Discussion

Methods for analysing hydrological sensitivity to changes in air temperature, precipitation, vegetation, and soils in Wolf Creek Research Basin (WCRB), Marmot Creek Research Basin (MCRB), and Reynolds Mountain East (RME) along the North American Cordillera (NAC) were introduced. These three mountain basins were chosen as they have high quality and high elevated meteorological stations with sufficient length of records, parameter measurements, and varying vegetation cover. RME and low elevations in MCRB have air temperatures above

−5°C in winter and few freeze days, which makes these areas more sensitive to warming. A large portion of snow fraction of total precipitation in RME and at low elevations in MCRB is expected to convert to rainfall, which can shorten the snowcover season and advance the spring freshet. These changes were also suggested by Knowles et al. (2006) and Stewart et al. (2004) in basins with similar elevation range and winter temperatures. The availability of long term data from high and low elevation stations in each basin representing multiple biomes makes them suitable case studies for comparing and contrasting the hydrological processes under climate and vegetation changes.

Regional climate model outputs cannot be used directly as they are unable to capture the local processes with sufficient accuracy. The simulated precipitation by these models is more intense and clustered in winter and spring than the actual measurements at three basins. A systematic overestimation of the frequency of westerly flow in winter is responsible for overestimation of winter precipitation (Addor et al., 2016). MacDonald et al. (2016) also found an overestimation of the snowcover season duration and large differences in simulated snow depth, soil moisture, and evapotranspiration and an underestimation of the precipitation at high elevations in MCRB. The simulated dry days were also more frequent than real measurements in the three stations. Biases in the synoptic circulations can propagate to regional-scale precipitation and temperature (Addor et al., 2016). These evidences show the difficulties of atmospheric models in capturing hydrometeorological processes in cold regions and mountainous regions. Uncertain RCM outputs and an overestimation of main meteorological variables over mountains make direct application or bias correction of the RCM outputs in hydrological modelling challenging.

The climate perturbation sensitivity approach, proposed for hydrological sensitivity analysis in this chapter, is based on change factors rather than a direct application of the RCM outputs. The change factors were applied to baseline observations on an annual or a monthly basis. Similar to the delta change method (Semadeni-Davies et al., 2008), the climate perturbation sensitivity method assumes the same number of precipitation events in current and future climates and relative rather than absolute changes in climate. Despite these

limitations, the climate perturbation sensitivity approach was used in hydrological sensitivity analysis in Chapter 5, Chapter 6, and Chapter 7 as uncertainty due to application of the change factors has not been shown to be higher than other statistical downscaling methods (Fowler et al., 2007; Kay et al., 2009; Sunyer et al., 2012).

The methods proposed in this chapter and their application to three mountain basins with varying mean annual temperature and precipitation, elevation range, and vegetation are initial steps to assess sensitivity of the mountain basins along the NAC to potential changes in climate, vegetation, and soils. More rigorous research needs to be done to understand regional impacts of climate and vegetation changes on hydrology of the NAC. The modelling strategy in this study can be applied to similar basins along the NAC to obtain a broad picture of the regional impacts of the changes on headwater basins until models are able to adequately project future climate in the mountains.

3.4 Summary

In this chapter, similarities and contrasts among three basins along the North American Cordillera were discussed. Hydrological models used for hydrological sensitivity analysis in the mountain basins were presented. The performance of the hydrological models developed in this chapter in simulating snow, soil moisture, soil temperature, and streamflow in each basin is assessed in Chapter 4. Two approaches for climate perturbation sensitivity analysis on an annual or a monthly basis were proposed: Chapter 5 describes how annually perturbed climate was used with current climate to study sensitivity of snow and streamflow regimes to annual shifts in air temperature (0°C to 5°C) and precipitation (–20% to +20%); Chapter 6 and Chapter 7 describe how monthly perturbed climate and transient vegetation and soil changes were used to study the hydrological sensitivity to climate and vegetation changes incorporating monthly variability in climate changes. Statistical methods and criteria for assessing significance of the hydrological changes under climate, vegetation, and soil changes are given, which are used in Chapter 5, Chapter 6, and Chapter 7.

Chapter 4

SIMULATION PERFORMANCE OF THE HYDROLOGICAL MODELS

In this chapter, hydrological field measurements and calibration of uncertain parameters are described and the performance of the Cold Regions Hydrological Modelling (CRHM) platform in simulating snow regime, soil moisture/temperature, and streamflow regime are evaluated with statistical and visual performance measures. The snowpack was simulated for alpine, shrub tundra, and forest biomes in Wolf Creek Research Basin (WCRB); alpine, subalpine, and forest clearcut biomes in Marmot Creek Research Basin (MCRB); and a sheltered forest clearing in Reynolds Mountain East (RME) catchment. The simulated soil surface temperatures and soil moisture were compared against available observations. The accuracy performance of the models in simulating streamflow at the outlets of WCRB, MCRB, and RME was also assessed. Section 4.1 and panels of Figures 4.1 and 4.7 for WCRB (Rasouli et al., 2014) and RME (Rasouli et al., 2015b) have been published in two papers led by Kabir Rasouli under supervision of John Pomeroy. Full citations are provided below.

[1] Rasouli, K., J. W. Pomeroy, J. R. Janowicz, S. K. Carey, and T. J. Williams, 2014. Hydrological sensitivity of a northern mountain basin to climate change. *Hydrological Processes*, 28(14):4191–4208.

[2] Rasouli, K., J. W. Pomeroy, and D. G. Marks, 2015b. Snowpack sensitivity to perturbed climate in a cool mid-latitude mountain catchment. *Hydrological Processes*, 29(18):3925–3940.

4.1 Hydrological Field Measurements

In Chapter 3, the hydrological processes and modules applied in the three models for each basin are presented. In this section, field measurements and model parameters are introduced. Model parameters were estimated and/or measured in previous cold regions modelling studies in Smoky River (Pomeroy et al., 2011, 2013), Wolf Creek Research Basin (Pomeroy et al., 1999; Pomeroy and Granger, 1999), and Marmot Creek Research Basin in Canada (MacDonald et al., 2009), and Reynolds Creek Experimental Watershed in Idaho, USA (Marks et al., 1999).

Field measurements in WCRB have been collected over the last two decades. Blowing snow fetch distances in the alpine and shrub tundra hydrological response units (HRUs) are taken from the study of MacDonald et al. (2009). Values of the blowing snow redistribution factor are chosen to be 2 and 5 for the alpine and shrub tundra HRUs, respectively (MacDonald et al., 2009) and blowing snow is inhibited for the forest HRUs. Vegetation heights determined by field surveys are used for the model simulations. Initial soil saturation prior to the snowmelt infiltration is estimated from both volumetric soil moisture content observations during pre-melt period and soil porosity measurements. The yearly antecedent soil moisture is measured by water content reflectometer measurements at each station. Soil types in WCRB (organic and mineral soils) and their porosity values were measured by Carey and Woo (2005) and Quinton et al. (2005). Initial soil temperature is measured by soil thermocouples prior to the major snowmelt. The environment coefficient and surface saturation for frozen soil infiltration are set up based on the recommended values from Gray et al. (2001). Infiltration opportunity time is calculated by model simulation of snowmelt duration. Studies on soil properties in WCRB (Carey and Woo, 2001; Carey and Quinton, 2004; Carey and Woo, 2005; Quinton et al., 2005) found that the active soil layer was composed of an upper organic soil layer over a mineral soil layer. Measured depth and porosity values for both the organic and mineral soil layers are used to approximate the capacity of the soil column layer. The soil recharge zone, a top layer of the soil column, is assumed to be shallow and initially saturated.

Field measurements in MCRB have been collected since 1962 and over the last decade after a break in the research in this basin from 1988 to 2003. Field measurements that were used in a previously developed model (Fang and Pomeroy, 2016) are applied in this research. Due to the short upwind distance, a uniform blowing snow fetch distance is used for all HRUs. Values of the blowing snow redistribution factor are chosen to be 1 for non-forest HRUs and 0 for forest HRUs (Fang and Pomeroy, 2016). Vegetation height measurements for the regenerated forest at clearing blocks, the circular forest clearing HRUs, and the other forest-cover HRUs were measured by MacDonald (2010). Leaf area index (LAI) values used are from Bewley et al. (2010) and Ellis et al. (2011). The canopy snow interception capacity for lodgepole pine forest HRU is adapted from Schmidt and Gluns (1991) and for the forest clearing HRUs, spruce forest, and mixed spruce and lodgepole pine forest HRUs were estimated by Ellis et al. (2011). The soil properties are adapted from Beke (1969). A value of 1 was estimated for the soil surface saturation due to preferential flow of early meltwater through the snowpack (Marsh and Pomeroy, 1996). Similar to WCRB, infiltration opportunity time was estimated within the model run. Relatively impermeable bedrock at high elevations and a deep layer of coarse and permeable soil in the rest of basin were reported by Jeffrey (1965). For the detailed set of parameters used in the MCRB model, please refer to Fang et al. (2013).

Parameter estimation in RME basin is based on previous studies in Reynolds Mountain East (RME) catchment and other headwater basins in Reynolds Creek Experimental Watershed (RCEW) and similar snow-dominated basins. Parameters adapted from measurements in the research basins included those that represented the characteristics of vegetation across the catchment and the parameters of snowmelt and blowing snow modules. Similar to MCRB, a uniform blowing snow fetch distance is used for all HRUs due to the short upwind distance. Blowing snow is inhibited for the sheltered HRUs. Snow surface roughness length was estimated by Reba et al. (2012). Vegetation heights/density and leaf area index were estimated by Link et al. (2004), Seyfried et al. (2009), and Flerchinger et al. (2012). The soil characteristics and soil water storage capacity are adapted from Seyfried et al. (2009). The soil surface saturation is adapted from Link et al. (2004). Initial soil temperature is measured by soil thermocouples prior to the major snowmelt. Thermal conductivity is set to 1.65 J

m^{-1} s^{-1} K^{-1}, a value for wet sand taken from Oke (1978). A list of parameters obtained from different studies in each of the three headwater basins applied for the hydrological modelling in this study is provided in Table 4.1.

4.1.1 Calibration of Uncertain Runoff Parameters

Minimum calibration is applied for timing and routing of streamflows and no calibration is applied for snow and soil moisture simulations. Representing the complex processes controlling streamflow generation in the models is challenging due to:

- the varying magnitude and timing of the hydrological processes over short distances (Carey and Woo, 2001);
- aufeis formation (Clark and Lauriol, 1997);
- river ice formation and breakup (Beltaos, 1990, 1995);
- snow dammed channels (Woo and Heron, 1987);
- discontinuous permafrost slopes (Carey and Woo, 2001; McCartney et al., 2006; Boucher and Carey, 2010); and
- ice layer formation from midwinter meltwater (Scherler et al., 2010).

Limited knowledge is available about the above-mentioned complex mechanisms that affect runoff routing. Lag and routing times in channels between subbasins have not been measured by any study in WCRB and RME. The ice-break in melt season in WCRB and the flashy nature of RME with its small drainage area and frequent rain-on-snow events make simulations of streamflow in these basins challenging. Understanding and quantifying the source, magnitude, and timing of contributions from each HRU to the main channel flow is difficult because it requires a very detailed study of surface and groundwater pathways, velocities, and soil characteristics (Quinton et al., 2005). The capacity of surface depressional storage is also unknown, so it is calibrated along with lag and routing parameters. Subsurface drainage factors may have been affected by subsurface flow perched over thawing frozen soil, which is

Table 4.1: Vegetation characteristics of the biomes and parameters used in the CRHM for hydrological modelling of the three research basins. HRUs are categorised as alpine, shrub tundra, and forest in Wolf Creek Research Basin (WCRB); alpine, treeline, forest, and forest clearing in Marmot Creek Research Basin (MCRB); and blowing snow regimes of wind-sheltered, source, sink, and forest (with intercepted snow) in Reynolds Mountain East (RME). Parameters for the WCRB model are obtained from Carey and Woo (2001); Carey and Quinton (2004); Carey and Woo (2005); Gray et al. (2001); MacDonald et al. (2009); Pomeroy et al. (2011, 2013); and Quinton et al. (2005). Parameters for the MCRB model are obtained from Bewley et al. (2010); Ellis et al. (2011); Fang et al. (2013); Fang and Pomeroy (2016); MacDonald (2010) and Schmidt and Gluns (1991). Parameters for the RME model are obtained from Oke (1978); Link et al. (2004); Flerchinger et al. (2012); Reba et al. (2012, 2014); and Winstral et al. (2013).

Basin	**WCRB**			**MCRB**				**RME**			
Biome	**alpine**	**shrub tundra**	**forest**	**alpine**	**treeline**	**forest**	**forest clearing**	**sheltered**	**source**	**forest**	**sink**
number of HRU	7	18	4	6	6	21	3	2	5	1	4
height [m]	0.1	1.5	15	0.14	3	15	8	8	0.75	12	12
veg. density [$1/m^2$]	1	1	2	1	1.5	1.5	1.5	0.2	2	0.2	2
stalk diameter [m]	0.1	0.8	1.5	0.003	0.6	0.8	0.6	0.45	0.01	0.45	0.45
max LAI [m^2m^{-2}]	–	–	–	0.5	2.5	2.07	2.5	5.4	1.2	5.9	3.6
mean LAI [m^2m^{-2}]	0.1	0.2	1	0.1	1.1	2.07	1.1	1.35	1.1	3	1.35
min LAI [m^2m^{-2}]	–	–	–	0.1	1.1	2.07	1.1	0.4	0.77	1.35	0.3
soil depth [m]	4	4	4	1.1	1.1	0.9	0.9	2.25	1.35	2.25	1.35
soil layers [-]	20	20	20	2	2	2	2	2	2	2	2
terrain emissivity [-]	0.98	0.98	0.98	0.98	0.98	0.98	0.98	0.98	0.98	0.98	0.98
snow roughness [m]	0.01	0.01	0.01	0.01	0.01	0.01	0.01	0.006	10^{-4}	0.006	0.006
fetch distance [m]	500	500	300	300	300	300	300	300	300	300	300
snow intercepted on canopy [kg m^{-2}]	0	0	2	0	6.6	8.8	6.6	0.5	1	6.6	0.5
snow active layer thickness [m]	0.15	0.15	0.15	0.15	0.15	0.15	0.15	0.15	0.15	0.15	0.15

Table 4.2: List and range of the Clark lag and route and drainage timing parameters calibrated using the dynamically dimensioned search (DDS) algorithm in watershed channel and HRUs

Parameter name	**unit**	**lower bound**	**upper bound**
Basin-scale groundwater lag time	hr	0	100
Basin-scale runoff lag time	hr	0	100
Groundwater storage constant	day	0	50
Groundwater lag time	hr	0	100
Drainage rate from groundwater	mm/day	0	0.5
Aggregated storage constant	day	0	50
Aggregated lag time	hr	0	100
Surface runoff storage constant	day	0	50
Surface runoff lag time	hr	0	100
Drainage rate from depressional storage to groundwater	mm/day	0	0.5

not yet fully parameterised in the CRHM and so is calibrated. Table 4.2 shows the routing and drainage parameters calibrated using the dynamically dimensioned search (DDS) algorithm (Tolson and Shoemaker, 2007) from measured streamflows at the outlets of WCRB and RME. This algorithm generally performs better for automatic calibration than uniform Monte Carlo random sampling. The DDS approach is used to calibrate the uncertain parameters based upon 1000 model runs over three years (1998–2001) in WCRB and four years (1993–1997) in RME for which measurement confidence is relatively high.

The DDS approach is a heuristic search method developed to obtain an acceptable optimal solution within a given number of model evaluation runs. First, the DDS algorithm searches the parameter set globally and then it looks for local solutions as the number of model evaluations approaches the specified try number. The transition from a global to a local search is carried out dynamically by reducing the size of the neighbourhood or dimensions of the model parameters. The calibrated parameters are the lag and route timing and storage constant, the sub-surface drainage rates and the depressional storage of the HRUs. The range

of the parameters is selected so that they are reasonable for the study area; the DDS search algorithm then optimises the parameters within this range. Quinton et al. (2005) attempted to obtain more physically accurate parameters of subsurface drainage, but the study was not sufficiently detailed to set parameters *a priori*. Therefore, calibration of the subsurface drainage was done as in Dornes et al. (2008).

4.2 Model Performance Measures

Verification/evaluation of the simulations by hydrological models is carried out using statistical (Willmott and Matsuura, 2005) and visual (Crout et al., 2008) performance measures. The statistical performance measures include the Nash-Sutcliffe model efficiency coefficient (NSE; McCuen et al., 2006), the Pearson correlation coefficient (Corr, Lawrence and Lin, 1989), mean absolute error (MAE, Willmott and Matsuura, 2005), and root mean squared error (RMSE, Willmott and Matsuura, 2005) for all simulations. A skill score measures the accuracy of the model simulations y relative to a reference model. The reference model usually applies a naive simulating method, such as climatology. A climatological simulation y_c simply represents the climatological mean of the observed data y_o. The NSE uses y_c as reference, i.e.

$$\mathrm{NSE} = 1 - \frac{\sum (y - y_o)^2}{\sum (y_c - y_o)^2} \tag{4.1}$$

Note NSE = 1 for a perfect model, and NSE < 0 when the model simulations are worse than those from the reference model.

While Pearson correlation coefficient is a good measurement of linear association between simulations and observations, it does not take simulation biases into account, and is sensitive to extreme events. It measures how strong is the linear relationships between the model simulations and observations.

$$\mathrm{Corr} = \frac{n \sum y.y_o - (\sum y)(\sum y_o)}{\sqrt{[n \sum y^2 - (\sum y)^2][n \sum y_o^2 - (\sum y_o)^2]}} \tag{4.2}$$

where n is the number of simulation–observation pairs. When $Corr = 1$, a perfect linear

relationship; $Corr = 0$, no linear relationship; and $Corr = -1$ when there is an inverse perfect linear relationship between simulations and observations.

MAE, which measure the average magnitude of the simulation errors, is a cleaner, hence preferable, measure of the average error (Willmott and Matsuura, 2005) than RMSE. RMSE and MAE are defined as:

$$\text{RMSE} = \sqrt{\frac{1}{n}\sum(y - y_o)^2} \tag{4.3}$$

$$\text{MAE} = \frac{1}{n}\sum|y - y_o| \tag{4.4}$$

When $RMSE = 0$ or $MAE = 0$, the model perfectly simulates the observations. While statistical performance measures are widely used to evaluate model performance, visual performance measures can provide valuable insight into model drawbacks, which may not be captured by statistical performance measures (Crout et al., 2008). The following visual measures (adapted from Crout et al., 2008) are used to assess the CRHM model performance in simulating snow, soil temperature and moisture, and discharge in this study:

1. duration curves of observed and simulated values (e.g., streamflow duration curve), which represent exceedance probability of occurrence for a full range of flow magnitudes. These can be used to compare the distribution of observations and simulations and to assess the over- or under-estimation of the extreme events;

2. a simple scatter plot of observed and simulated values on a linear scale, which shows the model agreement in magnitude;

3. a simple scatter plot of observed and simulated values on a logarithmic scale,which can illustrate the hydrograph shape; and

4. autocorrelation of residuals, which can display the errors in timing of peaks and systematic over- or under-estimation.

With the approaches applied in this research, a transparent assessment of the models and their outputs relative to observations is carried out and strengths and weakness of the simulations are more rigorously described. With an ideal visualisation technique, one can see model

errors both in the timing and magnitude of the predictions.

4.3 Assessment of Snow Modelling Performance

With the parameter setup for the modules listed in Chapter 3, snow water equivalent (SWE) was modelled for each HRU and biome in the three basins. Figure 4.1 compares simulated SWE against observations in three biomes in WCRB from 1993 to 2011, in three biomes in MCRB from 2008 to 2014, and in the sheltered site in the RME from 1983 to 2008. Observations from snow surveys at these three stations are available to test the performance of the model with respect to snow simulation. Hourly SWE time series recorded from a pillow in the sheltered site in RME are used for evaluating the CRHM model developed for RME catchment. The energy balance snowmelt model (Appendix B) was developed by Marks and Dozier (1992) in the alpine region of the Sierra Nevada and tested in RME catchment (Marks et al., 1998). The model simulates snow regime well in RME, where snowpack is shallower than Sierra Nevada. The snow model performance in RME is better than other two basins. Statistical performance measures also show that RME model performed better than the models for WCRB and MCRB in simulating snowpack (Table 4.3). RME has the highest SWE (Figure 4.1) and average basin elevation. Snowpack in the forest and shrub tundra biomes in WCRB is simulated with a low RMSE and MAE. Despite an overestimation of peak SWE in 2009 in WCRB, 2010 in MCRB, and 1995 in RME and a slight underestimation of peak SWE in the alpine and shrub tundra biomes in 2010 in WCRB and 1984 in RME, the overall performance of the uncalibrated snow model with a moderate complexity developed for each basin is encouraging.

For assessment of the model performance in simulating snowpack, a visual measure in the three basins is also illustrated in Figure 4.2. This figure illustrates the performance of the developed hydrological model on the CRHM platform in simulating two decades of snow regime in alpine, shrub tundra, and forest biomes in WCRB, on top of Fisera Ridge, on the Fisera Ridge south-facing slope, and in the Upper Clearing station in MCRB, and

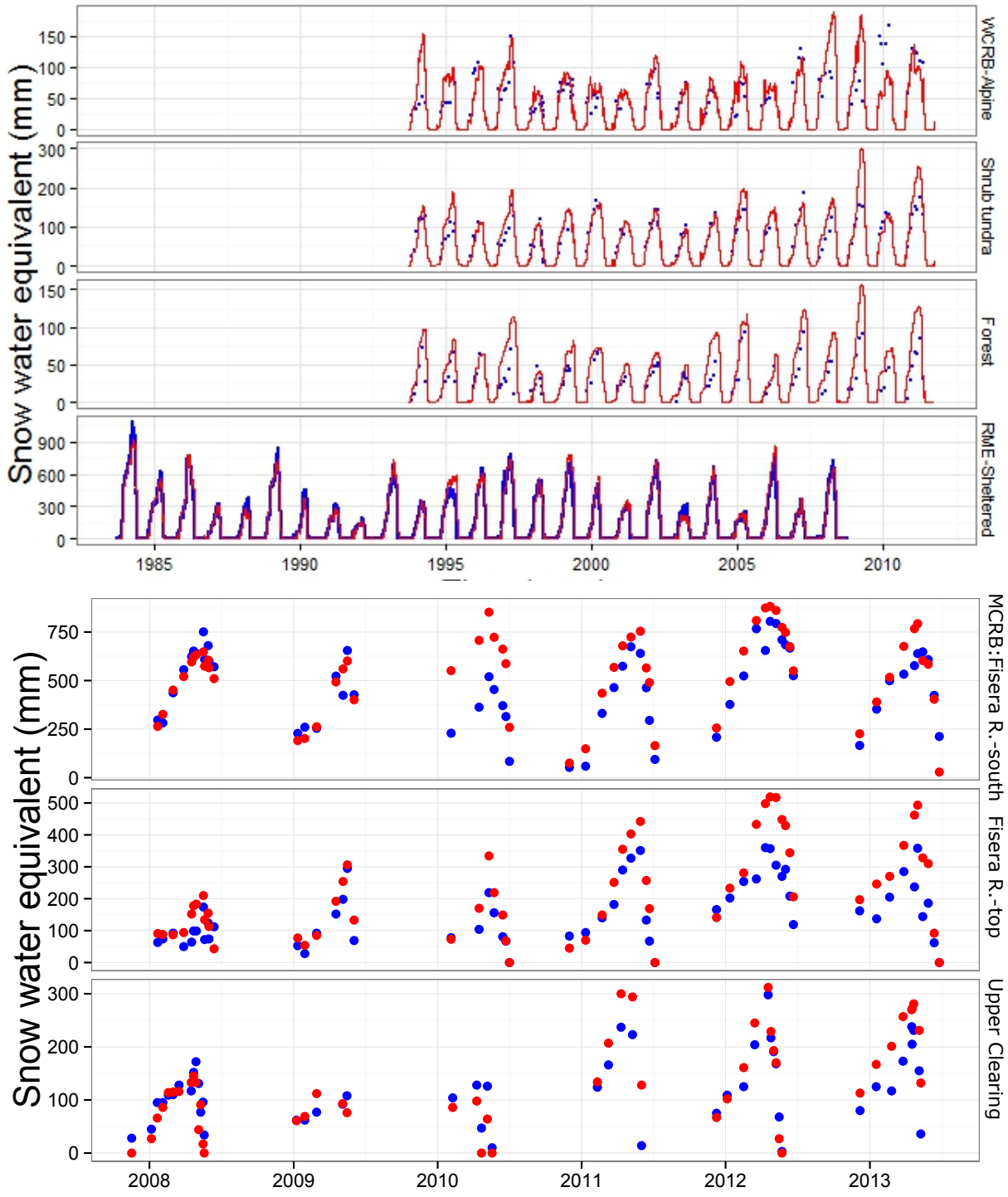

Figure 4.1: Performance of the Cold Regions Hydrological Model (CRHM) in capturing snow water equivalent (SWE). Snow measurements (blue) are compared against simulations (red) for three stations representing three biomes in Wolf Creek Research Basin (WCRB), a snow pillow in the wind sheltered site in Reynolds Mountain East (RME), and three stations in Marmot Creek Research Basin (MCRB). Snow measurements in MCRB are available from three stations including Fisera Ridge top, Fisera Ridge south facing slope, and Upper clearing, which represent different biomes (Fang and Pomeroy, 2016). No calibration is applied in snowpack simulation.

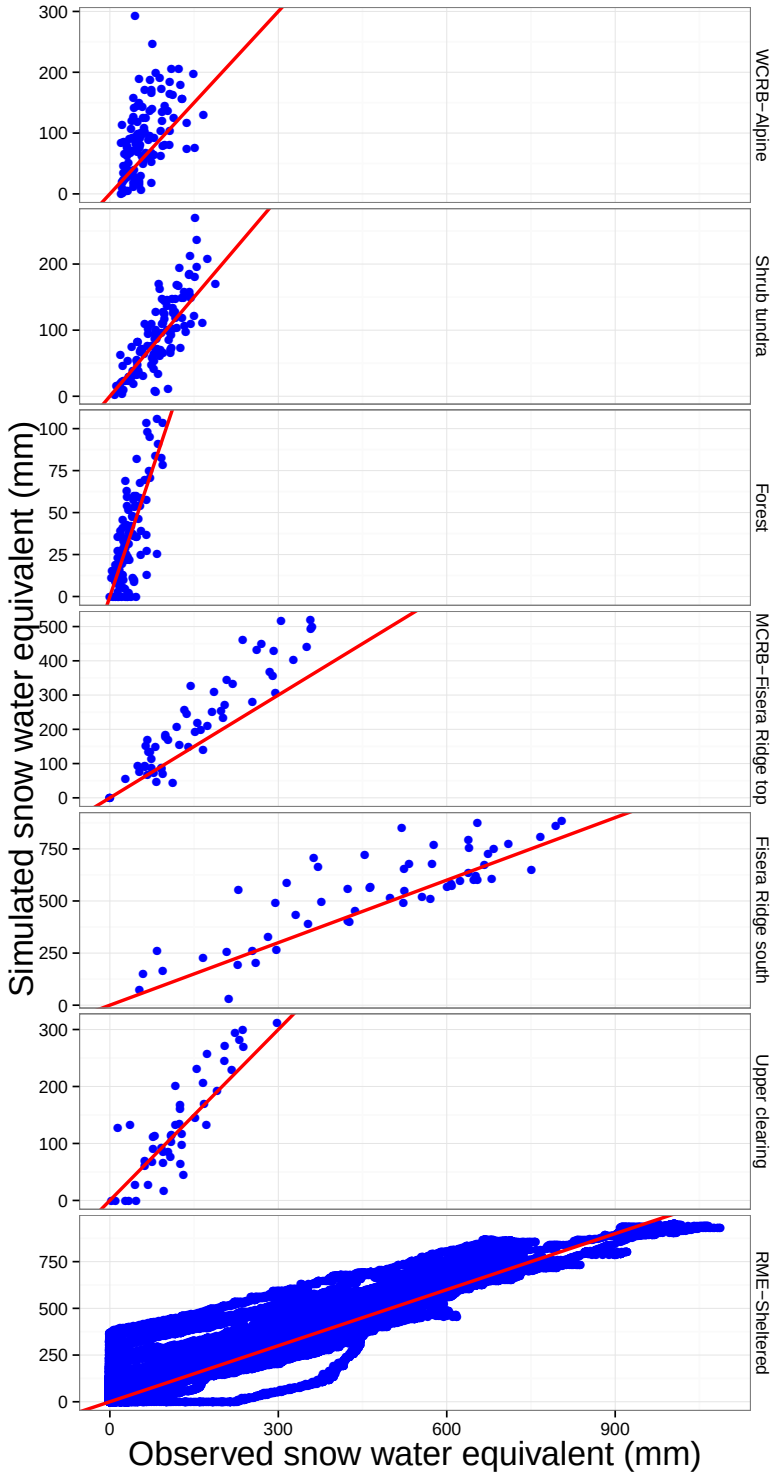

Figure 4.2: Visual assessment of model performance in simulating snow water equivalent (SWE) in three stations representing three biomes in Wolf Creek Research Basin (WCRB), three stations in Marmot Creek Research Basin (MCRB), and a snow pillow in the wind sheltered site in Reynolds Mountain East (RME). The red line has a 1:1 slope, which indicates that the models overestimate the SWE in almost all of the three basins.

Table 4.3: Accuracy of model performance in simulating snowpack based on statistical performance measures in the three basins across the North American Cordillera

Criteria	**WCRB**			**MCRB**			**RME**
	alpine	shrub tundra	forest	Fisera R. top	Fisera R. South	Upper Clearing	sheltered site
Corr [–]	0.74	0.81	0.73	0.93	0.85	0.88	0.98
RMSE [mm]	35	34	19	90	131	45	56
MAE [mm]	28	26	14	70	97	34	29

the sheltered site in RME. Fang and Pomeroy (2016) presented a rigorous assessment of the model performance in MCRB. Visual assessment for all three basins is in good agreement with statistical performance measures and shows that snow is simulated well in RME, in forest and shrub tundra biomes in WCRB, and in Fisera Ridge-south in MCRB. Apparently, there is a slight under-estimation of peak SWEs in RME. Models over-estimate the snowpack, especially in the alpine biomes. Uncertainty and high spatial variability of wind speed and wind direction might be the reason for slight over-estimation of snowpack in the alpine bimoes in WCRB and MCRB. Considering the complexity of the processes and high spatial variability of hydrometeorological variables in headwater basins, the performance of the models in capturing the snow regime in the three basins is encouraging and simulated snow regimes are in good agreement with the observations. The statistical performance scores with a moderate complexity model and no calibration are encouraging and a sensitivity analysis of snow regimes can be conducted based on these models.

4.4 Assessment of Soil Temperature and Moisture Modelling Performance

Soil temperature in frozen soils and soil moisture in non-frozen soils control infiltration, subsurface flow, and groundwater recharge. Two soil layers in MCRB and RME and 20 soil layers in WCRB are considered in the soil modules. Soil temperatures are simulated by

Table 4.4: Accuracy of model performance in simulating soil surface temperature and moisture over entire record period in the three basins across the North American Cordillera.

Criteria	**Soil temperature, t**		**Soil moisture, θ**	
	WCRB		**MCRB**	**RME**
Station	alpine	forest	Level Forest	sheltered site
Corr [t: –; θ: –]	0.84	0.81	0.36	0.87
RMSE [t: °C; θ: m^3m^{-3}]	4.6	5.5	0.06	0.054
MAE [t: °C; θ: m^3m^{-3}]	3.3	4.1	0.04	0.045

permafrost module only for WCRB. In the WCRB model, the ground surface temperatures are estimates from the air temperature, net radiation, and antecedent frost table depth (Williams et al., 2015). Figure 4.3 illustrates the measured and simulated soil temperature at ground surface in two alpine and forest stations in WCRB over the period from 1993 to 2011. There is a strong linear relationships between simulated and observed ground temperatures ($Corr > 0.80$, Table 4.4) and average error is less than 4.1°C, which mainly originates from over-estimation of low temperatures in both alpine and forest stations in WCRB.

Figure 4.4 shows the simulation performance of the permafrost module in modelling soil surface temperatures in WCRB. It shows that soil surface temperatures above the freezing point were well simulated, especially in the alpine biome, which has the most reliable data. The duration curve in Figure 4.4 shows that the simulated soil surface temperatures were overestimated for below-freezing temperatures in the alpine biome and for all ranges of soil surface temperature in the forest biome. Extreme temperatures also were slightly over-estimated by the model. The measurements of soil temperature were collected from a depth of 5cm, while simulations were done for the soil surface. This can be a potential reason for over-estimation of the soil temperatures by the model. The depth differences between observations and simulations make assessment of the model performance challenging.

Observed soil moisture measurements were not reliable in WCRB. Therefore, the results

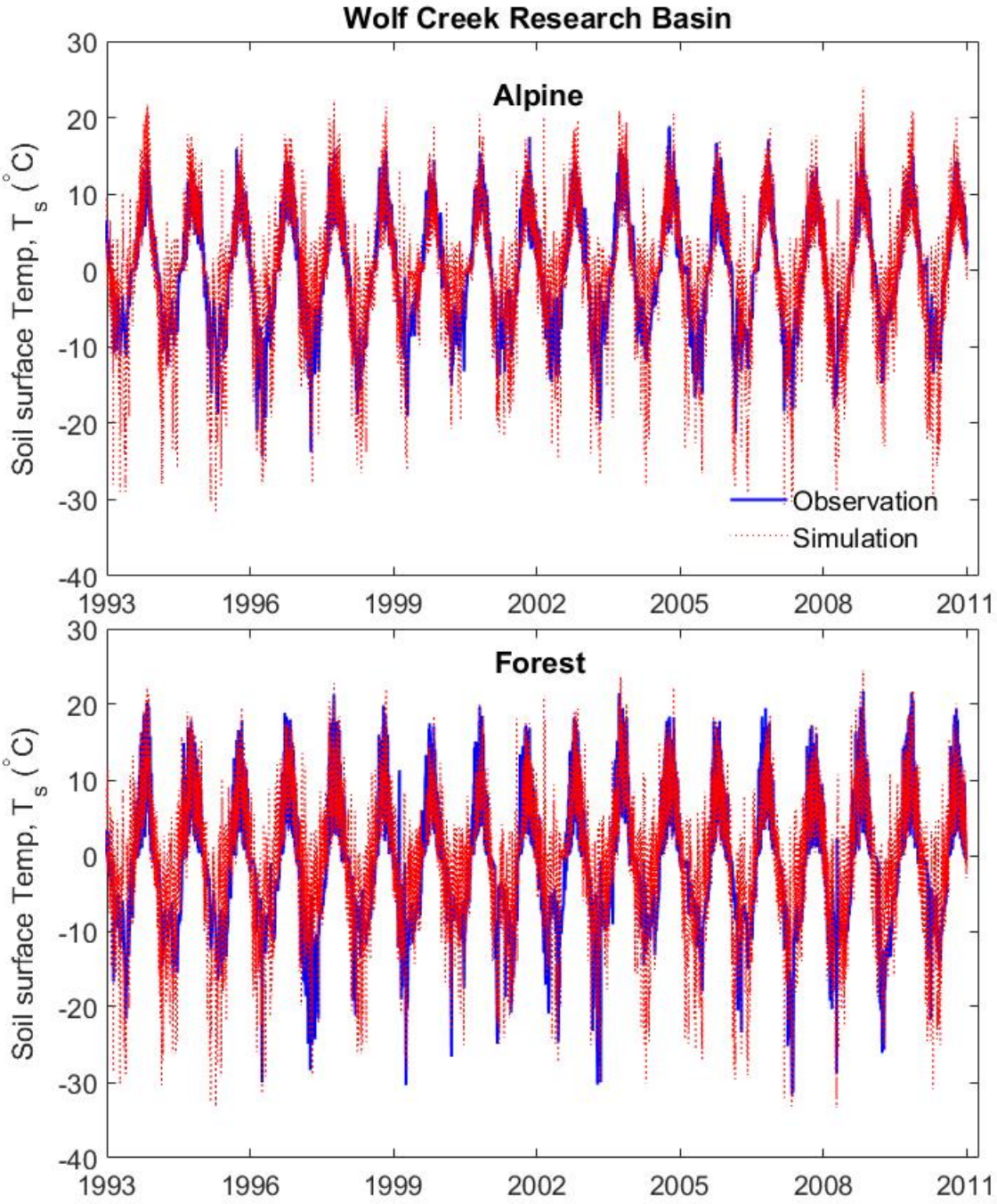

Figure 4.3: Comparison of observed and simulated soil temperature at ground surface in Wolf Creek Research Basin. Higher fluctuations in soil surface temperatures simulated by the model relative to observations are due to differences in measurement and simulation depths. Simulations are for the soil surface while observations are for soil depths of 5cm.

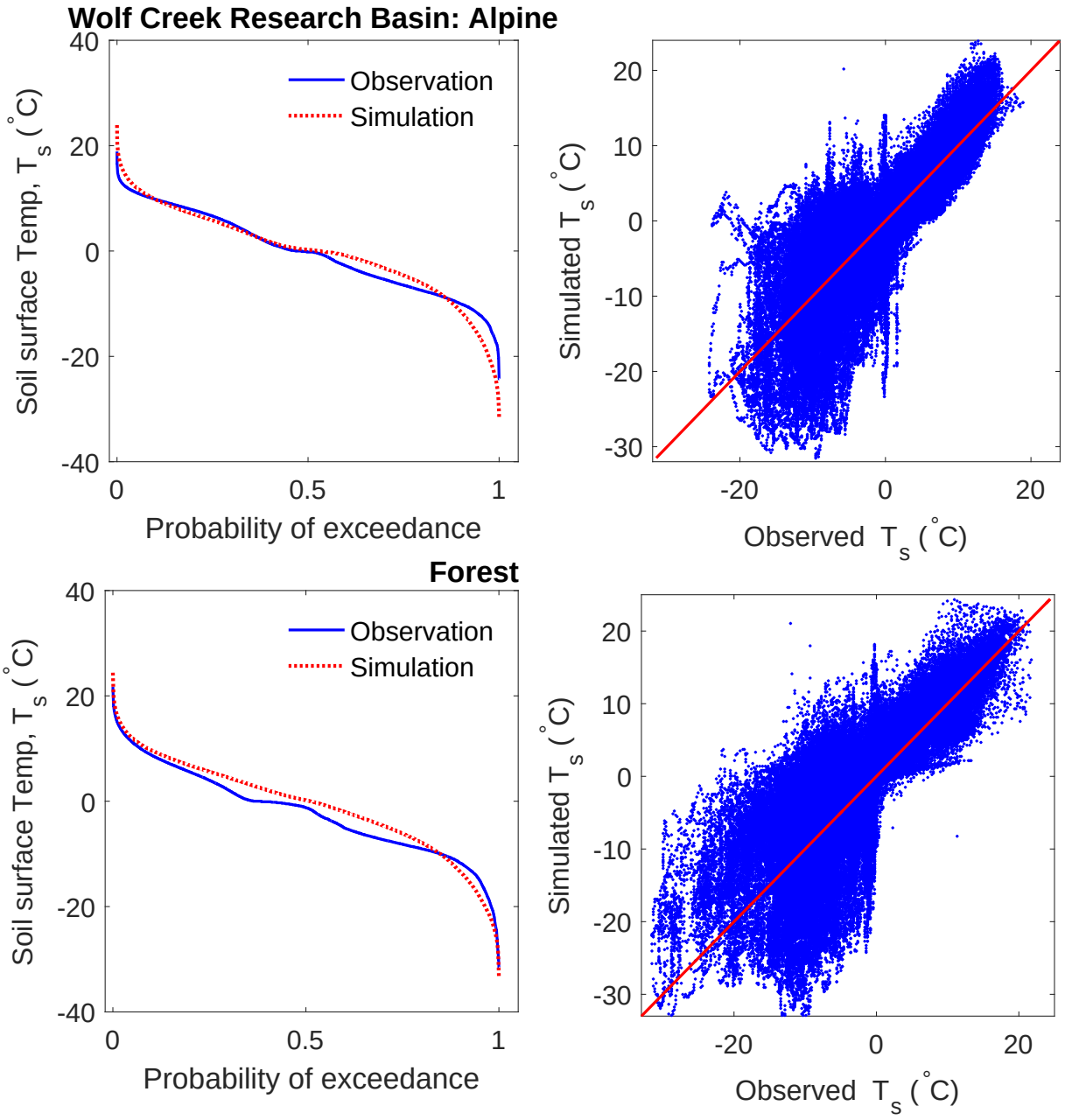

Figure 4.4: Model performance in simulating soil temperature at ground surface in Wolf Creek Research Basin. Simulations are for soil surface while observations are for 5cm of soil depth. The red line has a 1:1 slope, which indicates that the models overestimate the below-freezing soil temperatures in the alpine and forest biomes.

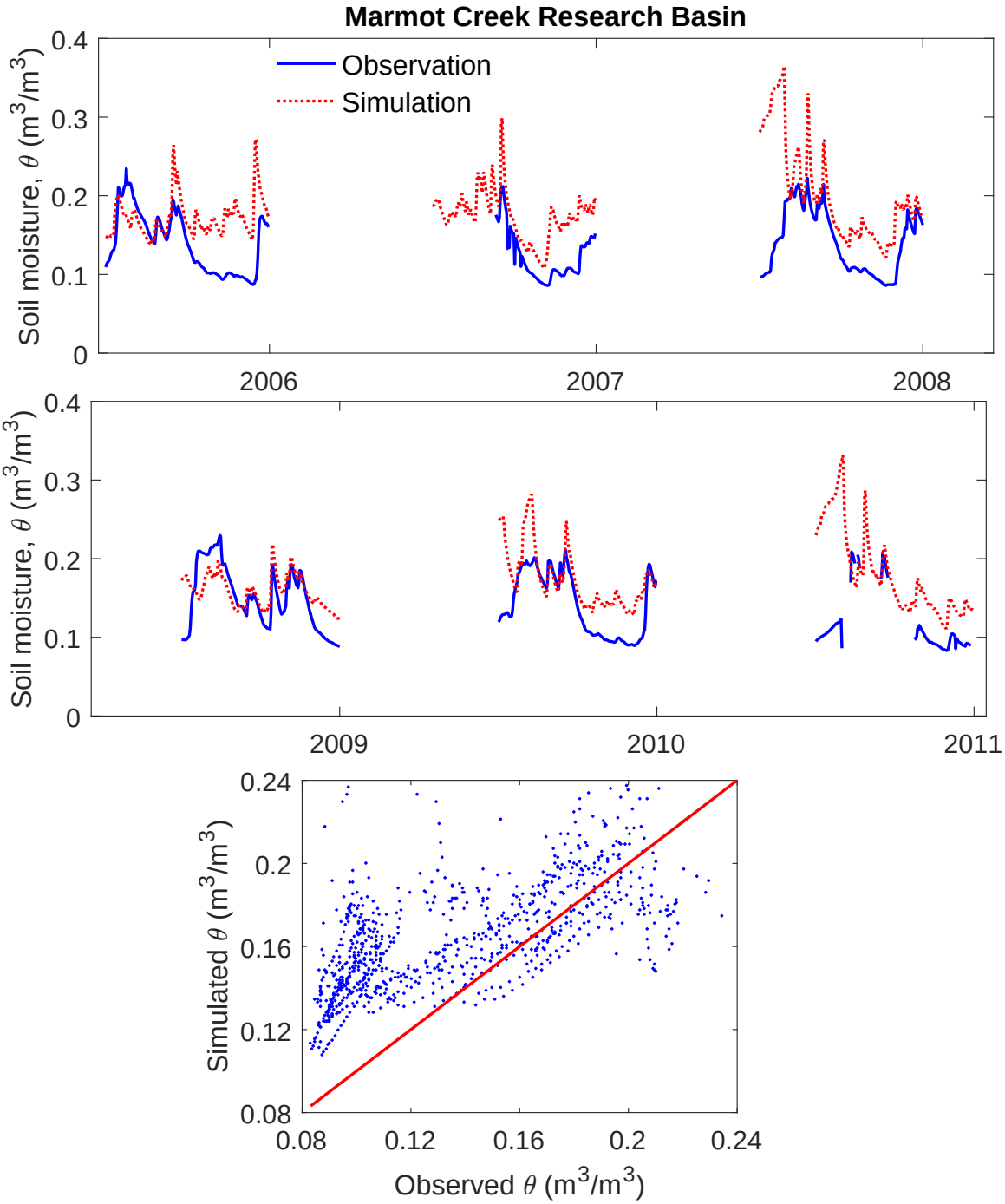

Figure 4.5: Comparison of observed and simulated soil moisture at Level Forest site (low elevation) in Marmot Creek Research Basin for the non-frozen period; 1 April to 30 September (figure was regenerated from Fang et al., 2013). The red line has a 1:1 slope, which indicates that the model overestimates the soil moisture.

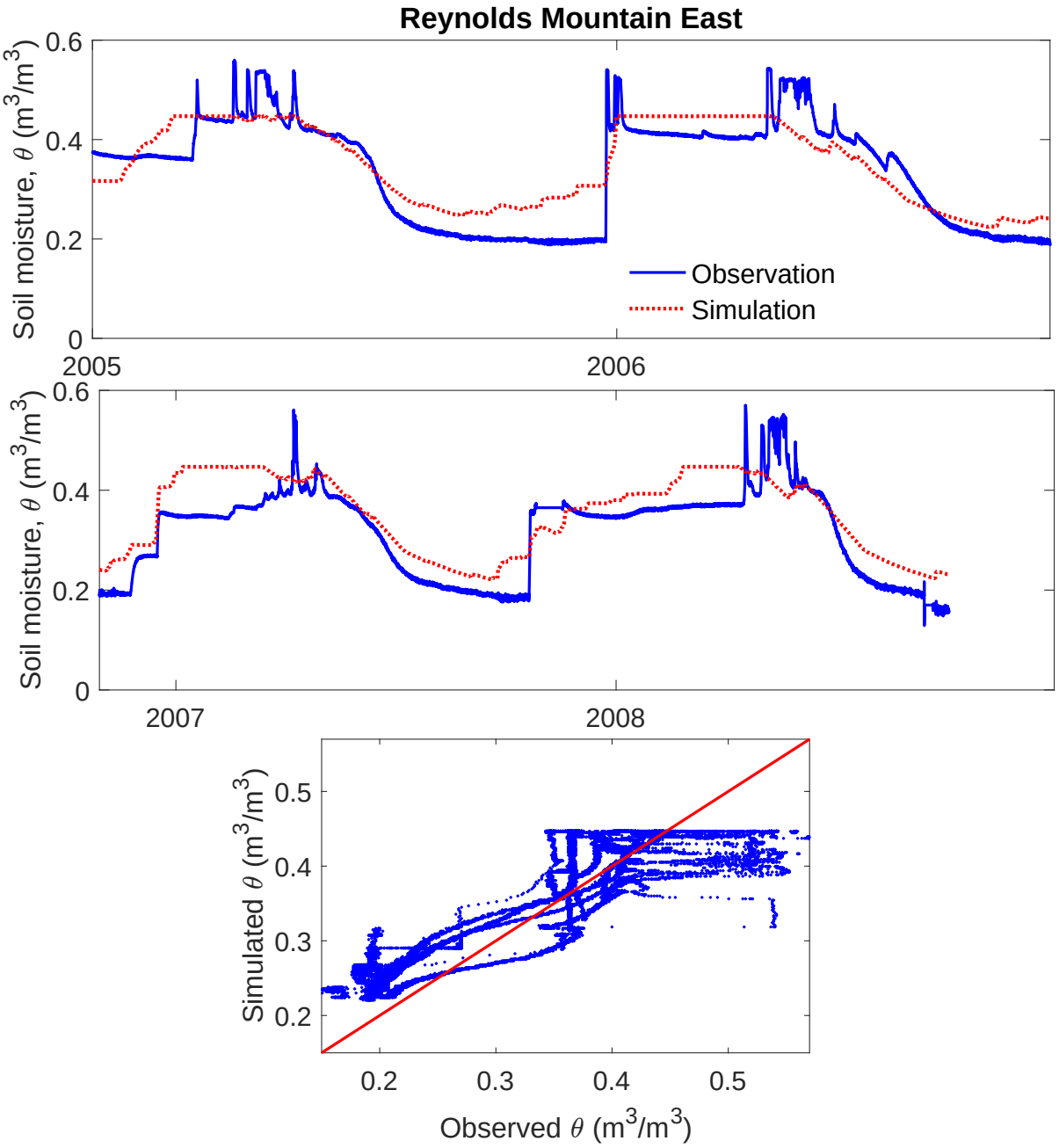

Figure 4.6: Comparison of observed and simulated soil moisture year round and visual assessment of model performance in Reynolds Mountain East (sheltered site). The ground does not freeze in winter in this basin. The red line has a 1:1 slope, which indicates that the model underestimates soil moisture in early spring. The model captures soil moisture well in late spring and in summer.

for soil moisture for this basin are not provided here. Figures 4.5 and 4.6 illustrate volumetric soil moisture at low elevations in MCRB and the sheltered station in RME. Statistical performance measures show that average error between observed and simulated soil moisture values is below 0.045 m^3m^{-3} (Table 4.4 and Figures 4.5 and 4.6). Visual assessment for RME shows that the model fails to capture high soil moisture events. This can be a potential reason why high streamflows are underestimated at the outlet of this basin. Differences in simulated and observed soil moisture values correspond to the differences in measurement and simulation depths. Soil moistures are simulated for the top 50 cm of the soil (recharge layer) in the model, while soil sensors are located 30 cm deep (Reba et al., 2011a).

4.5 Assessment of Streamflow Modelling Performance

Accuracy of hydrological model performance in simulating streamflow regimes depends mainly on the accuracy of the simulations for snow accumulation and ablation and accuracy of the soil temperature and moisture modelling, which control infiltration and subsurface flows. For routing streamflows, WCRB is divided into five subbasins (Figure A.2): Upper Wolf Creek (6 HRU), Coal Lake (10 HRU), Granger (4 HRU), Mid Wolf Creek (5 HRU), and Lower Wolf Creek (4 HRU). MCRB is divided into four subbasins: Cabin Creek (12 HRU), Middle Creek (7 HRU), Twin Creek (9 HRU), and Marmot Creek (8 HRU). RME (12 HRU) is not divided into subbasins as it is a relatively small basin and is one of the subbasins of the larger Reynolds Creek Experimental Watershed. The ability of the model to simulate daily stream discharge was tested statistically and visually at the gauged outlet of the basins. Figure 4.7 compares the observed and simulated discharge from the basin outlet for each basin. The models for WCRB and RME were calibrated only over three and four years, respectively, and the MCRB model is not calibrated at all. Minimal calibration is applied in this research. Apparently, if one calibrates the models with full or over 70% of the recorded data length, scores of the statistical performance measures for calibration period can improve. The question is whether a good agreement between the observed and simulated values is due to a stronger physical representation in the model or due to over-relying on uncertain observed data,

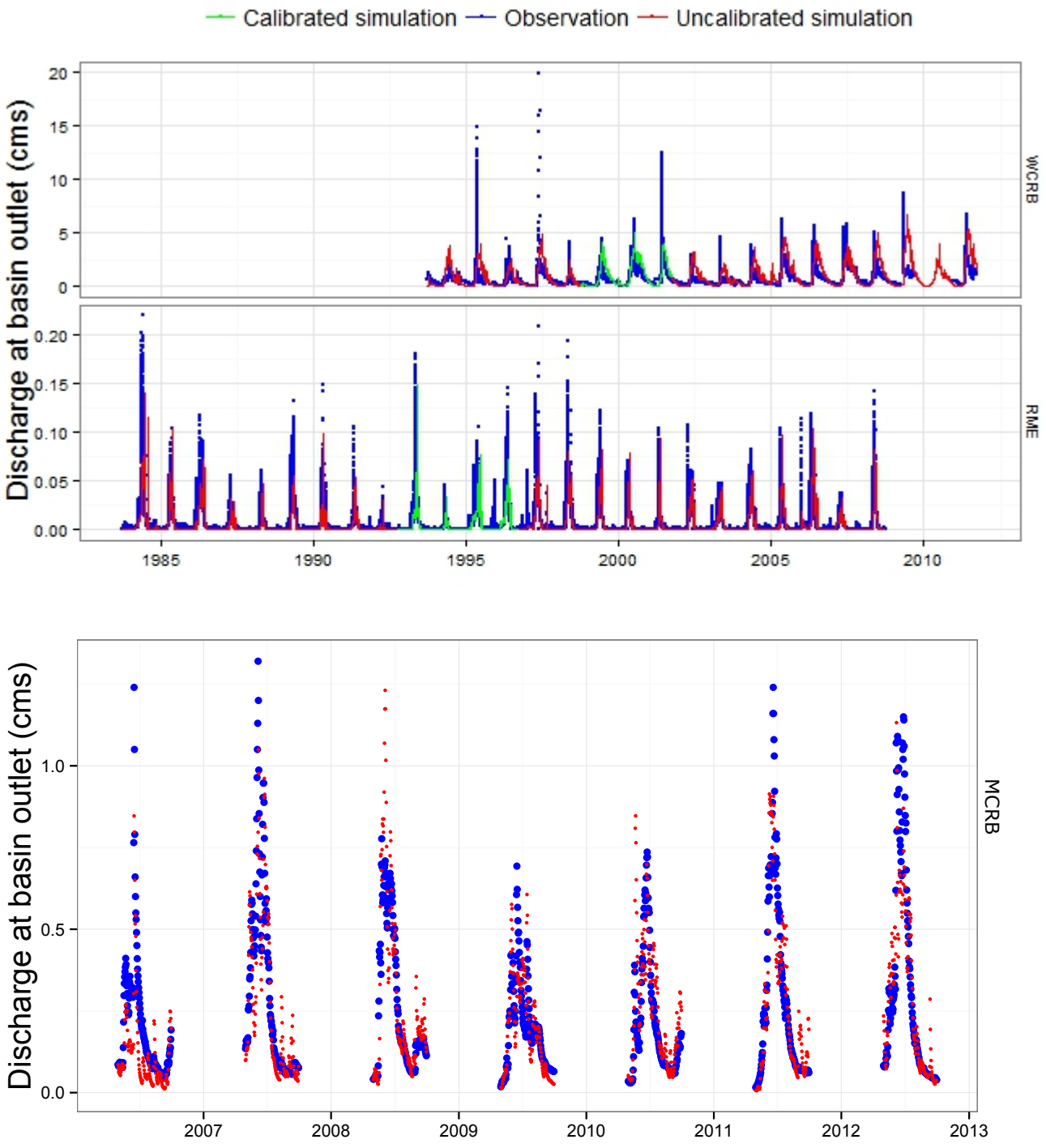

Figure 4.7: Performance of the Cold Regions Hydrological Model (CRHM) in capturing streamflow at the outlets of Wolf Creek Research Basin (WCRB), Marmot Creek Research Basin (MCRB), and Reynolds Mountain East (RME). The MCRB model is developed and assessed by Fang and Pomeroy (2016). A few lag and route parameters were calibrated (shown in green) in the WCRB and RME models.

Table 4.5: Accuracy of model performance in simulating streamflow over calibration period and entire record period in the three basins across the North American Cordillera. No calibration is applied in the MCRB model.

Criteria	**Calibration**			**Record period**		
	WCRB	MCRB	RME	WCRB	MCRB	RME
NSE [–]	0.64	–	0.73	0.40	0.71	0.72
Corr [–]	0.80	–	0.88	0.70	0.84	0.87
RMSE $[m^3 s^{-1}]$	0.60	–	0.008	0.75	0.13	0.008
MAE $[m^3 s^{-1}]$	0.31	–	0.003	0.37	0.09	0.003

uncertain model structure, and uncertain model outputs. Allowing the computer to obtain a so-called optimal set of parameters over many model runs without physical meaning may provide good results but for the not necessarily right reasons. With minimum calibration and maximum possible knowledge (through field measurements) and relevant physical mechanism representation in the model, streamflow simulations will be less uncertain (but uncertainty in high flows will be unavoidable).

Statistical performance measures show that the RME model captures the streamflow better than other two models and the WCRB model has a moderate performance in modelling streamflow. The Nash–Sutcliffe efficiency (NSE) scores for three- and four-year calibration periods for WCRB and RME are 0.64 and 0.7, respectively (Table 4.5). The NSE score for 25 years of streamflow simulations in RME is 0.72, which shows that the CRHM captures mountain hydrology within a reasonable range of simulation errors. Correlation coefficient values for all three basins represent about 50% of the variations, which indicates a moderate relationship between simulated and observed streamflows.

Performance measures for streamflow are illustrated in Figures 4.8 for WCRB, 4.9 for MCRB, and 4.10 for RME. High flows were under-estimated by all of the models with large underestimation in WCRB. Medium range and low flows were simulated well by all three models, providing reliable streamflow results that are important in this study for water balance purposes. Amongst the three models, the MCRB model performed better

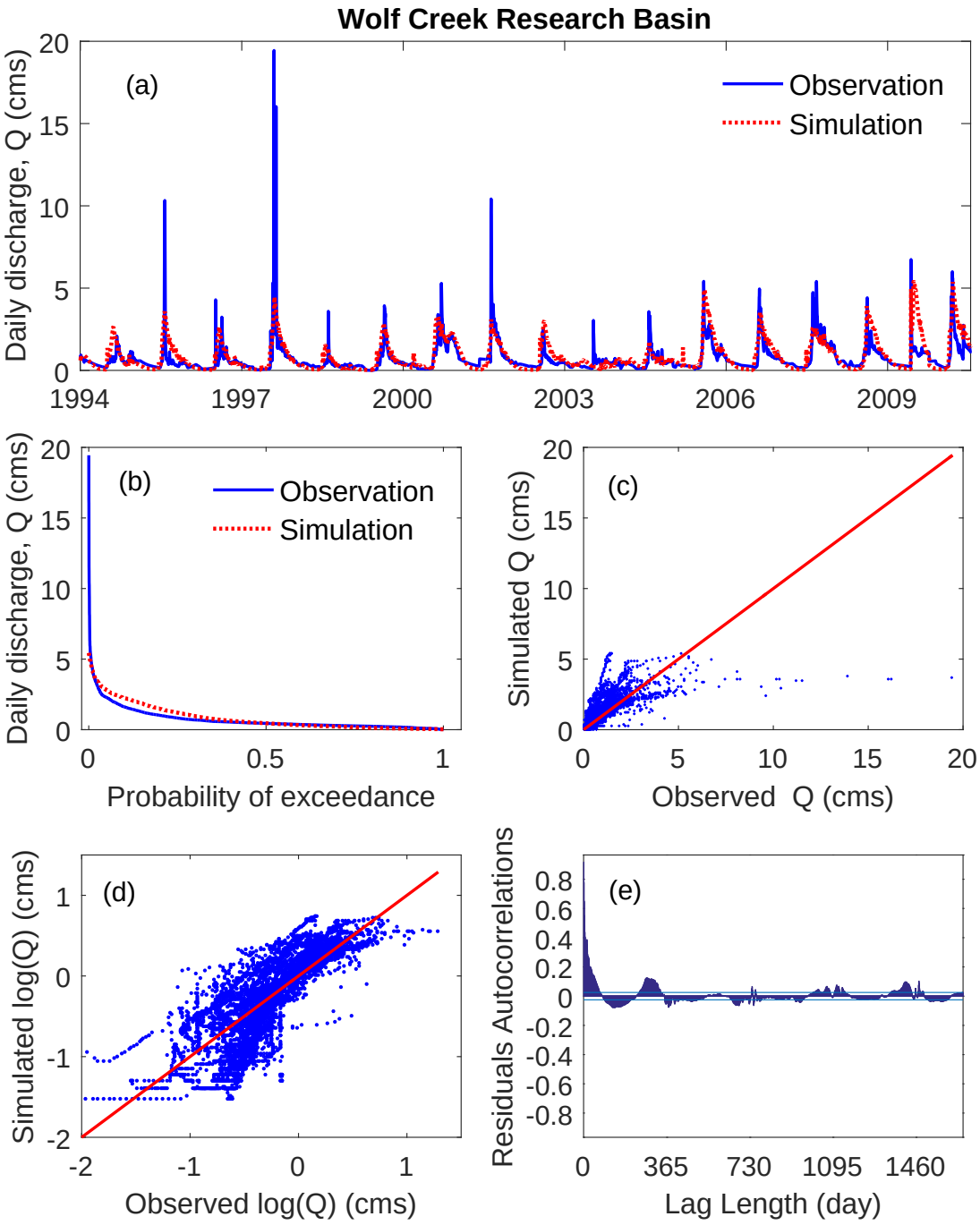

Figure 4.8: Assessment of the CRHM model performance in simulating discharge at the outlet of Wolf Creek Research Basin. (a) observation and simulation time series, (b) duration curves of the observed and simulated discharges, (c) observed and simulated discharges on a linear scale, (d) observed and simulated discharges on a logarithmic scale, and (e) autocorrelation of residuals. Flow duration curves show that model performance was good for flows with a probability of exceedance above 0.4 and that the model underestimates high flows and overestimates flows larger than the mean. The red lines in (c) and (d) have a 1:1 slope, which indicates that the model underestimates high flows. Autocorrelation of residuals (e) also shows that simulation errors reoccur at one-year intervals.

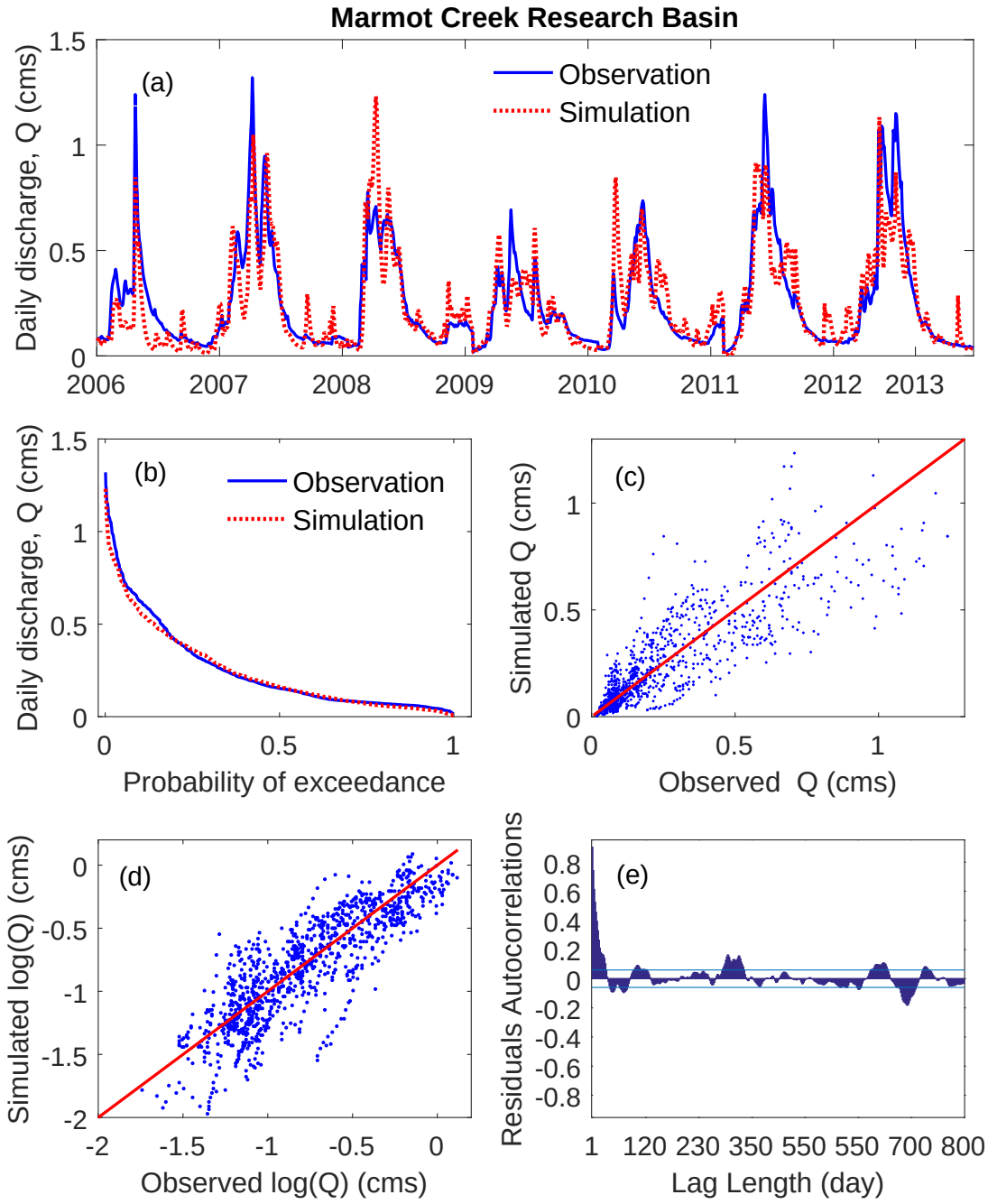

Figure 4.9: Assessment of the CRHM model performance in simulating discharge at the outlet of Marmot Creek Research Basin. (a) observation and simulation time series, (b) duration curves of the observed and simulated discharges, (c) observed and simulated discharges on a linear scale, (d) observed and simulated discharges on a logarithmic scale, and (e) autocorrelation of residuals. Flow duration curves show that the model performance was good for flows with a probability of exceedance above 0.2 and that the model underestimates high flows and overestimates flows with probability of exceedance below 0.2. The red lines in (c) and (d) have a 1:1 slope, which indicates that underestimated and overestimated flows by the model can offset each other. Because observations were sparse and not continuous in this basin, autocorrelation of residuals (e) cannot show the memory of the simulation errors at one-year intervals.

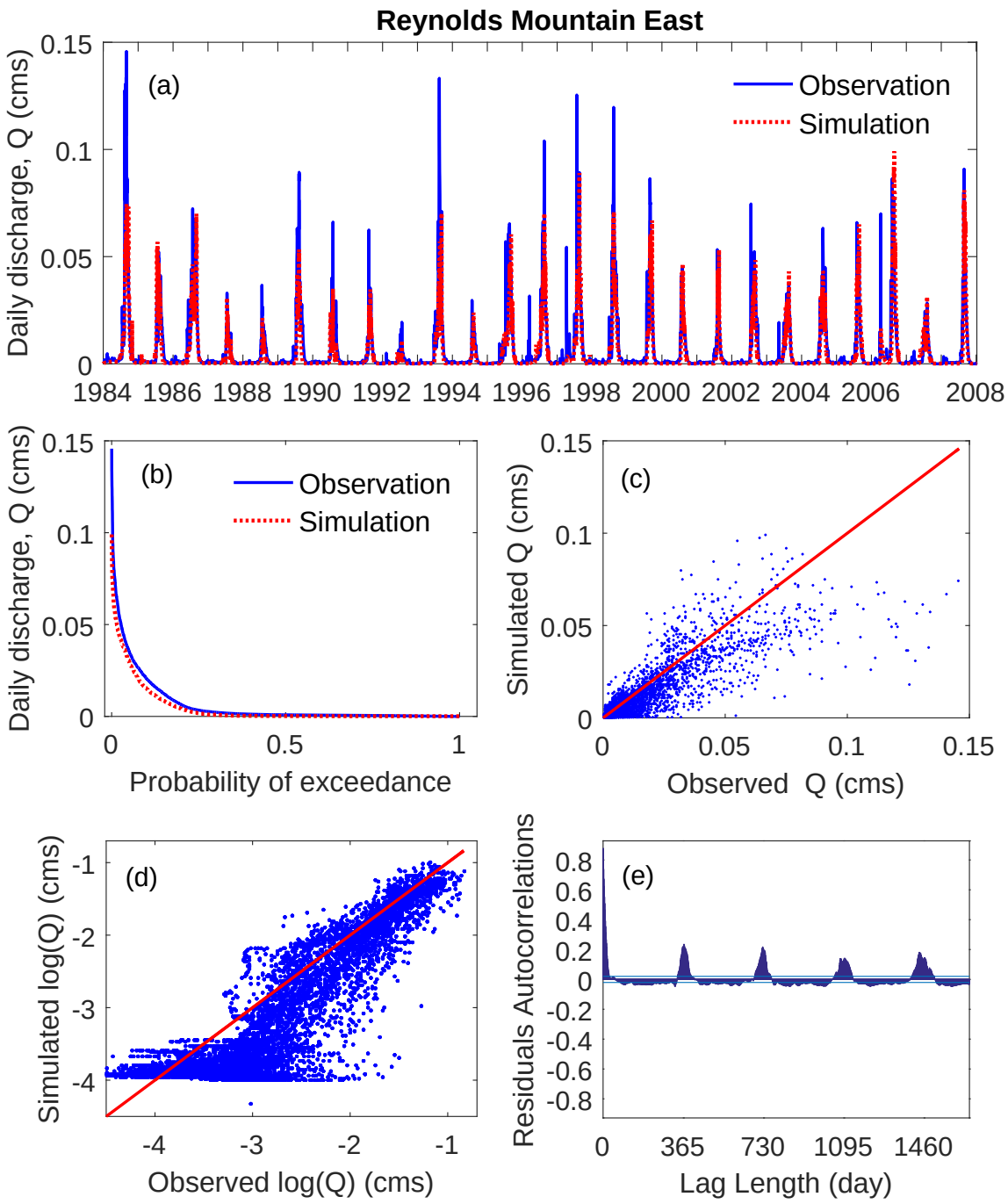

Figure 4.10: Assessment of the CRHM model performance in simulating discharge at the outlet of Reynolds Mountain East catchment. (a) observation and simulation time series, (b) duration curves of the observed and simulated discharges, (c) observed and simulated discharges on a linear scale, (d) observed and simulated discharges on a logarithmic scale, and (e) autocorrelation of residuals. Flow duration curves show that model performance was good for the full range of flows except for high flows. The red lines in (c) and (d) have a 1:1 slope, which indicates that the model underestimates high flows. Autocorrelation of residuals (e) also shows that simulation errors occur at one-year intervals and barely decline even after four years.

in simulating all ranges of streamflows. This is partly because of a short simulation period for MCRB (seven years) and lower interannual variability when compared with the two other basins.

The RME model slightly underestimates the peak streamflow (Figure 4.10b), which is related to antecedent soil moisture conditions that are not well simulated. Nayak (2008) showed that input of melt-water or rain at the soil surface was correlated to streamflow once soil became saturated during the snowmelt. Stream discharge was ≈90% of water input at the soil surface in cold and wet snow seasons (e.g., 1984), 67% in warm and wet years with antecedent dry conditions (e.g., 2006), and 42%–44% in dry years (e.g., 1987 and 2001). Most of the water at the soil surface infiltrates into the soil and recharges ground water prior to soil saturation. The model performance for basin-scale streamflow simulations, given the minimal calibration of model parameters and the strong physical basis of its structure, suggests that this model can be used for evaluating climate change effects on streamflow regimes in mountainous basins in the North American Cordillera. Some uncertainties, however, are unavoidable in capturing peak streamflows.

Table 4.6 summarises model performance assessment for low, medium, high, and peak values as well as timing of the simulated metrics in the three basins. It shows that performance of the models used in this research in capturing magnitude and timing of the peak values is fair and models performed reasonably good in simulating medium range and high values. Therefore, one needs to be cautious when interpreting the results for timing and peak changes under climate and transient vegetation changes.

4.6 Discussion

Uncertainties in simulated metrics such as snow water equivalent (SWE), soil moisture and temperature, and streamflow (Table 4.6) are associated with differences in spatial and temporal scales and inadequate representation of physical mechanisms, such as large spatial

Table 4.6: Modelling performance assessment of low, medium, high, and peak values of the hydrological metrics, along with the timing of the simulations (G: good with reliable simulation uncertainty; P: poor with high simulation uncertainty; F: fair with moderate simulation uncertainty)

			value ranges				
Variable	**Basin**	**Station**	**low**	**medium**	**high**	**peak**	**timing**
snow water equivalent	WCRB	alpine	G	G	G	F	F
		shrub tundra	G	G	G	F	G
		forest	F	G	G	F	F
	MCRB	F. Ridge S.	G	G	G	F	F
		F. Ridge top	G	G	G	F	F
		upper clearing	F	G	F	F	G
	RME	sheltered	F	G	G	F	F
soil temperature	WCRB	alpine	P	G	G	F	F
		forest	P	G	G	F	F
soil moisture	MCRB	level forest	F	G	F	F	F
	RME	level forest	F	G	F	P	P
streamflow	WCRB	outlet	F	G	G	P	F
	MCRB	outlet	F	G	G	G	F
	RME	outlet	F	G	F	P	F

variability of wind in the alpine biomes as well as large variability in orographic precipitation, midwinter meltwater refreeze, and river/lake ice break-up (in WCRB). Snow and soil data were collected from point measurements and their extrapolation to a hydrological response unit (HRU) scale introduces uncertainties to the simulations. Drainage area ranges from 0.4 km^2 in RME to 179 km^2 in WCRB. HRU-scale metrics such as soil moisture and temperatures, however, are uncertain as the spatial resolution of the HRUs varies in each basin (Table 3.2). Point measurements for soil moisture and temperature are not adequate for representing spatial variability within an HRU and also across the soil profile. The assessment of the model in simulating soil properties become challenging as models give an average soil moisture for entire soil depth and temperature at the soil surface rather than a specific point or depth.

To test the effect of spatial scale differences on snowpack, a small subbasin in WCRB with a relatively similar spatial scale as RME was used for comparison. Results confirm that basin-scale simulations for snowpack characteristics in WCRB are similar to the simulated small Granger subbasin within WCRB (Rasouli et al., 2015b). Therefore, comparing the basin-scale snow metrics in WCRB and RME in this research is valid.

Uncertainties in parameters and model structure and differences in depth of the soil between observations and simulations lead to an uncertain soil moisture and streamflows. To reduce the uncertainties, models needs more soil and streamflow measurements and more physical representation of the hydrological mechanisms. Incorporating approaches that can simulate complex wind fields, aufeis/river ice formation, lake/river ice breakup, discontinuous permafrost slopes, and thin ice layer formation from midwinter meltwater can reduce uncertainties. This, however, will turn a moderately complex model into a highly complex model, which will have limited applications to any other basin. The depth to frost table and soil properties play a key role in the amount of subsurface storage, runoff, contribution to groundwater, vegetation cover, and evapotranspiration. The shallow unfrozen and saturated layer on top of a frost table controls the surface runoff and plays an especial role in rain-on-snow events, when snow ablation starts and high flows are generated in spring and early summer. A thermal gradient between the ground surface and frost table affects changes

in the active layer, where freezing and thawing processes happen. These processes were not appropriately simulated in the hydrological models. Understanding these mechanisms will help to improve streamflow simulations. The uncertainty in observed air temperature, net radiation, and antecedent frost table depth lead to uncertainty in ground surface temperatures (Williams et al., 2015) and soil moisture content. A primary permafrost module in the CRHM tracks the evolution of thawing and freezing fronts (Xie and Gough, 2013). A more comprehensive permafrost module may be needed for appropriate modelling of the thawing and freezing processes. To test the effect of permafrost on the performance of the streamflow simulations, the WCRB model was calibrated with and without the permafrost module. Results highlight that the NS efficiency score for streamflow improves from 0.49 to 0.64 in the calibration period after incorporating thawing and freezing processes into the WCRB model. This suggests that an appropriate permafrost module may reduce the streamflow uncertainty in cold regions with frozen grounds.

4.7 Summary

Models developed in Chapter 3 were forced with observation time series and measured parameters in each basin and were assessed using statistical (e.g., RMSE) and visual performance measures (e.g., duration curve) in this chapter. Patterns of the snow regimes during the accumulation and ablation periods were simulated well in three biomes in Wolf Creek Research Basin (WCRB), three biomes in Marmot Creek Research Basin (MCRB), and a sheltered site in Reynolds Mountain East (RME). Models slightly overestimate the snow water equivalent (SWE) values; however, performance of the models in simulating the snow regimes in the complex terrains is encouraging as no calibration and complex wind model were applied. Therefore, results of the climate perturbation sensitivity method in Chapter 5, Chapter 6, and Chapter 7 can be sufficiently reliable. Despite the mismatch of the soil depths between observations and simulations and extrapolation of point-scale measurements to HRU-scale, above-freezing soil temperatures in WCRB and soil moistures in MCRB and RME are reasonably well simulated. Soil moitures, however, are underestimated by the RME model

during the early melt season, when soils become saturated. This can lead to an overestimation of infiltration and consequently an underestimation of peak streamflows in RME. Streamflow regimes in each basin are simulated well for full ranges of the streamflows, except for the high flows that are underestimated by all models. The model assessments show that streamflow simulations can be reliably applied for sensitivity analysis of the water balance components under climate and transient vegetation changes. Results for the magnitude and timing of the peak flows, however, are uncertain.

Chapter 5

HYDROLOGICAL SENSITIVITY TO ANNUALLY PERTURBED CLIMATE

This chapter is largely based on materials already published as Rasouli et al. (2014, 2015b). These works were led by Kabir Rasouli under supervision of John Pomeroy. All of the sections, except for results of Marmot Creek Research Basin (MCRB) model and Section 5.2.2, have been published in the journal of Hydrological Processes. In this chapter, same results from published works for two study areas and unpublished results for the third study area were combined and presented together. Additional results in each paper were not presented in this chapter to keep consistency among the three study areas. Rasouli et al. (2014) examined the hydrological sensitivity of a northern Canadian mountain basin (Wolf Creek Research Basin, WCRB) to perturbation in temperature and precipitation. Kabir Rasouli's contribution in Rasouli et al. (2014) was to clean the data, model the hydrological processes, to parameterise a physically based hydrological model for WCRB, and to write up the first draft of the paper. Kabir Rasouli generated all maps and figures for WCRB. All authors read and contributed equally to writing of final version of the paper. Model setup and results were checked by John Pomeroy. Tyler Williams helped on initial data cleaning. Rasouli et al. (2015b) studied the sensitivity of snowpack to similar perturbed climate in a mountain basin in the US northwestern interior (Reynolds Mountain East). Kabir Rasouli's contribution in Rasouli et al. (2015b) was to model the hydrological processes, to parameterise a physically based hydrological model for RME, and to write up the first draft of the paper. Kabir Rasouli generated all maps and figures for RME. All authors read and contributed equally to writing of final version of the paper. Model setup and results were checked by John Pomeroy. Danny Marks provided the data. Full citations are provided below. All of the

figures have been revised to match with unpublished results for MCRB. Results presented in this chapter and two published papers address thesis objective one, quantifying the sensitivity of simulated mountain hydrological processes to climate change. The sensitivity of snowpack and streamflow regimes are discussed with emphasis on changes in the magnitude and timing of annual peak flows and snow water equivalent (SWE). The sensitivity analysis involves increasing air temperatures by one degree increments for each hourly interval up to 5°C and increasing or decreasing hourly precipitation by ±10% and ±20%. Sensitivity analysis based on measurements and a plausible range of perturbations can avoid the added uncertainties of bias correction and downscaling of climate model outputs.

[1] Rasouli, K., J. W. Pomeroy, J. R. Janowicz, S. K. Carey, and T. J. Williams, 2014. Hydrological sensitivity of a northern mountain basin to climate change. *Hydrological Processes*, 28(14):4191–4208.
[2] Rasouli, K., J. W. Pomeroy, and D. G. Marks, 2015b. Snowpack sensitivity to perturbed climate in a cool mid-latitude mountain catchment. *Hydrological Processes*, 29(18):3925–3940.

5.1 Sensitivity of Mountain Snowpack to Annually Perturbed Climate

In this section, the sensitivity of hydrological variables to perturbed climatic conditions is investigated. The sensitivity of the simulated snowpack in three biomes in Wolf Creek Research Basin (WCRB), four biomes in Marmot Creek Research Basin (MCRB), and four blowing snow regimes in Reynolds Mountain East (RME) catchment are assessed. To compare and contrast snow accumulation and ablation amongst sites, HRUs in WCRB are grouped into three snow regimes (alpine, shrub tundra, and forest) with varying biomes and elevation bands; in MCRB are grouped into four snow regimes (alpine, treeline affected by blowing snow from alpine, forest, and forest clearings); and in RME catchment are grouped into three snow regimes (affected by blowing snow, snow interception on the canopy, or sheltered/not affected by wind or interception, e.g., in forest gap). The effect of raising hourly air temperatures by 0, 1, 2, 3, 4, and 5°C on seasonal snow regime is investigated for

the alpine, shrub tundra, and forest biomes in WCRB using observations from October 1993 to September 2011. Warming of up to 5°C decreases the simulated annual peak snowpacks in WCRB by 30% to 45% in different biomes. There are substantial declines in snow accumulation and duration of snowcover season with increasing temperature over most winters, with some seasons (e.g., 2002–2003) showing large sensitivities (over 120 mm snow loss) and some (e.g., 1997–98) almost no sensitivity to temperature increases (see Appendix A and Figure A.3). Warming affects the phase of precipitation when air temperature is near the freezing point, causing a large fraction of snowfall to convert to rainfall in the spring and fall transition seasons. This causes the snowcover season to start later and end earlier. Warming also can accelerate the initiation of snowmelt, which in some years slows the melt rate as the melt period is shifted into a period of lower local solar irradiance. Despite this effect, in most years snowmelt ends earlier with increased warming as the snow cover season becomes shorter.

The mean annual peak SWE is calculated as the maximum snow water equivalent over the year; this generally occurs in April or May of each calendar year in WCRB. In some years, there are large decreases in peak SWE when modelling increasing temperature (e.g., 2000, 2005, 2006), while in other years there are very small decreases (e.g., 1998, 2002, 2007). The most sensitive years are the wetter years, as these often included late spring snowfall that occurs under relatively warm conditions and so is the most vulnerable to phase change with warming.

The sensitivity analysis allows us to assess whether changes in precipitation would offset or magnify the effect of warming climate on WCRB. The overall response of mean annual peak SWE magnitude and timing in each biome to changing precipitation with warming is shown in Figure 5.1. Mean annual peak SWE responds to both temperature and precipitation in all biomes, with slightly stronger response to precipitation in the shrub tundra biome, slightly stronger response to temperature in the alpine, and fairly equal response to both temperature and precipitation in the forest. The response of mean annual peak SWE to changing precipitation with less than 2°C warming is non-linear, suggesting a greater sensitivity to the combination of warming and drying. The curvature and slope of the

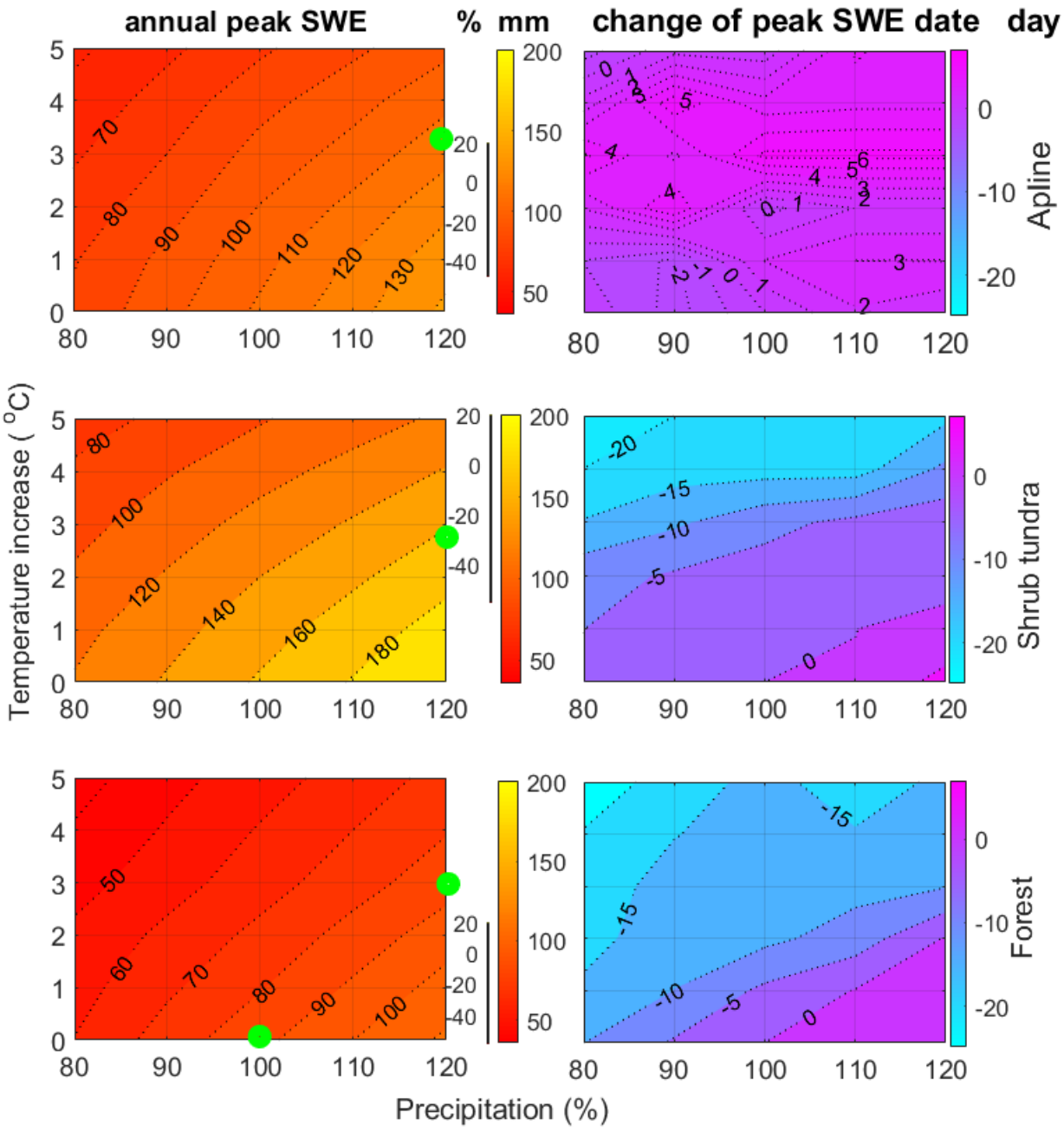

Figure 5.1: Sensitivity of mean annual peak SWE to 0°C to 5°C warming and varying changes in precipitation in the alpine, shrub tundra, and forest biomes in Wolf Creek Research Basin. Changes in magnitude and timing of peak snow water equivalent are illustrated in the left and right panels, respectively. The same scale is used for each biome for comparison purposes. Green markers show that a 20% precipitation increase is needed to offset a 3°C warming effect on peak SWE in the forest and shrub tundra biomes and to offset a 3.5°C warming effect in the alpine biome. Negative signs in the peak SWE date plot represent advances in time and positive signs denote delays in peak SWE timing. Contours in this figure and similar figures in this research were obtained from climatological means for 30 combinations (corners of the grids) of warming (0°C to 5°C with intervals of 1°C, 6 states) and precipitation change (-20% to +20% with intervals of 10%, 5 states).

contours of Figure 5.1 indicate that a complex interaction between air temperature and precipitation occurs in the alpine and shrub tundra biomes and less so in the forest in this basin. The timing of mean annual peak SWE advances largely with increases in temperature and is only slightly retarded or accelerated by increases or decreases in precipitation in the forest and shrub tundra biomes. Besides a general advance in the date of the mean annual peak SWE with warming and drying, there is no clear pattern in the alpine biome due to the complex interaction of blowing snow transport from the alpine snowpack with air temperature and precipitation.

The mean annual peak SWE in the shrub tundra biome shows the largest sensitivity to the most extreme simultaneous change in precipitation and warming; a 20% decrease in precipitation, along with 5°C warming, results in a 87 mm decline in magnitude from 162 mm to 75 mm and a 25 day advance in timing. The relatively high sensitivity of the shrub tundra peak snow accumulation to warming temperatures is partly due to diminished redistribution of blowing snow from alpine to shrub tundra as the winter temperature warms (see Appendix A and Figure A.4). The relatively low sensitivity of the alpine peak SWE date to temperature is due to colder temperatures at high elevations, which moderate the decrease in snowfall but not always the reduction in blowing snow transport with increasing temperature. Reduced snowfall and reduced snow removal counteract each other to some degree, but this will vary with the meteorological characteristics of each snowstorm. The relatively lower sensitivity of the forest peak snow accumulation is due to temperature-sensitive intercepted snow unloading processes in forests counteracting reduced snowfall at higher temperatures; warmer temperatures lead to greater unloading of intercepted snow and lesser sublimation loss (Gelfan et al., 2004). An interesting question regarding the effect of climate change on snowpack is whether an increase in precipitation of 20% (maximum likely) can offset the reduced mean annual peak SWE caused by climate warming. This is explored in Figure 5.1, where a 20% increase in precipitation can offset the effect of a 3°C warming on peak SWE in the forest and shrub tundra biomes and a 3.5°C warming in the alpine biome.

The response of mean annual peak SWE magnitude and timing in each biome in MCRB

to changing precipitation and warming is shown in Figure 5.2. Mean annual peak SWE in all of the biomes in MCRB responds more strongly than in WCRB, with the treeline zone losing the most snowpack (422 mm under the warmest and driest state). Because it has the highest snow accumulation, even after 39% snow loss, snow is still deeper than other biomes with over 80% snowpack loss. The response of the peak SWE timing to temperature and precipitation changes in MCRB shows a strong interaction in all biomes, except for the treeline biome where it responds moderately to warming and to a lesser extent to precipitation. The mean annual peak SWE is sensitive to precipitation changes in the alpine biome, to warming in the forest and forest clearing biomes, and to the interaction of temperature and precipitation in the treeline zone. In contrast to the magnitude of the peak SWE, its timing is mainly affected by warming and remains almost unchanged with increased or decreased precipitation. Under a 10% increase in precipitation and a 2°C warming, the most common scenario that is projected by 11 RCMs (see Chapter 6) for 2041–2070 for MCRB, mean annual peak SWE is expected to drop from a current level of 129 mm to 123 mm in the alpine biome, from 1076 mm to 1032 mm in the treeline zone, from 98 mm to 75 mm in the forest, and from 238 mm to 195 mm in the forest clearings (Figure 5.2). Mean annual peak SWE advanced 10 days at high elevations and up to 19 days at low elevations under the same climatic conditions. Under the most pessimistic scenario, snow loss is the most in the treeline, and almost all snow is lost in the forest and forest clearing, suggesting high sensitivity of the forest located at low elevations in MCRB. This may alter the vegetation of this biome over time. This shows that snowpacks at high elevations are very resilient and snowpacks at low elevations are very sensitive to the climatic changes in MCRB. The response of the peak SWE to warming and precipitation changes shows that in each biome in MCRB a 20% increase in precipitation can offset the effect of a 2.5°C warming on peak SWE in the alpine biome and a 2°C warming effect in the other biomes. This shows that more precipitation in MCRB than in WCRB is needed to offset the effect of the same warming on peak snowpacks.

Figure 5.3 shows the magnitude and associated percentage changes of mean annual peak SWE in RME with warming and changes in precipitation. Peak SWE shows a strong sensitivity to increases in air temperature and a secondary sensitivity to changes in precipitation.

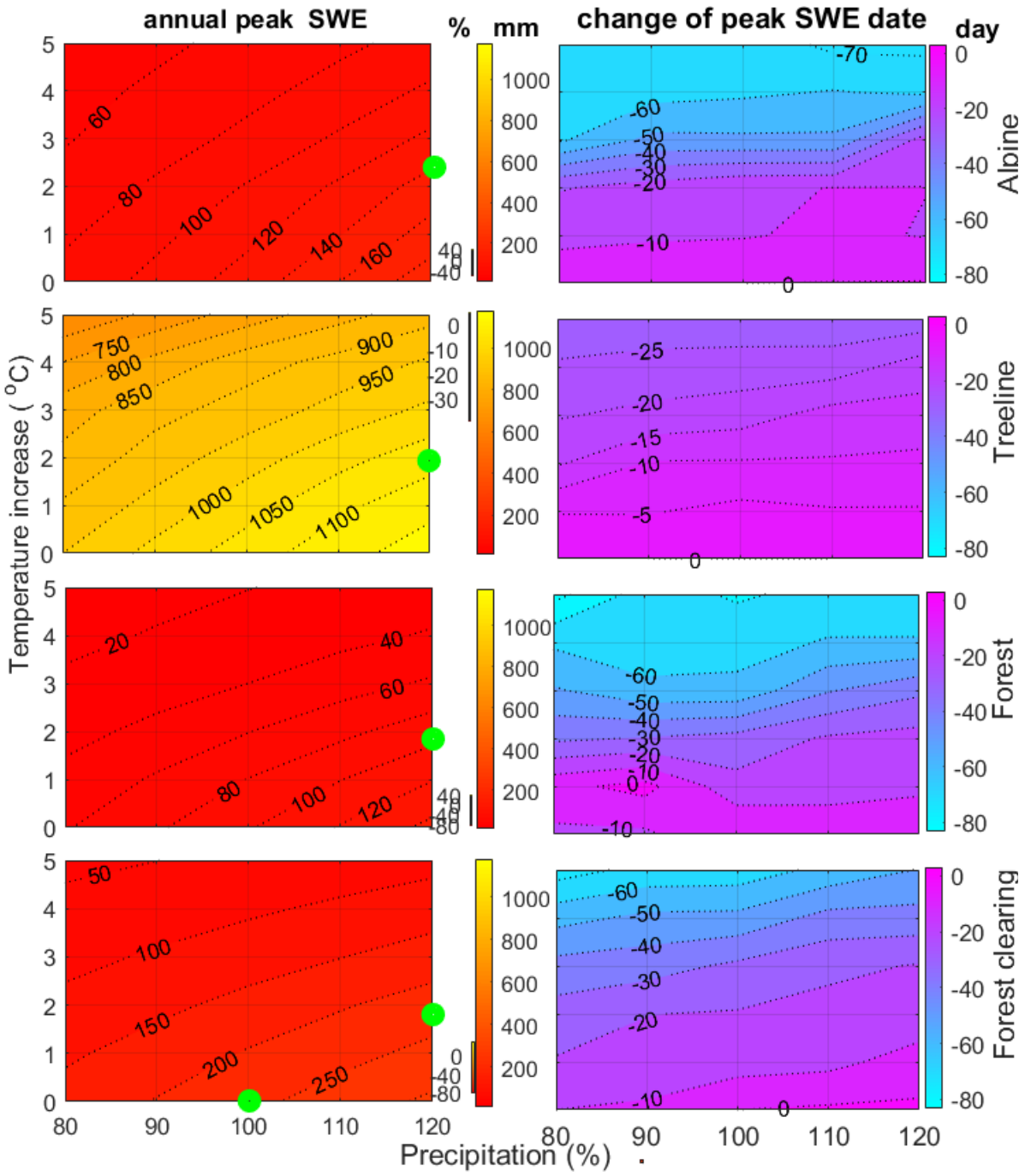

Figure 5.2: Sensitivity of mean annual peak SWE to 0°C to 5°C warming and varying changes in precipitation in the alpine, treeline, forest, and forest clearing biomes in Marmot Creek Research Basin. Changes in magnitude and timing of peak snow water equivalent are illustrated in the left and right panels, respectively. The same scale is used for each biome for comparison purposes. A percentage scale bar indicates the percentage of the changes. Green markers show that a 20% precipitation increase is needed to offset a 2.5°C warming effect on peak SWE in the alpine biome and a 2°C warming effect in the other biomes. Negative signs in the peak SWE date plot represent advances in time and positive signs denote delays in peak SWEs.

Further, curvature of the snow contours in Figure 5.3 shows that there is a complex interaction between air temperature and precipitation and that the sensitivity to precipitation change decreases as temperature increases. This suggests that peak snowpack in RME is sensitive to warming and that increased precipitation cannot offset the effects of warming on SWE when warming exceeds 1°C. For instance, warming of 5°C and precipitation change of ±20% leads to an 84–90% drop in the peak SWE. In the most extreme climate change case, a warming of 5°C and decline in precipitation of 20% causes the peak SWE to decline by 90%, from 570 mm to 58 mm in blowing snow sink HRUs and from 427 mm to 39 mm in the HRUs with intercepted snow. Maximum snow accumulation is lower in the blowing snow source HRUs when compared to other snow regimes, and therefore these drop the least, declining from 250 mm to 39 mm. The response of the mean annual peak SWE timing to warming in RME is strong in all of the blowing snow regimes. The response of the peak SWE to warming shows that a 20% increase in precipitation in RME can offset the effect of a 1°C warming on peak SWE in the sink and source snow regimes and a 1.3°C warming effect in the intercepted and sheltered snow regimes. This shows that more precipitation in RME than in WCRB and MCRB is needed to offset the effect of the same warming on peak snowpacks.

In RME, the response of snow characteristics to warming and precipitation change is complex and nonlinear because snow redistribution processes by wind and forest canopy add complexity and spatial variability to snow accumulation. For instance, mean annual peak SWE responds variably to a 20% increase of precipitation without warming, increasing by 100 mm in blowing snow sink HRUs and 58 mm in the intercepted HRUs. Results show that, under severe warming and reduction in precipitation, peak snowpack becomes relatively uniform in all of the snow regimes in RME because of the suppression of snow redistribution processes. Climate warming would have to be less than 1°C and be accompanied by a precipitation increase of at least 20% to allow peak SWE to remain within its historical range. All climate model scenarios predict greater warming than this for the 21st century for western North America including the RME region (Stewart et al., 2004) and substantial warming has already occurred. For instance, Nayak et al. (2010) analyzed 45 years of data (1962–2006) from RME and other subbasins in Reynolds Creek Experimental Watershed

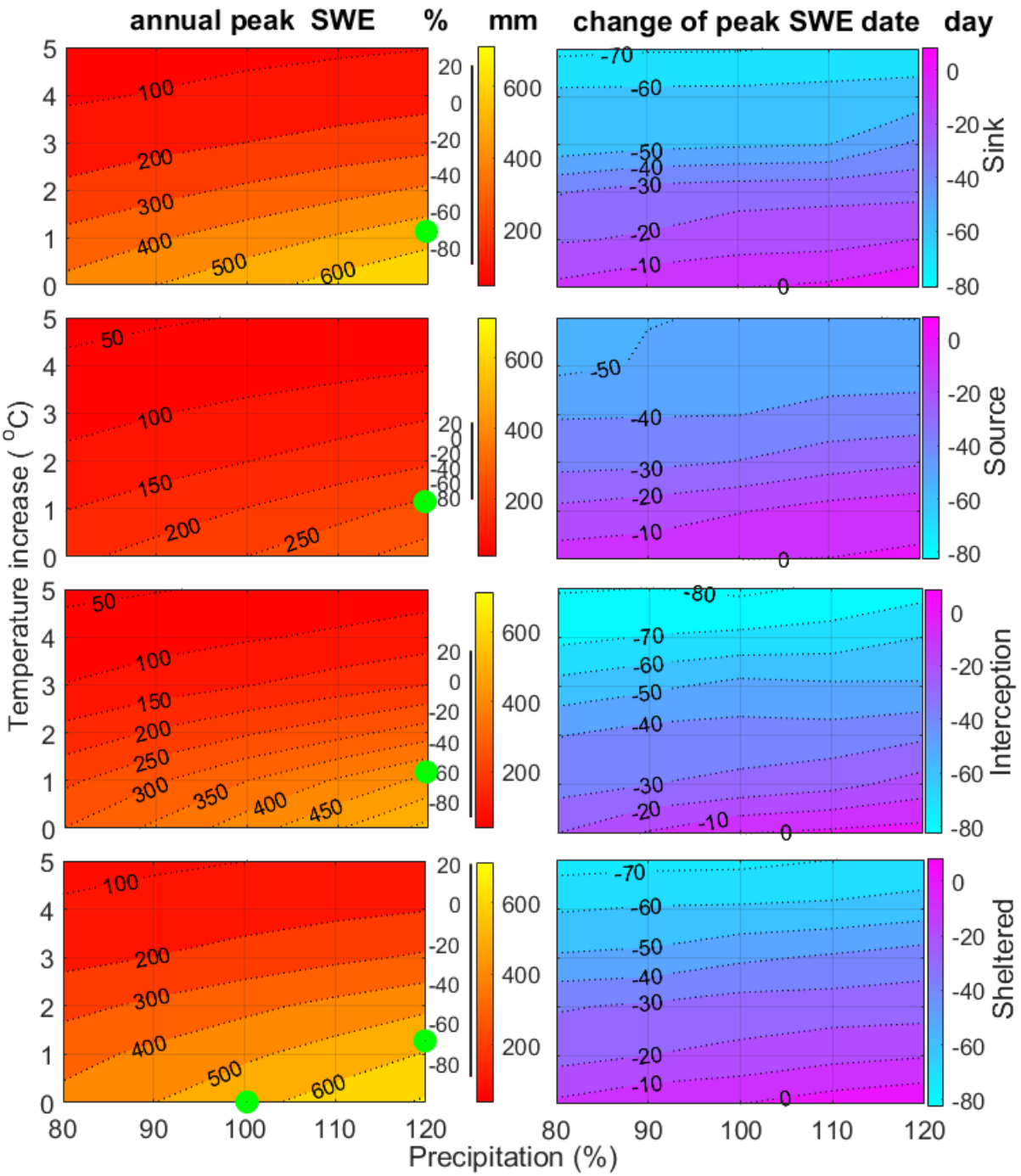

Figure 5.3: Sensitivity of mean annual peak SWE to 0°C to 5°C warming and varying changes in precipitation in the blowing snow sink and source snow regimes, forest with intercepted snow on the canopy, and a wind-sheltered site in Reynolds Mountain East catchment. Changes in magnitude and timing of peak snow water equivalent are illustrated in the left and right panels, respectively. The same scale is used for each biome for comparison purposes. A percentage scale bar indicates the percentage of the changes. Green markers show that a 20% precipitation increase is needed to offset a 1°C warming effect on peak SWE in the sink and source snow regimes and a 1.3°C warming effect in the intercepted and sheltered snow regimes.

(RCEW); they reported for the RME catchment a trend showing an increase in the mean annual temperature of +0.5°C per decade, and a trend showing a reduction of April 1 SWE of 58 mm per decade. Their analysis showed that mean annual temperature in RME catchment increased from around 4.0°C in 1962 to 5.8°C in 2006 and, during the same 45-year period, April 1 SWE decreased from around 648 mm in 1962 to 436 mm in 2006. This represents an approximate 18.5% reduction in April 1 SWE per degree of warming, and is within the 13–30% reduction in mean annual peak SWE that is expected per 1°C of future warming based on the analysis in this research. Annual maximum snow accumulation decreases 2–16% per 10% reduction in precipitation with and without warming; however, as air temperature increases above 3°C, the sensitivity of snowpack to changes in precipitation decreases.

In WCRB, the sensitivity of hourly SWE to warming air temperatures and precipitation change in the alpine, shrub tundra, and forest snow regimes is simulated using measured and perturbed meteorology (Figure 5.4). To estimate the probability density function (PDF) of the snowpack in Figure 5.4, the kernel density estimation (a non-parametric approach) is used. This estimation is based on a normal kernel function and a window parameter (bandwidth) that is a function of the length of the time series (n = 18 years ×365 days ×24 hours). Figure 5.4 shows that PDFs have much wider spreads if temperature warms by up to 2°C and a tendency for narrower spreads if temperature warms by more than 3°C and precipitation decreases. Compensation for warming by precipitation increase is large; a warming of 3°C can be offset by a precipitation increase of 20% for all SWE values in all snow regimes. Warming of more than 3°C, however, cannot be offset by an increase in precipitation of 20%. The temporal frequency distributions of different snowpack regimes show that the forest is the most resilient to impacts of warming and changes in precipitation because of its cold sub-canopy temperatures. Current mean snowpacks are expected to become the peak SWEs with a warming of 5°C and a 20% decrease in precipitation. The warming impacts medium range SWEs in early winter during the accumulation period or early spring during the melt season more than peak snowpacks in all of the snow regimes. This is because most of the precipitation falls in winter and an increase in future precipitation will likely increase winter precipitation. An increase in precipitation can offset the impacts of warming

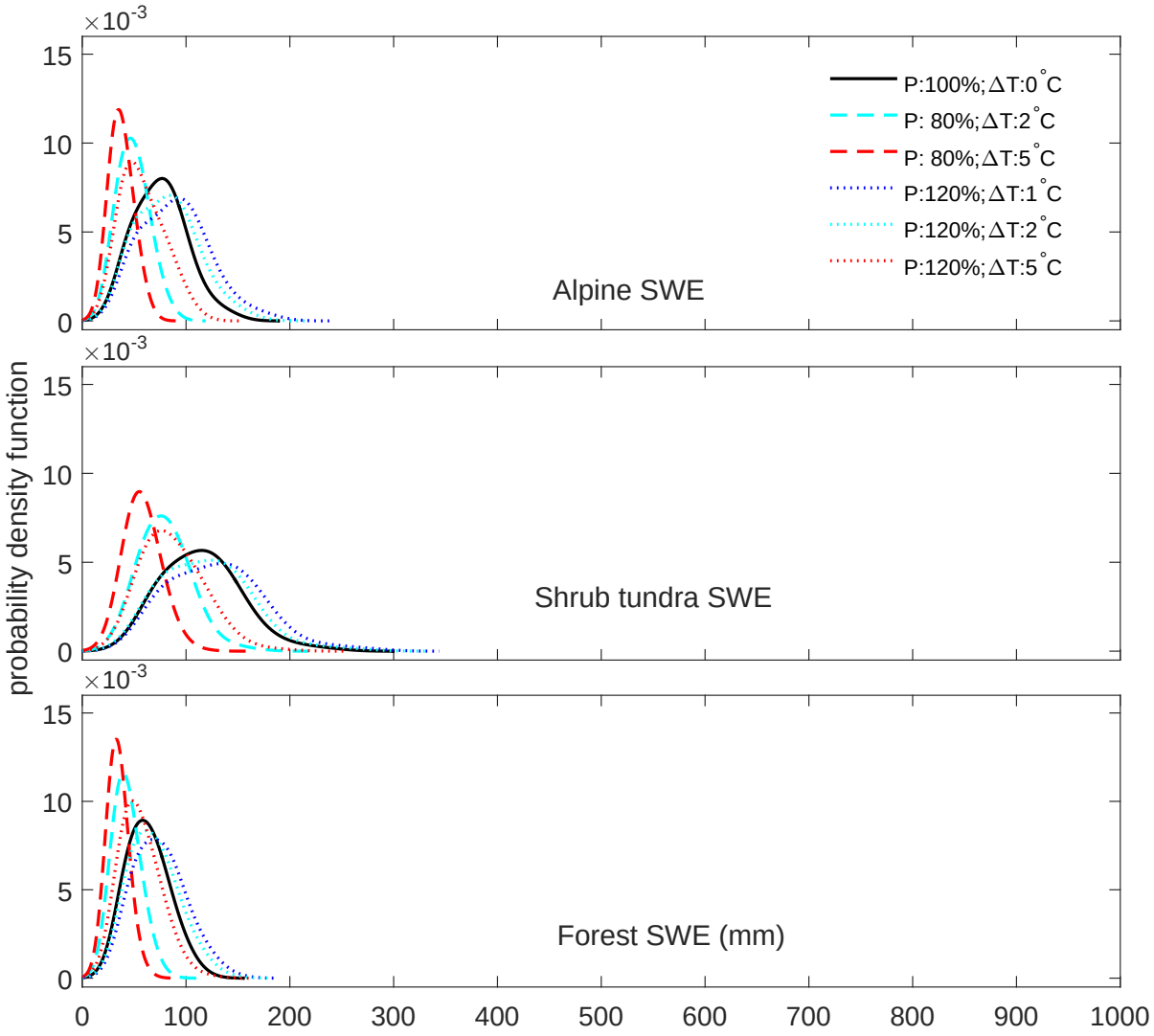

Figure 5.4: Sensitivity of snow water equivalent to warming and precipitation change in each of the three biomes shown as probability density functions for 18 years of hourly simulation in Wolf Creek Research Basin. All of the five distributions for the warming and changed precipitation scenarios in each biome are significantly (p–value < 0.05) different than the snowpack distribution in the control period based on the Kolmogorov-Smirnov (K–S) test (Massey Jr., 1951). The K–S test is a nonparametric hypothesis test that evaluates the differences between simulated SWE distribution in control period ($P = 100\%$ and $\Delta T = 0°\text{C}$) and simulated SWE distributions for perturbed climates over 18 years × 365 days × 24 hours.

and affects the high and medium range values of SWE the most and low range SWEs only slightly (Figure 5.4). In general, the snowpack regime in WCRB is more sensitive to changes in precipitation than to warming.

In MCRB, the sensitivity of hourly SWE to warming air temperatures and precipitation change for the four snow regimes is simulated (Figure 5.5). The PDF of snowpack in Figure 5.5 is estimated by the kernel density estimation for time series of $n = 9$ years $\times 365$ days $\times 24$ hours length. Figure 5.5 shows that PDFs have much narrower spreads if temperature warms by more than 2°C and a moderate tendency for wider spreads if precipitation increases. Compensation for warming by precipitation increase is notable; a warming of 2°C can be offset by a precipitation increase of 20% for all SWE values in all snow regimes (Figure 5.5). An increase in precipitation of 20% cannot offset warming of more than 2°C. The temporal frequency distributions of different snowpack regimes show that a shallow snowpack (SWE < 100 mm) is expected in the forest and forest clearings biomes under 5°C warming and 20% decrease in precipitation and current medium range snowpacks are expected to become the peak SWEs. The medium range SWEs denote the SWE magnitudes in early snow accumulation and late snowmelt seasons. The warming impacts the peak SWE more than shallower snowpacks in all of the snow regimes. Snowpacks in forest and forest clearings are important for early summer runoff generation in some years and so their absence under a warmer climate is expected to have hydrological consequences. An increase in precipitation can offset the impacts of warming by increasing SWE, especially high values of SWE (Figure 5.5). In general, the snowpack regime in MCRB is equally sensitive to warming and changes in precipitation.

In RME, the sensitivity of hourly SWE to warming air temperatures and precipitation change for the four snow regimes is also simulated (Figure 5.6). The PDF of snowpack in Figure 5.6 is estimated by the kernel density estimation for time series of $n = 25$ years $\times 365$ days $\times 24$ hours length. Figure 5.6 shows that PDFs have much narrower spreads if temperature warms by more than 1°C and a slight tendency for wider spreads if precipitation increases. Offset of the warming impact by precipitation increase is less than in WCRB and

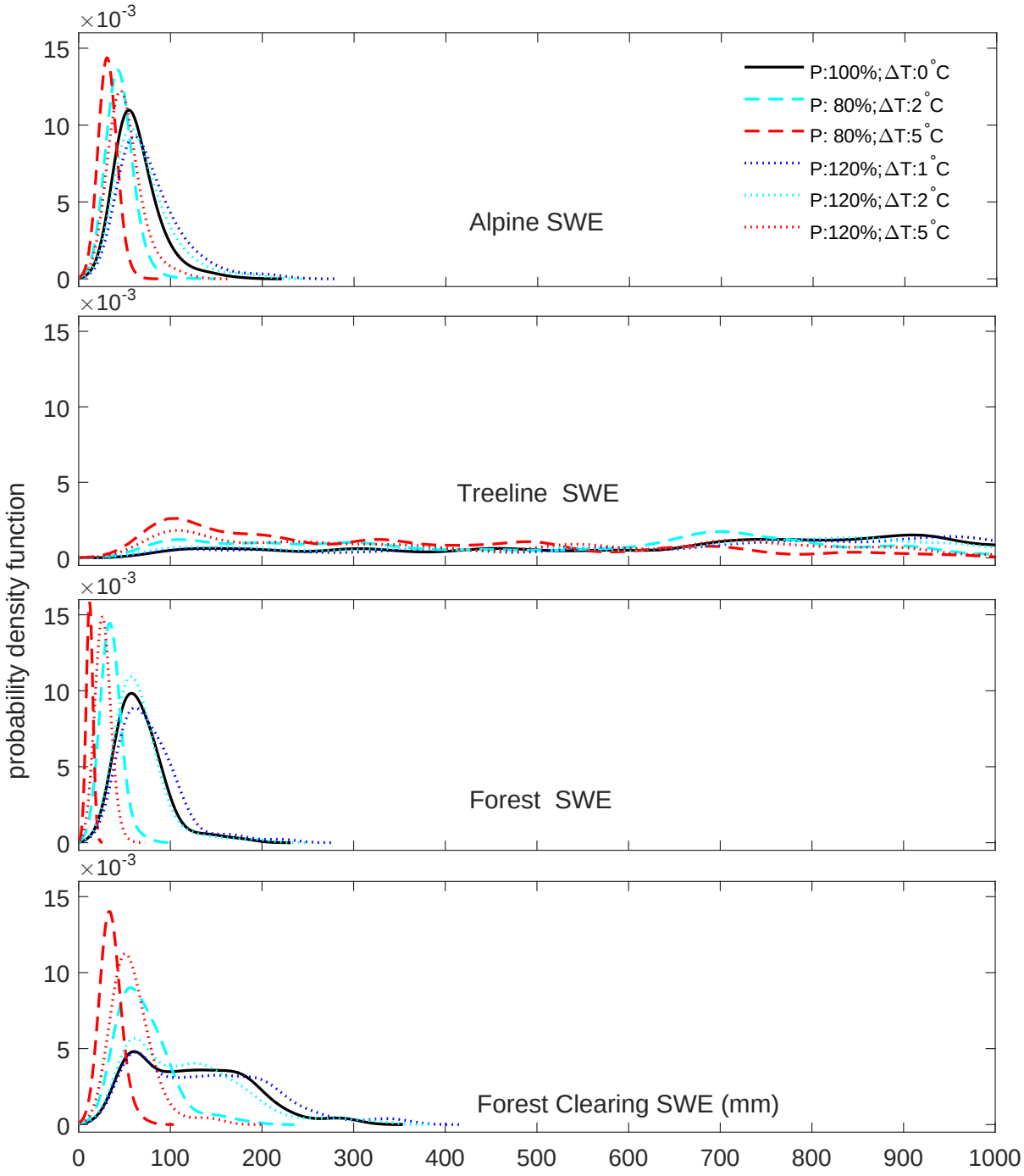

Figure 5.5: Sensitivity of snow water equivalent to warming and precipitation change in each of the four biomes shown as probability density functions for 9 years of hourly simulation in Marmot Creek Research Basin. All of the five distributions for the warming and changed precipitation scenarios in each biome are significantly (p–value $<$ 0.05) different than the snowpack distribution in the control period based on the K–S test. The K–S test is a nonparametric hypothesis test that evaluates the differences between simulated SWE distribution in control period (P = 100% and ΔT = 0°C) and simulated SWE distributions for perturbed climates over 9 years × 365 days × 24 hours.

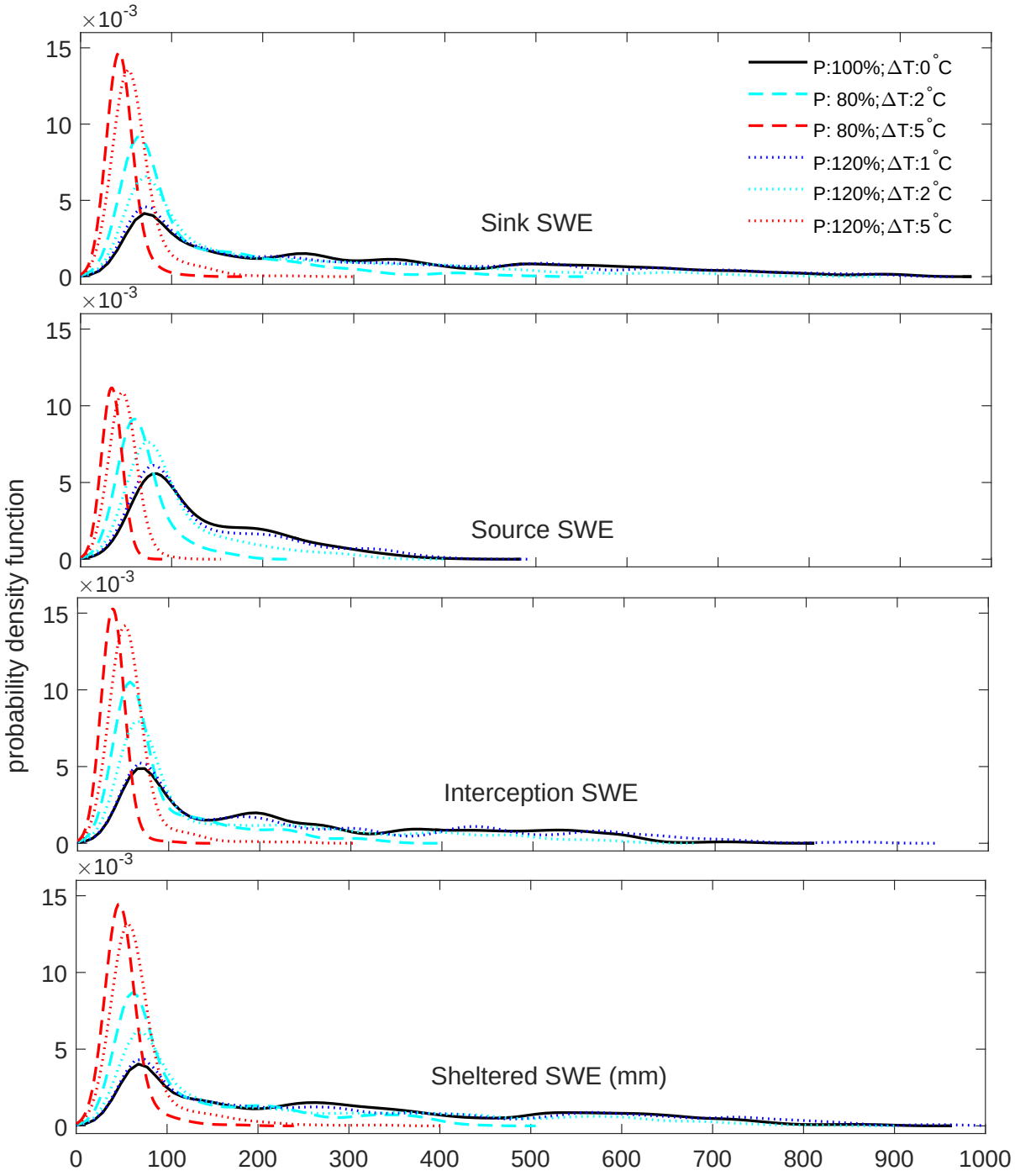

Figure 5.6: Sensitivity of snow water equivalent to warming and precipitation change in each of the four blowing snow regimes shown as probability density functions for 25 years of hourly simulation in Reynolds Mountain East. All of the five distributions for the warming and changed precipitation scenarios in each snow regime are significantly (p–value < 0.05) different than the snowpack distribution in the control period based on the K–S test. The K–S test is a nonparametric hypothesis test that evaluates the differences between simulated SWE distribution in control period ($P = 100\%$ and $\Delta T = 0°\text{C}$) and simulated SWE distributions for perturbed climates over 25 years $\times$ 365 days $\times$ 24 hours.

MCRB; a precipitation increase of 20% can offset the impact of a 1°C warming for all SWE values in all snow regimes (Figure 5.6). Warming of 2°C or more cannot be offset by an increase in precipitation of 20%. The temporal frequency distributions of different snowpack regimes show that all of the snow regimes are sensitive to impacts of 5°C warming and 20% decrease in precipitation and maximum SWE values are expected to drop below 240 mm from the current level of over 800 mm in the sheltered site, blowing snow sink HRUs, and forest HRUs with snow interception (Figure 5.6). Of particular interest is the disappearance of the rare high SWE values with warming from blowing snow sink and forest interception HRUs. Current mean snowpacks are expected to become the peak SWEs with warming and precipitation change scenarios. The warming impacts the peak SWE more than shallower snowpacks in all of the snow regimes. In general, the snowpack regime in RME is more sensitive to warming than to changes in precipitation, a finding supported by the results of Sproles et al. (2013) for the nearby but more temperate Cascades Mountains of Oregon, USA.

Changes in the distribution of SWEs in all of the biomes in each headwater basin show that all of the biomes in WCRB (especially forest) are least sensitive to air temperature and precipitation changes and blowing snow sink regimes in MCRB (treeline) and RME are the most sensitive snow regimes to the changes in terms of the absolute magnitude of snow loss. The impact of precipitation increase in WCRB can offset the impact of warming; however, the counteracting role of increasing precipitation is unable to match the impact of warming at low latitudes .

The timing of snowcover initiation (snow season start), snow-free date (snow season end), duration of snowmelt period, and length of the snow season, along with the magnitude of the peak snowpack, are five main characteristics that describe the snow regime including the effects of accumulation, redistribution, and ablation processes. Figure 5.7 illustrates the sensitivity of these characteristics to warming and change in precipitation averaged over WCRB. Change in precipitation is almost as important as warming that changes the magnitude of the peak SWE (Figure 5.7a). The values in Figure 5.7a reflect the similar influence of precipitation change when compared with the impact of warming. This suggests

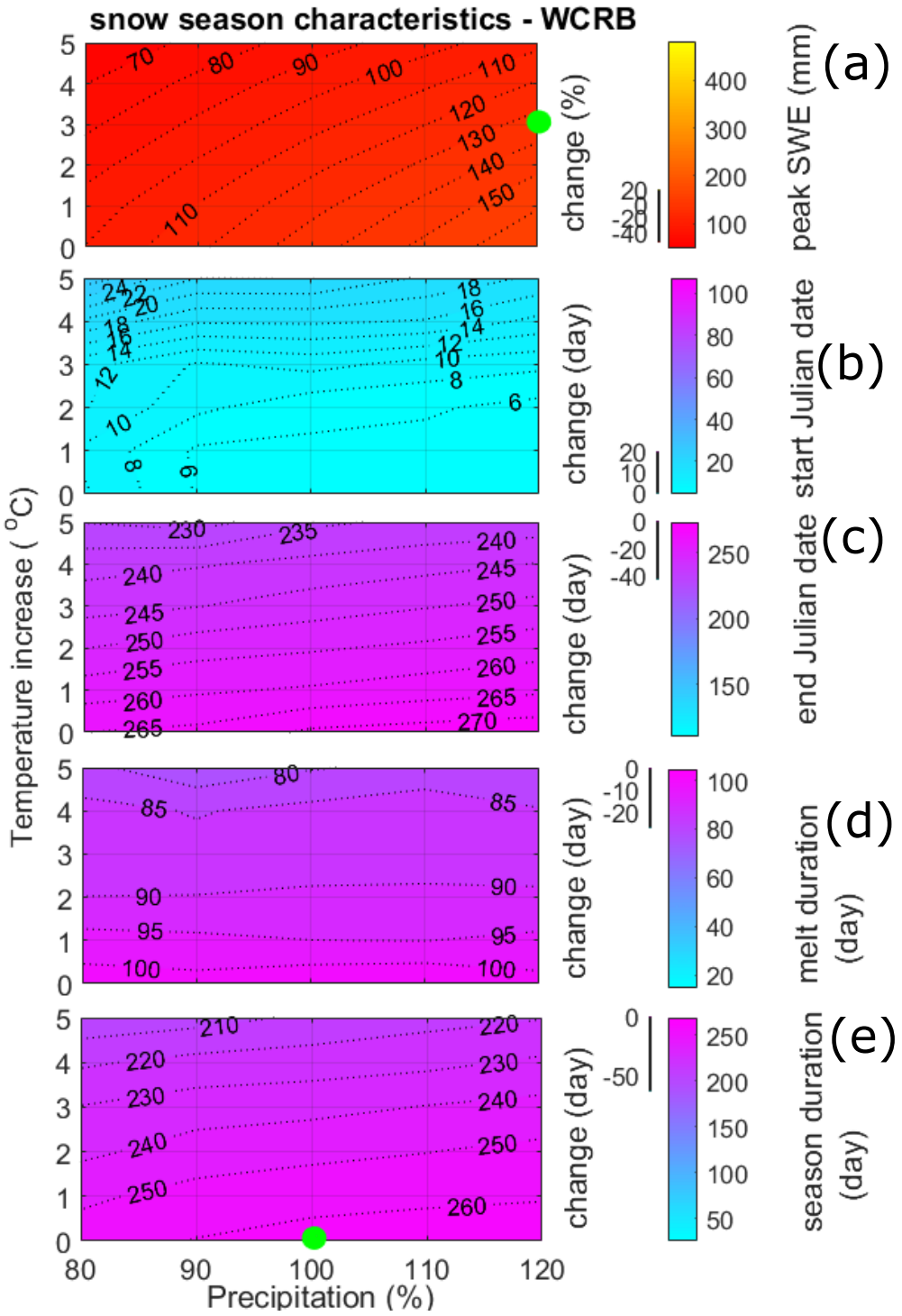

Figure 5.7: Magnitude and change of mean annual peak SWE, and the timing shift of the snow season start/end, snowmelt period, and snow season duration in Wolf Creek Research Basin with warming up to 5°C and precipitation change up to 20% in WCRB. Green markers show that a 20% precipitation increase is needed to offset a 3°C warming effect on peak SWE. Negative and positive values show advancing and delaying dates, respectively. Julian water year dates starting from October 1st are given for the first day of each month 1:Oct, 32:Nov, 62:Dec, 93:Jan, 124:Feb, 152:Mar, 183:Apr, 213:May, 244:Jun, 274:Jul, 305:Aug, 336:Sep.

that mean annual peak SWE is simultaneously affected by warming and changes in precipitation. The combination of air temperature increasing by at least 3°C and precipitation increasing by less than 20% results in declining peak SWE and deviation from the historical ranges of snowpack in WCRB. These temperature and precipitation conditions are considered likely in climate model projections for WCRB (see Chapter 6). Delay in initiation of snow accumulation is not sensitive to warming rates below 3°C and is sensitive to high rates of warming regardless of if precipitation changes or not (Figure 5.7b). The snow-free date advances from late-June in the recent climate to early June with a warming of 2°C (Figure 5.7c). Similar to ablation period, the snow-free date is also sensitive to warming and almost insensitive to precipitation changes. The mean timing difference between peak SWE and snow-free date indexes the snowmelt period and is sensitive to warming and almost insensitive to precipitation changes (Figure 5.7d). As shown in Figure 5.7, changes in the starting date of snow accumulation, snowmelt duration, and snow season length in WCRB are largely driven by warming and not by precipitation changes. This is because the snowpack is shallow and warm at the beginning and end of the season and shallow warm snow ripens and melts faster than deep cold snow.

Figure 5.8 illustrates the sensitivity of the snow regime characteristics to warming and change in precipitation averaged over MCRB. With warming of 5°C and decreasing precipitation (20%), the mean annual peak SWE drops from 220 mm to 92 mm (Figure 5.8a), snow ablates 83 days earlier (Figure 5.8b), and snowmelt period (Figure 5.8d) and snow season (Figure 5.8e) become, respectively, 12 days and 111 days shorter than those in the recent climate. In contrast to WCRB, initiation date of snow accumulation is sensitive to precipitation changes and would advance if warming rates are below 2°C and precipitation increases. The snow-free date advances from late-July in the recent climate to early July with a warming of 2°C (Figure 5.8c). Similar to ablation period, snow accumulation start date is sensitive to precipitation changes and to a lesser extent to warming. With concomitant warming (5°C) and decreasing precipitation, the snow-free date across the basin advances by 33 days to late-June (Figure 5.8c). As shown in Figure 5.8, snow-free date is sensitive to warming and insensitive to precipitation changes in MCRB and snow season length is affected by both warming and precipitation changes. Similar to WCRB, the combination of air temperature

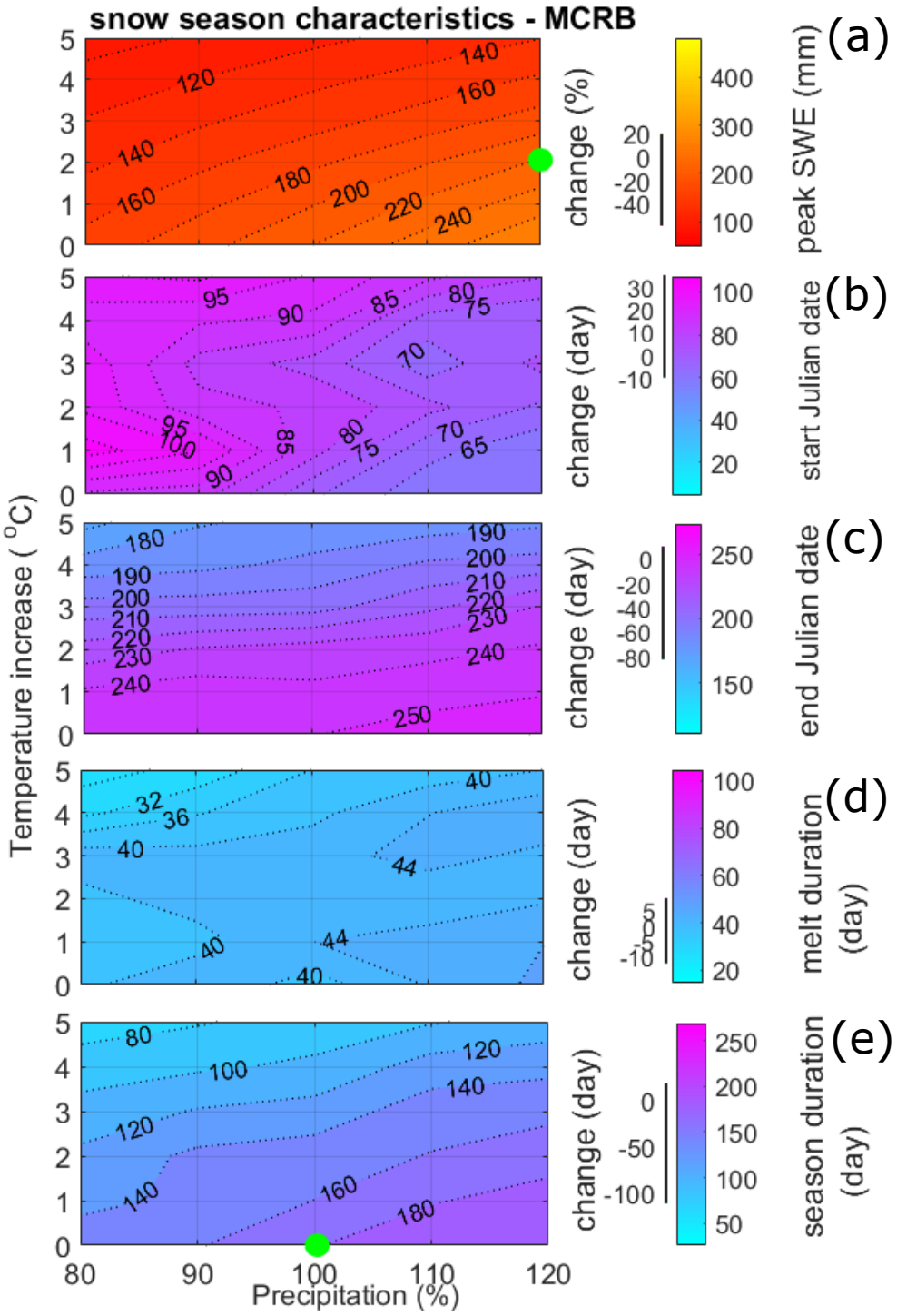

Figure 5.8: Magnitude and change of mean annual peak SWE, and the timing shift of the snow season start/end, snowmelt period, and snow season duration in Marmot Creek Research Basin with warming up to 5°C and precipitation change up to 20% in RME. Green markers show that a 20% precipitation increase is needed to offset a 2°C warming effect on peak SWE. Negative and positive values show advancing and delaying dates, respectively. Julian water year dates starting from October 1st are given for the first day of each month 1:Oct, 32:Nov, 62:Dec, 93:Jan, 124:Feb, 152:Mar, 183:Apr, 213:May, 244:Jun, 274:Jul, 305:Aug, 336:Sep.

increasing by at least 2°C and precipitation increasing by less than 20% results in declining peak SWE and deviation from the historical ranges of snowpack in MCRB.

Figure 5.9 illustrates the sensitivity of these characteristics to warming and change in precipitation averaged over the RME catchment. With warming of 5°C and decreasing precipitation (20%), the mean annual peak SWE drops 87% from 390 mm to 47 mm (Figure 5.9a), snow ablates two months earlier (Figure 5.9b), and snowmelt period (Figure 5.9d) and snow season (Figure 5.9e) become, respectively, 48 days and five months shorter than those in the recent climate. The mean snowmelt period is sensitive to warming but not to precipitation changes (Figure 5.9d). These results are generally supported by trend analysis by Nayak et al. (2010) in RME, as they found a 58 mm per decade reduction in peak SWE and a 6.4 day per decade delay in snowcover initiation over the past 50 years. Timing of the mean annual peak SWEs is not shown in Figure 5.9 but can be obtained from subtracting the melt duration from the snow-free date. It is estimated that a 1°C warming advances the timing of peak SWE by approximately 15 days; this can be offset by a 20% increase in precipitation. The date of the peak SWE in source HRUs is sensitive to warming of less than 3°C, but not to warming more than 3°C and changes in precipitation. The snow-free date (end of snowcover season) advances from mid-May in the recent climate to early April with a warming of 2°C. Similar to peak SWE timing, the snow-free date is also sensitive to warming but not to precipitation changes. As shown in Figure 5.9, changes in the snow season duration are largely driven by warming and not by precipitation changes. Change in precipitation is the secondary factor that affects the magnitude of peak SWE and snowmelt duration. The values in Figure 5.9 reflect the relatively small influence of precipitation change when compared with the impact of warming. This suggests that mean annual peak SWE is primarily affected by warming and to a lesser extent by changes in precipitation. The combination of air temperature increasing by at least 1°C (mean annual temperature exceeds 6.2°C) and precipitation increasing by less than 20% (mean annual precipitation less than 1030 mm) results in declining mean annual peak SWE and deviation from the historical ranges of snowpack in RME. Because snowpack in RME shows more sensitivity to air temperature and precipitation changes, variability of the snowpack is explored in more detail in Appendix B.

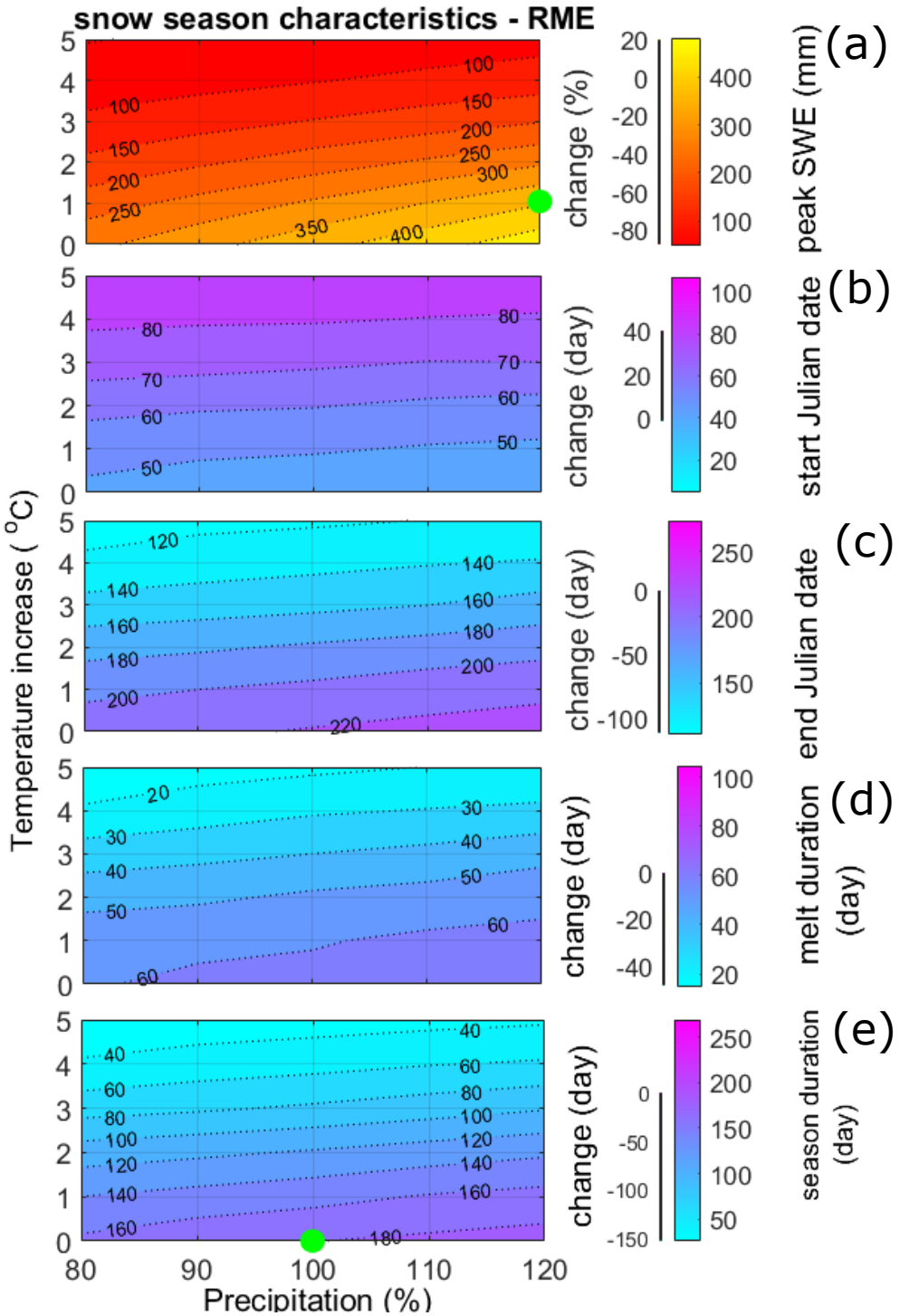

Figure 5.9: Magnitude and change of mean annual peak SWE, and the timing shift of the snow season start/end, snowmelt period, and snow season duration in Reynolds Mountain East catchment with warming up to 5°C and precipitation change up to 20% in RME. Green markers show that a 20% precipitation increase is needed to offset a 1°C warming effect on peak SWE. Negative and positive values show advancing and delaying dates, respectively. Julian water year dates starting from October 1st are given for the first day of each month 1:Oct, 32:Nov, 62:Dec, 93:Jan, 124:Feb, 152:Mar, 183:Apr, 213:May, 244:Jun, 274:Jul, 305:Aug, 336:Sep.

5.1.1 Similarities and Differences Between the Three Basins in Response to Annually Perturbed Climate: Snow

The sensitivity of snow regime characteristics to warming and precipitation changes is compared in the three basins along the NAC. Table 5.1 summarises the basin scale characteristics for current climatic conditions and for scenarios of warming and changes in precipitation. The long-term mean annual peak SWE is 136 mm in WCRB, 186 mm in MCRB, and 390 mm in RME; all occur in early March. The average peak SWE declines to 61 mm (55% decrease) in WCRB, to 90 mm (52%) in MCRB, and to 47 mm (88% decrease) in RME with warming of 5°C and a 20% decline in precipitation and increases to 169 mm (24%) in WCRB, to 242 mm in MCRB (30%), and to 486 mm (25%) in RME without warming and with a 20% increase in precipitation. With 5°C warming and no changes in precipitation, the onset of winter is delayed 17 days in WCRB, 22 days in MCRB, and 42 days in RME and the end of winter comes earlier by 37 days in WCRB, 33 days in MCRB, and 104 days in RME. When compared with historical winters, a 20% increase in precipitation would lengthen the winter season by only a few days in the three basins. The following shows the similarities and differences between biomes and basins:

- **Peak snowpack:**

    1. Sensitive to both warming and precipitation change in the south (RME) and less sensitive in the north (WCRB).
    2. Sensitive to warming in the sheltered site in RME and to both warming and precipitation change in the blowing snow sink regime in RME, treeline and forest biomes in MCRB, and shrub tundra biome in WCRB.

- **Peak snowpack timing:**

    1. Sensitive to warming in the south (RME) and centre (MCRB) and less sensitive to both warming and precipitation change in the north (WCRB).

Table 5.1: Sensitivity of the snow variables to warming and changes in precipitation in three basins long the North American Cordillera. The day of the water year starts from October 1st.

Variable		control	warm	warm	warm	–	warm
		period	–	–	dry	wet	wet
Warming [°C]		0	2	5	5	0	5
Precipitation [%]		100	100	100	80	120	120
(1) Wolf Creek Research Basin (WCRB)							
Peak SWE	[mm]	136	117	85	61	169	107
Snow initiation	[date]	Oct-05	Oct-07	Oct-22	Oct-27	Oct-04	Oct-18
Peak SWE date	[date]	Mar-16	Mar-12	Mar-03	Feb-25	Mar-21	Mar-04
Snow-free date	[date]	Jun-28	Jun-11	May-22	May-18	Jun-30	May-25
Season length	[day]	265	248	212	202	269	219
(2) Marmot Creek Research Basin (MCRB)							
Peak SWE	[mm]	186	141	81	90	242	103
Snow initiation	[date]	Oct-12	Oct-23	Nov-03	Oct-29	Oct-11	Oct-31
Peak SWE date	[date]	Apr-27	Apr-14	Mar-12	Apr-06	Apr-25	Mar-12
Snow-free date	[date]	Jul-19	Jul-04	Jun-16	Jun-26	Jul-23	Jun-18
Season length	[day]	280	254	225	241	285	229
(3) Reynolds Mountain East (RME)							
Peak SWE	[mm]	390	222	63	47	486	80
Snow initiation	[date]	Nov-11	Nov-28	Dec-25	Dec-23	Nov-09	Dec-23
Peak SWE date	[date]	Mar-07	Feb-08	Jan-07	Jan-04	Mar-11	Jan-09
Snow-free date	[date]	May-10	Apr-02	Jan-26	Jan-19	May-18	Jan-30
Season length	[day]	180	125	32	27	189	38

2. Treeline in MCRB is the most sensitive biome to changes amongst all biomes in the three basins.

- **Snow season (snow accumulation initiation/end, melt duration, and length of the snowcover season):**

1. Sensitive to warming in the south (RME) and north (WCRB) and to both warming and precipitation change in the centre (MCRB).

2. Interaction of warming and precipitation change is complicated with respect to affecting snow accumulation timing and melt duration in MCRB.

Sensitivity of annual peak snowpack timing to air temperature and precipitation changes in the three basins along the NAC shows that the response of peak SWE timing to precipitation changes becomes stronger moving from the southern basin to the northern basin: RME responds to warming only, MCRB responds to warming and to a lesser extent to precipitation; and WCRB responds to a complex interaction of warming and precipitation change. The role of precipitation with respect to counteracting the impact of warming on the magnitude of the annual peak snowpack, however, becomes less important moving from northern latitudes to southern latitudes. Therefore, regional responses to warming and changes to precipitation must be considered when evaluating future mountain hydrology. Simulations of future conditions for snow regimes in RME are in accord with the SWE magnitude and timing trends of the past 50 years. This indicates that the simulation results are similar to measured results, and therefore the model developed here can be applied to other mountainous regions. Higher rates of warming and increased precipitation are projected by RCMs (see Chapter 6) in the northern latitudes. Latitudinal change in the role of precipitation increase in offsetting the effect of warming on cold regions hydrology implies that, even though northern latitudes will warm more (Graversen et al., 2008), they will also have more precipitation. Therefore, the precipitation increase will largely offset the impact of warming in northern basins. It is also expected that the response of hydrological processes in different latitudes to the same climatic change will differ.

5.2 Sensitivity of Mountain Streamflows to Annually Perturbed Climate

Snowpack change and variability in mountains due to climatic changes can lead to runoff change and variability. Streamflow simulations are sensitive to changes in the entire range of hydrological processes and water balance components. Streamflow in WCRB shows a different response to changes in precipitation under warming than peak SWE. Under temperature increases of up to 4°C, annual mean discharge does not decrease in either low or high flow years from the current climate when precipitation increases by 20%. With 5°C of warming and 20% greater precipitation, low flows increase but high flows decrease compared to discharge under the current climate. The overall change in annual total runoff over the 18 years of simulation for WCRB, 9 years for MCRB, and 25 years for RME is shown in Figure 5.10. Change in annual runoff contrasts with the change in mean annual peak SWE (Figures 5.1, 5.2, and 5.3) in that it is more sensitive to precipitation than temperature. A 1°C increase in temperature in WCRB results in a 4% decrease in the annual runoff; decreases grow to 14% for a 5°C temperature increase (Figure 5.10a). The combination of 5°C of warming and 20% decreased precipitation in WCRB reduces simulated annual runoff by 44%, from 171 mm in the current climate to 96 mm. The sensitivity of runoff to temperature is because of the longer snow-free season and increased energy for evapotranspiration with increasing temperature. This is illustrated by the 45 mm increase in the annual actual evapotranspiration with 5°C of temperature rise (Appendix A). An 8% increase in precipitation is necessary to offset the impact of warming by 5°C on streamflow discharge from WCRB.

Simulated annual total runoff is more sensitive than snow regime to precipitation change in WCRB and the impact of up to 5°C of warming on annual runoff could be offset by an increase in precipitation of 8%. The uncertainty in the direction of change in precipitation causes uncertainty about the future hydrology of WCRB. A 5°C temperature increase can cause a 44% decrease in streamflow if precipitation declines by 20%, a 14% decrease if precipitation does not change, and a 20% increase in streamflow if precipitation increases by

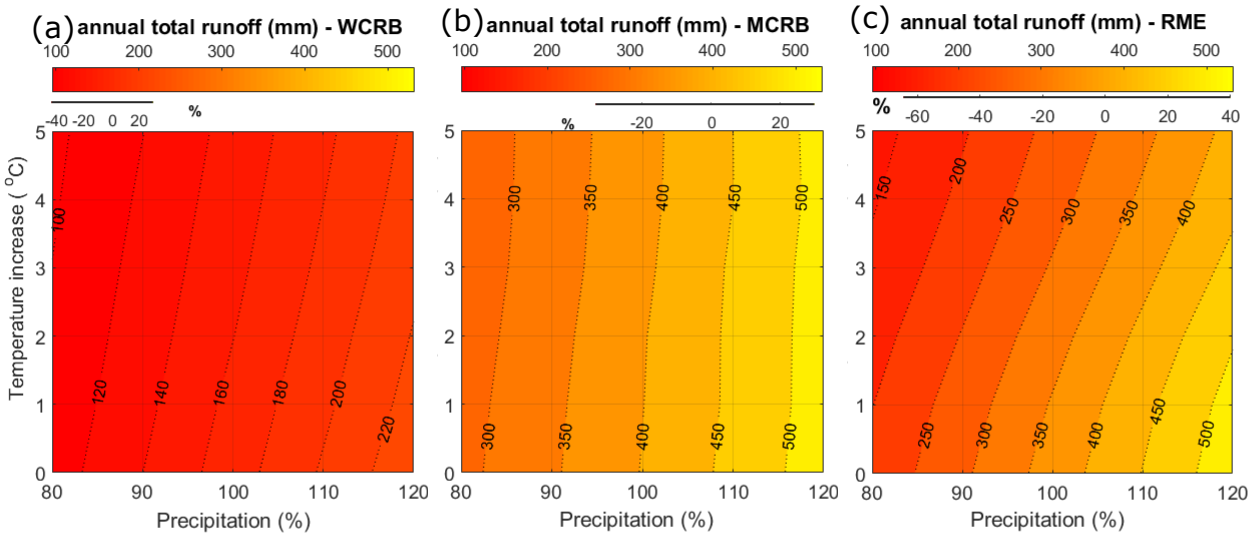

Figure 5.10: Sensitivity of mean annual runoff to increases in air temperature and changes in precipitation in (a) Wolf Creek Research Basin at the Alaska Highway, (b) outlet of Marmot Creek Research Basin, and (c) outlet of Reynolds Mountain East. Contours of the simulated annual total runoff were obtained from the model runs for 30 combinations of the warming and changes in precipitation and were averaged over simulation period.

20% (Figure 5.10b). The combination of climate warming and decreased precipitation causes larger declines in streamflow, but if precipitation increases there is some compensation. For instance, if precipitation increases by 20% then flow volumes increase 23% and peak runoffs remain nearly constant even with 4°C of warming.

In contrast to the equal response of the snowpack to both warming and precipitation change in MCRB (Figure 5.2), annual total runoff shows a stronger response to precipitation change and a smaller response to warming. The overall change in annual runoff over the 9 years of simulation is shown in Figure 5.10b. A 5°C increase in temperature results in a 4% decrease in the annual total runoff. The combination of 5°C of warming and 20% decreased precipitation reduces annual total runoff by 34%, from 402 mm in the current climate to 267 mm. Annual total runoff is sensitive to precipitation in MCRB because a large fraction of snowfall converts to rainfall, which contributes more to runoff. Therefore, change in total precipitation affects rainfall more than snowfall and runoff responds more quickly to rainfall than snowfall. A 3% increase in precipitation is necessary to offset the impact of warming

by 5°C on annual total runoff from MCRB.

In contrast to stronger response of snowpack to warming in RME (Figure 5.3), streamflow responds equally to both precipitation change and warming. The overall change in annual runoff over the 25 years of simulation is shown in Figure 5.10c. A 5°C increase in temperature results in a 29% decrease in the annual runoff. The combination of 5°C of warming and 20% decreased precipitation reduces annual runoff by 65%, from 371 mm in the current climate to 131 mm. In contrast to the sensitivity of snowpack to warming, annual runoff is less sensitive and the impact of warming can be partly offset by an increase in precipitation in RME. This is due to more snowfall conversion to rainfall under warmer climate that leads to a shallower snowpack and reduced sublimation from the snowpack and more rain-on-snow events. A 14% increase in precipitation is necessary to offset the impact of 5°C warming on streamflow discharge from RME.

Annual peak runoff is also important from a hydrological perspective. The performance of the models used in this research in capturing magnitude and timing of the peak values is fair. Therefore, one needs to be cautious when interpreting the results for timing and peak changes under climate changes. Figure 5.11a shows that annual peak runoff in WCRB increase proportionately more than changes in precipitation, demonstrating a high sensitivity of streamflow to changes in precipitation. Peak runoff timing advances in WCRB under most combinations of changed precipitation and warming (Figure 5.11b). For the combination of 2°C warming and 20% increased precipitation, peak streamflow advances 4 days and increases by 11%. Warming of 2°C and lower precipitation cause a reduction in peak flow; precipitation decreases of 10% and 20% cause decreases in peak flow rates by 25% and 35%, respectively. Increases in temperature in WCRB tend to reduce peak flows by desynchronising melt through accelerating the timing of spring flows (Table 5.2) and reducing summer and fall flows, as actual evapotranspiration increases in the longer snow-free period. The impact on peak flow rates of warming by 2°C and 4°C can be offset by increases in precipitation of 10% and 20%, respectively. With warming up to 5°C and a greater than 10% increase in precipitation, streamflow volumes increase.

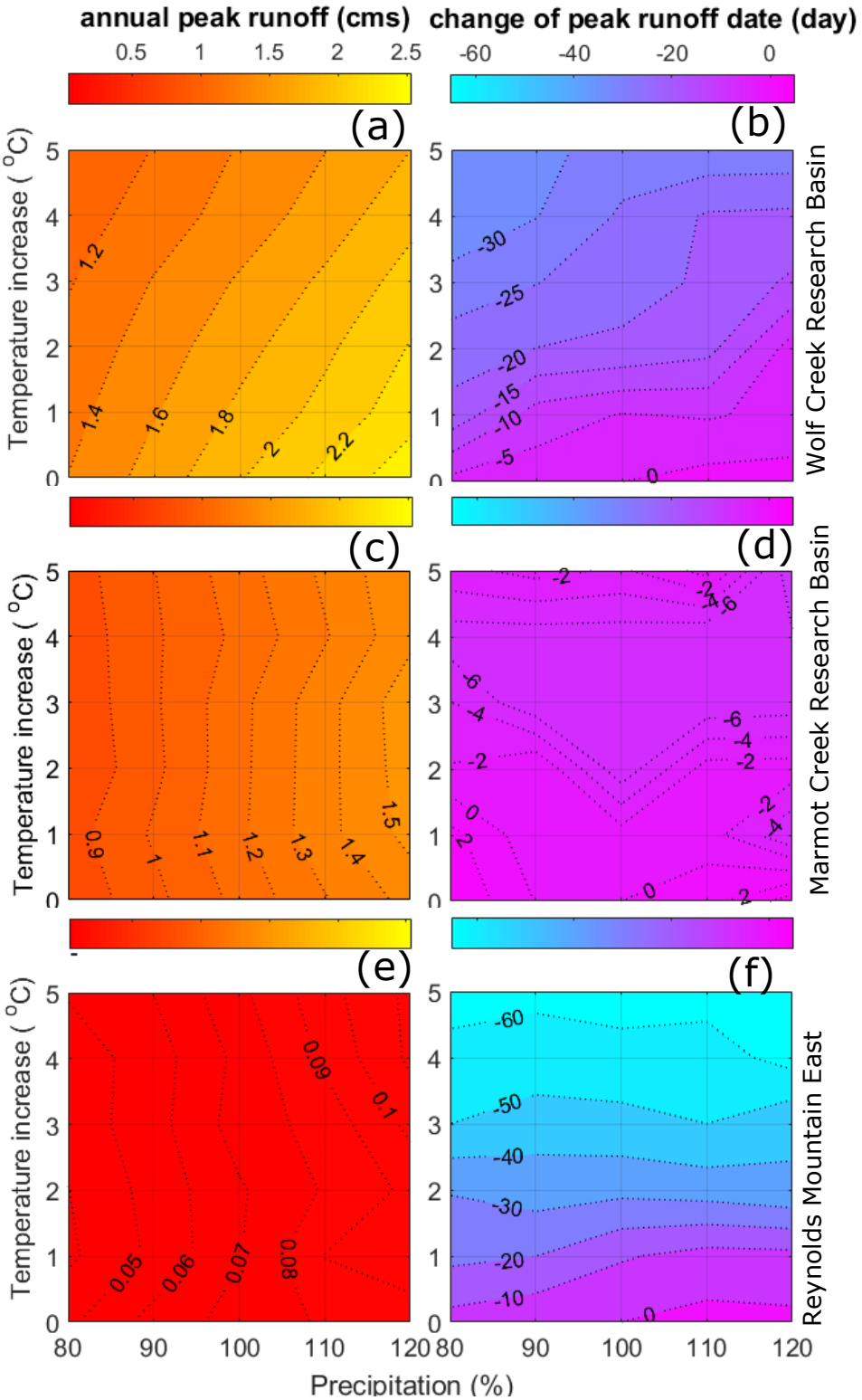

Figure 5.11: Sensitivity of mean annual peak runoff rate and date change at outlets of WCRB, MCRB, and RME with increases in air temperature and varying precipitation (30 scenarios, corners of the grids). Mean annual peak runoff for each scenario was obtained over the simulation period (1993–2011 for WCRB, 2005–2014 for MCRB, and 1983–2008 for RME). Negative signs in the peak runoff date plot represent advances in time and positive signs show the delays in peak runoff.

Figure 5.11c shows that peak streamflows in MCRB are sensitive to changes in precipitation (even more than WCRB) and almost insensitive to increases in air temperature. Peak runoff timing changes slightly with changes in precipitation and warming advances irregularly up to 9 days under most combinations of changed precipitation and warming (Figure 5.11d). For the combination of 2°C warming and 20% increased precipitation, peak streamflow advances 1 day and increases from 1.13 m^3s^{-1} to 1.55 m^3s^{-1} (38% increase). Warming of 2°C and lower precipitation cause a reduction in peak flow in MCRB; precipitation decreases of 10% and 20% cause decreases in peak flows of 14% and 29%, respectively. Figure 5.11e shows that peak streamflows in RME increase with increases in precipitation. Peak runoff timing advances up to 64 days under warmer and wetter scenarios (Figure 5.11f). For the combination of 2°C warming and 20% increased precipitation, peak streamflow advances 39 days and increases by 25%. Warming of 2°C and a lower precipitation cause a reduction in peak flow; precipitation decreases of 10% and 20% cause a decreases in peak flow rates of 28% and 46%, respectively. In contrast to the magnitude of the annual peak runoff, changes in timing of the peak runoff are driven by warming. The combined impact of warming, early freshet, and increased precipitation causes an increase in RME peak runoff.

5.2.1 Similarities and Differences Between the Three Basins in Response to Annually Perturbed Climate: Streamflow

Annual total runoff changes and peak runoff magnitude and timing under different scenarios of warming and changes in precipitation are given in Table 5.2. Annual total runoff responds strongly to precipitation changes in MCRB, to warming in RME, and to both precipitation and air temperature changes in WCRB. The annual runoff is the most resilient in MCRB and most sensitive to climate changes in RME. Under 5°C and a 20% increased precipitation, annual peak runoff decreases from 4.1 m^3s^{-1} to 3.7 m^3s^{-1} (9%) in WCRB and increases from 1.13 m^3s^{-1} to 1.49 m^3s^{-1} (28%) in MCRB and from 0.074 m^3s^{-1} to 0.112 m^3s^{-1} (50%) in RME (Table 5.2). This shows that increased precipitation with warming increases the high

Table 5.2: Sensitivity of streamflow characteristics to warming and changes in precipitation in the three basins along the North American Cordillera (NAC). The streamflow characteristics include magnitude of annual total runoff and annual peak runoff and timing of peak runoff, rising and falling limbs, and length of flow season. The day of the water year starts from October 1st.

Variable		control	warm	warm	warm	–	warm
		period	–	–	dry	wet	wet
Warming [°C]		0	2	5	5	0	5
Precipitation [%]		100	100	100	80	120	120
(1) Wolf Creek Research Basin (WCRB)							
Total annual	[mm]	171	160	147	96	236	206
Annual Peak	[cms]	4.1	3.6	2.9	2.1	5.3	3.7
Rising flow	[date]	Mar-09	Feb-16	Jan-27	Jan-02	Mar-10	Jan-27
Peak date	[date]	Jun-20	Jun-01	May-24	May-20	Jun-22	May-23
Recession end	[date]	Sep-18	Sep-02	Sep-08	Sep-05	Sep-22	Sep-01
Season length	[day]	193	197	225	246	196	217
(2) Marmot Creek Research Basin (MCRB)							
Total annual	[mm]	402	397	384	270	527	518
Annual Peak	[cms]	1.13	1.17	1.16	0.82	1.43	1.49
Rising flow	[date]	Jan-03	Dec-15	Jan-28	Feb-05	Jan-04	Dec-27
Peak date	[date]	Jun-10	Jun-03	Jun-08	Jun-06	Jun-15	Jun-01
Recession end	[date]	Sep-19	Sep-09	Sep-04	Sep-02	Sep-13	Sep-02
Season length	[day]	259	269	219	209	252	250
(3) Reynolds Mountain East (RME)							
Total annual	[mm]	371	331	263	161	533	415
Annual Peak	[cms]	0.074	0.069	0.078	0.044	0.088	0.112
Rising flow	[date]	Feb-02	Dec-17	Nov-28	Dec-19	Jan-19	Nov-18
Peak date	[date]	May-18	Apr-15	Mar-14	Mar-29	May-20	Mar-15
Recession end	[date]	Sep-23	Sep-25	Sep-24	Sep-24	Sep-23	Sep-24
Season length	[day]	233	283	300	280	246	310

flows in the southern basin more than the northern and central basins. This is due to more snowfall conversion to rainfall at low latitudes. Under warmer conditions, snow melts earlier but slower in WCRB, which leads to an earlier annual peak runoff. Changes in the timing of annual peak runoff affect runoff intensity. Under climate change, peak runoffs occur earlier and with less intensity.

The response of annual peak runoff to precipitation changes becomes stronger moving from the south to the north of the NAC. In contrast to the two northern basins, the impact of precipitation increase on annual peak runoff in RME is enhanced by the impact of warming. Peak runoff increases up to 52% and advances two months under 5°C warming and 20% increased precipitation (Table 5.2, Figure 5.11) as basin climate shifts from snow-dominated to rain-dominated and the freshet is two months earlier. Snowpack has lower spatial variability (Figure B.3) and higher spring variability (Figure B.2) under warmer and wetter conditions. This saturates the soils, which leads to runoff increase in spring. The magnitude of annual peak runoff is affected by precipitation changes while date of annual peak runoff is affected more by warming in all three basins. Advancing the peak runoff timing in spring when deep snow is on the ground and an increase in rainfall rather than snowfall enhances peak runoff in both MCRB and RME. Peak runoff in WCRB, however, responds differently: it decreases as air temperature increases and earlier snowmelt shifts toward a lower irradiance time of the year and it increases with precipitation increase if increased precipitation can offset the warming effect. In this basin, precipitation increase does not necessarily increase rainfall and runoff during the time of peak flows.

5.2.2 Offsetting Warming Effect by Precipitation Change

How much precipitation increase is needed to offset the warming effect on peak snowpack, annual total runoff, and annual peak runoff under future climate can be estimated from this sensitivity analysis. Figure 5.12 shows that, when warming is limited to 2°C, increased precipitation of 10% is able to offset the effect of warming in WCRB and peak snowpacks increase; but, with warming of 5°C, peak snowpacks decrease in all scenarios even with an

increased precipitation of 20%. In MCRB, the impact of a 1°C warming on peak snowpack can be offset by an 8% increase in precipitation. In RME, the impact of a 1°C warming on peak snowpack can be offset by a 16% increase in precipitation. Maximum projected precipitation increase by RCM–GCMs is 34% in WCRB, which is sufficient to offset the 5°C warming effect on peak snowpack. Maximum projected precipitation increases in MCRB and RME are 18% and 16%, respectively, which are not sufficient to offset the ≥ 3°C and ≥ 2°C warming effect on mean annual peak SWE in MCRB and RME, respectively.

Annual total runoff is not as sensitive as peak snowpack to warming and an increased precipitation of $\leq$8% in WCRB, $\leq$3% in MCRB, and $\leq$14% in RME can offset the effect of 5°C warming. These differences are due to varying fractions of snow to rain conversions in each basin under warmer climate. Deep snowpacks at high elevations in MCRB melt faster, which can increase overland flows under warmer conditions. Therefore, annual peak runoff can remain within the range of recorded values in MCRB and even a 2% in precipitation does not affect the high flows. In the north, precipitation must increase 20% to offset the effect of warming up to 3°C on peak snowpack and peak annual flows. The precipitation role in offsetting the impact of warming on total annual runoff becomes less effective in the south of the NAC as a 14% increase in precipitation in RME is needed to offset the impact of warming by 5°C on annual runoff, while precipitation increases of 8% in WCRB and 3% in MCRB are needed (Figure 5.12). The role of precipitation in offsetting the impact of warming on peak runoff is opposite to that of annual total runoff.

5.3 Discussion

Snow hydrology in mountains has a strong sensitivity to "loss of cold", which is connected to large decreases in snowpack with warmer temperatures. The proportional drop in peak snow accumulation is closely reflected in the proportional drop in annual total runoff in WCRB and MCRB, highlighting the importance of correctly estimating changes in snowpack when assessing changing hydrology in these two basins. Although the MCRB snow regime is as sensitive as the snow regime in WCRB to warming and a decrease in precipitation, its

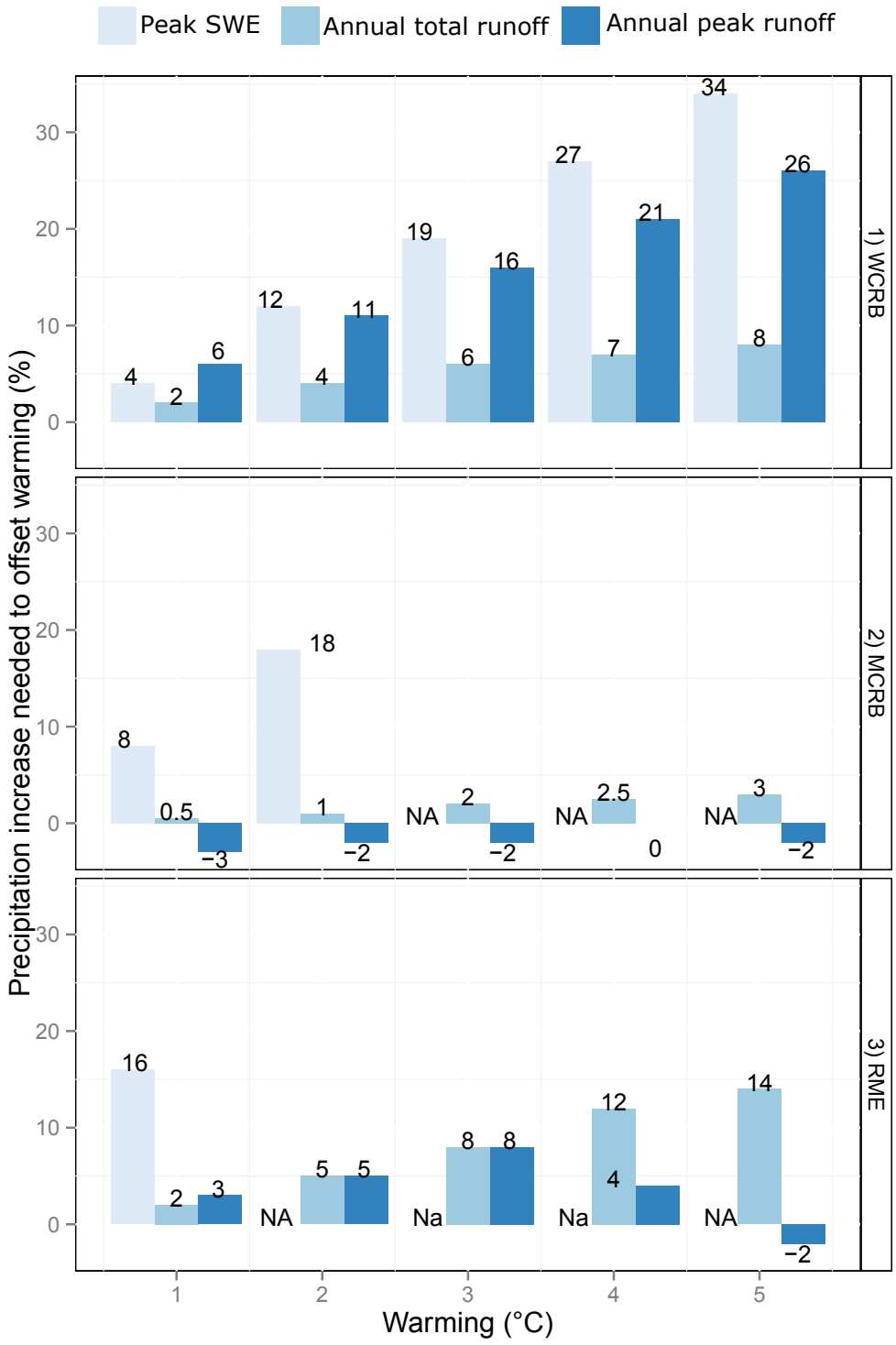

Figure 5.12: Percentage of precipitation change is needed to offset warming effect on peak snow water equivalent (SWE), annual total runoff, and annual peak runoff based on sensitivity analysis in the three headwater basins across the North American Cordillera. The highest possible increase in precipitation projected by NARCCAP RCM–GCMs is 34% for WCRB, 18% for MCRB, and 16% for RME. Because of insufficient increase in precipitation, effects of a ≥ 3°C warming in MCRB and a ≥ 2°C warming in RME (denoted by NA) on mean annual peak SWE cannot be offset.

streamflow regime is less sensitive than the streamflow regime in WCRB. This is because of the higher resiliency of the MCRB snowpack to changes at high elevations and in the blowing snow sink zone of the treeline in which a deep snowpack is deposited. The snowpack lasts longer on the ground at high elevations in MCRB, which moderates the impact of snow loss at low elevations on streamflow. A high elevation band with air temperatures similar to that in low elevations in WCRB and a rainy environment in spring and summer explain why the drop in peak snow accumulation is not reflected by a proportional drop in annual streamflow volume in MCRB. This highlights the role of the spatial redistribution of snow on heterogeneous hydrological responses at different elevations in MCRB. The snow and streamflow regimes are the most sensitive to warming in RME because of the (i) higher annual mean air temperature, (ii) near-freezing air temperatures in winter, and (iii) fewer number of days with freezing temperatures (120 days a year). Under moderate warming, much of the precipitation is converted from snow to rain and causes a large decrease in SWE and runoff in RME.

Snowpack reduction per degree increase of temperature is 7.5% in WCRB, 10% in MCRB, and 17% in RME. Snowpack loss per degree increase of temperature in WCRB is similar to reduction in the Svalbard Archipelago ($\approx 79^\circ$ N, López-Moreno et al., 2016). Snowpack loss in MCRB is in the range of 11–20% reduction reported for the Pyrenees (López-Moreno et al., 2013, 2014) and comparable to a 15% reduction reported for the Swiss Alps (Beniston et al., 2003). Snow loss per degree of warming in RME is similar to a 20% reduction reported for the Washington Cascades (Casola et al., 2009). This shows that findings in this research are consistent with other basins with similar climates and that climate change affects snowpack in mountain basins across the globe with large reductions at mid-latitudes and relatively small reductions at high latitudes. The impact of warming of 1°C on SWE values over the winter and spring seasons can be offset by a precipitation increase of 20% for almost all SWE values in all snow regimes in RME. However, warming of 2°C or more cannot be offset by increases in precipitation of less than 20%. The sensitivity of SWE in the blowing snow source and sink HRUs to warming is higher than that in the forested intercepted snow and sheltered forest gap HRUs; this is due to suppression of blowing snow redistribution processes

by warming. The low temporal variability in the forest gap and blowing snow sink SWE from December to May relative to other sites shows how snow regimes in small forest clearings and snow drifts are relatively stable and not representative of the natural temporal variability of snow regimes in exposed source or forest zones. The sheltered HRU in RME catchment has insignificant snow redistribution processes and shows the least response to warming. The locations of United States Department of Agriculture (USDA) SNOTEL sites are usually in forest gaps, which may have implications for the ability of the SNOTEL network to detect and fully represent the dynamics involved in changing basin snow hydrology due to climate change.

Hydrological responses in different regions vary with latitude under the same climatic change. For instance, for every 3°C warming increase in WCRB, 2°C in MCRB, and 1°C in RME, an increase of 20% in precipitation is needed for the peak snowpack to remain equal to that under current climate conditions. López-Moreno et al. (2016) also found that, for 5°C warming, a 25% increase of precipitation is needed to offset the warming effect on snowpack in the Svalbard Archipelago ($\approx 79^\circ$ N). This suggests that the role of precipitation as a compensator for the warming impact becomes less effective from mid-latitudes toward high latitudes. In WCRB ($\approx 61^\circ$ N), not only higher warming but also an increase in precipitation is expected (Graversen et al., 2008), which indicates that precipitation increase could partly offset the impact of warming on cold regions hydrology. Despite the uniformity of high mountain climates and similar response per one degree increase in temperature, the implication of these results is that mountain snow regime responses to climate change differ substantially, as noted for the three basins across North America studied here, and therefore regional analysis is required. The great difference between snowpack response in RME and WCRB implies that warming in cool climates impacts the maximum accumulated snowpack more than it does in cold climates. Warming affects the phase of precipitation, causing a shift from snowfall to rainfall in the spring and fall transition seasons and a shift from March to January in RME and less than a month in WCRB and MCRB for timing of peak snow accumulation. As the rainfall to precipitation ratio increases, advective and turbulent fluxes (e.g., sensible and latent heat) associated with rain-on-snow events (Marks et al., 1999)

might facilitate more rapid snowmelt in the cool mountain climate of RME, the cold climate of MCRB, and the cold sub-Arctic climate of WCRB. Warming and accelerated rain–snow processes can accelerate the initiation of snowmelt in RME, as the melt period is shifted forward into a lower solar irradiance period. Despite this effect, snowmelt ends earlier as temperatures increase and the snow season shortens. The impacts of warming on snowpacks can be partly offset by a precipitation increase in the cold WCRB and MCRB climates but not in the cool RME climate. The snow season is expected to shorten by about 2 months in the sub-Arctic WCRB, 1.5 months in the cold MCRB, and 5 months in the cool RME basin with concomitant warming and a decline in precipitation. This implies that, if warming occurs, the sensitivity of the snow hydrology to a precipitation increase changes with latitude from almost insensitive in RME to sensitive in WCRB. However, the snow hydrology is sensitive to warming and precipitation phase change in the southern basin and is relatively resilient in MCRB.

5.4 Summary

Annual perturbations of hourly air temperature and precipitation were used to investigate the sensitivity of snow and streamflow regimes modelled for the study sites. Consistent with the ideal gas law, relative humidity was held constant to allow water vapour pressure to change with temperature. The combination of a severe climate warming and decreased precipitation in all three basins causes declines in SWE and a shortened snow-covered period, which result in decreases in annual total runoff and average annual peak flow. The decrease in depth and advance in timing of peak snowpack are reflected in streamflow simulations in each basin. If precipitation decreases with warming, the impacts on snowpack multiply. This would have major implications for ecology, winter transportation, and hydrology. The smaller snowpacks and warmer weather would cause an increase in the snow-free period, which lengthens the evapotranspiration (ET) season, increases the annual ET loss, and increases the importance of rainfall–runoff mechanisms. Under changed climatic conditions, annual total runoffs and average annual peak flow rates decrease. Increased precipitation can partially offset the

warming impact on snow and total runoff. The role of precipitation as a compensator for the warming impact becomes less effective from mid-latitudes toward high latitudes. An annual perturbation in the proposed climate sensitivity analysis (Chapter 3 was applied in this chapter. Incorporating monthly variability of the future climate can show monthly variability of the future hydrological fluxes. This is investigated in Chapter 6.

Chapter 6

HYDROLOGICAL SENSITIVITY TO MONTHLY PERTURBED CLIMATE

This chapter presents results addressing the second objectives of this research. Objective two of the thesis includes documenting uncertainty in future hydrological processes due to uncertainty in climate models. Mountain basins and cold regions, which have long snow-covered periods and large snowmelt contributions to streamflow, are sensitive to warming and changes in precipitation (Rouse et al., 1997; Stewart et al., 2004) and their hydrological response may vary with the basin's elevation, slope, aspect, latitude, distance from an ocean, and vegetation. In temperate mountainous regions, where air temperature remains near freezing, small temperature perturbations can result in considerable snowpack loss, especially in subalpine biomes.

6.1 Climate Change Impacts on Mountain Hydrology

Based on North American Regional Climate Change Assessment Program (NARCCAP) RCM–AOGCM combinations, none of the climate models could capture the meteorological variables very well over the mountain basins. Part of this can be associated with elevation differences between climate model grid and site in which the measurements were collected. Table 6.1 shows the elevation differences between RCM–AOGCM grids that cover the basins and a weather station in each basin that matches the grid elevation most closely. The elevation biases between RCM grids and weather stations are not small; however, even when the elevation bias is small (e.g., 76 m between Hay Meadow station in Marmot Creek Research

Table 6.1: Elevation bias between RCM grids and a representative station in each of the three basins along the North American Cordillera

Basin	**Weather station**	**RCM**	**RCM grid elevation (m)**	**Station elevation (m)**	**elevation bias (m)**
WCRB	Alpine	WRFG	1163	1760	–597
		CRCM	1107		–653
		RCM3	1112		–648
		MM5I	1163		–597
		HRM3	1100		–660
		ECP2	1102		–658
MCRB	Hay Meadow	WRFG	1868	1436	432
		CRCM	2065		629
		RCM3	1654		218
		MM5I	1868		432
		HRM3	2298		862
		ECP2	1512		76
RME	Exposed site	WRFG	988	2094	–1106
		CRCM	1017		–1077
		RCM3	1336		–758
		MM5I	988		–1106
		HRM3	1389		–705
		ECP2	1179		–915

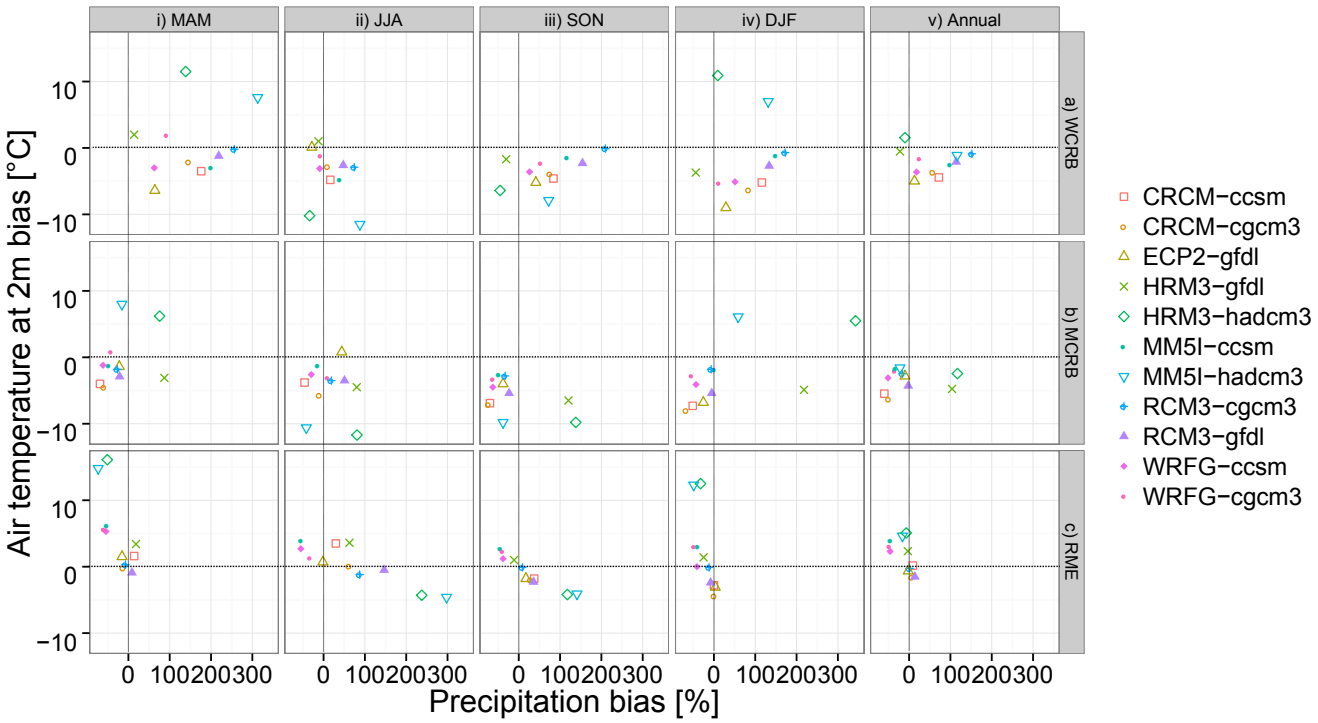

Figure 6.1: Seasonal and annual biases for air temperature and precipitation of current climate (1971–2000) from 11 combinations of NARCCAP regional and global climate models against local observations across the North American Cordillera

Basin (MCRB) and its associated ECP2 grid), the bias between observation and modelled air temperature and precipitation is large. The bias for air temperature and precipitation between regional climate model (RCM) outputs and locally observed data in the mountainous regions is plotted in Figure 6.1. The air temperature bias between climate model outputs and observations reaches 6°C in the annual step and 16°C in spring. The annual and seasonal precipitation biases increase from Reynolds Mountain East (RME) toward Wolf Creek Research Basin (WCRB), except for the summer. The annual precipitation biases in WCRB and MCRB are about an order of magnitude for some RCMs and the seasonal precipitation bias can be up to 300%. High seasonal and annual biases make NARCCAP products not directly applicable for hydrological modelling. Amongst all of the RCMs, HRM3–GFDL for WCRB, MM5I–CCSM for MCRB, and RCM3–CGCM3 for RME show the lowest annual and seasonal biases when compared with local precipitation and temperature data. The MM5I RCM driven by HadCM3 has the poorest performance in capturing the meteorological observations for all of the basins.

The future time series for assessing climate change impacts can be obtained based on bias correction and statistical–dynamical downscaling methods or alternatively by perturbing current climate with delta changes in the monthly climatology. In this section, the current hydrology of the three basins was compared to the response to a MPC that was introduced in Chapter 3. Because of the large biases in capturing the current climate by RCMs, changes in monthly climatology between current and future climate variables (Figures 6.2 and 6.3), along with the hourly observed data for precipitation, air temperature (at 2 m above the ground), relative humidity, and wind speed, were used in this study. The changes in monthly climatology are applied to further capture the variability in the climate variables. Based on NARCCAP's RCMs, changes in annual climatology obtained for the future climate (2041–2070) and current period (1971–2000) for annual precipitation (P) are over 2% and for air temperature (Ta) are greater than 2°C. Changes in annual climatology reached 16.3% for P and 2.6°C for Ta in WCRB, 6.6% for P and 2.2°C for Ta in MCRB, and 2.3% for P and 2.4°C Ta in RME (Figure C.11). The 11 RCM–GCM combinations used in this research are not fully independent ensemble members and some of them have similar dynamical cores, physics-dynamics coupling, and shared development history (e.g., RCMs driven by CGCM3 and GFDL).

Warming variability is high in spring and has an important controlling role in snowmelt rates. With variable warming conditions, higher uncertainties in spring streamflow are expected in the future. Snow and ice feedbacks, which are active in the lower atmosphere, are responsible for warming in spring, while atmospheric heat transport into the Arctic is the main mechanism for warming in summer (Graversen et al., 2008). It is expected that winter (December to February, DJF) warming will reach 2.5°C in MCRB and RME. The winter warming in the northern basin is expected to be affected by regional warming at high elevations and reach 3.5°C (Figure C.11) by 2070. This is consistent with "Arctic Temperature Amplification" caused by high phases of ocean and atmosphere circulations such as the Arctic Oscillation (AO) and changes in cloud, snow, and ice cover (Thompson and Wallace, 1998). Higher rates of warming well above the surface in the northern regions

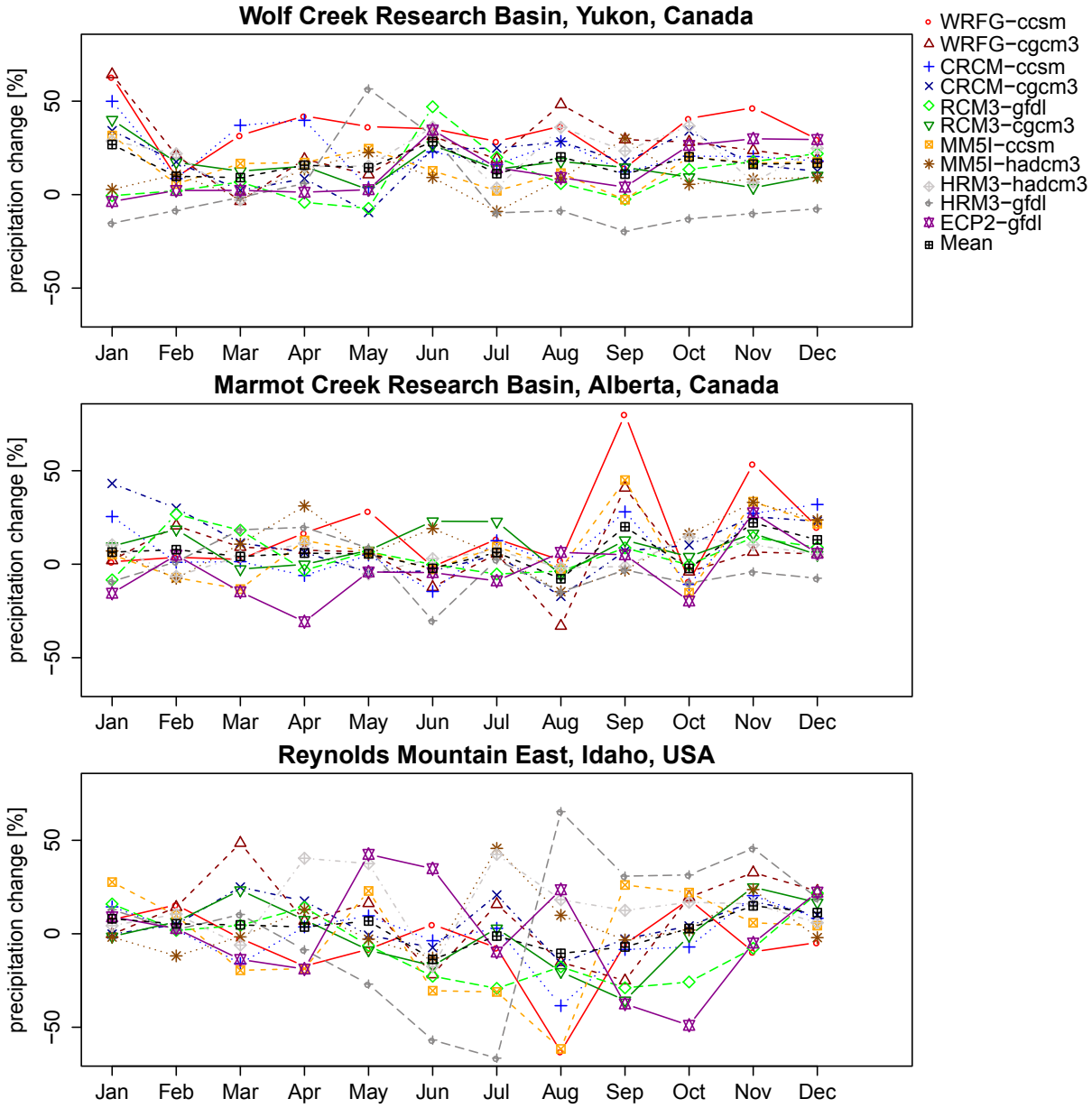

Figure 6.2: Monthly (30 daily) changes (deltas) in climatological precipitation obtained from all of the RCM–GCM combinations for the three basins across the North American Cordillera

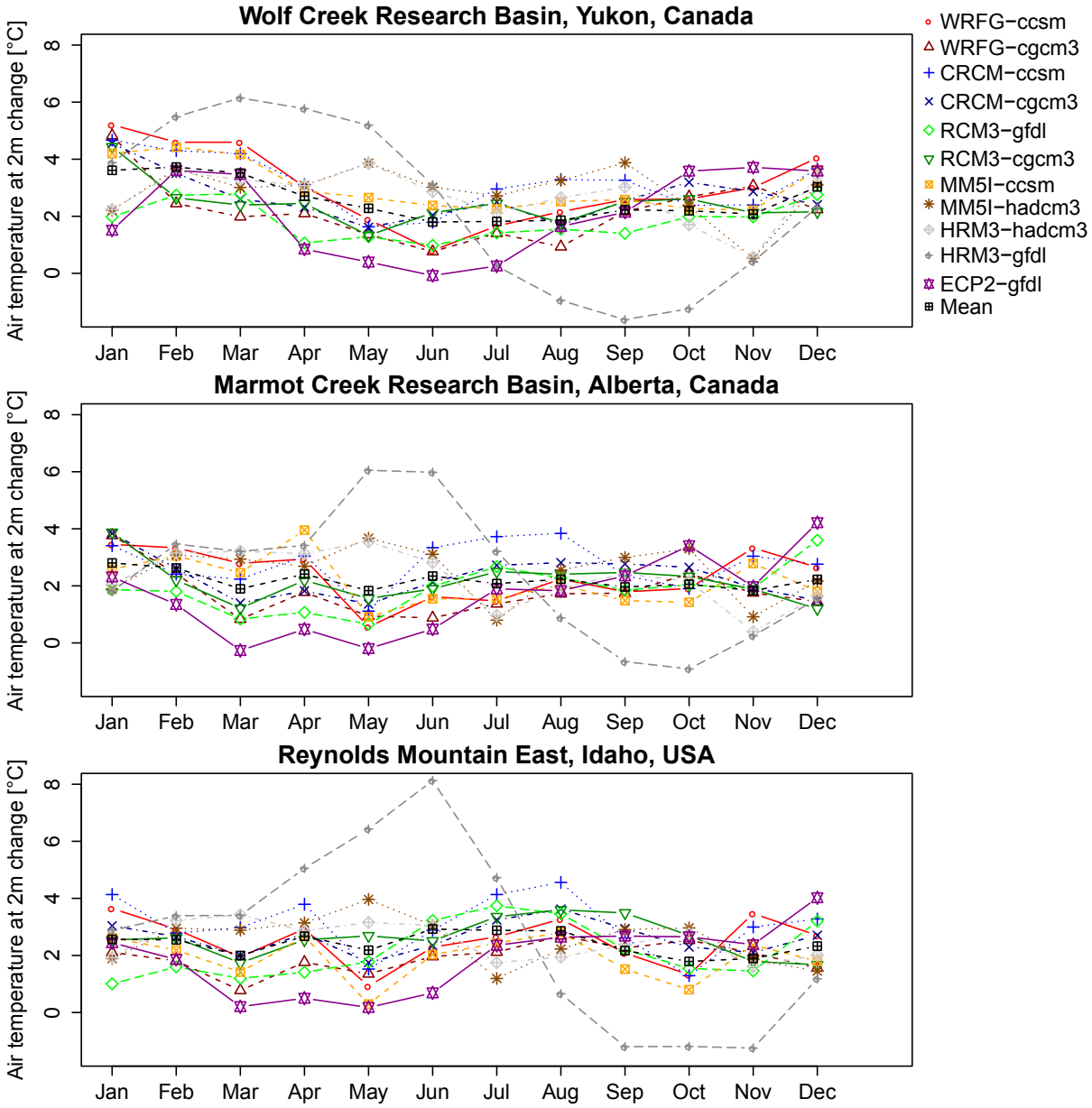

Figure 6.3: Monthly (30 daily) changes (deltas) in climatological air temperature obtained from all of the RCM–GCM combinations for the three basins across the North American Cordillera

(Graversen et al., 2008) are expected as sea ice becomes thinner and snow recedes in the northern latitudes. Albedo changes and increased refreezing of sea-ice in winter increase the heat and moisture transport from ocean to atmosphere and from atmosphere to Arctic (Graversen et al., 2008).

Examining the effect of warming and its seasonal fluctuations on hydrological processes in mountains will help to understand the response of snow and streamflow regimes. The processes used in the CRHM platform for each of the basins in the NAC are (see Chapter 3): theoretical global radiation, direct and diffuse solar radiation, short-wave radiation on the slope, incoming long-wave radiation, snow albedo, snowfall and rainfall interception on the canopy, unload/drip/sublimation/ evaporation from the forest canopy, sub-canopy snowfall and rainfall, sub-canopy radiation and turbulent transfer to snow, inter-HRU wind redistribution of snow, blowing snow sublimation losses, energy balance snowmelt, infiltration into frozen and unfrozen soils, actual evapotranspiration, soil moisture balance, depressional storage, surface/ sub-surface flows, groundwater discharge, lag and route timing, ground surface temperature, thawing, and freezing. Changes in the water, snow, and vapour fluxes and hydrological processes in cold regions are investigated to understand changes in discharge from the headwater basins.

6.2 Climate Change Impacts on Snow Regimes

The snowpack response to a MPC is compared against the control period. Figure 6.4 illustrates monthly variability of snow water equivalent (SWE) in different biomes across the NAC: alpine, shrub tundra, and forest biomes in WCRB; alpine, treeline, forest, and forest clearing (Gap) biomes in MCRB, and four biomes in RME including alpine representing blowing snow source (covered with grass and short mountain sage), blowing snow sink (valley bottoms and depressions with drifted snow), forest with intercepted snow, and a circular forest clearing (gap sheltered from blowing snow).

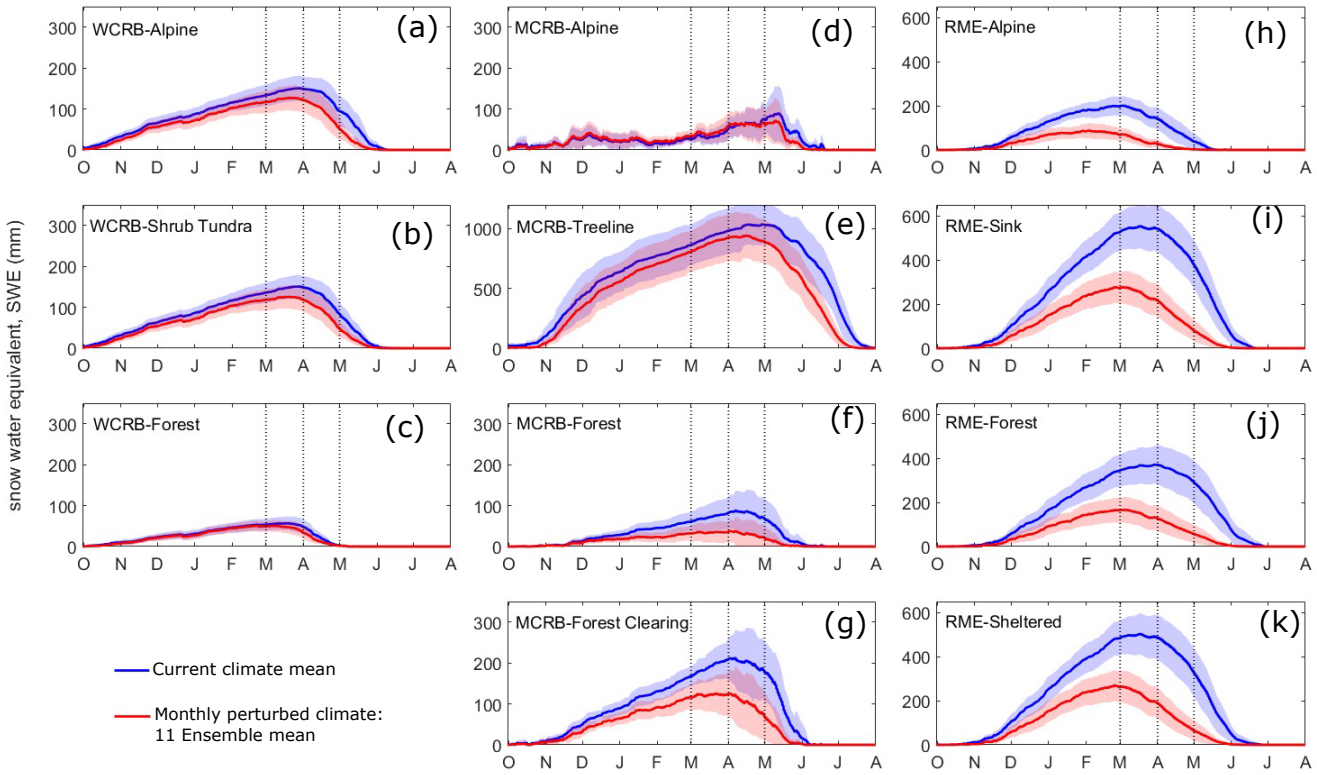

Figure 6.4: Snow accumulation and ablation under current and monthly perturbed climates in different biomes (a,b, c) in Wolf Creek Research Basin (WCRB) – Yukon Territory, (d, e,f, g) Marmot Creek Research Basin (MCRB) – Alberta, and (h, i, j, k) Reynolds Mountains East (RME) – Idaho along North American Cordillera. The y-axis has different scales for different subplots. The shaded area around the mean shows the interannual variability with ±95 confidence intervals. Mean response to ensemble of 11 RCM–GCMs is selected to study interannual variability in the future climate. The ensemble uncertainty is not shown. Slope of snow water equivalent curve during melt season under warmer climate (red line) is lower than current climate (blue line), which suggests a slower melt rate under warmer climate. This is because the melt period is shifted forward into a lower solar irradiance period.

Under MPC, the mean annual peak SWE decreases the most in the forest biomes in MCRB and RME with a large decline in MCRB from 88 mm to 38 mm (57%). In general, peak SWE in forests across the NAC drops 11–57% with a strong decline at low latitudes ($\approx 43^\circ$ N) and low elevations. The treeline in MCRB has the highest snow accumulation under current climate due to strong winds that scour snow from higher elevations to this zone. It also shows the highest resistance to climate change with only a 9% decline in the simulated peak SWE. A resilient alpine snowpack in MCRB leads to a minimum loss in water yield from the basin. This is because a higher SWE and a minimum sublimation loss due to climate change in this biome offset the negative effect of snow loss in other biomes. In contrast to the treeline in MCRB, all of the biomes in RME show an approximate 47% decline in maximum snowpack. This suggests that the reduction in the basin-scale peak SWE is high in RME but not in WCRB, where the reduction is small (Table 6.2). The RCM projections of the future climate (Figure C.11) show that WCRB anticipates the largest increase in warming and precipitation amongst the three basins, while RME is expected to experience only a small increase in precipitation under MPC. These heterogeneous climate changes across the NAC lead to a stronger response of the mean annual peak SWE in the southern basin and a resilient response in WCRB. In WCRB, the warming effect on the peak SWE is partly offset by the impact of precipitation increase (Rasouli et al., 2014). Not only is the magnitude of the mean annual peak SWE affected by climate change but also its timing. The peak SWE occurs 10 to 32 days earlier and snowcover season ends 13 to 33 days earlier in all three basins (Table 6.2). Interannual variability of the simulated SWE over 18 years in WCRB, 9 years in MCRB, and 25 years in RME is expressed as 95% confidence intervals (CI) in Figure 6.4. The interannual variability of SWE under MPC varies with latitude and elevation: it increases in biomes with blowing snow sink regimes such as shrub tundra in WCRB and treeline in MCRB, is almost unchanged in the alpine and forest biomes in WCRB and forest clearings in MCRB, and it decreases in lower forest in MCRB and all of the biomes in RME.

The mean annual peak snowpack in winter is important in terms of basin water yield. Changes in low and mean SWE values under monthly perturbed climate can also help to understand the snow seasonality and its distribution. Probability density functions for all

Table 6.2: Snow characteristics under current and monthly perturbed climates in the three basins along the western North American Cordillera. Bold values denote significant changes with p–values less than 0.05 based on the Mann–Whitney U-test. The simulated distributions with $n = 18$ years for WCRB, 9 years for MCRB, and 25 years in RMS over the control (Base) period for each hydrological variable are compared with the simulated future distributions obtained from 11 RCM–GCMs ($11 \times n$ values). Changes, which are relative to current climate and vegetation, are given in parentheses. The negative values represent advances in future timing while the positive values represent delays.

Variable	**Base**	**ΔClimate**		
		5%	**mean**	**95%**
(1) Wolf Creek Research Basin (WCRB)				
Peak SWE [mm]	133	73(–45)	118(–11)	153(15%)
Snow initiation [date]	Oct 5	Sep 31(–5)	Oct 7(2)	Nov 16(42 day)
Peak SWE timing [date]	Apr 4	Feb 20(–43)	**Mar 13(–22)**	Mar 27(–8 day)
Snow-free [date]	Jun 7	May 1(–37)	**May 23(–15)**	Jun 5(–2 day)
Season length [day]	224	160(–64)	**208(–16)**	242(18 day)
(2) Marmot Creek Research Basin (MCRB)				
Peak SWE [mm]	183	102(–45)	**141(–23)**	170(–7%)
Snow initiation [date]	Oct 9	Oct 4(–5)	**Oct 24(15)**	Dec 1(53 day)
Peak SWE timing [date]	Apr 29	Mar 26(–35)	Apr 18(–10)	May 4(6 day)
Snow-free [date]	Jul 21	Jun 14(–37)	**Jul 8(–13)**	Jul 22(1 day)
Season length [day]	283	204(–79)	**248(–35)**	277(–6 day)
(3) Reynolds Mountain East (RME)				
Peak SWE [mm]	368	105(-71)	**196(–47)**	277(–25%)
Snow initiation [date]	Nov 4	Oct 20(–15)	**Nov 19(15)**	Dec 26(50 day)
Peak SWE timing [date]	Mar 10	Jan 10(–59)	**Feb 6(–32)**	Feb 25(–13 day)
Snow-free [date]	Jun 3	Apr 2(–62)	**May 1(–33)**	May 22(–14 day)
Season length [day]	211	113(–98)	**161(–50)**	197(–14 day)

ranges of SWE (Figure 6.5) in the historical (control) period and under different perturbations present a platform to diagnose the changes in snow and streamflow regimes over mountainous basins. A large decrease in the future SWE values is suggested by the WRFG–CGCM3 model with a 41–58% decrease in peak snowpack. This model does not match well with other models in the sense that the snow response of this model is different. The average response of snow regimes to the changes given by all 11 ensemble members of RCMs (Figure 6.5) shows a large change in SWE values for all three basins, with the snow regime being the most sensitive to climate change in RME and the most insensitive in WCRB. In order to diagnose these changes, the sensitivity or resiliency in each biome in each basin is investigated.

Mean annual peak SWE is important with respect to generating high snowmelt runoffs and controlling the annual water yield changes over the mountains. Therefore, peak SWEs are examined in more detail in this chapter. The performance of the models used in this research in capturing magnitude and timing of the peak values is fair. Therefore, one needs to be cautious when interpreting the results for timing and peak changes under climate changes. Figure 6.6 illustrates the change in peak SWE in the alpine, shrub tundra, and forest biomes, along with outflow from WCRB under current climate and MPC. The annual maximum values are selected for each year in order to analyse the response of the snow and streamflow regimes to climate changes in wet, dry, and normal years. The interannual variability of peak SWEs under the current climate is high in the alpine and shrub tundra biomes and relatively small in the forest (Figure 6.6). The uncertainty of simulated peak SWE under MPC is also high in the alpine and shrub tundra biomes. The mean annual peak SWE decreases in the three biomes in WCRB with larger changes at high and low elevations. Even though the RCM ensemble mean suggests a decline in peak SWE across the WCRB, some of the RCM ensemble members suggest a slight increase in the peak SWE, especially in the forest biome. In a drier year with a low peak SWE (e.g., 2004), climate models project a substantial decline in the snowpack, which is reflected in the streamflows. This suggests that dry years in WCRB will have much lower snowpacks under MPC.

In contrast to WCRB, the maximum snowpack response to the changes in MCRB suggested

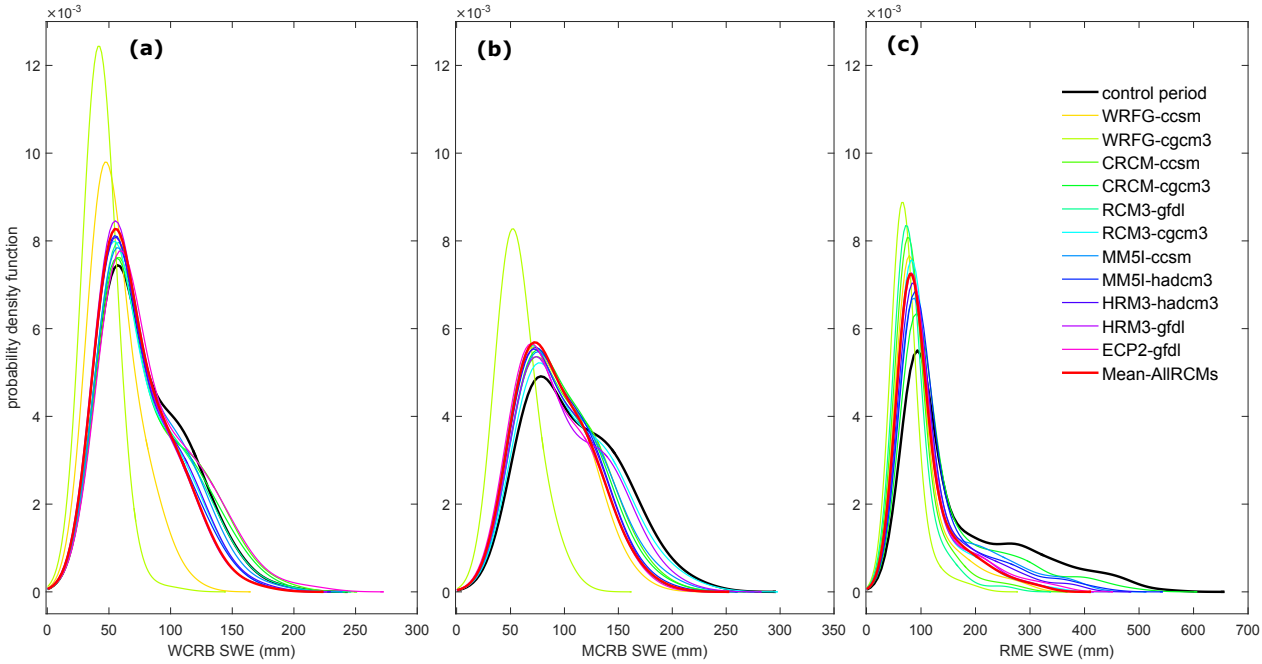

Figure 6.5: Differences in probability density functions of simulated snow water equivalent (SWE) in current and future climates in (a) Wolf Creek Research Basin (WCRB) – Yukon Territory, (b) Marmot Creek Research Basin (MCRB) – Alberta, and (c) Reynolds Mountains East (RME) – Idaho along the North American Cordillera. All 12 distributions of the simulated SWE under monthly perturbed climate in each basin are significantly (p–value < 0.05) different than the simulated SWE distribution in the control period based on the Kolmogorov-Smirnov (K–S) (Massey Jr., 1951). Future SWEs were simulated by the models applying change factors obtained from 11 RCM–GCMs and their ensemble mean to observed time series. The K–S test, which is a nonparametric hypothesis test, was used to evaluate the differences in hourly SWE distributions in control period (black line) and under perturbed climates (colored lines) over 25 years in WCRB, 9 years in MCRB, and 25 years in RME $\times$ 365 days $\times$ 24 hours.

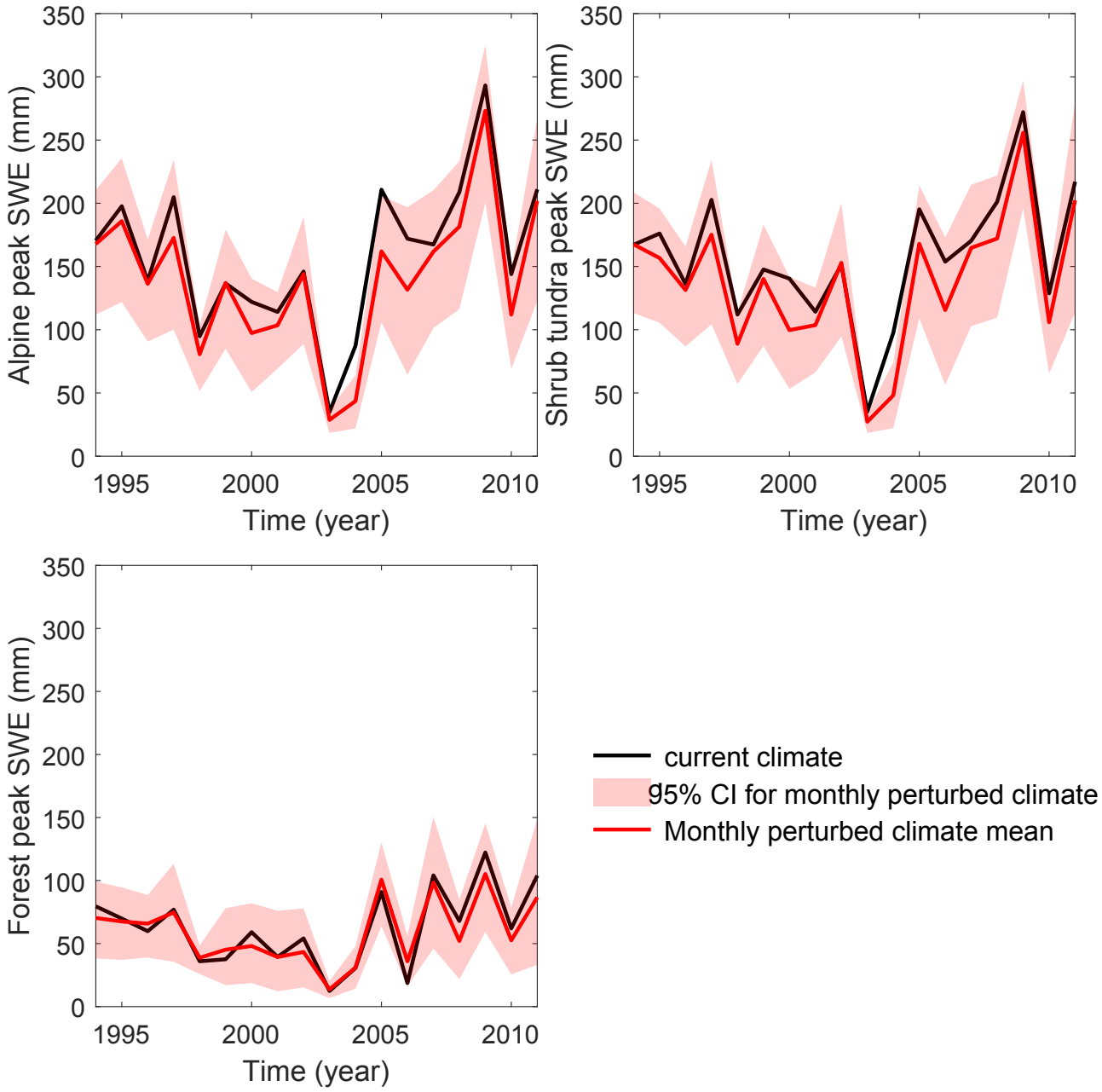

Figure 6.6: Simulated peak snow water equivalent (SWE) under current climate in Wolf Creek Research Basin (WCRB) and responses to monthly perturbed climate. The shaded area around the mean shows the ensemble uncertainty due to uncertainty in the climate models with ±95 confidence intervals. (WCRB coverage: Alpine 15%, Shrub tundra 65%, and Forest 20%).

by the climate models is a strong decline at low elevations and forest clearings and a moderate decline in the alpine biome, except for extreme cases such as in 2013 when the response of the snowpack is a slight increase (Figure 6.7). A high sublimation magnitude at low elevations in MCRB is responsible for snowpack decline in the forest. Figure 6.6 to Figure 6.8 show that uncertainty in peak SWE due to uncertainty in climate models is higher in the alpine and shrub tundra biomes of WCRB and in the sink and sheltered zones in RME under MPC. Uncertainty in maximum accumulated snow is low in the forest located in the low elevations in all three headwater basins. Comparing the range of uncertainty due to the climate models with the range of hydrological changes due to climate change shows that the uncertainty associated with snow regimes in WCRB and high elevations of MCRB is greater than due to climate change uncertainty. In contrast, the difference between snow regimes in current climate and MPCs is greater than the uncertainty of snow regimes in RME and low elevations of MCRB. The interannual variability of the high SWEs increases under MPC only in WCRB.

6.3 Snow Processes and Evapotranspiration Under Climate Change

Mean modelled water, vapor, and snow fluxes in three biomes of Wolf Creek Research Basin, four biomes of Marmot Creak Research Basin, and four snow regimes in Reynolds Mountain East catchment (alpine representing blowing snow source, sheltered from blowing wind, blowing snow sink, forest with intercepted snow), along with the basin-scale variables under (a) current climate and (b) monthly perturbed climate are illustrated in Figure 6.9. For convenience, values for each variable are given on the stacked bars and statistically significant changes with p–values less than 0.05 are represented by bold and red values. The Mann–Whitney U-test (Wilcoxon, 1945; Mann and Whitney, 1947 is used to test the significance of the changes in distribution of the simulated variables. The Mann–Whitney U-test is a nonparametric test for equality of distributions of two independent samples. Simulated distributions with $n = 18$ years for WCRB, 9 years for MCRB, and 25 years for RME over the control (base) period for each hydrological variable are compared with

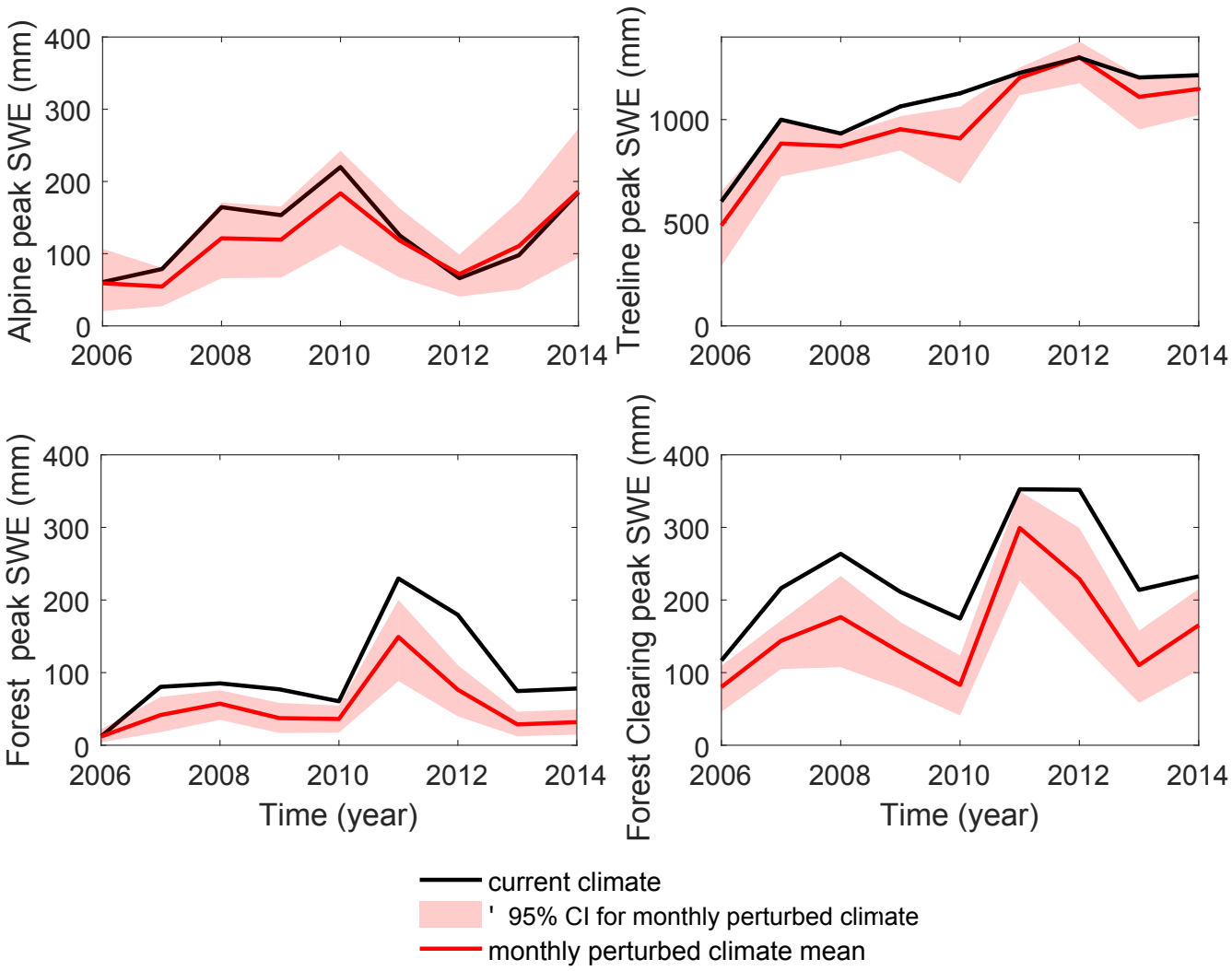

Figure 6.7: Simulated peak snow water equivalent (SWE) under current climate in Marmot Creek Research Basin (MCRB) and responses to monthly perturbed climate. The shaded area around the mean shows the ensemble uncertainty due to uncertainty in the climate models with ±95 confidence intervals. (MCRB coverage: Alpine 34%, Treeline 10%, Forest 46%, and Forest clearing 10%).

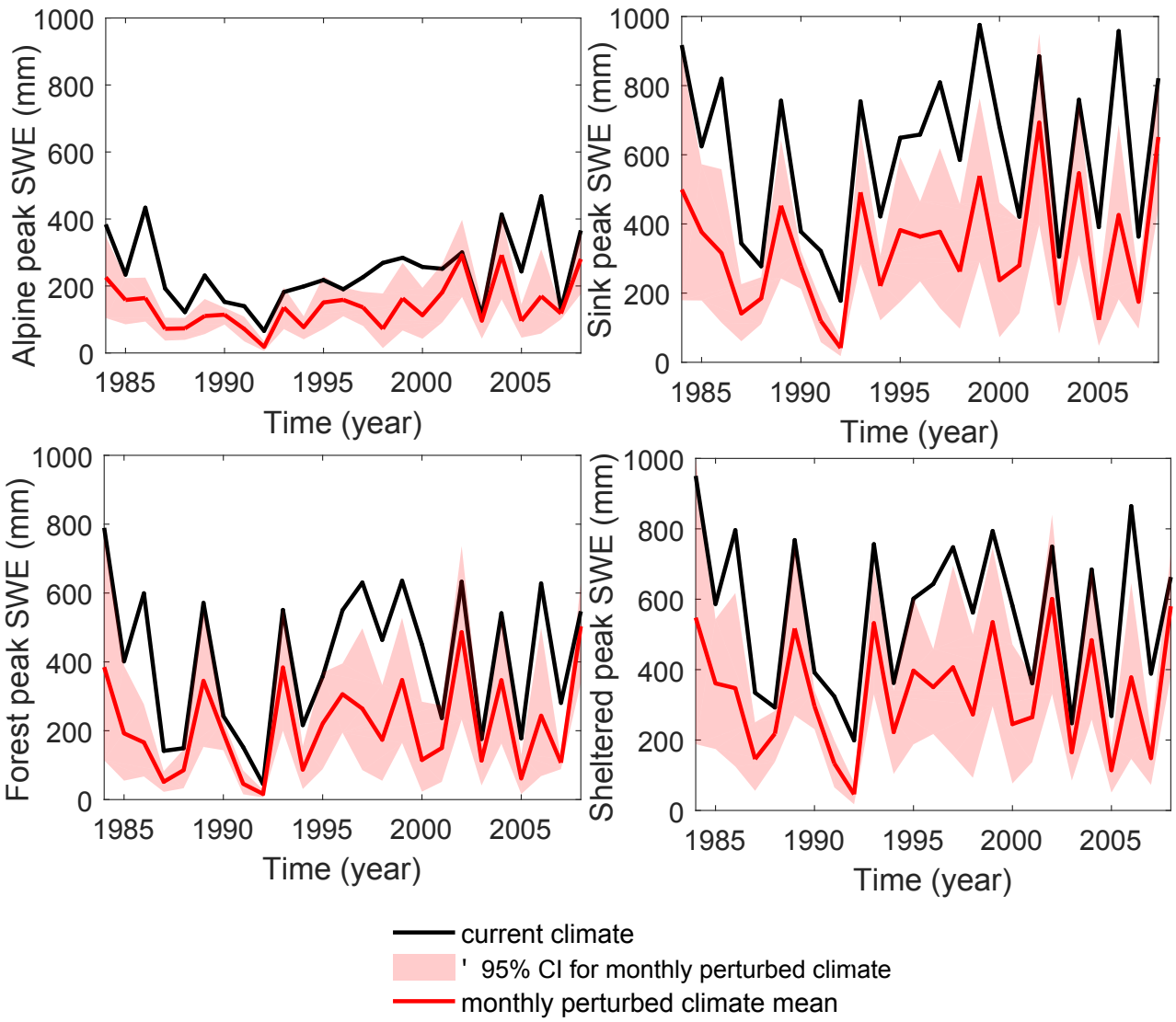

Figure 6.8: Simulated peak snow water equivalent (SWE) under current climate in Reynolds Mountain East (RME) catchment and responses to monthly perturbed climate. The shaded area around the mean shows the ensemble uncertainty due to uncertainty in the climate models with ±95 confidence intervals. (RME coverage: Alpine 57%, Sink 27%, Forest 5%, and Sheltered snow regime from blowing wind 10%).

the simulated future distributions obtained from 11 RCM-GCMs ($11 \times n$ values). The null hypothesis is that the distribution under current climate is equal to the distribution under MPC. The alternative hypothesis is that the distribution under current climate is not equal to the distribution under MPC.

6.3.1 Precipitation Phase

The headwater basins studied in this research are snow-dominated with a current climate rain to total precipitation ($\frac{R}{P}$) ratio of 49% in WCRB, 39% in MCRB, and 30% in RME of the NAC. WCRB has the highest area and latitude, lowest elevation, and shortest distance from the Pacific Ocean amongst the three basins. Therefore, a high $\frac{R}{P}$ ratio in WCRB is expected. Under MPC, a large proportion of the annual precipitation changes phase from snow to rain. This causes statistically significant (p–value < 0.05) changes in $\frac{R}{P}$ ratios. Rain to total precipitation ratios increase to 59% in WCRB, 53% in MCRB, and 54% in RME and all of the basins become rain-dominated under MPC. The sensitivity analysis of the mountain hydrology to changes in precipitation and air temperature studied in Chapter 5 shows that precipitation phase changes significantly under warmer and wetter conditions (Rasouli et al., 2015b). The change in $\frac{R}{P}$ is higher in the south than in the north even although the absolute value of $\frac{R}{P}$ is higher in the north. Under MPC, precipitation is expected to increase by 16.3% in WCRB (Figure C.11), which leads to a heterogeneous increase in rainfall across the basin, 42% in the alpine and shrub tundra biomes at high and medium elevations, and 36% in the forest at low elevations (Figure 6.9). The change rate of the $\frac{R}{P}$ ratio in MCRB does not change with elevation. For instance, the $\frac{R}{P}$ ratio increases from 30% to 44% (14% increase) in the alpine biome and from 48% to 63% (15% increase) in the forest in MCRB under climate change. These values show that a substantial portion of annual precipitation, which falls as snow in current climate, will turn to rainfall under future conditions. Changes in precipitation phase may change the frequency of rain-on-snow events in basins with near zero winter temperatures (Chae et al., 2015).

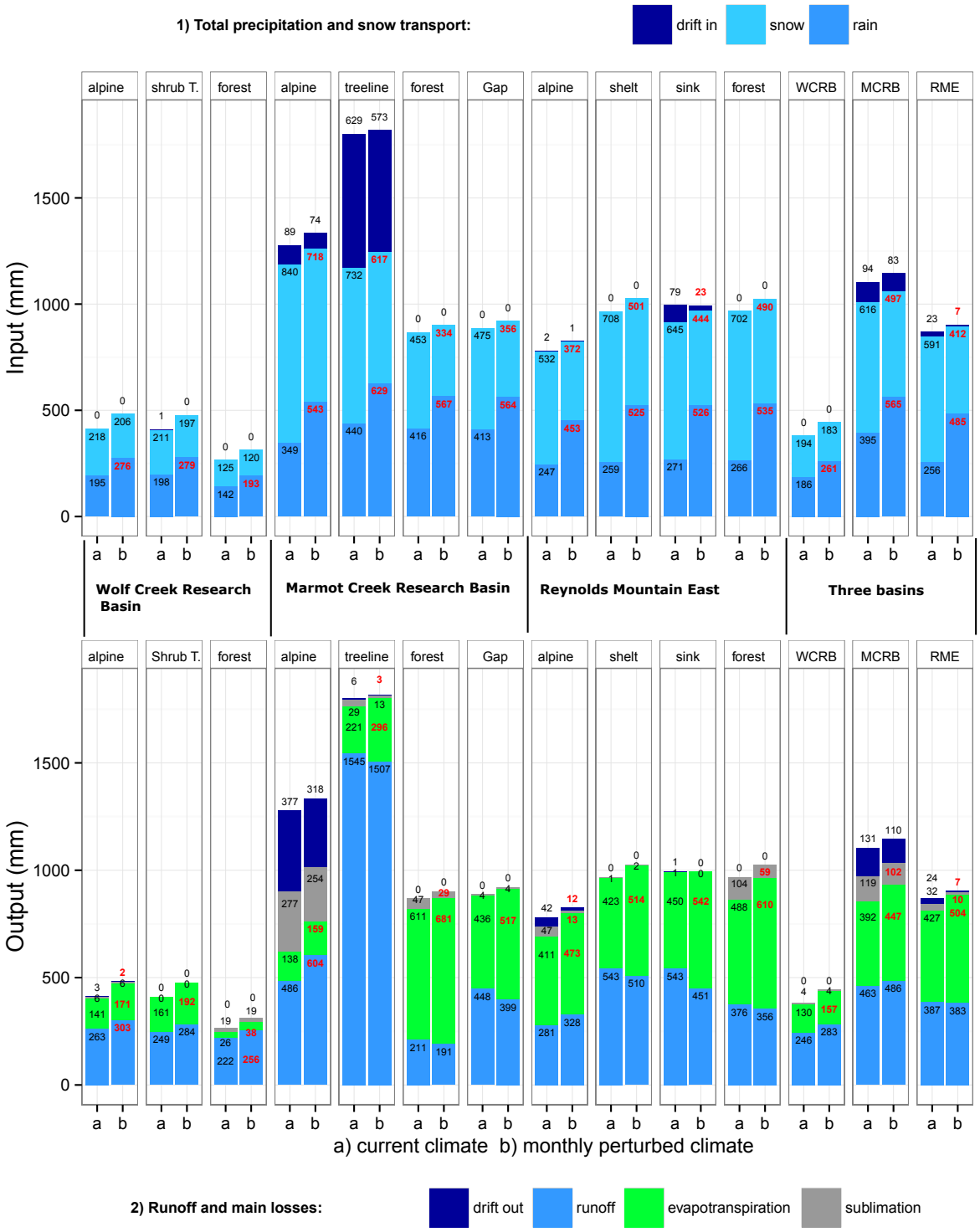

Figure 6.9: Mean modelled water, vapor, and snow fluxes under (a) current climate and (b) monthly perturbed climate. For convenience, values for each variable are given on the stacked bars. The statistically significant changes in distributions of the simulated variables with p–values less than 0.05 based on the Mann–Whitney U-test are represented by bold and red values between pairs. The simulated distributions with n = 18 years for WCRB, 9 years for MCRB, and 25 years for RME in the control period for each hydrological variable are compared with the simulated future distributions obtained from 11 RCM-GCMs (11×n values).

6.3.2 Snow Transport

Figure 6.9 shows that snow transport (drift in) from the alpine biome to treeline in MCRB decreases by 9% (from 629 mm to 573 mm) under MPC, which is reflected in the changes in the snow transported out of the alpine biome (drift out). Snow transport from the treeline in MCRB decreases by half. Snow transport to the sink zone in RME drops dramatically from 79 mm to 23 mm (71%, p–value <0.05) under perturbed climatic conditions, which is reflected in the decline in snow transport from the source zone in this basin (Figure 6.9). Basin-scale snow transport shows that RME and MCRB are sensitive to climate changes, with blowing snow decreasing by 16 mm in RME and by 11 mm in MCRB. In contrast, WCRB is resilient and changes in snow transport in this basin are negligible.

6.3.3 Sublimation

The effect of climate change on sublimation from the following sources is discussed here: (i) sublimation from blowing snow, (ii) sublimation from intercepted snow on the canopy, and (iii) sublimation from the snow surface. The magnitude of sublimation is usually small relative to annual precipitation and snowmelt rates, but can be considerable in some biomes and may negatively contribute to water loss from a basin. Sublimation from blowing snow in forest zones is negligible as these biomes are sheltered from the wind. Sublimation from blowing snow decreases significantly in the source zone in RME from 51 mm to 14 mm (37 mm, p–value < 0.05). The change in blowing snow sublimation is negligible in WCRB. The change in sublimation from blowing snow in the alpine biome in MCRB is similar to the source zone in RME as it decreases by 24 mm (from 289 mm to 265 mm). WCRB is the most insensitive basin to changes in sublimation from blowing snow, while alpine biomes within RME and MCRB are sensitive. Sublimation from intercepted snow on the canopy is sensitive to climate change and decreases from 27 mm to 17 mm (10 mm, p–value < 0.05) in MCRB and from 7 mm to 4 mm in RME. The decrease in WCRB is negligible. RME shows the greatest sensitivity in surface sublimation response to climate change in terms of magnitude and percentage, whilst MCRB shows the least sensitivity. In general sublimation from the

snow surface is less than other two sources of sublimation. Under MPC, it is expected that total sublimation for all three sources (Figure 6.9) decreases by 22 mm in RME and by 18 mm in MCRB (These changes are statistically significant with p–value < 0.05). In contrast, snow sublimation in WCRB remains almost unchanged.

6.3.4 Evapotranspiration (ET)

Under MPC, evapotranspiration (ET) increases in all of the biomes within the three study basins across the NAC (Figure 6.9). Amongst all of the biomes, forest in RME shows the highest increase (122 mm) in ET, which is due to higher annual precipitation and the fact that ET in the forest is water mass balance dominated and not energy balance dominated. The ET change across the NAC depends on both warming and precipitation changes. The warmer and wetter a climate, the higher the ET rate. This is the case in RME, where the basin-scale ET increase is the highest (74 mm increase, from 427 mm to 504 mm). ET increases from 392 mm to 447 mm (55 mm increase, p–value <0.05) in MCRB (Figure 6.9). WCRB ET is relatively insensitive to climate change and ET only increases 27 mm (from 130 mm to 157 mm) even though warming under MPC is slightly higher in this basin (2.6°C) than in the other two basins. This is because of the lower annual precipitation in this basin, larger drainage area relative to the other two basins, and because ET in WCRB is not water mass balance dominated, but is energy balance dominated. The ET response in WCRB is smaller due to a wetter summer climate (summer rainfall is relatively higher than other two basins). The increase in ET at WCRB is due to a longer snowfree period. Net radiation energy fluxes for ET, however, remain low in summer at this latitude.

6.4 Climate Change Impacts on Streamflow Regimes

Total overland and subsurface runoff fluxes are investigated under current and monthly perturbed climates for each biome. Results show that annual total runoff remains unchanged in RME and increases in all of the biomes in WCRB and MCRB, except for the forest

in MCRB (Figure 6.9). The annual total runoff in WCRB increases from 246 mm under current climate to 286 mm under future climate (16% increase, p–value < 0.05) and remains almost unchanged in RME at 371 mm (Figure 6.9). Simulated annual total runoff is 402 mm in MCRB, which rises 6% under MPC (Table 6.3). The annual total runoff increases with latitude under MPC, because the annual precipitation projected by 11 RCMs increases with latitude (Figure C.11) across the NAC; the runoff ratio changes slightly in RME and remains almost unchanged in the other two basins (Table 6.3). The increased precipitation and unchanged runoff ratio are two factors that both are consistent with an annual total runoff increase in WCRB and MCRB.

In contrast to the annual total runoff, the peak annual runoff does not match with the precipitation increases, decreasing in WCRB and RME and increasing in MCRB. The magnitude and timing of the simulated annual peak runoff in MCRB is resilient to climate change because: (1) this basin features the highest elevation band (up to 2800 m) amongst the three basins, (2) mean annual temperature at high elevations in this basin is –1.8°C; and (3) peak runoffs occur in June, when a large portion of precipitation falls as rain, which is also insensitive to warming. The average annual peak runoff increases only in MCRB, as the absolute value of the SWE in the higher elevations of this basin remains high (Figure 6.4). The runoff ratio is similar in the southern and central basins (≈0.46) and is higher in WCRB (0.64) under the current climate. The runoff ratio, however, decreases slightly in RME and remains unchanged in other two basins under MPC. An 18% increase in simulated evapotranspiration rate and a 2.3°C warming are two main factors that slightly decrease the runoff ratio in RME. In contrast, the effect of a 16.3% increase in precipitation in WCRB on runoff ratio under MPC is offset by an increase in evapotranspiration rate (21%) and in soil moisture content with permafrost degradation described later.

Streamflows with high intensity in WCRB (e.g., 2009) show a large decline in magnitude while the medium range streamflows (e.g., 1999 to 2002) do not change much under MPC (Figure 6.10). Figure 6.10 shows that uncertainty in annual total runoff and annual peak runoff due to uncertainty in climate models under MPC is high in the three basins. Uncertainty

Table 6.3: Simulated runoff characteristics under current and monthly perturbed climates in the three basins along the North American Cordillera. Bold values denote significant changes with p–values less than 0.05 based on the Mann–Whitney U-test. The simulated distributions with $n = 18$ years for WCRB, 9 years for MCRB, and 25 years for RMS over the control (Base) period for each hydrological variable are compared with the simulated future distributions obtained from 11 RCM–GCMs ($11 \times n$ values). Changes, which are relative to current climate and vegetation, are given in parentheses. The negative values represent advances in future timing while the positive values represent delays.

Variable		**Control**	**ΔClimate**		
		Period	**5%**	**mean**	**95%**
(1) Wolf Creek Research Basin (WCRB)					
Annual volume	[mm]	246	207(–16)	286(16%)	343(39)
Annual peak	[cms]	3.2	1.9(–42)	3.0(–7%)	3.9(22)
Peak timing	[date]	Apr 24	Feb 23(–59)	Apr 13(–11 day)	May 16(22)
(2) Marmot Creek Research Basin (MCRB)					
Annual volume	[mm]	402	342(–15)	426(6%)	481(20)
Annual peak	[cms]	1.01	0.80(–21)	1.11(9%)	1.33(31)
Peak timing	[date]	Jun 11	Jun 1(–10)	Jun 10(–1 day)	Jun 15(4)
(3) Reynolds Mountain East (RME)					
Annual volume	[mm]	371	262(–30)	375(1%)	459(24)
Annual peak	[cms]	0.053	0.033(–38)	0.045(–15%)	0.054(2)
Peak timing	[date]	May 14	Mar 7(–68)	**Apr 4(–40 day)**	Apr 22(–22)

in peak runoff under MPC is the greatest in WCRB and the least in MCRB. The uncertainty of streamflow regimes due to climate model uncertainty is greater than the differences due to climate change in all three basins. The interannual variability of high flows is expected to increase in all three study basins, with higher rates in MCRB and lower rates in WCRB. The response of mean annual peak runoff to changes in each of the three basins across the NAC is different. For instance, the spread of RCM responses (95% confidence interval) and their ensemble mean shows an increase in the variability of high flows in MCRB. From a flood control point of view, it is important to know how high flows recorded in the historical period would occur under climate changes. The performance of the models used in this research in capturing magnitude and timing of the peak values is fair. Therefore, one needs to be cautious when interpreting the results for changes in timing of the variables under climate changes.

6.4.1 Early Freshet and Changes in Streamflow Timing

Changes in timing of snow accumulation and ablation have great hydrological consequences and can alter the soil moisture, infiltration rate, and runoff intensity. Shallower snowpacks and the substantial shift forward in the melt period into lower solar irradiance periods with warming cause an early ablation of the snowpack, which decelerates the snowmelt (Pomeroy et al., 2015). This might affect the intensity of high flows over frozen ground. The initiation date of snow accumulation does not change under MPC and is only delayed by 2–15 days in the three basins across the NAC (Table 6.2). In contrast to the snowpack initiation date, timing of the peak SWE changes substantially and advances 22 days from April 4 to March 13 in WCRB, 10 days from April 29 to April 18 in MCRB, and 32 days from March 10 to February 6 in RME. The snow-free date advances 15 days in WCRB, 13 days in MCRB, and 33 days in RME. The reason that the peak SWE date in MCRB shows higher resiliency to climate changes is that precipitation is high in this basin and falls as snow, usually at the end of snowcover season and under sufficiently cold conditions, especially at high elevations. This shows that timing of the peak SWE date and snowcover season in MCRB because of its unique snow regime and high elevation range will be more resilient to further warming

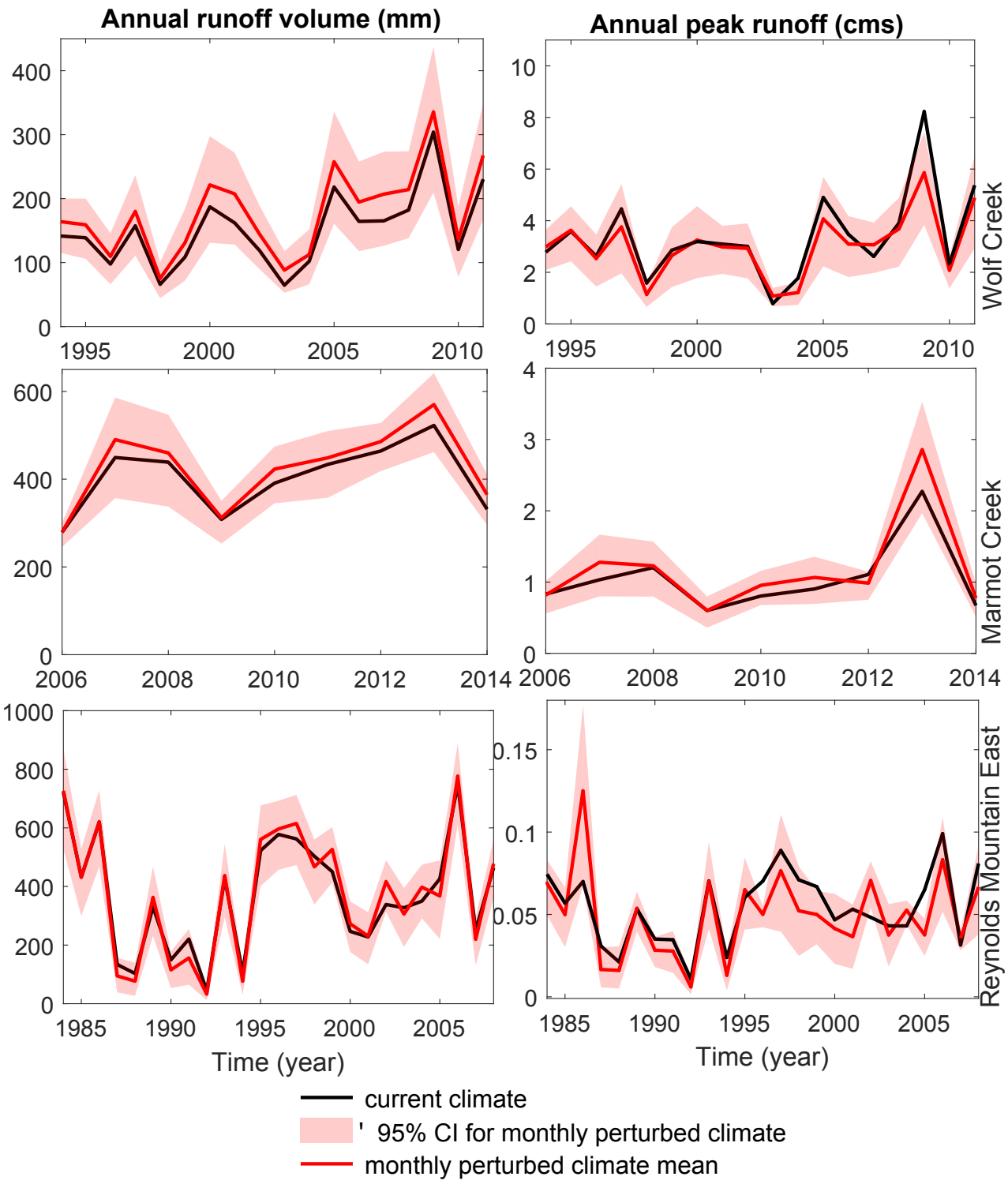

Figure 6.10: Differences in annual total runoff and annual peak runoff under current and monthly perturbed climates in the three basins across the North American Cordillera. The 2013 peak runoff in MCRB would occur with higher intensity and reach 2.859 m^3s^{-1} under monthly perturbed climate.

under MPC. Under MPC, the length of the snow season is expected to be 16 days less in the north, 35 days less in the centre, and 50 days less in the south of the NAC. The peak snowpack date advances toward a time of year with lower solar irradiance. Annual total runoff and variability of peak streamflows increase more in the north and less in the south of the NAC under MPC. Consistent with the date of the annual peak snowpack, average annual peak streamflow occurs 11 days earlier in the north and 40 days earlier in the south, but remains unchanged in MCRB under MPC (Table 6.3). The performance of the models used in this research in capturing magnitude and timing of the peak values is fair. Therefore, one needs to be cautious when interpreting the results for changes in timing of the variables under climate changes.

6.5 Discussion

Average changes in monthly climatology of air temperature are 2.6°C in WCRB, 2.2°C in MCRB, and 2.4°C in RME, while average changes in monthly climatology of precipitation are 16.3% in WCRB, 6.6% in MCRB, and 2.3% in RME. Under MPC, the peak SWE in the forests across the North American Cordillera (NAC) is expected to decrease with a large decline in RME and lower elevations in the other two basins. Snowpack is the most sensitive in RME and the most insensitive to climatic changes in WCRB. Basin-scale snow transport shows that RME and MCRB are sensitive to climate changes, while WCRB is the most resilient. Sublimation from blowing snow, snow surface, and snow intercepted on the canopy drops in the study areas with MCRB being the most insensitive to changes in total sublimation from all sources and RME the most sensitive. Basin-scale peak SWE declines under MPC in all three basins with varying rates. This is in contrast to a work by MacDonald et al. (2012) in which peak SWE does not change under future warming scenarios in headwater basins of the North Saskatchewan River watershed in Canada.

Under monthly perturbed climate, the interannual variability of snowpack decreases in low-elevation forests and basins located at low latitudes ($\approx 43^\circ$ N). Annual peak snowpack in

the alpine biome is more resilient to climate change than that in the forest. The main factors responsible for this are colder conditions at high elevations and warmer and higher rain to total precipitation ratios at lower elevations. The decline in peak snowpack in northern and southern basins is reflected in the decline in peak runoff. An increase in the rainfall to snowfall events increases the variability of the annual peak flows in the northern part of the NAC. Uncertainty in projected changes in timing and the magnitude of peak snowpack and peak runoffs is greatest in the northern basin and similar in the centre and southern basins. This suggests that representation of the interactions between atmosphere and cold regions ecohydrological processes in RCMs needs to be improved. Because of a colder climate in the north, sublimation from the snow surface as well as snowmelt decreases less in WCRB than in the other two basins. Loss due to sublimation from blowing snow or from snow intercepted on the canopy is least in MCRB and most in RME.

Under monthly perturbed climate in WCRB, peak SWE and sublimation decline, snow season period shortens, ET increases, thawing depth becomes deeper, and "rain to total precipitation" ratio increases which, when combined, result in an increase in annual total runoff and a decrease in average annual peak flow. This suggests that the snow and streamflow regimes in WCRB are relatively resilient to the combination of warming and precipitation increase under MPC. This is due to the colder climate of WCRB and a compensating role of increased precipitation that offsets the impact of warming. Thawing associated with permafrost degradation under the warmer MPC increases soil moisture storage in winter, which may restrict the infiltration to deep soil and increase spring runoff. The thawing front becomes deeper than that under the current climate while the freezing front becomes shallower. The thawing and freezing processes moderate the high flows in the northern latitudes by increasing the storage capacity of the soil. In MCRB, similar changes with different intensities are expected in snowcover season, evapotranspiration, and rain to total precipitation ratio, except for average annual peak flow, which increases under MPC. The snow regime at low elevations in MCRB is sensitive to changes; however, the streamflow regime and the snow regime at high elevations in MCRB are resilient to changes. This is due to a high elevation band reaching 2800 m with mean annual temperatures of -1.8°C

and a rainy environment in spring and summer. In RME, large changes are expected in snowcover season, evapotranspiration, rain to total precipitation ratio, and average annual peak flow and no change in annual total runoff is expected under MPC. The changes reported in this research are in agreement with findings in Nayak (2008), in which a +2°C warming scenario resulted in more rain, less snow, a decrease in SWE, earlier peak SWE, and earlier snowmelt. The results of this research suggest that the snow regime and to some extent the streamflow regime are sensitive to changes in RME. This is due to the higher annual mean air temperature in RME and a large change from historically being a snow-dominated basin to being a rain-dominated basin under MPC, which together make this basin sensitive to warming. A trend analysis by Nayak (2008) shows large reductions in snowpack in RME due to precipitation phase change. The greater precipitation phase change in this basin has an important role with respect to the resiliency of the annual total runoff to changes and allows rainfall to form runoff under MPC instead of infiltrating or sublimating from the snowpack under the current climate.

Under monthly perturbed climate, the simulated runoff ratio remains almost unchanged in all three basins with only a slight decline in RME. Multiple changes in the hydrological processes lead to more homogenous responses of runoff across the NAC. In WCRB, the impact of annual precipitation increase on runoff ratio is moderated by increased evapotranspiration and annual runoff increases. The rainfall ratios are expected to become similar in all elevation bands from mid-latitudes to high latitudes. The rainfall ratio in WCRB is the highest amongst the basins (note that WCRB has the lowest elevation and coldest temperatures) and, based on NARCCAP RCM–GCMs, the warming and precipitation increase in this basin are the greatest. In MCRB, the impacts of the snowfall to rainfall conversion and slight increase in precipitation on runoff ratio are offset by an increase in ET and a mild increase in annual runoff. In contrast, the impact of the higher snowfall to rainfall conversion rate on runoff ratio in RME is almost canceled out by the impact of the higher ET rates, and therefore no change in annual runoff is expected.

The interannual variability of the high flows increases in all three study basins with

climate changes. Annual total runoff and variability of peak streamflows increase under MPC from south to north across the NAC. Annual peak streamflow occurs earlier under monthly perturbed climate in the north and south of the NAC but remains unchanged in the central basin. This is consistent with a previous study in RME that shows a seasonal shift to earlier spring runoffs (Nayak, 2008). All three basins are vulnerable to warming and show drops in annual ET. Warming counteracts the impact of the precipitation increase on water yield by increasing ET and converting snowfall to rainfall in the headwater basins along the North American Cordillera.

Hydrological sensitivity of mountain basins to a warming climate depends on the elevation of the basins (Stewart et al., 2004). Snow regime and snowmelt runoff timing in high elevation basins with winters well below the freezing point are shown to be less sensitive to warming than low elevation basins (Stewart et al., 2004; McCabe and Clark, 2005). Precipitation phase is also sensitive to warming in basins with winter temperatures warmer than -5°C (Knowles et al., 2006). Winter temperatures in RME are above -5°C (Figure 3.2), which make this basin sensitive to warming. As discussed earlier in this chapter, there are similarities in high elevation (MCRB) and high latitude (WCRB) basins with winter temperatures remaining below the freezing point despite the modelled warming.

To compare hydrological changes between annually and monthly perturbed climates, changes in monthly climatology of air temperature and precipitation were averaged over 12 months to obtain similar annual changes under monthly perturbed climate. Hydrological response to the same changes under annually and monthly perturbed climate show that annual total runoff in WCRB and MCRB and peak SWE in MCRB and RME show similar responses to annually and monthly perturbed climates. For a 2.6°C warming and a 16.3% increase in precipitation projected by 11 NARCCAP RCMs for the period 2041–2070, peak SWE in WCRB decreases by –11% under monthly perturbed climate and does not change under the same warming and increased precipitation of annually perturbed climate. This is due to considerable warming in spring (2.8°C) and winter months (3.5°C) in WCRB. For a 2.4°C warming and a 2.3% increase in precipitation, annual total runoff in RME decreases by

–6% under annually perturbed climate and does not change under monthly perturbed climate.

The application of the monthly delta change factors to hourly or daily observed variables may introduce some uncertainties to snow and streamflow regimes and may not represent the changes in extremes, sequences of wet and dry spans, and duration of droughts and floods. Uncertainty of streamflow regimes is high under MPC because of the considerable uncertainty in the climate models. Therefore, responses of annual total runoff, annual peak runoff, and timing of peak flows to climatic changes projected by different RCMs are uncertain.

6.6 Summary

Monthly perturbed climate (MPC) in this chapter is based on monthly changes in climatological values of air temperature and precipitation from current to future climate. This is different to Chapter 5 where only annually perturbed climate (APC) was constructed. Monthly perturbed climate (equivalent to the 2041–2070 period) is reconstructed based on observations in the research basins and changes in monthly climatology obtained from the North American Regional Climate Change Assessment Program (NARCCAP) RCMs to understand how current hydrology would respond to climate changes. Uncertainties in simulated hydrological variables due to uncertainties in the climate models are quantified. Comparing hydrological sensitivities to APC (Chapter 5) and MPC (this chapter) approaches reveals the importance of seasonality in climate change impact studies. Hydrological response to the same changes under APC and MPC show that annual total runoff in Wolf Creek Research Basin and Marmot Creek Research Basin and peak SWE in Marmot Creek Research Basin and Reynolds Mountain East show similar responses to annually and monthly perturbed climates. The range of uncertainties in simulated snow regimes in Wolf Creek Research Basin and high elevations of Marmot Creek Research Basin and simulated streamflow regimes in all three basins along the North American Cordillera are greater than the range of differences due to climate change. The uncertainties in peak runoff and timing of peak runoff and peak snowpack suggest caution in using these results for future flood control planning in mountainous

regions. Smaller uncertainties in water balance components (e.g., annual total runoff) relative to peak values, however, suggest that the results for water balance components can be used to anticipate future water resources management and aquatic ecosystem conservation strategies.

Chapter 7

HYDROLOGICAL SENSITIVITY TO TRANSIENT CLIMATE, VEGETATION, AND SOIL CHANGES

This chapter presents results that address the third objective of this research. Objective three of the thesis includes quantifying the response of the simulated mountain hydrology to transient climate, vegetation, and soil changes. Warming may lengthen the growing season and reduce the snowpack, which may lead to changes in soil moisture and infiltration rates in high elevation and high latitude basins (Inouye et al., 2000). High elevation and high latitude ecosystems are more sensitive to climate changes as warming causes snow recession at high elevations with an albedo feedback (Nogués-Bravo et al., 2007) and permafrost degradation at high latitudes (Zhang et al., 2008). Changes in precipitation under a warmer climate affect snow accumulation and ablation rates, soil moisture, and vegetation growth (Billings and Bliss, 1959). The hydrological responses to the interactive vegetation and climate changes were examined over three mountain basins along the North American Cordillera (NAC).

Interaction between vegetation and snow in the mountain basins, where snowpack acts as a main source of water availability for vegetation growth, is also hydrologically important. A change in vegetation composition can alter snow redistribution and sublimation from snow intercepted on the canopy. Snowmelt affects soil and leaf temperatures, surface microclimate, nutrient transport, and length of the growing season. The sensitivity of snow accumulation to warming and precipitation changes under future climate needs to be investigated. Similarities and contrasts between mountain basins at high latitudes and low latitudes make them

interesting for the study of heterogeneous effects of climate and vegetation change on hydrology in different mountain basins. Some of the similarities in the hydrological processes in high elevation and high latitude basins include:

- Air temperature decreases with elevation and latitude. There is a negative linear relationship between air temperature and elevation in mountain basins and a negative relationship between air temperature and latitude;
- Similar to upward movement of the treeline in high elevation mountains, coverage by shrubs is also expanding to high elevations (Hallinger et al., 2010) and higher latitudes (Tape et al., 2006).

There are distinct differences between a mountain ecosystem located at high latitude and a mountain ecosystem located at mid-latitude, such as RME. Two important differences from a hydrological perspective are:

- The lapse rate for precipitation increases with elevation, but decreases with latitude moving northward (Singh and Goyal, 2016).
- In contrast to high latitude basins – where there is a high chance of permafrost presence – only seasonally frozen ground (Ireson et al., 2013) is present in the mid-latitude basin and the ground does not freeze at all in the low-latitude basin.

7.1 Future Vegetation and Soils: Regrowth and Deforestation Mechanisms

Under climatic changes, vegetation cover and associated soils are expected to change in response to warming (Jorgenson et al., 2010), snowcover season changes (Stanton et al., 1994), extended growing season (Billings and Bliss, 1959; Euskirchen et al., 2010), wildfires (Shakesby et al., 1996), mountain pine beetle (Macias Fauria and Johnson, 2009), and terrestrial changes (Bosch and Hewlett, 1982) caused by anthropogenic activities. Figure 7.1 represents typical vegetation cover over mountain basins across the North American Cordillera (NAC) under current and future climates. The vegetation cover in WCRB, a high latitude

watershed ($\approx 61^\circ$ N), includes forest at low elevations, shrub tundra at medium elevations, and alpine tundra at high elevations. MCRB in the Canadian Rockies is covered by mixed forest at low elevations, larch trees at the treeline, and alpine vegetation and rocks/bare ground at high elevations. Approximately 10% of the basin's forest was harvested a few decades ago and is expected to regrow under a warmer climate and a lengthened growing season (Schneider, 2013). Low elevations in MCRB are likely to be influenced by wildfires (Schneider, 2013) and/or mountain pine beetle (Macias Fauria and Johnson, 2009) and convert to grassland. The southern basin in the US northwestern interior is presently covered by mountain sages/shrubs, alpine grass, a deciduous aspen and willow forest, and a needle-leaf fir forest.

Large changes in vegetation cover and height are expected in all three headwater basins as shown schematically in Figure 7.1. Elmendorf et al. (2012) tested the alpine vegetation response to warming in summer months between 1980 to 2010 over a wide range of locations and found that abundance of tundra vegetation was high in warmer summers, canopy height increased, and the abundance of tall shrubs expanded over bare grounds in the Arctic and sub-Arctic. Shrub tundra expansion was also reported by Tape et al. (2006), Sturm et al. (2005), and Hallinger et al. (2010). Based on these studies and the physiography of the basins, three future vegetation scenarios for WCRB are estimated based on shrub expansion and treeline movement as shown in Figure 7.1.

Hydrological model parameters under transient vegetation and soil changes are adapted from parameters that represent vegetation and soil characteristics under current climate. For instance, if a hydrological response unit (HRU) in the model is currently covered by grass and it is expected to be afforested under future climate, parameters for the new afforested HRU can be adapted from an HRU that has been historically covered by forest. HRU parameters are transferred to represent transient changes in two approaches: (i) only transferring vegetation parameters and (ii) transferring both vegetation and soil parameters. Table 7.1 shows a list of parameters that change under transient vegetation and soil changes. Changes in organic layer of soils following transient vegetation changes can alter the soil

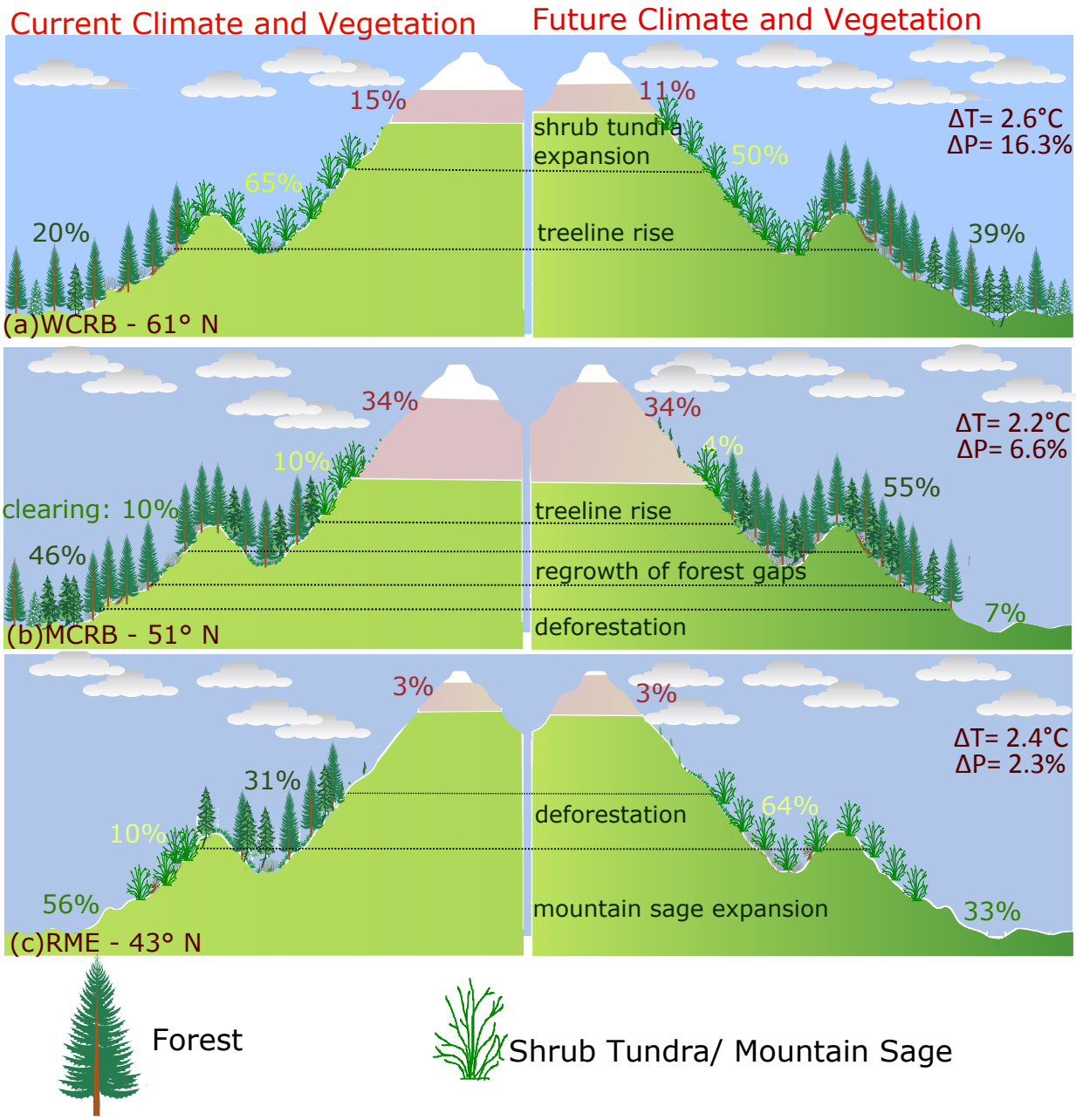

Figure 7.1: Schematic illustration of the vegetation cover under current and monthly perturbed climates in the three basins along a north–south transect of the North American Cordillera (NAC). The numbers show the areal percentage of alpine, forest, shrub tundra, grassland, and forest clearing biomes. The estimated future vegetation changes are: (a) upward movement of the treeline and a shrub tundra expansion in Wolf Creek Research Basin (WCRB), (b) upward movement of the treeline, afforestation of the harvested forest, and deforestation of the lower elevations in Marmot Creek Research Basin (MCRB), and (c) deforestation and mountain sage expansion across the Reynolds Mountain East (RME) catchment. The vegetation changes were estimated from the literature (e.g., Sturm et al., 2005; Tape et al., 2006; Hallinger et al., 2010; Macias-Fauria and Johnson, 2013; Schneider, 2013) and adapted to the physiography (e.g., soil/moisture availability) of each basin. ΔT and ΔP, which are projected by 11 RCM–GCM combinations, denote annual warming and precipitation increases, respectively.

Table 7.1: List of hydrological model parameters that their values are transferred from a hydrological response unit under current climate to a changed hydrological response unit under (i) only transient vegetation change and (ii) both transient vegetation and soil changes

Parameter	**Vegetation change**	**Vegetation/Soil change**
canopy or clearing or gap	✓	✓
ground cover	✓	✓
vegetation height	✓	✓
vegetation density	✓	✓
stomatal resistance	✓	✓
stalk diameter	✓	✓
Leaf Area Index (LAI)	✓	✓
snow interception capacity of canopy	✓	✓
sky view factor	✓	✓
blowing snow inhibition	✓	✓
fetch distance	✓	✓
representative station	✓	✓
soil depth		✓
soil porosity		✓

characteristics including soil macro-pores and hence, alter snowmelt/rainfall infiltration, thawing/freezing processes, recharge into groundwater, and runoff mechanisms.

Climate products from 24 GCMs, used in the Intergovernmental Panel on Climate Change Fourth Assessment, show a 2.8°C to 4.2°C rise in mean annual temperature, a 7.2% to 9.4% rise in mean annual precipitation, and a 33% to 56% increase in growing degree days by the end of the century in the Canadian Rockies and Alberta, where MCRB is located (Schneider, 2013). With these projections for the future climate in this region, a change in vegetation cover is expected. The upward movement of the treeline in the Rocky Mountains depends on soil depth, soil moisture, and the obstructing effect of the rock (Macias-Fauria and Johnson, 2013), and varied from no change to a 150 m vertical shift over the past century (Luckman

and Kavanagh, 2000). In MCRB, the treeline is expected to rise toward higher elevations as suitable soil and moisture conditions become present (Figure 7.1). Therefore, alpine vegetation will be gradually replaced by forest. Vegetation in the lower elevations, now covered with lodgepole pine is expected to turn to shrubs and grass; grasslands are already extending toward higher elevations in the foothills of the Canadian Rockies (Schneider, 2013). Vegetation in forest clearings with deep snowpacks in winter is expected to continue growing under warmer conditions and the forest gaps infilled by the end of the century (Macias-Fauria and Johnson, 2013). Uncertainties in future forest management in MCRB would add more modelling uncertainty. In this study, it is assumed that harvesting in MCRB will not be allowed in the future. Despite the positive impacts of warming on vegetation at high elevations, a warmer temperature can increase tree mortality by increasing the possibility of fire and bark beetle attacks (Williams et al., 2013; Brando et al., 2014; Johnstone et al., 2016). Drought also increases the mortality rate of coniferous trees as they become vulnerable to bark beetle attack under drought conditions (Raffa et al., 2008). In RME, a large change from snowfall to rainfall, with projected warming, will cause snowpack accumulation to drop significantly from a present-day climate value of 368 mm to 196 mm under MPC (47% decrease, p–value < 0.05; refer to Table 7.2). The loss of snowpack in RME threatens the survival of aspens. Drifted snowpacks in the surface depressions and subsequent snowmelt during late spring and summer are critical to sustaining the vegetation in RME (Marks et al., 2001). Johnstone et al. (2016) showed that understanding ecosystem resilience to any natural or anthropogenic disturbance is not possible unless characteristics of the disturbance (e.g., severity, frequency, and size) are understood. Therefore, all deciduous and coniferous trees, which cover 31% of the basin, can die off in response to warming and water deficit stressors. Given the high uncertainty in future vegetation scenarios, disturbance by a wildfire or MPB infestation is not assessed and only warming disturbance, the severity of which can be characterised by climate model projections, is investigated.

7.2 Impacts of Climate and Transient Vegetation Change on Snow Regimes

To assess the uncertainty in the mountain hydrology due to uncertainty in future vegetation, three different scenarios for each basin were chosen based on vegetation projections for the late 21st century and physiography of the mountain basins. Vegetation change scenarios are: (1) an upward movement of the treeline and shrub tundra expansion, (2) only shrub tundra expansion, and (3) only an upward movement of the treeline in WCRB; (1) an upward movement of the treeline, afforestation of the harvested forest, and deforestation of the lower elevations, (2) an upward movement of the treeline and afforestation of the harvested forest, and (3) afforestation of the harvested forest and deforestation of the lower elevations in MCRB; and (1) deforestation of all trees (aspen, fir, willow) and mountain sage expansion, (2) deforestation of fir trees and mountain sage expansion, and (3) deforestation of aspen and fir trees and mountain sage expansion across RME catchment. Figure 7.2 shows the differences between distributions of hourly modelled snow for the control (current climate) period and the three vegetation scenarios for each basin mentioned above. All SWE values, modelled under current climate with no changes in vegetation and under three vegetation scenarios, are given in this figure. Snow regimes are mainly sensitive to the upslope treeline movement and to a lesser extent to shrub tundra expansion in WCRB, to treeline movement and infill of the harvested forest in MCRB, and willow tree deforestation and mountain sage expansion in RME. In general, the hydrological uncertainty due to uncertainty in future vegetation is high in MCRB and low in RME. The first scenario, which includes all of the potential changes in vegetation cover of each basin, is selected for further analysis and comparison of the hydrological responses to vegetation and climate changes.

Figure 7.3 shows monthly variability of simulated snow water equivalent (SWE) with elevation (blowing snow regimes in RME). The high, medium, and low elevations each match a vegetation type under the current climate. Under future climate, however, each elevation band may include two types of vegetation. For comparing the snow regime changes, each

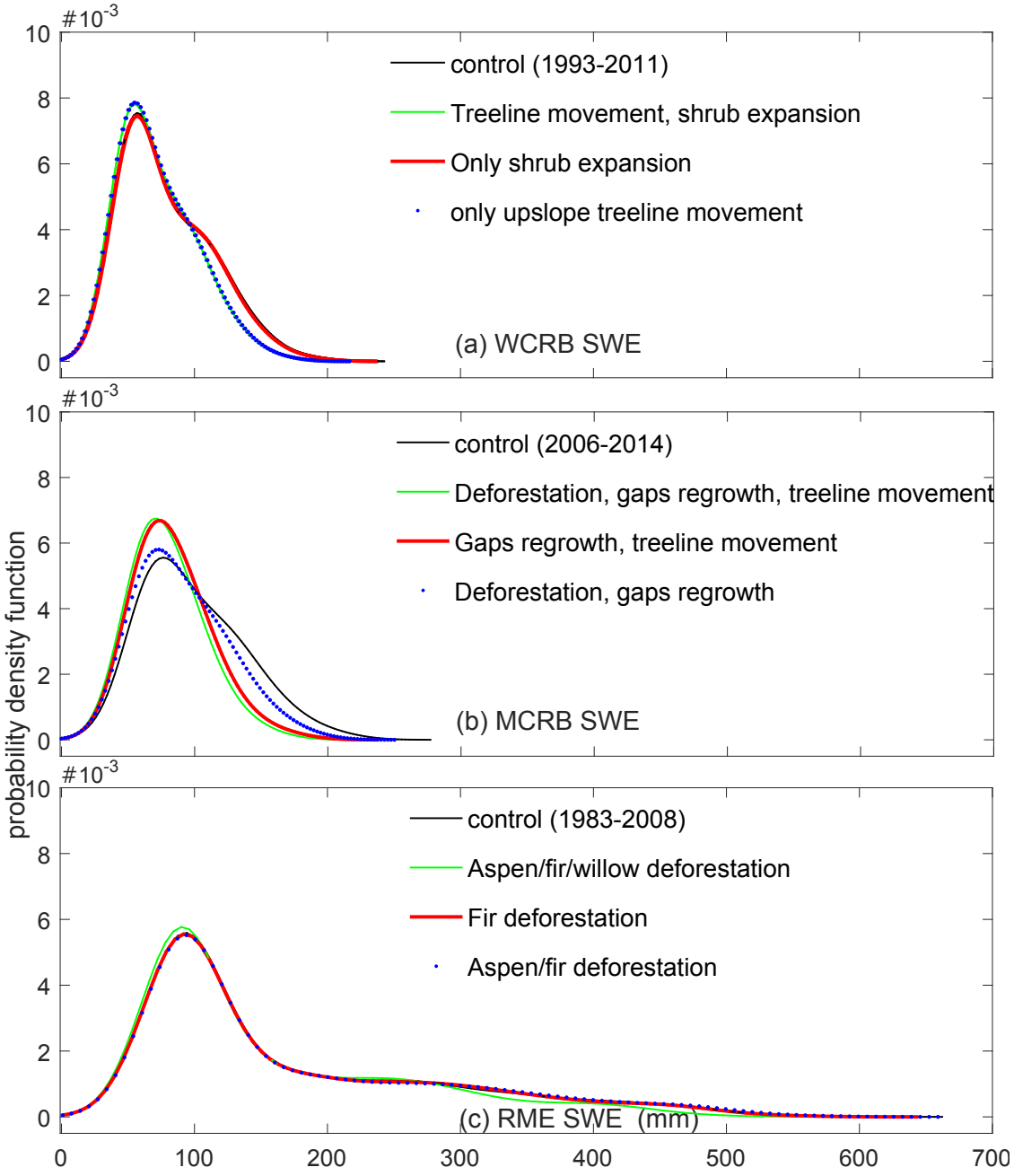

Figure 7.2: Differences in the distributions of simulated snow water equivalent (SWE) in the current climate/vegetation and three vegetation change scenarios in the three basins along the North American Cordillera. No climate change is considered with transient vegetation changes. All three simulated SWE distributions for vegetation change scenarios in each basin are significantly (p–value < 0.05) different than the simulated SWE distribution for the control period based on the Kolmogorov-Smirnov (K–S) test. The K–S test, which is a nonparametric hypothesis test, was used to evaluate differences between distribution of modelled hourly SWE for the control period and distributions of the modelled hourly SWE under three vegetation change scenarios over 18 years in WCRB, 9 years in MCRB, and 25 years in RME ($\times$ 365 days $\times$ 24 hours).

basin was divided into three elevation bands each covering multiple HRUs. In addition to different elevation bands, the snowpack accumulation and ablation in a forest clearing in MCRB and in a sheltered site in RME are examined. Shaded areas in Figure 7.3 show the interannual variability of snowpack under (i) the present-day climate, (ii) a transient vegetation change, (iii) climate change, and (iv) a combined climate and vegetation change within the three headwater basins across the NAC. Uncertainty due to ensemble uncertainty of climate models will be discussed later in this chapter for peak snowpack. Under a transient vegetation change scenario with an unchanged climate, the peak snow close to a latitude of 61° N becomes deeper, and snowpack ablates slower, and snowcover season becomes longer (Figure 7.3a). This is due to shrub expansion to higher elevations, which reduces snow transport and subsequent sublimation from blowing snow. In contrast, under climate change with unchanged vegetation, less snow accumulates and ablation rates are greater. Under a combined climate and vegetation change scenario, the effect of climate change on the alpine snowpack is moderated in the northern basin by the impact of the shrub tundra expansion to higher elevations. At medium elevations, shrubs are expected to be replaced from below by treeline upward movement; therefore, under the vegetation change scenario and the combined climate and vegetation change scenario, peak snowpack decreases from 156 mm in the current climate to 127 mm (19% decrease, Figure 7.3b). Transient vegetation change is negligible at low elevations in the northern latitudes (Figure 7.3). Therefore, the snowpack in the lower elevations in WCRB is not disturbed by transient vegetation change but is disturbed by climate change in these simulations.

In the medium latitude basin ($\approx$ 51° N), MCRB in the Canadian Rocky Mountains, an upward movement of the treeline causes an increase in the simulated peak snowpack with slower ablation rates at high elevations (Figure 7.3d). In contrast to the snowpack enhancement under treeline upward movement, climate change slightly decreases the peak SWE in the alpine in MCRB. The treeline has an important role in snow redistribution and acts as a blowing snow sink. The effect of treeline rise on the alpine snowpack is greater than that of climate change alone. This is due to the higher sublimation rate of forest in comparison to shrubs and alpine vegetation in the treeline zone. Even though the drifted

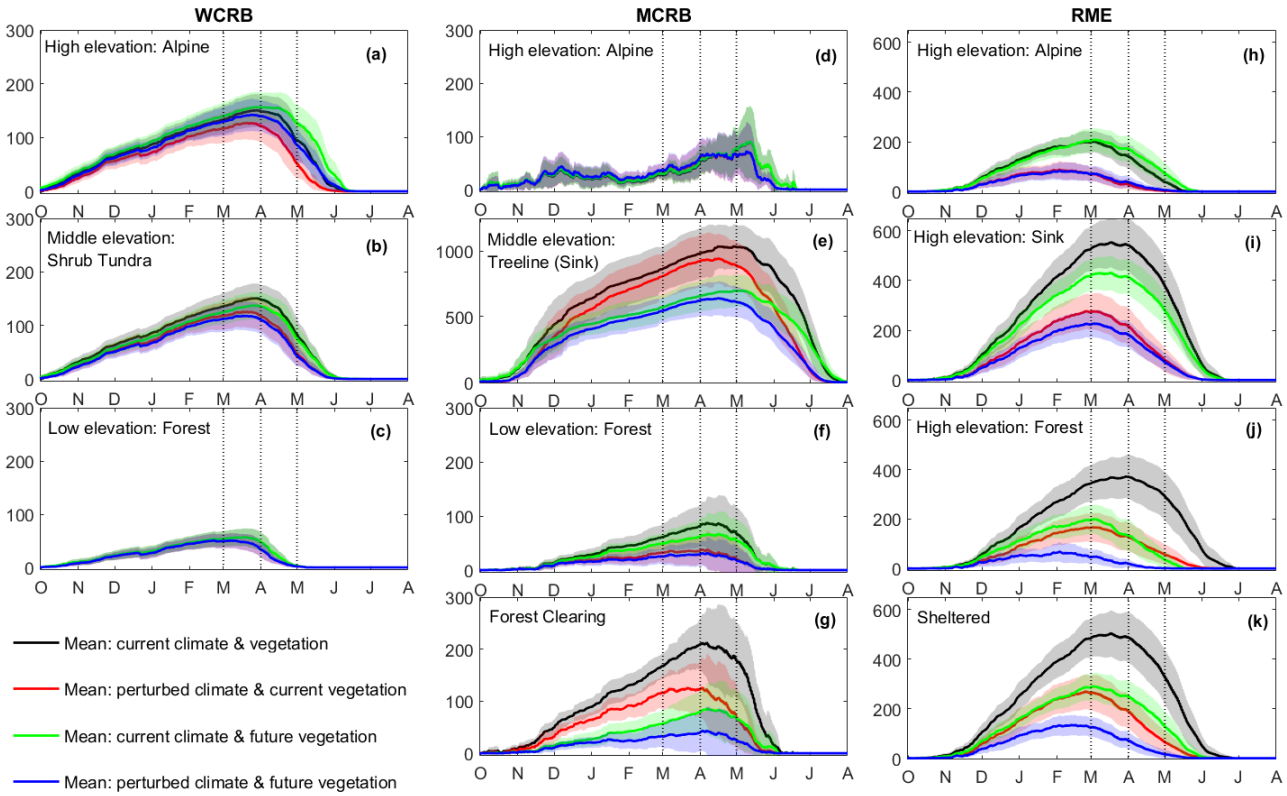

Figure 7.3: Simulated snow accumulation and ablation under current climate and vegetation and climate changes in different elevation bands in Wolf Creek Research Basin (WCRB) – Yukon Territory, Marmot Creek Research Basin (MCRB) – Alberta, Reynolds Mountains East (RME) – Idaho along the North American Cordillera. RME has only one elevation band but multiple blowing snow regimes. The shaded areas around the mean show the interannual variability with ±95 confidence intervals. Ensemble uncertainty is not considered and ensemble mean is instead selected for analysing the interannual SWE under current and perturbed climatic conditions.

snow regime in the treeline zone and the alpine snow regime in MCRB are the most resilient biomes to climate change amongst all other biomes in the northern and southern NAC, these biomes are susceptible to the combined impact of climate change and upward movement of the treeline (Figure 7.3e). At low elevations in MCRB, snow accumulation decreases from 87 mm to 39 mm (48 mm) under climate change and conversion of forest to shrub and grass (Figure 7.3f due to potential wildfire and mountain pine beetle (MPB) (Macias Fauria and Johnson, 2009). This is because of the shift in the forest role from slowing snowmelt by shading the snow and sheltering the snow from wind to accelerating midwinter snowmelt by removal of forest canopy (Lundquist et al., 2013). Forest clearings store deep snowpacks under present-day climate; however, with regrowth of harvested forest the peak snow will decrease (Figure 7.3g). The impact of climate change is less important than the impact of forest regrowth in the harvested clearings due to increased interception losses. Another impact of forest regrowth is the delay in snow ablation because of the lower net radiation under the canopy relative to clearings with no canopy. In general, the impact of vegetation change is offsetting the impact of climate change on peak snowpack timing. The date of the peak SWE is delayed with only vegetation conversion in MCRB and advanced with only climate change impacts.

In RME ($\approx 43^\circ$ N), all blowing snow regimes except for the depressions and valley bottom (Figure 7.3i) will receive a uniform SWE under vegetation changes as the forest canopy disappears. Despite the small impact of vegetation change in the alpine biome covered with grass and short mountain sages, the impact of climate change on snowpack in this biome is large (Figure 7.3h). The most sensitive biome in RME to both climate and vegetation changes is the forest, based on a large decrease in the peak snowpack (Figure 7.3j). The interannual variability of SWE, which is expressed as 95% confidence intervals (CI) in Figure 7.3, becomes smaller in all of the biomes within the three basins under MPC because the snowpack becomes shallow under the combined climate and the vegetation change and variability of the shallow snowpacks becomes smaller. This can occur despite an increased variability of precipitation under the future climate conditions. The interannual variability of SWE does not change in the alpine biomes under a transient vegetation change scenario with an unchanged climate.

To understand the impact of vegetation and climate changes on the distribution of SWE, a probability density function of basin-scale SWE is shown in Figure 7.4 for the three basins. Under the (i) vegetation change only, (ii) climate change only, and (iii) combined climate and vegetation change scenarios, all ranges of SWE decrease the most in the southern basin. SWE in the northern basin shows some insensitivity to the changes. Amongst three basins, MCRB is the most sensitive to vegetation change. The impact of vegetation on snowpack varies between basins and can be as important as the impact of climate change on high SWEs in WCRB. The impact of vegetation change on both low and high SWEs is more important than the impact of climate change in MCRB, while the opposite is true in RME where snowpack is more susceptible to climate change than to transient vegetation change.

The distribution of SWE values throughout the snow season helps to understand the accumulation and ablation rates under present-day climate and also under climate and transient vegetation changes in the future. Figure 7.5 to Figure 7.7 show the effect of vegetation, soil, and climate change on peak SWEs at different elevations and also on the peak outflows from the basins. The impact of the vegetation change counteracts the impact of climate change at higher elevations in WCRB, which makes this biome resilient to the combined changes in climate and transient vegetation (Figure 7.5). The vegetation change acts similarly to climate change in decreasing the peak snowpack at medium elevations in WCRB. In contrast, it counteracts the climate change impact on decreasing the peak snowpack at high elevations in WCRB. Therefore, snowpack decreases at high elevations under climate change will be offset by shrub tundra expansion. The impact of transient vegetation change with respect to the interaction with climate change on peak SWE varies with elevation in WCRB. It is small at low elevations and large at medium elevations and it offsets the climate change impact at high elevations. This suggests that understanding vegetation dynamics in mountain basins is important with respect to reducing the uncertainty in hydrological responses to climate change, because transient vegetation change can be as important as uncertainty due to climate models.

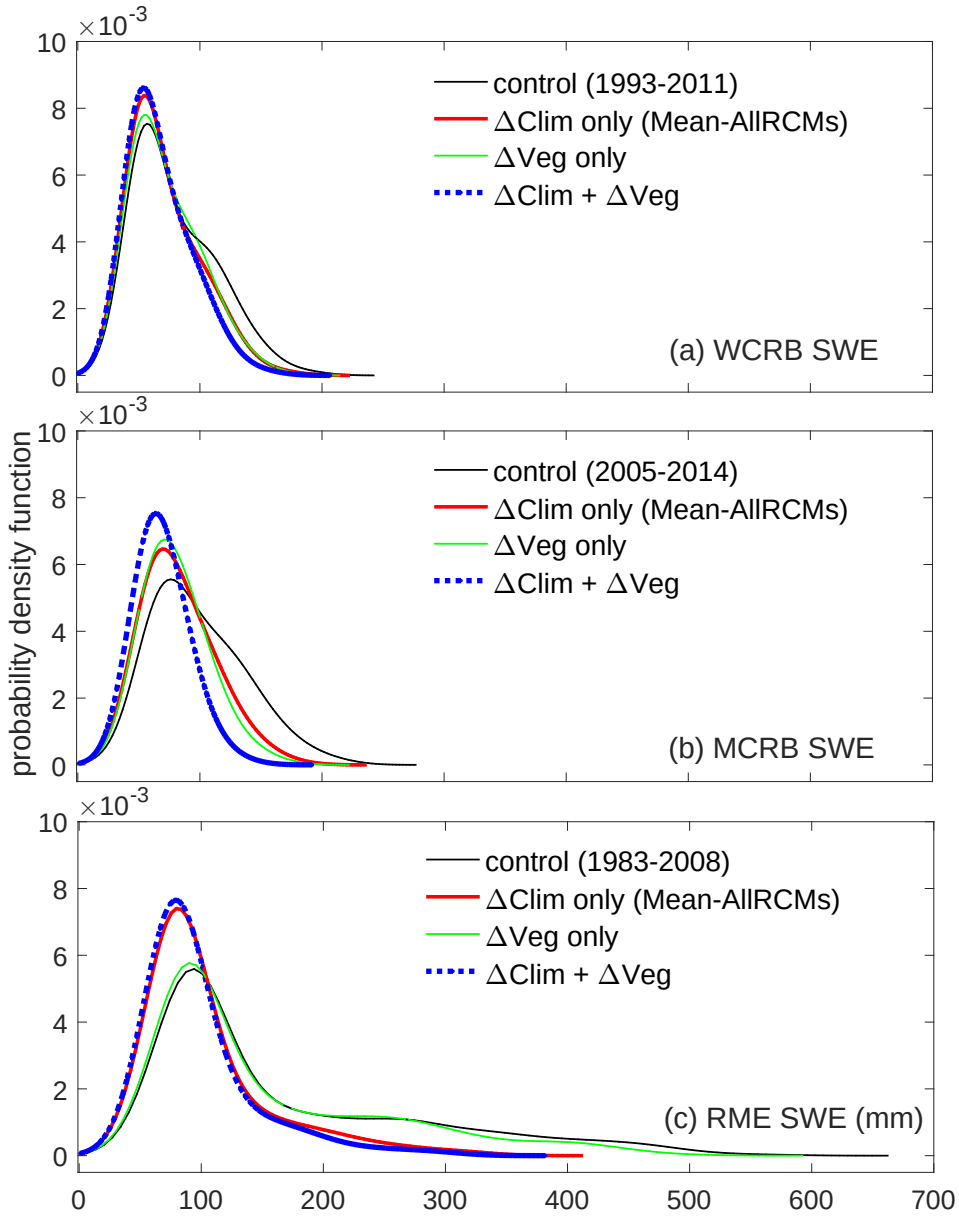

Figure 7.4: Differences in the probability density functions of snow water equivalent (SWE) between current climate with no change in vegetation, future climate with no change in vegetation, future vegetation with no change in climate, and combination of future climate and vegetation changes for (a) Wolf Creek Research Basin (WCRB) – Yukon Territory, (b) Marmot Creek Research Basin (MCRB) – Alberta, and (c) Reynolds Mountains East (RME) – Idaho, three headwater basins along the North American Cordillera (NAC). All three simulated SWE distributions for climate, vegetation, and both climate and vegetation changes in each basin are significantly (p–value < 0.05) different than simulated SWE distribution for the control period based on the Kolmogorov- Smirnov (K–S) test (Massey Jr., 1951). The K–S test, which is a nonparametric hypothesis test, was used to evaluate the differences between the distributions of modelled hourly SWE for the control climate and under transient vegetation and climate changes over 18 years in WCRB, 9 years in MCRB, and 25 years in RME ($\times$365day$\times$24 hour).

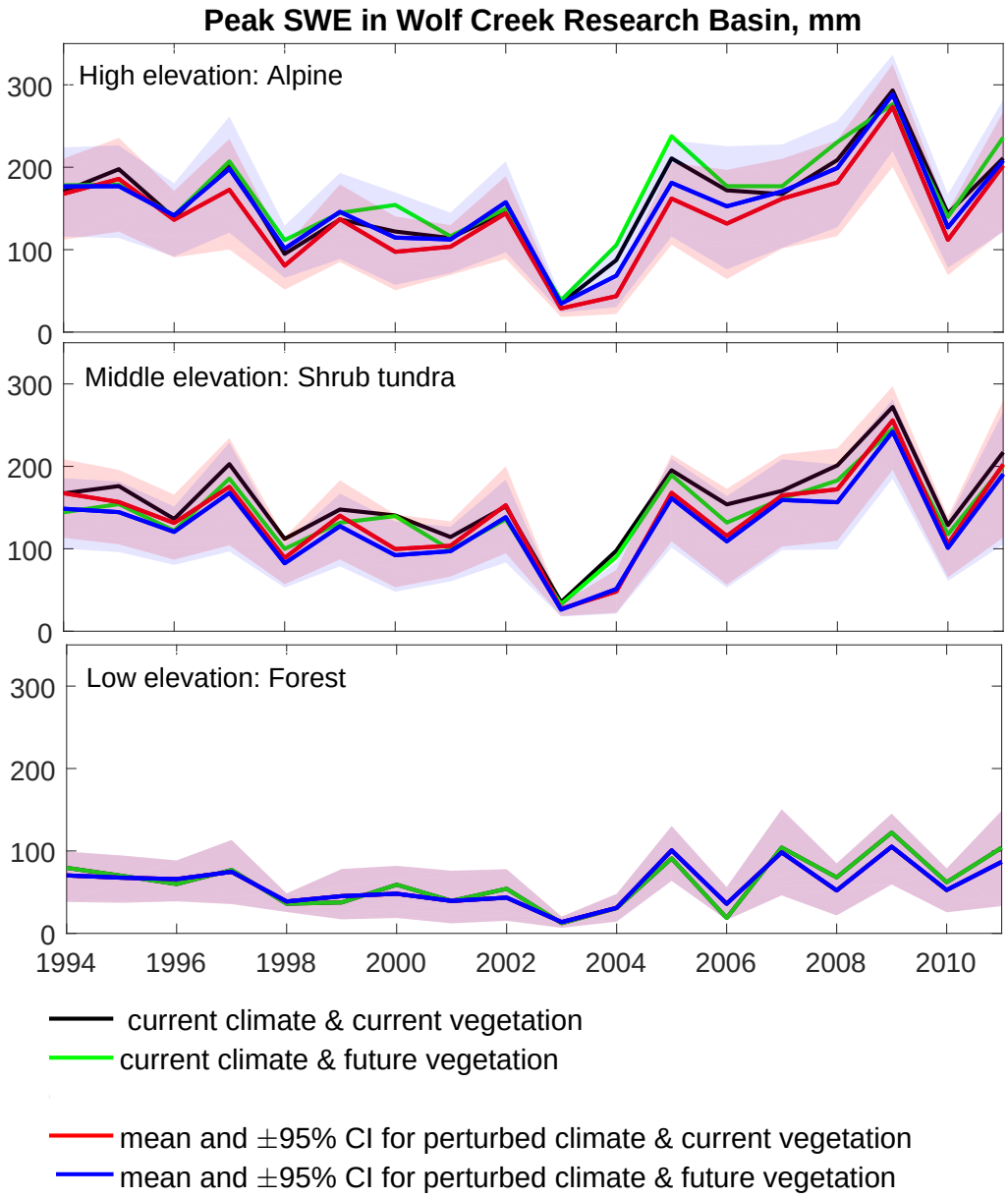

Figure 7.5: Differences in simulated peak snow water equivalent (SWE) between current climate and under climate and vegetation changes in Wolf Creek Research Basin (WCRB). Shaded area shows the associated response uncertainty of the climate models with 95% confidence intervals.

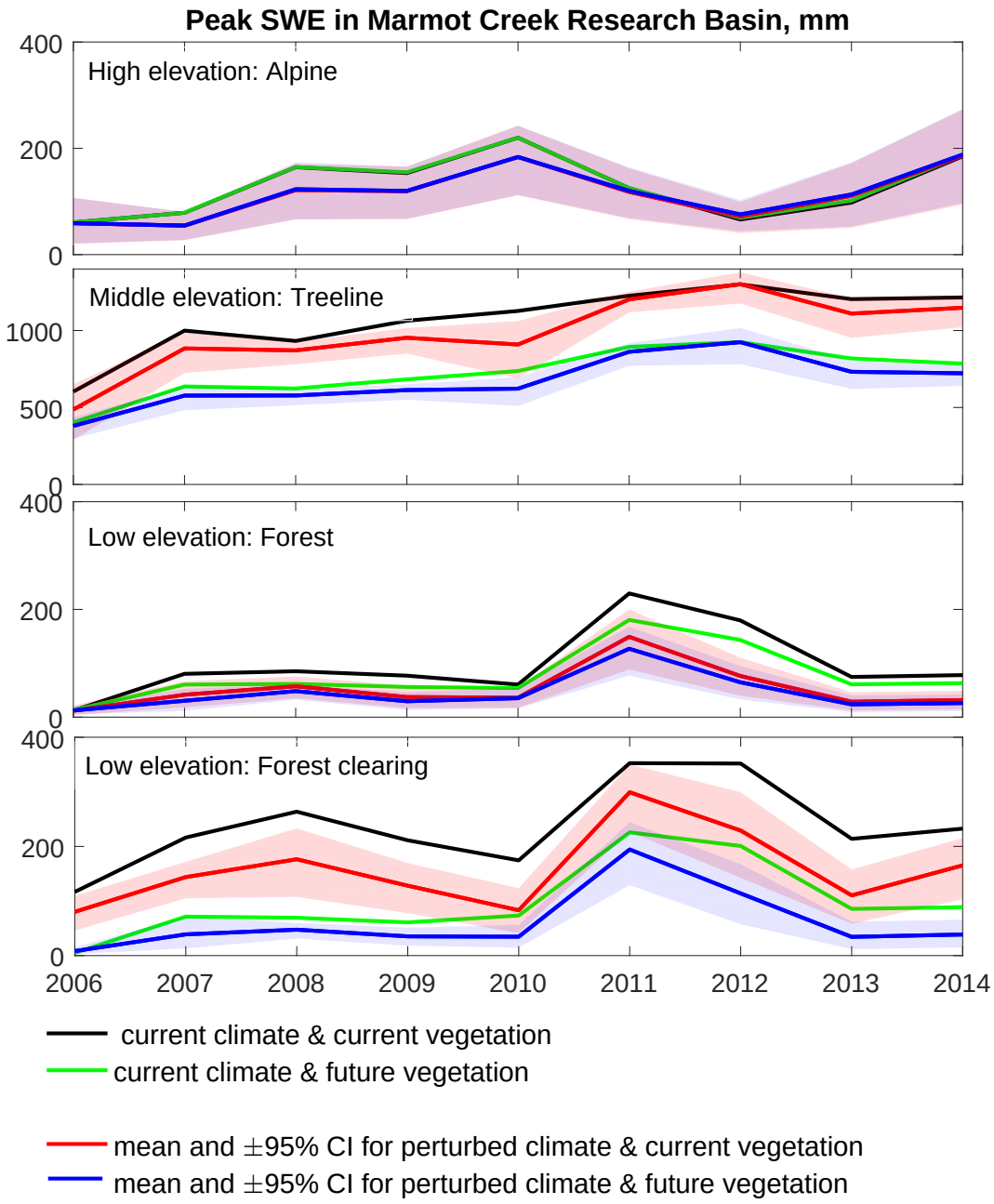

Figure 7.6: Differences in simulated peak snow water equivalent (SWE) between current climate and under climate and vegetation changes in Marmot Creek Research Basin (MCRB). Shaded area shows the associated response uncertainty of the climate models with 95% confidence intervals.

Similar to the alpine biome in WCRB, the impact of climate change on peak snowpacks at high elevations in MCRB is slightly offset by the impact of transient vegetation change. The treeline, which acts as a blowing snow sink zone, shifts upslope under future vegetation conditions, which causes the peak SWE to increase slightly at high elevations in MCRB (Figure 7.6). A deep snowpack is deposited at medium elevations in MCRB because of the strong winds, which scour blowing snow from the higher elevations to the treeline. Under vegetation growth, alpine vegetation and shrubs in the treeline will eventually convert to forest, which can change the snow regime from a present-day blowing snow sink to a future forest with intercepted snow on the canopy. A snow regime change at medium elevations in MCRB leads to a substantial decrease in the maximum accumulated snowpack. The peak SWE at low elevations also declines under future deforestation in MCRB (Figure 7.6). This because sublimation from blowing snow within the deforested portion of the lower elevations becomes more important than sublimation from intercepted snow on the canopy before deforestation. A higher sublimation rate on the slopes with no vegetation cover was also reported by Liston et al. (2002). The impact of afforestation on snowpack in the forest clearings is stronger than that of climate change. Therefore, an enhanced snowpack decline is expected in forest clearings under climate and vegetation changes (Figure 7.6).

RME has a small drainage area and elevation range. Therefore, separating RME into different elevation bands is not necessary. The snow regimes of blowing snow source and sink, sheltered from blowing wind, and forest with intercepted snow are chosen to examine the impact of climate and vegetation changes. Snow simulations in the alpine zone in RME, which is covered with grass and short mountain sages, show that snowpack in this biome is sensitive to climate change but almost insensitive to transient vegetation change (Figure 7.7). In all other zones, the impact of transient vegetation change on snowpack is as important as the impact of climate change. Except for the blowing snow source zone in RME, the role of vegetation change is to intensify the impact of climate change on the decreased snowpack. Peak SWE decreases the most in the present-climate forest under deforestation in the future. Under vegetation change, the simulated future peak snowpack becomes spatially uniform across the basin.

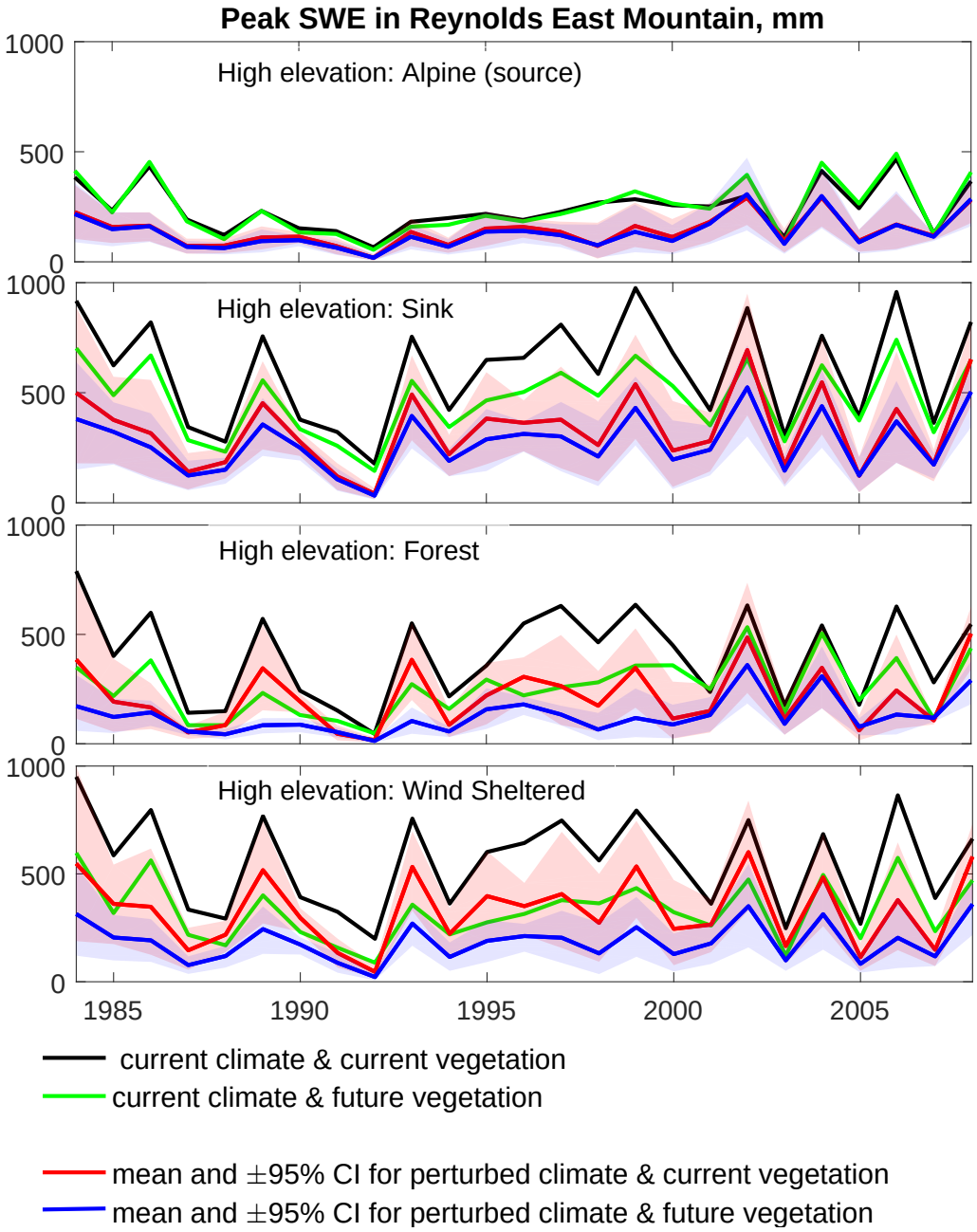

Figure 7.7: Differences in simulated peak snow water equivalent (SWE) between current climate and under climate and vegetation changes in Reynolds Mountain East (RME) catchment. Shaded area shows the associated response uncertainty of the climate models with 95% confidence intervals.

Snow regimes are the most resilient to both climate and transient vegetation changes at high elevations in WCRB and MCRB and low elevations in WCRB, with less than 10% decrease in the annual peak SWE. In contrast, snow regimes in the forest clearings in MCRB and in the forest and sheltered sites in RME are sensitive to the changes, with 80% and 68% decreases, respectively. Under transient vegetation change, the peak SWE drops from 87 mm to 46 mm (47% decrease) at low elevations in MCRB with expansion of the grasslands into the forest. Impacts of climate change on snow regimes can be enhanced or dampened by the impact of transient vegetation changes. Shrub tundra expansion into the higher elevations in WCRB can substantially dampen the impact of climate change on snowpack, even though it cannot completely offset the impact of climate change. Active vegetation growth in the treeline or in forest clearings enhances climate change impacts on the snowpack. Therefore, the impact of afforestation on the snowpack can be as important as the impact of climate change.

The basin-scale peak SWE is affected by both climate and vegetation changes, with p–values less than 0.05 indicating the changes are statistically significant based on the Mann–Whitney U-test. Distributions of the simulated peak SWE for $n = 18$ years for WCRB, 9 years for MCRB, and 25 years for RME over the control (base) period are compared with the future distributions obtained from 11 RCM-GCMs ($11 \times n$ values). Table 7.2 shows that it decreases from 133 mm under the current climate to 118 mm (11% decrease) under a climate change scenario in WCRB. The peak SWE decreases to 107 mm (20%) when a transient vegetation change scenario is also considered in combination with a climate change scenario. In the central basin, the peak SWE declines from a current climate SWE of 183 mm to 141 mm (23% decrease) under climate change and declines to 106 mm (42% decrease) under a combined climate and transient vegetation change. An increase in precipitation in the north and a large vegetation change in MCRB and its effect on accumulated snow lead to almost an equal peak snowpack in both MCRB and WCRB. The peak SWE in the southern basin decreases from 368 mm under the current climate to 196 mm (47% decrease) under climate change and decreases to 168 mm (54% decrease) under both climate and vegetation changes.

Table 7.2: Simulated snow characteristics including peak snow water equivalent (SWE), length of snow season, timing of snow initiation, mean annual peak SWE, and snow-free date under current and monthly perturbed climate and future vegetation in three basins along the North American Cordillera. Because only three scenarios are applied for future vegetation, only the range of changes is provided. Bold and underlined values denote significant changes with p–values less than 0.05 and 0.1, respectively, based on the Mann–Whitney U-test. Simulated distributions with $n = 18$ years for WCRB, 9 years for MCRB, and 25 years for RME over the control (Base) period for each hydrological variable are compared with the simulated future distributions obtained from 11 RCM–GCMs ($11 \times n$ values). Changes, which are relative to current climate/vegetation, are given in parentheses. Dates are given in Julian water year, starting October 1st.

Variable	**Base**	**ΔClimate** **5%, mean, 95%**	**ΔVegetation change range**	**ΔClimate+ΔVeg.** **5%, mean, 95%**
(1) Wolf Creek Research Basin (WCRB)				
Peak SWE [mm]	133	73, 118(–11), 153	118–133(–11 to 0)	64, **107(–20)**, 142
Initiation [date]	5	0, 7(2), 47	5(0)	0, 7(2), 45
Peak SWE [date]	186	143, **164(–22)**, 178	182–185(–4 to –1)	148, **162(–24)**, 170
Snow-free [date]	250	213, **235(–15)**, 248	250–252(0 to 2)	216, **236(–14)**, 249
Season length [day]	224	160, **208(–16)**, 242	224–226(0 to 2)	164, **215(–9)**, 251
(1) Marmot Creek Research Basin (MCRB)				
Peak SWE [mm]	183	102, **141(–23)**, 170	136–168(–26 to –8)	74, **106(–42)**, 130
Initiation [date]	9	4, **24(15)**, 62	9(0)	4, **24(15)**, 63
Peak SWE [date]	210	175, 200(–10), 216	211(1)	177, 205(–5), 223
Snow-free [date]	294	257, **281(–13)**, 295	294–296(0 to 2)	257, **283(–11)**, 299
Season length [day]	283	204, **248(–35)**, 277	283–284(0 to 1)	200, **246(–37)**, 276
(3) Reynolds Mountain East (RME)				
Peak SWE [mm]	368	105, **196(–47)**, 277	326–375(–11 to 2)	91, **168(–54)**, 237
Initiation [date]	35	20, **50(15)**, 85	35(0)	19, **49(14day)**, 83
Peak SWE [date]	161	102, **129(–32)**, 148	162–168(1 to 7)	96, **127(–34)**, 149
Snow-free [date]	246	184, **213(–33)**, 232	247(1)	195, **220(–26)**, 236
Season length [day]	211	113, **161(–50)**, 197	212–213(1 to 2)	129, **171(–40)**, 200

1st day of	Oct	Nov	Dec	Jan	Feb	Mar	Apr	May	Jun	Jul	Aug	Sep
Water year date	1	32	62	93	124	152	183	213	244	274	305	336

Considering only vegetation changes under the current climate, the peak SWE decreases more in MCRB (26%) than in WCRB and RME (11%). Therefore, under the combined climate and transient vegetation change studied in this research, the maximum accumulated snowpack is the most resilient in WCRB and the most sensitive in RME.

7.3 Snow Processes and Evapotranspiration under Climate and Transient Vegetation Changes

Differences in snow processes and evapotranspiration under monthly perturbed climate and transient changes in vegetation and soils are simulated. The Mann–Whitney U-test is applied to test whether differences between current climate and future climate/vegetation variables are statistically significant or not. The null hypothesis is that the distribution mean under current climate is equal to the distribution mean under climate and vegetation change scenarios. The alternative hypothesis is that the climatological means are not equal.

7.3.1 Precipitation Phase

With warmer air temperatures and increased precipitation, the snowfall events become less frequent as the precipitation phase changes from snowfall to rainfall. As shown in Figure 7.8, the rain to total precipitation ratio ($\frac{R}{P}$) increases in all of the basins under climate and transient vegetation changes. Furthermore, the annual rainfall reaches 238 mm out of 413 mm total annual precipitation ($\frac{R}{P}$=0.58) in WCRB, 550 mm out of 1027 mm total precipitation ($\frac{R}{P}$=0.54) in MCRB, and 473 mm out of 866 mm total precipitation ($\frac{R}{P}$=0.55) in RME. Based on the results for the three basins constituting a north–south transect through the NAC, snow-dominated regions with elevations ranging between 650 m and 2500 m are expected to become rain-dominated under similar monthly perturbed climatic conditions to these basins.

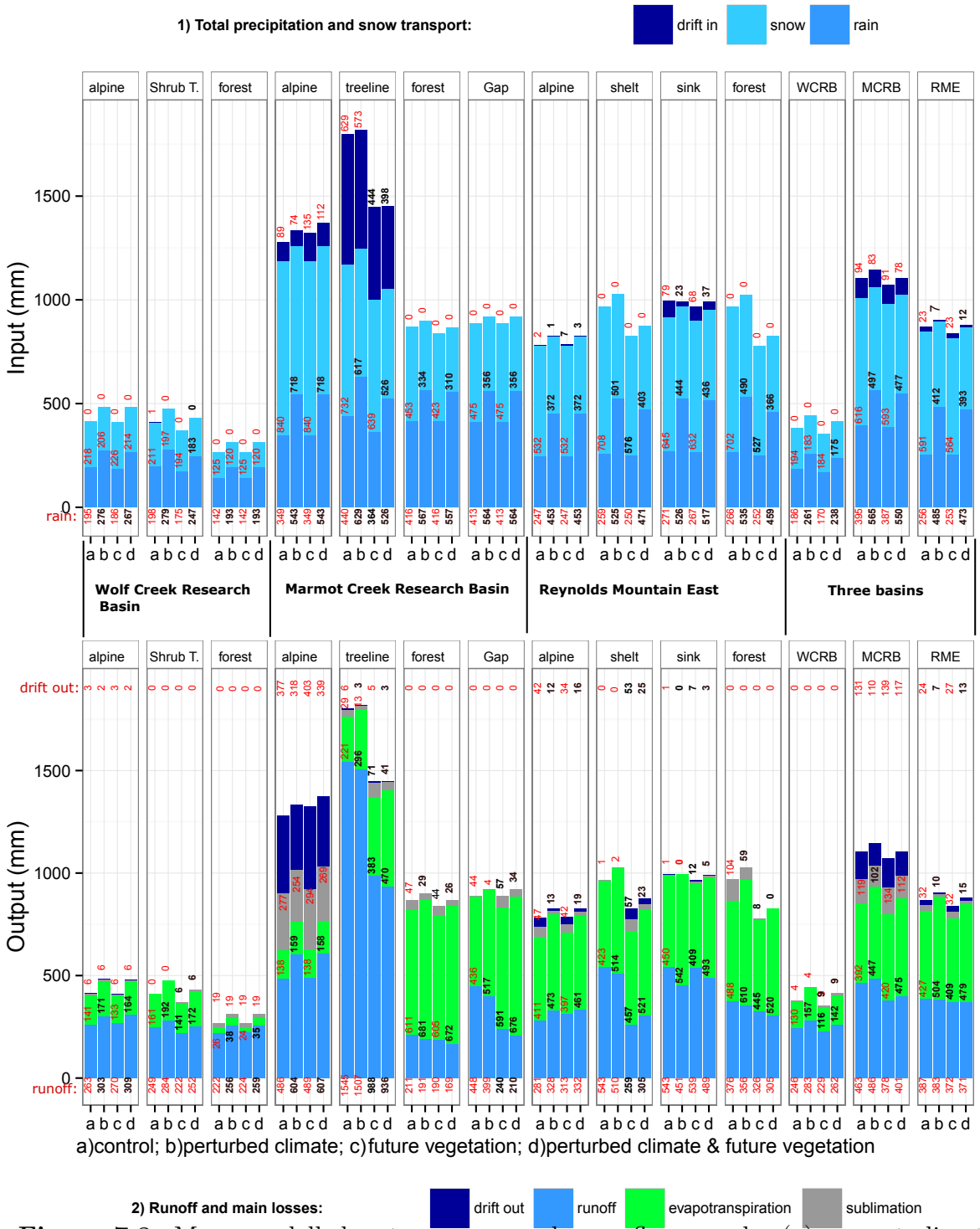

Figure 7.8: Mean modelled water, vapor, and snow fluxes under (a) current climate, (b) monthly perturbed climate, (c) transient vegetation change, and (d) both transient vegetation and climate changes. For convenience, values for each variable are given on the stacked bars. The statistically significant changes in climatological mean of the simulated variables with p–values less than 0.05 based on the Mann–Whitney U-test are represented by bold and black values. The simulated distributions with $n = 18$ years for WCRB, 9 years for MCRB, and 25 years for RME in the control period for each hydrological variable are compared with the simulated future distributions obtained from 11 RCM-GCMs ($11 \times n$ values).

7.3.2 Snow Transport

Under climate and transient vegetation changes, the annual average snow transport remains unchanged in WCRB, while it declines 14 mm in MCRB and 11 mm in RME (Figure 7.8). Snow drifting at high elevations in MCRB declines 11 mm under climate change and increases 23 mm due to shorter fetches as the treeline moving upslope. Therefore, the impact of climate change on snow transport in the alpine biome in MCRB is almost completely offset by vegetation change. Under both climate and vegetation changes at medium elevations in MCRB, where the treeline currently exists, snow transport decreases 56 mm under MPC. Snow transport in the valley bottom and blowing snow sink regime in RME, now covered with a willow forest, also decreases substantially from present-day 79 mm to 37 mm (42 mm decrease, p–value <0.05) under MPC and deforestation.

7.3.3 Sublimation

The total annual sublimation from all sources including snow intercepted on the canopy, snow surface, and blowing snow was examined under climate and transient vegetation changes (Figure 7.8). Sublimation from snow intercepted on the canopy in WCRB dominates the total sublimation, which is expected to increase in this basin as the treeline moves upward and shrub tundra expands to higher elevations. In MCRB, total annual sublimation increases 14 mm under vegetation changes, but decreases 8 mm under both vegetation and climate changes. The impact of vegetation on sublimation rate in RME is negligible, while climate change decreases sublimation from 31 mm to 10 mm. Transient vegetation change enhances the sublimation with varying rates on different biomes across the NAC. It causes the amount of sublimation to increase moderately in the central and northern basins. Transient vegetation change does not affect sublimation magnitudes in the southern basin.

Sublimation losses do not only vary from one basin to another, but vary among the different elevation bands within each basin. For instance, at high elevations in WCRB, a shrub tundra expansion enhances the sublimation by increasing the snowpack. In contrast,

both snowpack and sublimation decrease under climate change. This shows that, in the alpine biome of WCRB, the impact of transient vegetation change on sublimation can be as important as the impact of climate change and a combined climate and transient change leads to an unchanged sublimation rate. At medium elevations in WCRB covered currently by shrub tundra, a treeline shift into the shrub tundra biome increases sublimation, while the opposite is true under climate change when snowpack and sublimation both decrease. No changes are expected in the sublimation at low elevations in WCRB. Similar to WCRB, the impact of a combined climate and transient vegetation change on sublimation in MCRB varies with elevation. It causes a 8 mm decrease at high elevations as a result of the upward movement of the treeline, a 12 mm increase in the treeline blowing snow sink regime as shrubs turn to forest, and a 21 mm decrease at low elevations as forest becomes uncovered and snowpack becomes shallower with warming. Different mechanisms are responsible for these changes, total sublimation decreases in the alpine biome with the upward movement of the treeline as sublimation from blowing snow drops with upslope forest expansion. At medium elevations, bushes are replaced by trees and sublimation from intercepted snow on their canopy slightly increases. The combination of topographic gradients and types of vegetation plays an important role in snow redistribution and blowing snow sublimation. The highest wind-driven redistribution of snow and the highest sublimation occurs on leeward slopes, where there is little or no vegetation cover (Liston et al., 2002). At low elevations in MCRB, sublimation from intercepted snow on the canopy decreases as deforestation occurs. This also occurs in the deforested zone in RME in which sublimation significantly decreases from 104 mm to 8 mm as a result of decreased available snow combined with deforestation under climate change.

7.3.4 Evapotranspiration (ET)

The change in vegetation composition also alters the amount of evapotranspiration (ET). The vegetation composition in all three basins in this study are projected to change under future conditions. The simulations show that, under transient vegetation change, annual ET increases 8 mm as a result of afforestation of the clearings and upward movement of the

treeline in MCRB. In contrast, ET decreases 14 mm in WCRB and 18 mm in RME. An increase in ET due to climate change can be offset to some degree by a transient vegetation change in WCRB and RME. ET increases the most in MCRB, from 392 mm to 475 mm (83 mm, p–value < 0.05), and the least in WCRB, from 130 mm to 142 mm (12 mm), under both vegetation and climate changes. Under a combined climate and transient vegetation change, statistically significant changes in ET are expected in different elevation bands. The increase in ET varies with elevation within each basin and reaches 23 mm at high elevations and 9 mm at low elevations in WCRB, 61 mm at low elevations and 249 mm in the treeline elevations in MCRB, and 32 mm in the forest and 98 mm in the sheltered site in RME. This shows a high variability of the annual ET in the three basins along the NAC.

7.3.5 Permafrost

Permafrost in the northern latitudes and in high mountains affects the runoff process, subsurface storage, and the infiltration from snowmelt and rainfall. Permafrost degradation under warmer climates has important hydrological consequences and can substantially alter runoff processes. Only WCRB in the southern Yukon has permafrost, and therefore freezing and thawing mechanisms as well as response of the permafrost to perturbed climatic conditions are also examined for this basin. As soil moisture and heat conductivity varies with soil depth, multiple layers are considered in permafrost modelling (Xie and Gough, 2013). Figure 7.9 shows total soil moisture of all layers and depths from ground surface to freezing front and thawing front at different elevations under the current climate and their response to both climate and transient vegetation changes. The average soil depth across the WCRB is considered to be 4 m based on previous studies (e.g., Quinton et al., 2005).

Under a combined climate and transient vegetation change scenario, soil moisture in WCRB does not change and remains similar to that in the current climate. In spring and summer, slight decrease in the soil moisture is found under both vegetation and climate changes. At low elevations, a decrease in the soil moisture is expected; vegetation does not change much in this elevation band and only climate change is responsible for the simulated

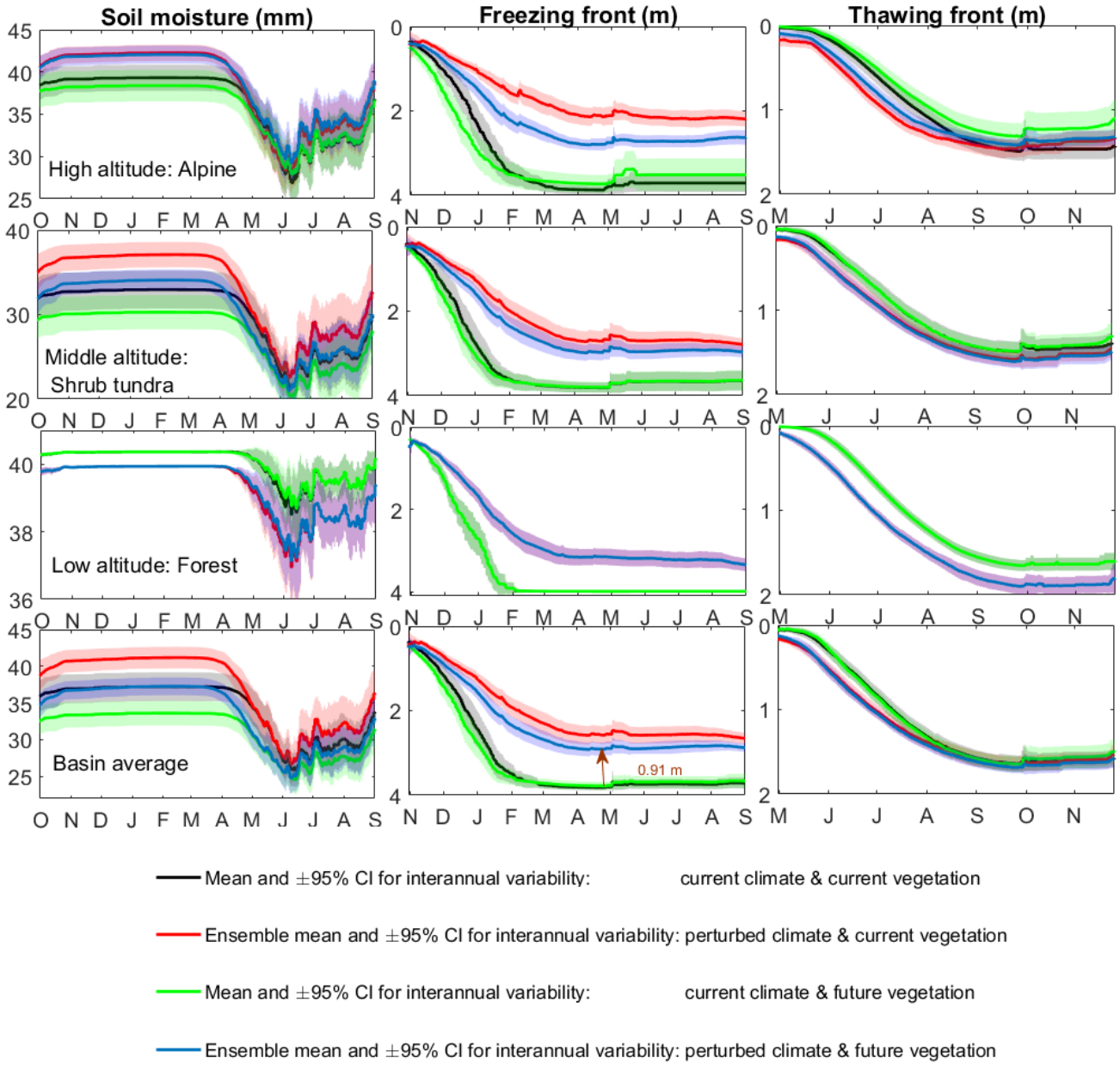

Figure 7.9: Simulated permafrost characteristics including soil moisture and depths from the ground surface to freezing and thawing fronts under vegetation and climate changes in Wolf Creek Research Basin for different elevations. Simulated permafrost characteristics are not affected by a moderate change in soil properties associated to transient vegetation changes in this basin. The shaded areas around the mean show the interannual variability with ±95 confidence intervals. No ensemble uncertainty of climate models is included in interannual variability.

soil moisture reduction. Depth of the simulated frozen layer is 0.34 m in mid-October under current climate conditions. It becomes thicker gradually and reaches its maximum depth of 3.81 m in late April. Under climate change, the maximum frost depth decreases to 2.55 m (1.26 m drop), and under both vegetation and climate changes, decreases to 2.9 m (0.91 m decrease). This suggests that the impact of climate change on permafrost can be moderated by the impact of transient vegetation change. Under the current climate, the depth to thawing front starts to increase in May as the ground warms up and reaches 1.63 m in September. Under climate change and vegetation changes, the depth to thawing front increases in spring and summer up to 0.26 m in June on average across the basin. Upward movement of the treeline and shrub tundra expansion at high elevations in WCRB counteract the impact of climate change; the impact of climate changes on permafrost degradation is reduced by vegetation abundance. This is consistent with a previous study by Sturm et al. (2005) that reported permafrost enhancement by shrub tundra expansion in the Arctic and sub-Arctic. The responses of the simulated permafrost characteristics to both transient vegetation and associated soil changes are not strong and a moderate change in soil properties associated to transient vegetation changes in this basin would not affect soil moisture and thawing or freezing fronts.

7.4 Impact of Climate and Transient Vegetation Change on Streamflow Regimes

Similar to other hydrological variables, runoff is also affected by vegetation and climate changes. Afforestation or deforestation alters the surface roughness, infiltration, soil moisture, and depth to the frozen soil layer. The impact of transient vegetation and soil changes on annual total runoff and peak runoff is high (Figure 7.8, Figure 7.10, and Table 7.3). Annual total runoffs gradually increase from south to north (1% to 16%) under climate change (Table 7.3 and Figure 7.10); however, a transient vegetation change decreases the annual total runoff up to 16%. Under both vegetation and climate change, a 8% increase in WCRB's annual runoff is expected and annual runoff decreases from 371 mm to 351 mm

Table 7.3: Simulated runoff characteristics including annual volume, annual peak, and timing of the annual peak under current and monthly perturbed climates and future vegetation in basins along the North American Cordillera. Bold and underlined values denote significant changes with p–values less than 0.05 and 0.1, respectively, based on the Mann–Whitney U-test. Simulated distributions with $n = 18$ years for WCRB, 9 years for MCRB, and 25 years for RME over the control (Base) period for each hydrological variable are compared with the simulated future distributions obtained from 11 RCM–GCMs ($11 \times n$ values). Changes, which are relative to the current climate/vegetation, are given in parentheses. Dates are given in Julian water year, starting October 1st; for convenience, a guide for the first day of each month is given.

Variable	**Base**	**ΔClimate** **5%, mean, 95%**	**ΔVegetation** **change range**	**ΔClimate+ΔVeg.** **5%, mean, 95%**
(1) Wolf Creek Research Basin (WCRB)				
Volume [mm]	246	207, 286(16), 343	228–262(–7 to +7)	194, 265(8%), 317
Peak [cms]	3.2	1.9, 3.0(–7),3.9	2.4–3.3(–26 to +2)	1.5, **2.5(–22%)**, 3.3
Peak [date]	206	147,195(–11), 228	209–213(3 to 7)	141, 183(–23day), 212
(2) Marmot Creek Research Basin (MCRB)				
Volume [mm]	402	342, 426(6), 481	336–373(–16 to –7)	284, 359(–11%), 409
Peak [cms]	1.01	0.80, 1.11(9), 1.33	0.91–0.96(–10 to –5)	0.70, 0.98(–3%), 1.18
Peak [date]	254	244, 253(–1), 258	254–256 (0 to 2)	254, 256(2day), 261
(3) Reynolds Mountain East (RME)				
Volume [mm]	371	262, 375(1), 459	340–379(–8 to +2)	248, 351(–5%), 427
Peak [cms]	0.05	0.03, 0.045(–15), 0.05	0.045–0.05(–16 to 2)	0.03, **0.044(–17%)**, 0.05
Peak [date]	226	158, **186(–40)**, 204	226–228(0 to 2)	154, **179(–47day)**, 195

1st day of	Oct	Nov	Dec	Jan	Feb	Mar	Apr	May	Jun	Jul	Aug	Sep
Water year date	1	32	62	93	124	152	183	213	244	274	305	336

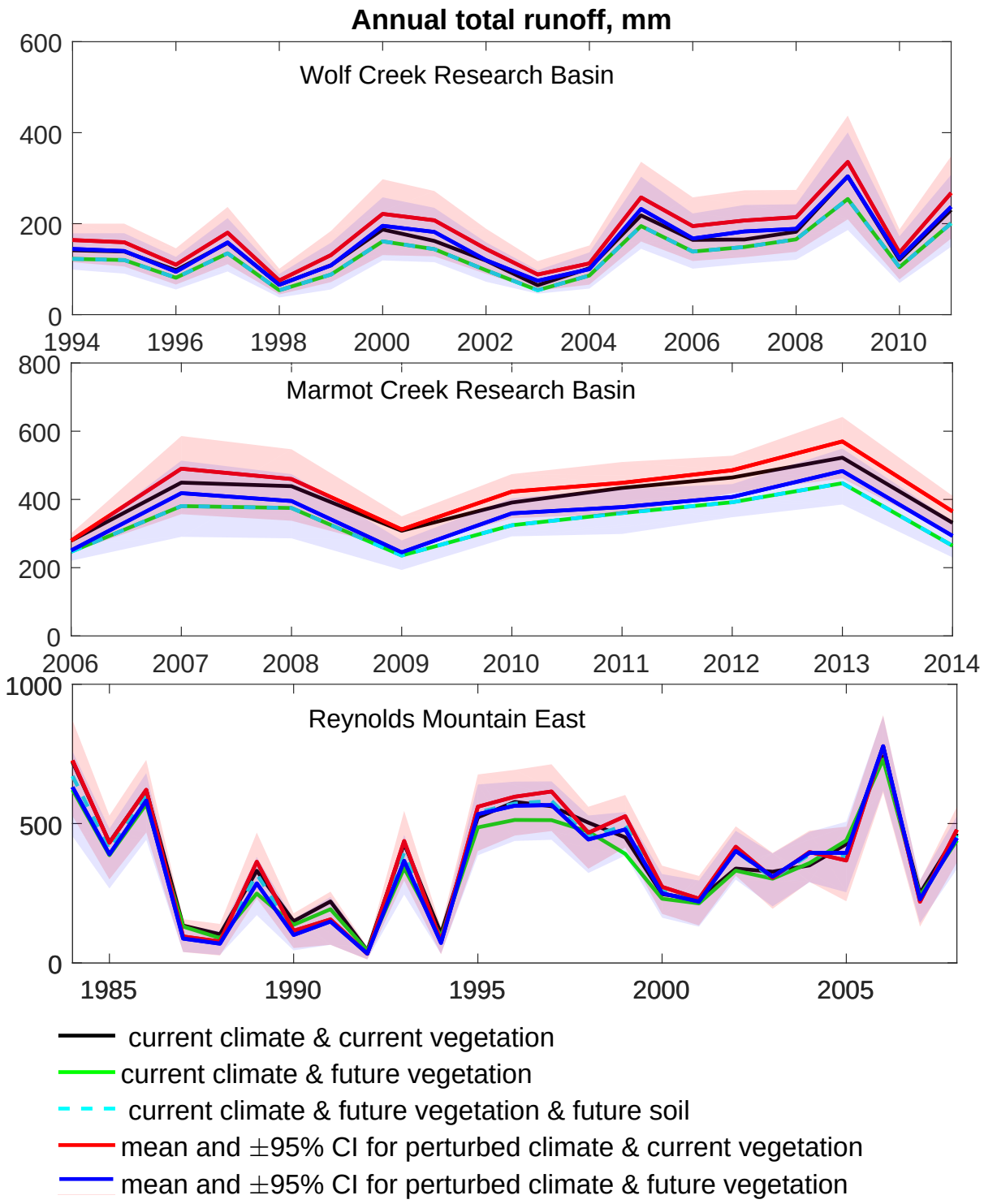

Figure 7.10: Differences in annual total runoff between current climate and under climate, vegetation, and soil changes in the three basins across the North American Cordillera. Shaded area shows the associated response uncertainty of the climate models with 95% confidence intervals. Time series for both vegetation and soil changes and only vegetation change almost overlap in Wolf Creek Research Basin and Marmot Creek Research Basin.

(5% decrease) in RME. Under both vegetation and soil changes, annual total runoff does not change in WCRB and MCRB and only slightly changes are expected in RME (Figure 7.10). Slightly changed soils in WCRB and MCRB as a result of treeline movement do not affect the annual total runoff in these two basins. Deforestation in RME, however, can change soil properties over a long period of time, which can affect annual total runoff.

Results show that transient vegetation changes contribute more than transient soil changes to changes in annual total runoff. The contribution of increased precipitation under MPC to annual total runoff in WCRB is moderated by increased surface roughness due to alpine afforestation, and shrub tundra expansion. The impact of slightly increased precipitation on annual total runoff in MCRB is dampened by alpine and clearings afforestation and deforestation at low elevations. Therefore, annual total runoff decreases from 402 mm under current climate to 359 mm under both climate and vegetation changes (11% decrease, p–value < 0.05) in MCRB. Response of the peak SWE to transient vegetation change is reflected in the response of the annual runoff. Not only does the total annual outflow from each basin respond differently to changes in climate and vegetation, but the response of runoff to changes in vegetation and climate also varies with elevation in each basin. At high elevations in WCRB, annual total runoff increases from 264 mm to 308 mm (17% increase) largely due to vegetation change that intensifies the climate change impact on decreased snow accumulation by a shrub tundra expansion.

Despite the dominant impact of climate change at high elevations, the impact of transient vegetation changes become as important as the impact of climate change on runoff at medium elevations in WCRB. Runoff decreases with shrub tundra to forest conversion (27 mm, 11%) but increases under climate change (38 mm, 15%, p–value < 0.05) and slightly increases (4 mm, 2%) under both vegetation and climate changes. This suggests that the impact of climate change on decreasing runoff at medium elevations in WCRB can be offset by changes in the vegetation. Runoff at high elevations in MCRB remains almost unchanged under afforestation, increases from current climate value of 486 mm to 604 mm (24%) under climate change, and to 607 mm (25%, p–value < 0.05) under both vegetation and climate

changes. Runoff at low elevations in MCRB is modelled to decrease from 211 mm to 107 mm (19%, p–value < 0.05) under the combined impact of deforestation and climate change.

The maximum accumulated snowpack, along with the melt rates, rain-on-snow intensity and frequency, soil characteristics, antecedent soil moisture conditions, and time of the year, are important factors in runoff generation. Despite some dampening impacts of transient vegetation change on the peak SWEs, the impact of transient vegetation change on peak streamflows enhances the impact of climate change in all three basins (Table 7.3). Mean annual peak runoff increases under MPC only in MCRB assuming no vegetation change occurs (Figure 7.11). Under both vegetation and climate changes, peak runoff drops in all three basins, with the largest drop in WCRB from current climate peak runoff of 3.2 $m^3 s^{-1}$ to 2.5 $m^3 s^{-1}$ (22% decrease, p–value < 0.05). MCRB is the most resilient basin to the changes in terms of annual peak runoff with only a 3% decrease (from 1.01 $m^3 s^{-1}$ to 0.98 $m^3 s^{-1}$). The forest expansion into shrubs and shrub tundra expansion into alpine tundra affect the maximum runoff from WCRB and decrease its intensity and variability (Figure 7.11). Similar to WCRB, peak streamflows are mainly affected by vegetation changes and to a lesser extent by climate change in MCRB. Peak runoff decreases in RME and remains unchanged in WCRB and MCRB under both vegetation and soil changes. The impact of transient soil changes, as a result of transient vegetation changes, on peak runoff can be as important as climate and vegetation change impacts in RME. Vegetation change slightly reduces the intensity of the peak flows but not enough to keep them within the range of historical flows (Figure 7.11). The expected deforestation and expansion of tall mountain sages intensify the peak streamflow in RME, but not enough to reach historical ranges. The only case in which a future peak streamflow exceeds the historical range of peak streamflows occurs in 1986 (Figure 7.11). This is due to a rare circumstance with a rapidly melting snowpack following a warm week and a severe rainfall event.

The performance of the models used in this research in capturing magnitude and timing of the peak values is only fair. Therefore, one needs to be cautious when interpreting the results for changes in timing of the variables under climate changes.

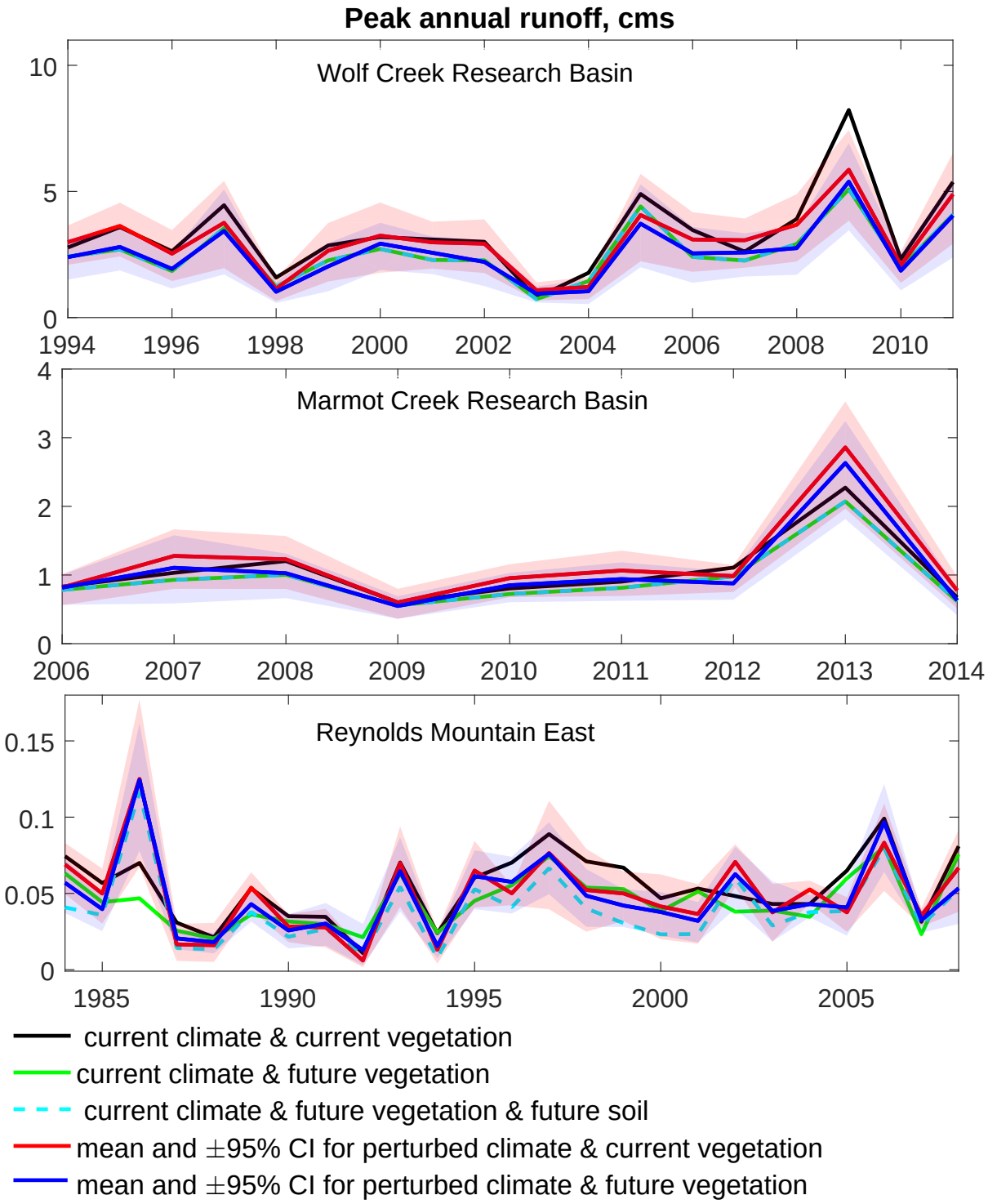

Figure 7.11: Differences in annual peak runoff between current climate and under climate, vegetation, and soil changes in the three basins across the North American Cordillera. Shaded area shows the associated response uncertainty of the climate models with 95% confidence intervals. Time series for both vegetation and soil changes and only vegetation change almost overlap in Wolf Creek Research Basin and Marmot Creek Research Basin.

Table 7.4: Simulated runoff ratio, which is the ratio of annual total runoff to annual total precipitation, under current and monthly perturbed climates and future vegetation in basins along the North American Cordillera. Changes, which are relative to current climate/vegetation, are given in parentheses. The bold values represent statistically significant changes with p–values less than 0.05 based on the Mann–Whitney U-test. The simulated distributions with $n = 18$ years for WCRB, 9 years for MCRB, and 25 years for RME over the control (Base) period for each hydrological variable are compared with the simulated future distributions obtained from 11 RCM–GCMs ($11 \times n$ values).

Basin	**Base**	**ΔClim.**	**ΔVeg.**	**ΔClim.+ΔVeg.**
Wolf Creek Research Basin	0.64	0.64(0)	0.65(0.01)	0.63(–0.01)
Marmot Creek Research Basin	0.46	0.46(0)	**0.38(–0.08)**	**0.39(–0.07)**
Reynolds Mountain East	0.46	0.43(–0.03)	0.46(0)	0.43(–0.03)

Climate change slightly affects the runoff ratio only in RME. In contrast, the transient vegetation change affects the runoff ratio only in MCRB (Table 7.4). The runoff ratios in the three basins across the NAC change slightly (1–7%) under both vegetation and climate changes.

7.4.1 Early Freshet and Changes in Streamflow Timing

Not only the magnitudes but also timing of the maximum snowpack and peak streamflow are affected by climate and transient vegetation changes. The impact of transient vegetation change on delaying the snow-free date or lengthening the snow season can be important in some biomes, but not with respect to basin-scale timings, which do not exceed 2 days. Under a combined climate and transient vegetation change scenario, however, the date of the snow initiation is delayed 2 days in WCRB and about two weeks in the central and southern basins. The date of the maximum snow accumulation advances from April 4 to March 11 (24 days) in WCRB, while it advances from April 28 to April 23 (5 days) in MCRB and from March 10 to February 4 (40 days) in RME (Table 7.2). An early accumulation of maximum snowpack, when the solar irradiance is low may decrease melt rates and therefore peak streamflows in

all of the study basins. In contrast to peak SWE, the impact of vegetation on timing of peak streamflows in WCRB is slightly greater and the date of the peak streamflows delays 5 days. Under climate and transient vegetation changes, the date of the maximum streamflow advances from April 24 to April 1 (23 days) in WCRB, while it is delayed from June 11 to June 13 (2 days) in MCRB and advances from May 14 to April 26 (47 days) in RME (Table 7.3). Under the current climate, the average lag time between the peak SWE and peak streamflow, which represents the melt period, increases with latitude toward the equator. The lag time under the current climate is 20 days in WCRB, 44 days in MCRB, and 65 days in RME. Under climate and transient vegetation changes, this lag time becomes longer: 21 days in WCRB, 51 days in MCRB, and 81 days in RME. This suggests that the snowmelt will be slower and therefore the peak flows will be less intense under MPC than under present-day climate.

7.5 Discussion

Not only climate change but also transient vegetation and soil changes need to be considered in modelling of hydrological processes to reduce the uncertainties in the future mountain hydrology. Under combined climate and transient vegetation changes in WCRB, peak SWE declines, ET and sublimation increases, snow season period shortens, and thawing depth becomes deeper, which result in an increase in annual total runoff and a decrease in average annual peak flow. This implies that the increased total runoff in WCRB under MPC is dampened while the decreased peak runoff is decreased even more by the transient vegetation change. Unlike WCRB, sublimation and annual total runoff declines under combined climate and transient vegetation changes in MCRB and RME. The impact of transient vegetation change on total runoff and peak runoff would offset the impact of the climate change in MCRB. Increases in total and peak runoff are expected under MPC while both total and peak runoff decline under a combined climate and transient vegetation change.

The response of simulated annual total runoff to varies: it increases with climate change

and decreases with vegetation change in WCRB and MCRB but is insensitive to changes in RME. Despite the snow regime and annual peak runoff in RME, which are sensitive to both climate and transient vegetation changes, neither transient vegetation change nor climate change plays a role with respect to annual total runoff in RME and no change in its magnitude is expected. Annual total runoff gradually increases from south to north under climate change, decreases under transient vegetation change, and under a combined climate and transient vegetation change, increases in WCRB and decrease in the other two basins. This shows the importance of vegetation in runoff processes. A transient vegetation change moderates the impact of climate change on ET to some extent by decreasing ET in WCRB and RME. Under a combined climate and transient vegetation change, ET increases across the NAC. The response of the peak SWE to transient vegetation change is reflected in the response of the annual runoff, with the highest response in MCRB compared to the other basins. Changes in runoff characteristics become statistically significant when combined climate and vegetation changes occur.

7.6 Summary

A series of monthly perturbed climate (MPC) constructed in Chapter 6 were used to understand how current hydrology would respond to combined climate, vegetation, and soil changes. Uncertainties in simulated hydrological variables due to uncertainties in the climate models when there are transient vegetation and soil changes are quantified. The importance of the interaction of climate, vegetation, and soil changes is examined in this chapter from a hydrological perspective. Vegetation cover and associated soils are expected to change by upslope treeline movement and shrub tundra to forest conversion in Wolf Creek Research Basin; upslope treeline movement, reforestation in the forest clearings, and conversion to grasses at low elevations in Marmot Creek Research Basin; and deforestation and mountain sage expansion in Reynolds Mountain East. The results show that transient vegetation and associated soils changes are as important as climate changes in decreasing the simulated peak SWE and the annual peak runoff in all three basins. The impact of climate change

is moderated by the impact of vegetation change on peak SWE at high elevations, peak SWE timing, peak runoff, snow transport, evapotranspiration, annual total runoff, soil moisture, and permafrost degradation. The impact of climate change on decreased peak SWE (at medium elevations), spatial variability of peak SWE, and sublimation, however, is intensified by vegetation change. Soil changes associated with transient vegetation changes affect peak runoff in Reynolds Mountain East but not in Wolf Creek Research Basin and Marmot Creek Research Basin. Impact of transient vegetation changes is more important on annual total runoff, annual peak runoff, and peak SWEs at low elevations in MCRB and high elevations in WCRB and RME. All climate, vegetation, and soil changes must be considered in regional climate change assessments to understand uncertainties in future hydrology of the cold regions.

Chapter 8

SUMMARY AND CONCLUSIONS

A brief description of the workflow is presented here and main findings of this research are listed. Snow regimes in three headwater basins along the North American Cordillera (NAC), which provides a remarkable proportion of the needed water resources for agriculture, industry, and water supply, are vulnerable to climate and transient vegetation changes. Wolf Creek Research Basin (WCRB) is the Yukon's most intensively studied headwaters basin and has an archive of high elevation weather, snowpack, soils, and streamflow data that have been collated and corrected. Marmot Creek Research Basin (MCRB) in the Canadian Rockies and Reynolds Mountain East (RME) in the US northwestern interior feature intensive measurements. Therefore, these basins were selected in this research to analyse the sensitivity and response of mountain hydrology to climate and transient vegetation changes. A physically based semi-distributed hydrological model using hydrological response unit (HRU) spatial discretisation was developed from the Cold Regions Hydrological Modelling (CRHM) platform for each basin. The models were used to simulate snowpack and streamflow magnitude and timing, along with the other mass balance fluxes, for an 18-year period for WCRB, a 9-year period for MCRB, and a 25-year period for RME with minimal calibration of the Clark lag and routing timing parameters in WCRB and RME. The models developed on the CRHM platform were parameterised using the results of scientific research in the research basins and were able to adequately predict snow accumulation and melt in alpine, shrub tundra, and forest zones in WCRB, alpine and the treeline blowing snow sink in MCRB, forest clearing in RME, and basin streamflow over the period of simulation. The models were then perturbed on an annual basis with increases in hourly air temperatures from 1°C to 5°C, and both increases (to +20%) and decreases (to –20%) in hourly precipitation. Relative humidity was held constant to allow water vapour pressure to increase with warming. In this study,

instead of direct application of regional climate model (RCM) outputs with large biases when compared against local observations, monthly perturbed climate (MPC) was reconstructed based on the historical observations and changes in monthly climatology. Changes in monthly climatology were obtained from 11 RCMs driven by a few representative general circulation models (GCMs). The main findings and concluding points of the simulated changes in the three headwater basins in this research are as follows:

1. The model simulations of SWE accumulation and melt with no calibration are encouraging when compared to measurements in the three basins based on statistical (e.g., root mean square error and mean absolute error) and visual (e.g., duration curves) assessment criteria. The assessment criteria show that the streamflow simulations match reasonably well with measurements in the three basins. A sensitivity analysis of mountain hydrology to changing climate shows that the impact of warming on peak snowpack and annual runoff can be offset by an increase in precipitation; however, the role of increased precipitation in offsetting the impact of warming varies with latitude. The increased precipitation needs to be greater than 5% in WCRB, 10% in MCRB, and 20% in RME to offset the impact of 1°C warming on simulated peak snowpack. The increased precipitation needs to be 8% in WCRB, 3% in MCRB, and 14% in RME to offset the impact of warming by 5°C on annual total runoff. Annual total runoff responds strongly to precipitation changes in MCRB and to both warming and precipitation change in WCRB and RME. The sensitivity of snowpack to air temperature and annual total runoff to precipitation changes along the NAC showed that the role of precipitation in offsetting the impact of warming on snow regimes becomes less effective at southern latitudes. In contrast, the role of precipitation in offsetting the impact of warming on annual total runoff becomes less effective at northern latitudes. A varying role of precipitation increase in offsetting the impact of warming on cold regions hydrology implies that the impact of the same warming and precipitation change at different latitudes will not necessarily be similar. This suggests that, even though air temperatures in northern latitudes will warm up more, but precipitation will also increase, which its offsetting role will make northern basins less sensitive to changes

relative to basins at mid-latitudes.

2. The impacts of warming and decreased precipitation on simulated hydrology of the three basins are severe and result in a large decrease in snow accumulation, annual total runoff, and peak streamflow and lengthening of the snow-free period. Increased precipitation, however, can partly offset the impact of warming. The results show that, while the impacts of warming on cold regions hydrological processes are unequivocal – reduced snow contribution to streamflow, shorter snow-covered period, greater evapotranspiration – the magnitude and direction changes in simulated streamflow under warming will depend on whether warming is accompanied by precipitation increases or decreases. Therefore, both warming and changes in precipitation, along with the simulated processes that are describing the detailed changes, must be considered when evaluating future hydrology in mountainous basins.

3. The results for RME contrast with those for the colder WCRB, where precipitation changes could offset the declining SWE as temperature rises. For instance, with a 5°C warming and a 20% increase in precipitation, mean annual peak SWE still drops 79% in RME. This indicates that precipitation increases can partially offset the impact of warming in the cold climate WCRB but not in the cool climate RME. These results show that the impacts of warming on cold regions hydrological processes in mountain basins vary along the North American Cordillera, with stronger sensitivity to warming and moderate sensitivity to precipitation change in the central part and moderate sensitivity to warming and precipitation change in the northern part. Therefore, regional responses to warming and changes to precipitation must be considered when evaluating future alpine hydrology. Simulations of future conditions for snow regimes in this research are consistent with the SWE magnitude and timing trends of past years. This indicates that the simulation results are similar to measured results, and therefore the model developed here can be applied to other mountainous regions.

4. Under monthly perturbed climate, the peak SWE decreases the most in forests, especially in RME. The interannual variability of peak SWE in WCRB and peak flows in all three study basins are projected to increase. Basin-scale snow transport shows that RME and MCRB are sensitive to climate changes in peak snowpack and snow transport while WCRB is the most resilient to such changes. Sublimation from blowing snow, snow surface, and snow intercepted on the canopy drops in the study areas; MCRB is the most resilient to changes in total sublimation from all sources, whilst RME is the most sensitive. Warming counteracts the impact of precipitation increase on water yield by increasing ET and converting a portion of snowfall to rainfall in the headwater basins along the North American Cordillera.

5. Not only climate changes but also vegetation and associated soil changes affect cold regions hydrological mechanisms. Vegetation changes act similarly to climate changes and decrease peak SWE at middle elevations, the spatial variability of peak SWE, and sublimation amounts. However, the impact of climate change is partially offset by the impact of vegetation change on peak SWE at high elevations, peak SWE timing, peak streamflow, snow transport in MCRB, ET, annual total runoff, soil moisture, and permafrost degradation. Under both climate and transient vegetation changes, a more uniform snowpack is simulated in the basin located in the US northwestern interior. Simulations show that annual total runoff is expected to gradually increase from south to north under only climate change, decrease under only transient vegetation change, and slightly increase in WCRB and decrease in the other two basins under combined climate and transient vegetation changes. Soil changes as a result of transient vegetation changes also affect peak runoff in Reynolds Mountain East.

6. Comparing the range of hydrological uncertainty due to uncertainty of the climate models with the hydrological difference due to climate and vegetation changes shows that the range of uncertainty in snow regimes in WCRB and high elevations of MCRB is greater than the range of differences due to climate and vegetation changes. In contrast,

the range of snow regime differences between current and monthly perturbed climates and between current and future vegetation is greater than the range of simulated snow uncertainty in RME and low elevations of MCRB. Uncertainty of streamflow regimes due to uncertainty of climate models is greater than the streamflow differences due to climate and vegetation changes in all three basins. Simulations of peak streamflow are more uncertain than the snow simulations.

Further investigation is needed to consider the impact of temperature and precipitation changes in other mountainous regions around the world. In the meantime, the results of this study can inform water resources stakeholders regarding the vulnerability of alpine headwaters to first-order climate change impacts and second-order transient vegetation change impacts. The models proposed here can be applied to other mountainous regions with cold climate to assess the sensitivity to warming in environments with different climate, vegetation, and frozen ground conditions. The models used here can be applied to investigate impacts of the combined climate and vegetation changes and to detect snow and streamflow regime shifts due to transient vegetation and soil changes. Mountains with near freezing winter temperatures are more vulnerable to climate changes. The methods applied in this research can be used to identify water resources systems that are vulnerable to warming. Improvements in climate modelling can reduce hydrological uncertainties. Results of this study show that impacts of warming on cold regions hydrology can be offset by precipitation increases. Ultimately, the results of this study may be used for the development of adaptation strategies, which may include water resources management and improving flood forecasting and warning systems. This research is the first approach to understanding the characteristics of mountain snowmelt and runoff generation under varying warming conditions in a north–south transect of the North American Cordillera covering three headwater basins in the Yukon Territory, the Canadian Rockies, and Idaho. The results will help to assess the vulnerability and resiliency of water resources that are dependent on mountain snow.

References

Abramopoulos, F., C. Rosenzweig, and B. Choudhury, 1988. Improved ground hydrology calculations for global climate models (GCMs): Soil water movement and evapotranspiration. *Journal of Climate*, 1(9):921–941.

Addor, N., M. Rohrer, R. Furrer, and J. Seibert, 2016. Propagation of biases in climate models from the synoptic to the regional scale: Implications for bias adjustment. *Journal of Geophysical Research: Atmospheres*, 121(5):2075–2089.

Alberta-Natural-Regions-Committee, 2006. In *Natural Regions and Subregions of Alberta. Compiled by D. J. Downing and W. W. Pettapiece*. Government of Alberta Publication Number T/852. pp. 254.

Alila, Y., P. K. Kuraś, M. Schnorbus, and R. Hudson, 2009. Forests and floods: A new paradigm sheds light on age-old controversies. *Water Resources Research*, 45(8). doi:10.1029/2008WR007207.

Armstrong, R. N., J. W. Pomeroy, and L. W. Martz, 2010. Estimating evaporation in a Prairie landscape under drought conditions. *Canadian Water Resources Journal*, 35(2):173–186. doi:10.4296/cwrj3502173.

Arnold, J. G., R. Srinivasan, R. S. Muttiah, and J. R. Williams, 1998. Large area hydrologic modeling and assessment part I: Model development. *Journal of the American Water Resources Association*, 34(1):73–89.

Ayers, H., 1959. Influence of soil profile and vegetation characteristics on net rainfall supply to runoff. In *Proceedings of Hydrology Symposium*, number 1, Pp. 198–205.

Bales, R. C., J. W. Hopmans, A. T. O'Geen, M. Meadows, P. C. Hartsough, P. Kirchner, C. T. Hunsaker, and D. Beaudette, 2011. Soil moisture response to snowmelt and rainfall in a Sierra Nevada mixed-conifer forest. *Vadose Zone Journal*, 10(3):786–799.

Bales, R. C., N. P. Molotch, T. H. Painter, M. D. Dettinger, R. Rice, and J. Dozier, 2006. Mountain hydrology of the western United States. *Water Resources Research*, 42(8). doi:10.1029/2005WR004387.

Balling Jr, R. C., P. J. Michaels, and P. C. Knappenberger, 1998. Analysis of winter and summer warming rates in gridded temperature time series. *Climate Research*, 9(3):175–181.

Ban, N., J. Schmidli, and C. Schär, 2014. Evaluation of the convection-resolving regional climate modeling approach in decade-long simulations. *Journal of Geophysical Research: Atmospheres*, 119(13):7889–7907.

Barnett, T., L. Dümenil, U. Schlese, E. Roeckner, and M. Latif, 1989. The effect of Eurasian snow cover on regional and global climate variations. *Journal of the Atmospheric Sciences*, 46(5):661–686.

Barros, V. R., C. B. Field, D. J. Dokke, M. D. Mastrandrea, K. J. Mach, T. E. Bilir, M. Chatterjee, K. L. Ebi, Y. O. Estrada, R. C. Genova, B. Girma, E. S. Kissel, A. N. Levy, S. MacCracken, P. R. Mastrandrea, and L. L. White, 2014. *Climate Change 2014: Impacts, Adaptation, and Vulnerability. Part B: Regional Aspects. Contribution of Working Group II to the Fifth Assessment Report of the Intergovernmental Panel on Climate Change*. Cambridge University Press. pp. 190.

Barry, R. G., 1992. Mountain climatology and past and potential future climatic changes in mountain regions: a review. *Mountain Research and Development*, 12(1):71–86.

Beke, G. J., 1969. *Soils of three experimental watersheds in Alberta and their hydrologic significance*. PhD thesis, PhD Thesis, University of Alberta, Edmonton. pp. 456.

Bellprat, O., S. Kotlarski, D. Lüthi, and C. Schär, 2013. Physical constraints for temperature biases in climate models. *Geophysical Research Letters*, 40(15):4042–4047.

Beltaos, S., 1990. Fracture and breakup of river ice cover. *Canadian Journal of Civil Engineering*, 17(2):173–183.

Beltaos, S., 1995. *River Ice Jams*. Water Resources Publication. pp. 372.

Benestad, R. E., I. Hanssen-Bauer, and D. Chen, 2008. *Empirical-statistical downscaling*. World Scientific Publishing Co Inc. pp. 228.

Beniston, M., 2003. Climatic change in mountain regions: a review of possible impacts. In *Climate variability and change in high elevation regions: past, present & future*, Pp. 5–31. Springer.

Beniston, M., F. Keller, B. Koffi, and S. Goyette, 2003. Estimates of snow accumulation and volume in the Swiss Alps under changing climatic conditions. *Theoretical and Applied Climatology*, 76(3):125–140.

Bennett, K. E., A. T. Werner, and M. Schnorbus, 2012. Uncertainties in hydrologic and climate change impact analyses in headwater basins of British Columbia. *Journal of Climate*, 25(17):5711–5730.

Bergstrom, S., 1995. The HBV model. In *V.P. Singh (Ed.), Computer Models of Watershed Hydrology, Water Resources Publications, Highlands Ranch, CO (1995)*. Pp. 443–476.

Beven, K., 2011. I believe in climate change but how precautionary do we need to be in planning for the future? *Hydrological Processes*, 25(9):1517–1520.

Beven, K. and A. Binley, 1992. The future of distributed models: model calibration and uncertainty prediction. *Hydrological Processes*, 6(3):279–298.

Bewley, D., R. Essery, J. Pomeroy, and C. Ménard, 2010. Measurements and modelling of snowmelt and turbulent heat fluxes over shrub tundra. *Hydrology and Earth System Sciences*, 14(7):1331–1340.

Billings, W. D. and L. Bliss, 1959. An alpine snowbank environment and its effects on vegetation, plant development, and productivity. *Ecology*, 40(3):388–397.

Binley, A. M., K. J. Beven, A. Calver, and L. Watts, 1991. Changing responses in hydrology: assessing the uncertainty in physically based model predictions. *Water Resources Research*, 27(6):1253–1261.

Bintanja, R. and E. Van der Linden, 2013. The changing seasonal climate in the Arctic. *Scientific Reports*, 3. doi:10.1038/srep01556.

Bonsal, B. R. and T. D. Prowse, 2003. Trends and variability in spring and autumn 0°c-isotherm dates over Canada. *Climatic Change*, 57(3):341–358.

Borden, J. H., 1982. Aggregation pheromones. In *Bark beetles in North American conifers: A system for the study of evolutionary biology, edited by J. B. Mitton and K. B. Sturgeon*, Pp. 74–139. Univ. of Tex. Press, Austin.

Bosch, J. M. and J. Hewlett, 1982. A review of catchment experiments to determine the effect of vegetation changes on water yield and evapotranspiration. *Journal of Hydrology*, 55(1):3–23.

Boucher, J. L. and S. K. Carey, 2010. Exploring runoff processes using chemical, isotopic and hydrometric data in a discontinuous permafrost catchment. *Hydrology Research*, 41(6):508–519.

Bourdin, D. R. and R. B. Stull, 2013. Bias-corrected short-range member-to-member ensemble forecasts of reservoir inflow. *Journal of Hydrology*, 502:77–88.

Brabets, T. P. and M. A. Walvoord, 2009. Trends in streamflow in the Yukon River Basin from 1944 to 2005 and the influence of the Pacific Decadal Oscillation. *Journal of Hydrology*, 371(1):108–119.

Brando, P. M., J. K. Balch, D. C. Nepstad, D. C. Morton, F. E. Putz, M. T. Coe, D. Silvério, M. N. Macedo, E. A. Davidson, C. C. Nóbrega, et al., 2014. Abrupt increases in Amazonian tree mortality due to drought–fire interactions. *Proceedings of the National Academy of Sciences*, 111(17):6347–6352.

Brooks, R. and A. Corey, 1964. Hydraulics properties of porous media. *Hydrology Paper, Colorado State University*, (3):1–29.

Brown, A. E., L. Zhang, T. A. McMahon, A. W. Western, and R. A. Vertessy, 2005. A review of paired catchment studies for determining changes in water yield resulting from alterations in vegetation. *Journal of Hydrology*, 310(1):28–61.

Brown, D. G., C. Polsky, P. Bolstad, S. D. Brody, D. Hulse, R. Kroh, T. R. Loveland, and A. Thomson, 2014. Land use and land cover change. In *Climate Change Impacts in the United States: The Third National Climate Assessment*, J. M. Melillo, T. R. Terese, and G. W. Yohe, eds., chapter 13, Pp. 318–332. U.S. Global Change Research Program.

Brown, R. D. and D. A. Robinson, 2011. Northern Hemisphere spring snow cover variability and change over 1922-2010 including an assessment of uncertainty. *The Cryosphere*, 5(1):219–229.

Bunbury, J. and K. Gajewski, 2012. Temperatures of the past 2000years inferred from lake sediments, southwest Yukon Territory, Canada. *Quaternary Research*, 77(3):355–367.

Burney, J. A., S. J. Davis, and D. B. Lobell, 2010. Greenhouse gas mitigation by agricultural intensification. *Proceedings of the National Academy of Sciences*, 107(26):12052–12057.

Burton, A., C. Kilsby, H. Fowler, P. Cowpertwait, and P. O'Connell, 2008. RainSim: A spatial–temporal stochastic rainfall modelling system. *Environmental Modelling & Software*, 23(12):1356–1369.

Cannon, A. J., 2008. Probabilistic multisite precipitation downscaling by an expanded bernoulli-gamma density network. *Journal of Hydrometeorology*, 9(6):1284–1300.

Carey, S. and W. Quinton, 2004. Evaluating snowmelt runoff generation in a discontinuous permafrost catchment using stable isotope, hydrochemical and hydrometric data. *Hydrology Research*, 35(4-5):309–324.

Carey, S. K., W. L. Quinton, and N. T. Goeller, 2007. Field and laboratory estimates of pore size properties and hydraulic characteristics for subarctic organic soils. *Hydrological Processes*, 21(19):2560–2571.

Carey, S. K. and M.-k. Woo, 2001. Slope runoff processes and flow generation in a subarctic, subalpine catchment. *Journal of Hydrology*, 253(1):110–129.

Carey, S. K. and M.-k. Woo, 2005. Freezing of subarctic hillslopes, Wolf Creek Basin, Yukon, Canada. *Arctic, Antarctic, and Alpine Research*, 37(1):1–10.

Casola, J. H., L. Cuo, B. Livneh, D. P. Lettenmaier, M. T. Stoelinga, P. W. Mote, and J. M. Wallace, 2009. Assessing the impacts of global warming on snowpack in the Washington Cascades. *Journal of Climate*, 22(10):2758–2772.

Chae, Y., S. M. Kang, S.-J. Jeong, B. Kim, and D. M. Frierson, 2015. Arctic greening can cause earlier seasonality of Arctic amplification. *Geophysical Research Letters*, 42(2):536–541.

Chapin III, F. S., T. V. Callaghan, Y. Bergeron, M. Fukuda, J. Johnstone, G. Juday, and S. Zimov, 2004. Global change and the boreal forest: thresholds, shifting states or gradual change? *AMBIO: A Journal of the Human Environment*, 33(6):361–365.

Chapman, W. L. and J. E. Walsh, 1993. Recent variations of sea ice and air temperature in high latitudes. *Bulletin of the American Meteorological Society*, 74(1):33–47.

Clark, C., 1945. Storage and the unit hydrograph. *Transactions of the American Society of Civil Engineers*, 110(1):1419–1446.

Clark, I. D. and B. Lauriol, 1997. Aufeis of the Firth River basin, northern Yukon, Canada: Insights into permafrost hydrogeology and karst. *Arctic and Alpine Research*, Pp. 240–252.

Clark, P. E. and S. P. Hardegree, 2005. Quantifying vegetation change by point sampling landscape photography time series. *Rangeland Ecology & Management*, 58(6):588–597.

Clark, P. E., M. S. Seyfried, and B. Harris, 2001. Intermountain plant community classification using Landsat TM and SPOT HRV data. *Journal of Range Management*, 54:152–160.

Crochet, P., T. Jóhannesson, T. Jónsson, O. Sigurdsson, H. Björnsson, F. Pálsson, and I. Barstad, 2007. Estimating the spatial distribution of precipitation in iceland using a linear model of orographic precipitation. *Journal of Hydrometeorology*, 8(6):1285–1306.

Crocker, R. L. and J. Major, 1955. Soil development in relation to vegetation and surface age at Glacier Bay, Alaska. *The Journal of Ecology*, Pp. 427–448.

Crout, N., T. Kokkonen, A. Jakeman, J. Norton, L. Newham, R. Anderson, H. Assaf, B. Croke, N. Gaber, J. Gibbons, et al., 2008. Chapter two good modelling practice. *Developments in Integrated Environmental Assessment*, 3:15–31.

Dale, V. H. and J. F. Franklin, 1989. Potential effects of climate change on stand development in the Pacific Northwest. *Canadian Journal of Forest Research*, 19(12):1581–1590.

Daly, C., M. Halbleib, J. I. Smith, W. P. Gibson, M. K. Doggett, G. H. Taylor, J. Curtis, and P. P. Pasteris, 2008. Physiographically sensitive mapping of climatological temperature and precipitation across the conterminous United States. *International Journal of Climatology*, 28(15):2031–2064.

DeAngelis, A., F. Dominguez, Y. Fan, A. Robock, M. D. Kustu, and D. Robinson, 2010. Evidence of enhanced precipitation due to irrigation over the Great Plains of the United States. *Journal of Geophysical Research: Atmospheres*, 115(D15). doi:10.1029/2010JD013892.

DeBano, L. F., 1991. The effect of fire on soil properties, General Technical Report. Technical report, United States Department of Agriculture, Forest Service INT-280. Pp. 151 – 156.

DeFries, R. and K. N. Eshleman, 2004. Land-use change and hydrologic processes: A major focus for the future. *Hydrological Processes*, 18(11):2183–2186.

Denmead, O. and R. H. Shaw, 1960. The effects of soil moisture stress at different stages of growth on the development and yield of corn. *Agronomy Journal*, 52(5):272–274.

Déry, S. J. and R. D. Brown, 2007. Recent northern hemisphere snow cover extent trends and implications for the snow-albedo feedback. *Geophysical Research Letters*, 34(22). doi:10.1029/2007GL031474.

Deser, C., R. Knutti, S. Solomon, and A. S. Phillips, 2012. Communication of the role of natural variability in future North American climate. *Nature Climate Change*, 2(11):775–779.

Diaz, H. F., M. Grosjean, and L. Graumlich, 2003. Climate variability and change in high elevation regions: past, present and future. In *Climate Variability and Change in High Elevation Regions: past, present & future*, Pp. 1–4. Springer.

Dornes, P. F., J. W. Pomeroy, A. Pietroniro, S. K. Carey, and W. L. Quinton, 2008. Influence of landscape aggregation in modelling snow-cover ablation and snowmelt runoff in a sub-arctic mountainous environment. *Hydrological Sciences Journal*, 53(4):725–740.

Duan, J., N. McIntyre, and C. Onof, 2012. Resolving non–stationarity in statistical downscaling of precipitation under climate change scenarios. In *British Hydrological Society Eleventh National Symposium, Hydrology for a Changing World, Dundee, UK*.

Ehret, U., E. Zehe, V. Wulfmeyer, K. Warrach-Sagi, and J. Liebert, 2012. HESS Opinions: "should we apply bias correction to global and regional climate model data?". *Hydrology and Earth System Sciences*, 16(9):3391–3404.

Ellis, C., J. Pomeroy, T. Brown, and J. MacDonald, 2010. Simulation of snow accumulation and melt in needleleaf forest environments. *Hydrology and Earth System Sciences*, 14(6):925–940.

Ellis, C., J. Pomeroy, R. Essery, and T. Link, 2011. Effects of needleleaf forest cover on radiation and snowmelt dynamics in the Canadian Rocky Mountains. *Canadian Journal of Forest Research*, 41(3):608–620.

Ellis, C., J. Pomeroy, and T. Link, 2013. Modeling increases in snowmelt yield and desynchronization resulting from forest gap-thinning treatments in a northern mountain headwater basin. *Water Resources Research*, 49(2):936–949.

Ellis, C. R. and J. W. Pomeroy, 2007. Estimating sub-canopy shortwave irradiance to melting snow on forested slopes. *Hydrological Processes*, 21(19):2581–2593.

Elmendorf, S. C., G. H. Henry, R. D. Hollister, R. G. Björk, N. Boulanger-Lapointe, E. J. Cooper, J. H. Cornelissen, T. A. Day, E. Dorrepaal, T. G. Elumeeva, et al., 2012. Plot-scale evidence of tundra vegetation change and links to recent summer warming. *Nature Climate Change*, 2(6):453–457.

Elsner, M. M., S. Gangopadhyay, T. Pruitt, L. D. Brekke, N. Mizukami, and M. P. Clark, 2014. How does the choice of distributed meteorological data affect hydrologic model calibration and streamflow simulations? *Journal of Hydrometeorology*, 15(4):1384–1403.

Essery, R., P. Bunting, A. Rowlands, N. Rutter, J. Hardy, R. Melloh, T. Link, D. Marks, and J. Pomeroy, 2008. Radiative transfer modeling of a coniferous canopy characterized by airborne remote sensing. *Journal of Hydrometeorology*, 9(2):228–241.

Eum, H.-I., Y. Dibike, T. Prowse, and B. Bonsal, 2014. Inter-comparison of high-resolution gridded climate data sets and their implication on hydrological model simulation over the Athabasca Watershed, Canada. *Hydrological Processes*, 28(14):4250–4271.

Euskirchen, E., A. McGuire, F. S. Chapin, and T. Rupp, 2010. The changing effects of Alaska's boreal forests on the climate system. *Canadian Journal of Forest Research*, 40(7):1336–1346.

Fall, S., N. S. Diffenbaugh, D. Niyogi, R. A. Pielke, and G. Rochon, 2010. Temperature and equivalent temperature over the United States (1979–2005). *International Journal of Climatology*, 30(13):2045–2054.

Fang, X., J. Pomeroy, C. Ellis, M. MacDonald, C. DeBeer, and T. Brown, 2013. Multi-variable evaluation of hydrological model predictions for a headwater basin in the Canadian Rocky Mountains. *Hydrology and Earth System Sciences*, 17(4):1635–1659.

Fang, X., J. Pomeroy, C. Westbrook, X. Guo, A. Minke, and T. Brown, 2010. Prediction of snowmelt derived streamflow in a wetland dominated prairie basin. *Hydrology and Earth System Sciences Discussions*, 7(1):1103–1141.

Fang, X. and J. W. Pomeroy, 2016. Impact of antecedent conditions on simulations of a flood in a mountain headwater basin. *Hydrological Processes*, 30(16):2754–2772.

Flerchinger, G. N., M. L. Reba, and D. Marks, 2012. Measurement of surface energy fluxes from two rangeland sites and comparison with a multilayer canopy model. *Journal of Hydrometeorology*, 13(3):1038–1051.

Forsythe, N., H. Fowler, S. Blenkinsop, A. Burton, C. Kilsby, D. Archer, C. Harpham, and M. Hashmi, 2014. Application of a stochastic weather generator to assess climate change impacts in a semi-arid climate: The Upper Indus Basin. *Journal of Hydrology*, 517:1019–1034.

Fowler, H., S. Blenkinsop, and C. Tebaldi, 2007. Linking climate change modelling to impacts studies: recent advances in downscaling techniques for hydrological modelling. *International Journal of Climatology*, 27(12):1547–1578.

Fowler, H., C. Kilsby, P. O'Connell, and A. Burton, 2005. A weather-type conditioned multi-site stochastic rainfall model for the generation of scenarios of climatic variability and change. *Journal of Hydrology*, 308(1):50–66.

Francis, S., S. Smith, and R. Janowicz, 1998. Data integration and ecological zonation of Wolf Creek watershed. In *Wolf Creek Research Basin–Hydrology, Ecology, Environment–Proceedings of a workshop held in Whitehorse, Yukon, edited by: Pomeroy, J. W. and Granger R. J.*, Pp. 93–100. Citeseer.

Fyfe, J. C. and G. M. Flato, 1999. Enhanced climate change and its detection over the Rocky Mountains. *Journal of Climate*, 12(1):230–243.

Gaitan, C. F., W. W. Hsieh, and A. J. Cannon, 2014. Comparison of statistically downscaled precipitation in terms of future climate indices and daily variability for southern Ontario and Quebec, Canada. *Climate Dynamics*, 43(12):3201–3217.

Garnier, B. and A. Ohmura, 1970. The evaluation of surface variations in solar radiation income. *Solar Energy*, 13(1):21–34.

Gelfan, A., J. Pomeroy, and L. Kuchment, 2004. Modeling forest cover influences on snow accumulation, sublimation, and melt. *Journal of Hydrometeorology*, 5(5):785–803.

Gibson, J. and T. Edwards, 2002. Regional water balance trends and evaporation-transpiration partitioning from a stable isotope survey of lakes in northern Canada. *Global Biogeochemical Cycles*, 16(2).

Gleick, P. H., 1986. Methods for evaluating the regional hydrologic impacts of global climatic changes. *Journal of Hydrology*, 88(1):97–116.

Goodison, B., P. Louie, and D. Yang, 1998. The WMO solid precipitation measurement intercomparison. *World Meteorological Organization-Publications-WMO TD*, Pp. 65–70.

Granger, R. and D. Gray, 1990. A net radiation model for calculating daily snowmelt in open environments. *Hydrology Research*, 21(4-5):217–234.

Granger, R., D. Gray, and G. Dyck, 1984. Snowmelt infiltration to frozen prairie soils. *Canadian Journal of Earth Sciences*, 21(6):669–677.

Granger, R. J., 1999. Partitioning of energy during the snow-free season at the Wolf Creek Research Basin. *Wolf Creek Research Basin–Hydrology, Ecology, Environment–Proceedings of a workshop held in Whitehorse, Yukon, edited by: Pomeroy, J. W. and Granger R. J.*, Pp. 33–43.

Granger, R. J. and D. Gray, 1989. Evaporation from natural nonsaturated surfaces. *Journal of Hydrology*, 111(1):21–29.

Granger, R. J. and J. W. Pomeroy, 1997. Sustainability of the western Canadian boreal forest under changing hydrological conditions. II. Summer energy and water use. *IAHS Publications-Series of Proceedings and Reports-Intern Assoc Hydrological Sciences*, 240:243–250.

Graversen, R. G., T. Mauritsen, M. Tjernström, E. Källén, and G. Svensson, 2008. Vertical structure of recent Arctic warming. *Nature*, 451(7174):53–56.

Gray, D., B. Toth, L. Zhao, J. Pomeroy, and R. Granger, 2001. Estimating areal snowmelt infiltration into frozen soils. *Hydrological Processes*, 15(16):3095–3111.

Gutmann, E., I. Barstad, M. Clark, J. Arnold, and R. Rasmussen, 2016. The Intermediate Complexity Atmospheric Research Model (ICAR). *Journal of Hydrometeorology*, 17(3):957–973.

Gutmann, E., T. Pruitt, M. P. Clark, L. Brekke, J. R. Arnold, D. A. Raff, and R. M. Rasmussen, 2014. An intercomparison of statistical downscaling methods used for water resource assessments in the United States. *Water Resources Research*, 50(9):7167–7186.

Hallinger, M., M. Manthey, and M. Wilmking, 2010. Establishing a missing link: warm summers and winter snow cover promote shrub expansion into alpine tundra in Scandinavia. *New Phytologist*, 186(4):890–899.

Hansell, R., D. Chant, and J. Weintraub, 1971. Changes in the northern limit of spruce at Dubawnt Lake, Northwest Territories. *Arctic*, 24(3):233–234.

Hanson, C., 2001. Long-term precipitation database, Reynolds Creek Experimental Watershed, Idaho, United States. *Water Resources Research*, 37(11):2831–2834.

Hanson, C., D. Marks, and S. Van Vactor, 2001. Long-term climate database, Reynolds Creek Experimental Watershed, Idaho, United States. *Water Resources Research*, 37(11):2839–2841.

Hay, L. E., R. L. Wilby, and G. H. Leavesley, 2000. A comparison of delta change and downscaled GCM scenarios for three mounfainous basins in the United States. *JAWRA Journal of the American Water Resources Association*, 36(2):387–397.

Hayashi, M., W. L. Quinton, A. Pietroniro, and J. J. Gibson, 2004. Hydrologic functions of wetlands in a discontinuous permafrost basin indicated by isotopic and chemical signatures. *Journal of Hydrology*, 296(1):81–97.

Hijmans, R. J., S. E. Cameron, J. L. Parra, P. G. Jones, and A. Jarvis, 2005. Very high resolution interpolated climate surfaces for global land areas. *International Journal of Climatology*, 25(15):1965–1978.

Hope, A. and D. Stow, 1995. Shortwave reflectance properties of Arctic tundra. In *J. Reynolds, & J. Tenhuenen (Eds.), Landscape function and disturbance in Arctic tundra. Ecological Studies*, volume 120. Heidelberg, Germany: Springer-Verlag. pp. 155–164.

Hsieh, W. W., 2009. *Machine learning methods in the environmental sciences: Neural networks and kernels*. Cambridge University Press, Cambridge, UK. pp. 349.

Hunt, J., 2005. Inland and coastal flooding: developments in prediction and prevention. *Philosophical Transactions of the Royal Society of London A: Mathematical, Physical and Engineering Sciences*, 363(1831):1475–1491.

Imeson, A., J. Verstraten, E. Van Mulligen, and J. Sevink, 1992. The effects of fire and water repellency on infiltration and runoff under Mediterranean type forest. *Catena*, 19(3-4):345–361.

Imeson, A. and M. Vis, 1984. Seasonal variations in soil erodibility under different land-use types in Luxembourg. *European Journal of Soil Science*, 35(2):323–331.

Innes, J., 1991. High-altitude and high-latitude tree growth in relation to past, present and future global climate change. *The Holocene*, 1(2):168–173.

Inouye, D. W., B. Barr, K. B. Armitage, and B. D. Inouye, 2000. Climate change is affecting altitudinal migrants and hibernating species. *Proceedings of the National Academy of Sciences*, 97(4):1630–1633.

Ireson, A., G. Van Der Kamp, G. Ferguson, U. Nachshon, and H. Wheater, 2013. Hydrogeological processes in seasonally frozen northern latitudes: understanding, gaps and challenges. *Hydrogeology Journal*, 21(1):53–66.

Isukapalli, S., A. Roy, and P. Georgopoulos, 1998. Stochastic response surface methods (SRSMs) for uncertainty propagation: application to environmental and biological systems. *Risk Analysis*, 18(3):351–363.

Janowicz, J., 1999. Wolf Creek Research Basin-overview. *Wolf Creek Research Basin–Hydrology, Ecology, Environment–Proceedings of a workshop held in Whitehorse, Yukon, edited by: Pomeroy, J. W. and Granger R. J., Canada: National Hydrology Institute*, Pp. 121–130.

Janowicz, J., D. Gray, and J. Pomeroy, 2003. Spatial variability of fall soil moisture and spring snow water equivalent within a mountainous sub-Arctic watershed. *In Proceedings of the Eastern Snow Conference*, 60:127–139.

Janowicz, J. R., 2008. Apparent recent trends in hydrologic response in permafrost regions of northwest Canada. *Hydrology Research*, 39(4):267–275.

Janowicz, J. R., 2010. Observed trends in the river ice regimes of northwest Canada. *Hydrology Research*, 41(6):462–470.

Jarosch, A. H., F. S. Anslow, and G. K. Clarke, 2012. High-resolution precipitation and temperature downscaling for glacier models. *Climate Dynamics*, 38(1-2):391–409.

Jeffrey, W. W., 1965. Experimental watersheds in the Rocky Mountains. In *Proceedings of the International Association of Scientific Hydrology Symposium, Budapest.* International Association of Scientific Hydrology, Gentbrugge. Pp. 502–521.

Johannessen, O. M., L. Bengtsson, M. W. Miles, S. I. Kuzmina, V. A. Semenov, G. V. Alekseev, A. P. Nagurnyi, V. F. Zakharov, L. P. Bobylev, L. H. Pettersson, et al., 2004. Arctic climate change: Observed and modelled temperature and sea-ice variability. *Tellus A*, 56(4):328–341.

Johnstone, J. F., C. D. Allen, J. F. Franklin, L. E. Frelich, B. J. Harvey, P. E. Higuera, M. C. Mack, R. K. Meentemeyer, M. R. Metz, G. L. Perry, et al., 2016. Changing disturbance regimes, ecological memory, and forest resilience. *Frontiers in Ecology and the Environment*, 14(7):369–378.

Jones, R. N., F. H. Chiew, W. C. Boughton, and L. Zhang, 2006. Estimating the sensitivity of mean annual runoff to climate change using selected hydrological models. *Advances in Water Resources*, 29(10):1419–1429.

Jorgenson, M. T., C. H. Racine, J. C. Walters, and T. E. Osterkamp, 2001. Permafrost degradation and ecological changes associated with a warming climate in central Alaska. *Climatic Change*, 48(4):551–579.

Jorgenson, M. T., V. Romanovsky, J. Harden, Y. Shur, J. O'Donnell, E. A. Schuur, M. Kanevskiy, and S. Marchenko, 2010. Resilience and vulnerability of permafrost to climate change. *Canadian Journal of Forest Research*, 40(7):1219–1236.

Joshi, M., E. Hawkins, R. Sutton, J. Lowe, and D. Frame, 2011. Projections of when temperature change will exceed 2°C above pre-industrial levels. *Nature Climate Change*, 1(8):407–412.

Kawase, H., T. Yoshikane, M. Hara, F. Kimura, T. Yasunari, B. Ailikun, H. Ueda, and T. Inoue, 2009. Intermodel variability of future changes in the baiu rainband estimated by the pseudo global warming downscaling method. *Journal of Geophysical Research: Atmospheres*, 114(D24). doi: 10.1029/2009JD011803.

Kay, A., H. Davies, V. Bell, and R. Jones, 2009. Comparison of uncertainty sources for climate change impacts: flood frequency in England. *Climatic Change*, 92(1):41–63.

Kilsby, C., P. Jones, A. Burton, A. Ford, H. Fowler, C. Harpham, P. James, A. Smith, and R. Wilby, 2007. A daily weather generator for use in climate change studies. *Environmental Modelling & Software*, 22(12):1705–1719.

Kirby, C. and R. Ogilvie, 1969. *The forests of Marmot Creek watershed research basin*, number 47–1259. Canadian Forestry Service, Queen's Press. pp. 37.

Kite, G., A. Dalton, and K. Dion, 1994. Simulation of streamflow in a macroscale watershed using general circulation model data. *Water Resources Research*, 30(5):1547–1559.

Kite, G. and U. Haberlandt, 1999. Atmospheric model data for macroscale hydrology. *Journal of Hydrology*, 217(3):303–313.

Klemeš, V., 1990. The modelling of mountain hydrology: the ultimate challenge. *IAHS-AISH publication*, 190:29–43.

Knowles, N. and D. R. Cayan, 2004. Elevational dependence of projected hydrologic changes in the San Francisco estuary and watershed. *Climatic Change*, 62(1):319–336.

Knowles, N., M. D. Dettinger, and D. R. Cayan, 2006. Trends in snowfall versus rainfall in the western United States. *Journal of Climate*, 19(18):4545–4559.

Köppen, W., 1936. Das geographische system der klimate.

Krogh, S. A., J. W. Pomeroy, and J. McPhee, 2015. Physically based mountain hydrological modeling using reanalysis data in Patagonia. *Journal of Hydrometeorology*, 16(1):172–193.

Kuchment, L. S. and A. N. Gelfan, 2002. Estimation of extreme flood characteristics using physically based models of runoff generation and stochastic meteorological inputs. *Water International*, 27(1):77–86.

Kumar, M., D. Marks, J. Dozier, M. Reba, and A. Winstral, 2013. Evaluation of distributed hydrologic impacts of temperature-index and energy-based snow models. *Advances in Water Resources*, 56:77–89.

Lawrence, I. and K. Lin, 1989. A concordance correlation coefficient to evaluate reproducibility. *Biometrics*, Pp. 255–268.

Leavesley, G. H., R. Lichty, B. Thoutman, and L. Saindon, 1984. *Precipitation-runoff modeling system: User's manual*, volume 83 of *Water-resources Investigations*. US Geological Survey Colorado, CO. pp. 207.

Leith, R. M. and P. H. Whitfield, 1998. Evidence of climate change effects on the hydrology of streams in south-central BC. *Canadian Water Resources Journal*, 23(3):219–230.

Lewkowicz, A. G. and M. Ednie, 2004. Probability mapping of mountain permafrost using the BTS method, Wolf Creek , Yukon Territory, Canada. *Permafrost and Periglacial Processes*, 15(1):67–80.

Li, L. and J. W. Pomeroy, 1997. Probability of occurrence of blowing snow. *Journal of Geophysical Research: Atmospheres*, 102(D18):21955–21964.

Link, T. E., G. N. Flerchinger, M. Unsworth, and D. Marks, 2004. Simulation of water and energy fluxes in an old-growth seasonal temperate rain forest using the simultaneous heat and water (SHAW) model. *Journal of Hydrometeorology*, 5(3):443–457.

Liston, G. E., J. P. Mcfadden, M. Sturm, and R. A. Pielke, 2002. Modelled changes in arctic tundra snow, energy and moisture fluxes due to increased shrubs. *Global Change Biology*, 8(1):17–32.

López-Moreno, J., J. Boike, A. Sanchez-Lorenzo, and J. Pomeroy, 2016. Impact of climate warming on snow processes in Ny-Ålesund, a polar maritime site at Svalbard. *Global and Planetary Change*, 146:10–21.

López-Moreno, J., J. Pomeroy, J. Revuelto, and S. Vicente-Serrano, 2013. Response of snow processes to climate change: spatial variability in a small basin in the Spanish Pyrenees. *Hydrological Processes*, 27(18):2637–2650.

López-Moreno, J. I., J. Revuelto, M. Gilaberte, E. Morán-Tejeda, M. Pons, E. Jover, P. Esteban, C. García, and J. Pomeroy, 2014. The effect of slope aspect on the response of snowpack to climate warming in the Pyrenees. *Theoretical and Applied Climatology*, 117(1-2):207–219.

Loveland, T. R. and R. Mahmood, 2014. A design for a sustained assessment of climate forcing and feedbacks related to land use and land cover change. *Bulletin of the American Meteorological Society*, 95(10):1563–1572.

Luckman, B. and T. Kavanagh, 2000. Impact of climate fluctuations on mountain environments in the Canadian Rockies. *Ambio: A Journal of the Human Environment*, 29(7):371–380.

Lundquist, J. D., S. E. Dickerson-Lange, J. A. Lutz, and N. C. Cristea, 2013. Lower forest density enhances snow retention in regions with warmer winters: A global framework developed from plot-scale observations and modeling. *Water Resources Research*, 49(10):6356–6370.

MacDonald, J. P., 2010. *Unloading of intercepted snow in conifer forests*. MSc Thesis, University of Saskatchewan, Canada. pp. 93.

MacDonald, M. K., B. J. Davison, M. A. Mekonnen, and A. Pietroniro, 2016. Comparison of land surface scheme simulations with field observations versus atmospheric model output as forcing. *Hydrological Sciences Journal*, 61(16):2860–2871.

MacDonald, M. K., J. W. Pomeroy, and A. Pietroniro, 2009. Parameterizing redistribution and sublimation of blowing snow for hydrological models: tests in a mountainous subarctic catchment. *Hydrological Processes*, 23(18):2570–2583.

MacDonald, R. J., J. M. Byrne, S. Boon, and S. W. Kienzle, 2012. Modelling the potential impacts of climate change on snowpack in the North Saskatchewan River Watershed, Alberta. *Water Resources Management*, 26(11):3053–3076.

Macias Fauria, M. and E. Johnson, 2009. Large-scale climatic patterns and area affected by mountain pine beetle in British Columbia, Canada. *Journal of Geophysical Research: Biogeosciences*, 114(G1). doi:10.1029/2008JG000760.

Macias-Fauria, M. and E. A. Johnson, 2013. Warming-induced upslope advance of subalpine forest is severely limited by geomorphic processes. *Proceedings of the National Academy of Sciences*, 110(20):8117–8122. Pp. 349.

Mahat, V. and A. Anderson, 2013. Impacts of climate and catastrophic forest changes on streamflow and water balance in a mountainous headwater stream in Southern Alberta. *Hydrology and Earth System Sciences*, 17(12):4941–4956.

Mahmood, T. H., J. W. Pomeroy, H. S. Wheater, and H. M. Baulch, 2016. Hydrological responses to climatic variability in a cold agricultural region. *Hydrological Processes*, 31(4):854–870. doi: 10.1002/hyp.11064.

Malmqvist, B. and S. Rundle, 2002. Threats to the running water ecosystems of the world. *Environmental Conservation*, 29(02):134–153.

Mann, D. H., T. Scott Rupp, M. A. Olson, and P. A. Duffy, 2012. Is Alaska's boreal forest now crossing a major ecological threshold? *Arctic, Antarctic, and Alpine Research*, 44(3):319–331.

Mann, H. B. and D. R. Whitney, 1947. On a test of whether one of two random variables is stochastically larger than the other. *The Annals of Mathematical Statistics*, 18(1):50–60.

Maples, A., M. McHugh, and E. Brown, 2014. Downscaled climate models in complex topographical regions: relevancy for water utility planning. *Journal of Water and Climate Change*, 5(4):540–555.

Maraun, D., 2012. Nonstationarities of regional climate model biases in European seasonal mean temperature and precipitation sums. *Geophysical Research Letters*, 39(6).

Maraun, D., F. Wetterhall, A. Ireson, R. Chandler, E. Kendon, M. Widmann, S. Brienen, H. Rust, T. Sauter, M. Themeßl, et al., 2010. Precipitation downscaling under climate change: Recent developments to bridge the gap between dynamical models and the end user. *Reviews of Geophysics*, 48(3). doi: 10.1029/2009RG000314.

Marks, D., K. R. Cooley, D. C. Robertson, and A. Winstral, 2001. Long-term snow database, Reynolds Creek Experimental Watershed, Idaho, United States. *Water Resources Research*, 37(11):2835–2838.

Marks, D., J. Domingo, D. Susong, T. Link, and D. Garen, 1999. A spatially distributed energy balance snowmelt model for application in mountain basins. *Hydrological Processes*, 13(12-13):1935–1959.

Marks, D. and J. Dozier, 1992. Climate and energy exchange at the snow surface in the alpine region of the Sierra Nevada: 2. Snow cover energy balance. *Water Resources Research*, 28(11):3043–3054.

Marks, D., J. Kimball, D. Tingey, and T. Link, 1998. The sensitivity of snowmelt processes to climate conditions and forest cover during rain-on-snow: A case study of the 1996 Pacific Northwest flood. *Hydrological Processes*, 12:1569–1587.

Marsh, P. and J. Pomeroy, 1996. Meltwater fluxes at an arctic forest-tundra site. *Hydrological Processes*, 10(10):1383–1400.

Martinec, J., A. Rango, R. Roberts, M. F. Baumgartner, and G. M. Apfl, 2008. *Snowmelt Runoff Model (SRM) User's Manual*. University of Berne, Department of Geography. pp. 178.

Massey Jr., F. J., 1951. The Kolmogorov-Smirnov test for goodness of fit. *Journal of the American Statistical Association*, 46(253):68–78.

Matott, L. S., J. E. Babendreier, and S. T. Purucker, 2009. Evaluating uncertainty in integrated environmental models: A review of concepts and tools. *Water Resources Research*, 45(6). doi:10.1029/2008WR007301.

McCabe, G. J. and M. P. Clark, 2005. Trends and variability in snowmelt runoff in the western United States. *Journal of Hydrometeorology*, 6(4):476–482.

McCartney, S. E., S. K. Carey, and J. W. Pomeroy, 2006. Intra-basin variability of snowmelt water balance calculations in a subarctic catchment. *Hydrological Processes*, 20(4):1001–1016.

McCuen, R. H., Z. Knight, and A. G. Cutter, 2006. Evaluation of the Nash–Sutcliffe efficiency index. *Journal of Hydrologic Engineering*, 11(6):597–602.

Mearns, L., W. Gutowski, R. Jones, L. Leung, S. McGinnis, A. Nunes, and Y. Qian, 2007. The North American regional climate change assessment program dataset. *National Center for Atmospheric Research Earth System Grid Data Portal, Boulder, CO*. doi:10.5065/D6RN35ST.

Meehl, G., T. Stocker, W. Collins, P. Friedlingstein, A. Gaye, J. Gregory, A. Kitoh, R. Knutti, J. Murphy, A. Noda, S. Raper, I. Watterson, A. Weaver, and Z.-C. Zhao, 2007. Global climate projections. In *Climate Change 2007: The Physical Science Basis. Contribution of Working Group I to the Fourth Assessment Report of the Intergovernmental Panel on Climate Change*, S. Solomon, D. Qin, M. Manning, Z. Chen, M. Marquis, K. Averyt, M. Tignor, and H. Miller, eds., chapter 10, Pp. 747–845. Cambridge, United Kingdom and New York, NY, USA: Cambridge University Press.

Ménard, C., R. Essery, and J. Pomeroy, 2014a. Modelled sensitivity of the snow regime to topography, shrub fraction and shrub height. *Hydrology and Earth System Sciences*, 18(6):2375–2392.

Ménard, C. B., R. Essery, J. Pomeroy, P. Marsh, and D. B. Clark, 2014b. A shrub bending model to calculate the albedo of shrub-tundra. *Hydrological Processes*, 28(2):341–351.

Meybeck, M., P. Green, and C. Vörösmarty, 2001. A new typology for mountains and other relief classes: An application to global continental water resources and population distribution. *Mountain Research and Development*, 21(1):34–45.

Minville, M., F. Brissette, and R. Leconte, 2008. Uncertainty of the impact of climate change on the hydrology of a nordic watershed. *Journal of Hydrology*, 358(1):70–83.

Moore, R., I. McKendry, K. Stahl, H. Kimmins, and Y.-H. Lo, 2005. Mountain pine beetle outbreaks in western Canada: coupled influences of climate variability and stand development. *Resources Naturelles Canada, Direction des impacts et de ladaptation liés aux changements climatiques, rapport final du Projet A*, 676. pp. 60.

Morris, M. D., 1991. Factorial sampling plans for preliminary computational experiments. *Technometrics*, 33(2):161–174.

Moss, R. H., J. A. Edmonds, K. A. Hibbard, M. R. Manning, S. K. Rose, D. P. Van Vuuren, T. R. Carter, S. Emori, M. Kainuma, T. Kram, et al., 2010. The next generation of scenarios for climate change research and assessment. *Nature*, 463(7282):747–756.

Mountain-Research-Initiative-EDW-Working-Group, 2015. Elevation-dependent warming in mountain regions of the world. *Nature Climate Change*, 5(5):424–430.

Muleta, M. K. and J. W. Nicklow, 2005. Sensitivity and uncertainty analysis coupled with automatic calibration for a distributed watershed model. *Journal of Hydrology*, 306(1):127–145.

Musselman, K., N. P. Molotch, and P. D. Brooks, 2008. Effects of vegetation on snow accumulation and ablation in a mid-latitude sub-alpine forest. *Hydrological Processes*, 22(15):2767–2776.

Nakicenovic, N., R. Swart, J. Alcamo, G. Davis, B. de Vries, J. Fenhann, S. Gaffin, K. Gregory, A. Grübler, T. Y. Jung, and et al., 2000. *Special report on emissions scenarios*. Cambridge University Press, Cambridge, UK. pp. 612, ISBN: 0521804930., July 2000.

Nayak, A., 2008. *The effect of climate change on the hydrology of a mountainous catchment in the western United States: A case study at Reynolds Creek, Idaho*. Utah State University. pp. 194.

Nayak, A., D. Marks, D. Chandler, and M. Seyfried, 2010. Long-term snow, climate, and streamflow trends at the Reynolds Creek Experimental Watershed, States, Owyhee Mountains, Idaho, United. *Water Resources Research*, 46(6). doi:10.1029/2008WR007525.

Neilson, R. P. and D. Marks, 1994. A global perspective of regional vegetation and hydrologic sensitivities from climatic change. *Journal of Vegetation Science*, 5(5):715–730.

Newman, A. J., M. P. Clark, A. Winstral, D. Marks, and M. Seyfried, 2014. The use of similarity concepts to represent subgrid variability in land surface models: Case study in a snowmelt-dominated watershed. *Journal of Hydrometeorology*, 15(5):1717–1738.

Nogués-Bravo, D., M. B. Araújo, M. Errea, and J. Martinez-Rica, 2007. Exposure of global mountain systems to climate warming during the 21st century. *Global Environmental Change*, 17(3):420–428.

Nossent, J., P. Elsen, and W. Bauwens, 2011. Sobol sensitivity analysis of a complex environmental model. *Environmental Modelling & Software*, 26(12):1515–1525.

Oke, T., 1978. *Boundary Layer Climates*. Methuen, New York. pp. 372.

Osterkamp, T., M. Jorgenson, E. Schuur, Y. Shur, M. Kanevskiy, J. Vogel, and V. Tumskoy, 2009. Physical and ecological changes associated with warming permafrost and thermokarst in interior Alaska. *Permafrost and Periglacial Processes*, 20(3):235–256.

Pachauri, R. K., L. Meyer, G.-K. Plattner, T. Stocker, et al., 2015. *IPCC, 2014: Climate Change 2014: Synthesis Report. Contribution of Working Groups I, II and III to the Fifth Assessment Report of the Intergovernmental Panel on Climate Change, Core Writing Team, R.K. Pachauri and L.A. Meyer (eds.)*. IPCC. pp. 151.

Patil, S. D., P. J. Wigington, S. G. Leibowitz, E. A. Sproles, and R. L. Comeleo, 2014. How does spatial variability of climate affect catchment streamflow predictions? *Journal of Hydrology*, 517:135–145.

Pechlivanidis, I., B. Jackson, N. McIntyre, and H. Wheater, 2011. Catchment scale hydrological modelling: A review of model types, calibration approaches and uncertainty analysis methods in the context of recent developments in technology and applications. *Global NEST Journal*, 13(3):193–214.

Perovich, D. K., B. Light, H. Eicken, K. F. Jones, K. Runciman, and S. V. Nghiem, 2007. Increasing solar heating of the Arctic Ocean and adjacent seas, 1979–2005: Attribution and role in the ice-albedo feedback. *Geophysical Research Letters*, 34(19).

Phillips, J. D., A. V. Turkington, and D. A. Marion, 2008. Weathering and vegetation effects in early stages of soil formation. *Catena*, 72(1):21–28.

Pielke, R. A., R. Avissar, M. Raupach, A. J. Dolman, X. Zeng, A. S. Denning, et al., 1998. Interactions between the atmosphere and terrestrial ecosystems: Influence on weather and climate. *Global Change Biology*, 4(5):461–475.

Pomeroy, J., D. Bewley, R. Essery, N. Hedstrom, T. Link, R. Granger, J.-E. Sicart, C. Ellis, and J. Janowicz, 2006. Shrub tundra snowmelt. *Hydrological Processes*, 20(4):923–941.

Pomeroy, J., X. Fang, and C. Ellis, 2012. Sensitivity of snowmelt hydrology in Marmot Creek, Alberta, to forest cover disturbance. *Hydrological Processes*, 26(12):1891–1904.

Pomeroy, J., X. Fang, and B. Williams, 2011. Modelling snow water conservation on the Canadian Prairies. Technical report, Centre for Hydrology, University of Saskatchewan. pp. 43.

Pomeroy, J., D. Gray, T. Brown, N. Hedstrom, W. Quinton, R. Granger, and S. Carey, 2007. The cold regions hydrological model: a platform for basing process representation and model structure on physical evidence. *Hydrological Processes*, 21(19):2650–2667.

Pomeroy, J., D. Gray, N. Hedstrom, and J. Janowicz, 2002. Prediction of seasonal snow accumulation in cold climate forests. *Hydrological Processes*, 16(18):3543–3558.

Pomeroy, J. and L. Li, 2000. Prairie and Arctic areal snow cover mass balance using a blowing snow model. *Journal of Geophysical Research*, 105(D21):26619–26634.

Pomeroy, J., P. Marsh, and D. Gray, 1997. Application of a distributed blowing snow model to the Arctic. *Hydrological Processes*, 11(11):1451–1464.

Pomeroy, J., J. Parviainen, N. Hedstrom, and D. Gray, 1998. Coupled modelling of forest snow interception and sublimation. *Hydrological Processes*, 12(15):2317–2337.

Pomeroy, J., K. Shook, X. Fang, T. Brown, C. Marsh, and R. Granger, 2013. *Development of a snowmelt runoff model for the Lower Smoky River. Centre for Hydrology Report: Report No. 13.* University of Saskatchewan, Saskatoon. pp. 89.

Pomeroy, J., B. Toth, R. Granger, N. Hedstrom, and R. Essery, 2003. Variation in surface energetics during snowmelt in a subarctic mountain catchment. *Journal of Hydrometeorology*, 4(4):702–719.

Pomeroy, J. W., X. Fang, and K. Rasouli, 2015. Sensitivity of snow processes to warming in the Canadian Rockies. In *72nd Eastern Snow Conference, Sherbrooke, Québec, Canada.* Pp. 22–33.

Pomeroy, J. W. and R. J. Granger, 1999. *Wolf Creek Research Basin: Hydrology, Ecology, Environment.* National Water Research Institute. Environment Canada, Saskatoon, Saskatchewan. pp. 160.

Pomeroy, J. W., N. Hedstrom, and J. Parviainen, 1999. The snow mass balance of Wolf Creek , Yukon: effects of snow sublimation and redistribution. *Wolf Creek Research Basin–Hydrology, Ecology, Environment–Proceedings of a workshop held in Whitehorse, Yukon, edited by: Pomeroy, J. W. and Granger R. J.*, Pp. 15–30.

Priestley, C. and R. Taylor, 1972. On the assessment of surface heat flux and evaporation using large-scale parameters. *Monthly Weather Review*, 100(2):81–92.

Quinton, W., T. Shirazi, S. Carey, and J. Pomeroy, 2005. Soil water storage and active-layer development in a sub-alpine tundra hillslope, southern Yukon Territory, Canada. *Permafrost and Periglacial Processes*, 16(4):369–382.

Quinton, W. L., R. K. Bemrose, Y. Zhang, and S. K. Carey, 2009. The influence of spatial variability in snowmelt and active layer thaw on hillslope drainage for an alpine tundra hillslope. *Hydrological Processes*, 23(18):2628–2639.

Quinton, W. L. and S. K. Carey, 2008. Towards an energy-based runoff generation theory for tundra landscapes. *Hydrological Processes*, 22(23):4649–4653.

Raffa, K. F., B. H. Aukema, B. J. Bentz, A. L. Carroll, J. A. Hicke, M. G. Turner, and W. H. Romme, 2008. Cross-scale drivers of natural disturbances prone to anthropogenic amplification: the dynamics of bark beetle eruptions. *Bioscience*, 58(6):501–517.

Rakovec, O., M. C. Hill, M. Clark, A. Weerts, A. Teuling, and R. Uijlenhoet, 2014. Distributed Evaluation of Local Sensitivity Analysis (DELSA), with application to hydrologic models. *Water Resources Research*, 50(1):409–426.

Rasmussen, R., C. Liu, K. Ikeda, D. Gochis, D. Yates, F. Chen, M. Tewari, M. Barlage, J. Dudhia, W. Yu, et al., 2011. High-resolution coupled climate runoff simulations of seasonal snowfall over Colorado: a process study of current and warmer climate. *Journal of Climate*, 24(12):3015–3048.

Rasouli, K., M. Hernández-Henríquez, and S. Déry, 2013. Streamflow input to Lake Athabasca, Canada. *Hydrology and Earth System Sciences*, 17(5):1681.

Rasouli, K., M. Hernández-Henríquez, and S. Déry, 2015a. Reply to DL Peters' comment on" Streamflow input to Lake Athabasca, Canada" by Rasouli et al.(2013). *Hydrology and Earth System Sciences*, 19(3):1287–1292.

Rasouli, K., J. W. Pomeroy, J. R. Janowicz, S. K. Carey, and T. J. Williams, 2014. Hydrological sensitivity of a northern mountain basin to climate change. *Hydrological Processes*, 28(14):4191–4208.

Rasouli, K., J. W. Pomeroy, and D. G. Marks, 2015b. Snowpack sensitivity to perturbed climate in a cool mid-latitude mountain catchment. *Hydrological Processes*, 29(18):3925–3940.

Rawlins, M. A., M. Steele, M. C. Serreze, C. J. Vörösmarty, W. Ermold, R. B. Lammers, K. C. McDonald, T. M. Pavelsky, A. Shiklomanov, and J. Zhang, 2009. Tracing freshwater anomalies through the air-land-ocean system: A case study from the Mackenzie river basin and the Beaufort Gyre. *Atmosphere-Ocean*, 47(1):79–97.

Razavi, S. and H. V. Gupta, 2016. A new framework for comprehensive, robust, and efficient global sensitivity analysis: 1. Theory. *Water Resources Research*, 52(1):423–439.

Razavi, S., B. A. Tolson, L. S. Matott, N. R. Thomson, A. MacLean, and F. R. Seglenieks, 2010. Reducing the computational cost of automatic calibration through model preemption. *Water Resources Research*, 46(11). doi:10.1029/2009WR008957.

Reba, M. L., D. Marks, T. E. Link, J. Pomeroy, and A. Winstral, 2014. Sensitivity of model parameterizations for simulated latent heat flux at the snow surface for complex mountain sites. *Hydrological Processes*, 28(3):868–881.

Reba, M. L., D. Marks, A. Winstral, T. E. Link, and M. Kumar, 2011a. Sensitivity of the snowcover energetics in a mountain basin to variations in climate. *Hydrological Processes*, 25(21):3312–3321.

Reba, M. L., D. Marks, A. Winstral, T. E. Link, and M. Kumar, 2011b. Sensitivity of the snowcover energetics in a mountain basin to variations in climate. *Hydrological Processes*, 25(21):3312–3321.

Reba, M. L., J. Pomeroy, D. Marks, and T. E. Link, 2012. Estimating surface sublimation losses from snowpacks in a mountain catchment using eddy covariance and turbulent transfer calculations. *Hydrological Processes*, 26(24):3699–3711.

Reiners, W., A. Bouwman, W. Parsons, and M. Keller, 1994. Tropical rain forest conversion to pasture: changes in vegetation and soil properties. *Ecological Applications*, 4(2):363–377.

Retana, J., J. Maria Espelta, A. Habrouk, J. Luis Ordoñez, and F. de Solà-Morales, 2002. Regeneration patterns of three Mediterranean pines and forest changes after a large wildfire in northeastern Spain. *Ecoscience*, 9(1):89–97.

Ritter, E., L. Vesterdal, and P. Gundersen, 2003. Changes in soil properties after afforestation of former intensively managed soils with oak and Norway spruce. *Plant and Soil*, 249(2):319–330.

Rodriguez-Iturbe, I., 2000. Ecohydrology: A hydrologic perspective of climate-soil-vegetation dynamics. *Water Resources Research*, 36(1):3–9.

Rouse, W. R., M. S. Douglas, R. E. Hecky, A. E. Hershey, G. W. Kling, L. Lesack, P. Marsh, M. McDonald, B. J. Nicholson, N. T. Roulet, et al., 1997. Effects of climate change on the freshwaters of arctic and subarctic North America. *Hydrological Processes*, 11(8):873–902.

Rutter, N., R. Essery, J. Pomeroy, N. Altimir, K. Andreadis, I. Baker, A. Barr, P. Bartlett, A. Boone, H. Deng, et al., 2009. Evaluation of forest snow processes models (SnowMIP2). *Journal of Geophysical Research: Atmospheres*, 114(D6). doi:10.1029/2008JD011063.

Safranyik, L., D. Shrimpton, H. Whitney, et al., 1975. An interpretation of the interaction between lodgepole pine, the mountain pine beetle and its associated blue stain fungi in western Canada. *Management of Lodgepole Pine Ecosystems*, 1:406–428.

Salathé, E. P., 2003. Comparison of various precipitation downscaling methods for the simulation of streamflow in a rainshadow river basin. *International Journal of Climatology*, 23(8):887–901.

Saltelli, A., M. Ratto, T. Andres, F. Campolongo, J. Cariboni, D. Gatelli, M. Saisana, and S. Tarantola, 2008. *Global sensitivity analysis: The primer*. John Wiley & Sons. pp. 304.

Scherler, M., C. Hauck, M. Hoelzle, M. Stähli, and I. Völksch, 2010. Meltwater infiltration into the frozen active layer at an alpine permafrost site. *Permafrost and Periglacial Processes*, 21(4):325–334.

Schindler, D. W. and W. F. Donahue, 2006. An impending water crisis in Canada's western prairie provinces. *Proceedings of the National Academy of Sciences*, 103(19):7210–7216.

Schmidt, R. and D. R. Gluns, 1991. Snowfall interception on branches of three conifer species. *Canadian Journal of Forest Research*, 21(8):1262–1269.

Schneider, R. R., 2013. *Alberta's natural subregions under a changing climate: past, present, and future*. Alberta Biodiversity Monitoring Institute, Edmonton, Canada. pp. 86.

Schneider, R. R., A. Hamann, D. Farr, X. Wang, and S. Boutin, 2009. Potential effects of climate change on ecosystem distribution in Alberta. *Canadian Journal of Forest Research*, 39(5):1001–1010.

Schuur, E. A., J. G. Vogel, K. G. Crummer, H. Lee, J. O. Sickman, and T. E. Osterkamp, 2009. The effect of permafrost thaw on old carbon release and net carbon exchange from tundra. *Nature*, 459(7246):556–559.

Semadeni-Davies, A., C. Hernebring, G. Svensson, and L.-G. Gustafsson, 2008. The impacts of climate change and urbanisation on drainage in Helsingborg, Sweden: Combined sewer system. *Journal of Hydrology*, 350(1):100–113.

Semmens, K. and J. Ramage, 2013. Recent changes in spring snowmelt timing in the Yukon River basin detected by passive microwave satellite data. *The Cryosphere*, 7(3):905–916.

Sevruk, B., 1997. Regional dependency of precipitation-altitude relationship in the Swiss Alps. *Climatic Change*, 36(3-4):355–369.

Seyfried, M., L. Grant, D. Marks, A. Winstral, and J. McNamara, 2009. Simulated soil water storage effects on streamflow generation in a mountainous snowmelt environment, idaho, usa. *Hydrological Processes*, 23(6):858–873.

Seyfried, M., R. Harris, D. Marks, and B. Jacob, 2001. Geographic database, Reynolds Creek Experimental Watershed, Idaho, United States. *Water Resources Research*, 37(11):2825–2829.

Seyyedi, H., E. Anagnostou, E. Beighley, and J. McCollum, 2014. Satellite-driven downscaling of global reanalysis precipitation products for hydrological applications. *Hydrology and Earth System Sciences*, 18(12):5077–5091.

Shakesby, R. A., D. J. Boakes, C. de OA Coelho, A. B. Gonçalves, and R. P. Walsh, 1996. Limiting the soil degradational impacts of wildfire in pine and eucalyptus forests in Portugal: a comparison of alternative post-fire management practices. *Applied Geography*, 16(4):337–355.

Shepherd, T. G., 2014. Atmospheric circulation as a source of uncertainty in climate change projections. *Nature Geoscience*, 7(10):703–708.

Sicart, J.-E., J. Pomeroy, R. Essery, and D. Bewley, 2006. Incoming longwave radiation to melting snow: observations, sensitivity and estimation in northern environments. *Hydrological Processes*, 20(17):3697–3708.

Siemens, E., 2016. *Effects of climate variability on hydrological processes in a Canadian Rockies headwaters catchment*. MSc Thesis, University of Saskatchewan, Canada. pp. 71.

Singh, V. and M. K. Goyal, 2016. Analysis and trends of precipitation lapse rate and extreme indices over north Sikkim eastern Himalayas under CMIP5ESM-2M (RCPs) experiments. *Atmospheric Research*, 167:34 – 60.

Skamarock, W. C., J. B. Klemp, J. Dudhia, D. O. Gill, D. M. Barker, W. Wang, and J. G. Powers, 2005. A description of the advanced research WRF version 2. Technical report, DTIC Document. pp. 88.

Slaughter, C. W., D. Marks, G. N. Flerchinger, S. S. Van Vactor, and M. Burgess, 2001. Thirty-five years of research data collection at the Reynolds Creek Experimental Watershed, Idaho, United States. *Water Resources Research*, 37(11):2819–2823.

Sobol, I. M., 1993. Sensitivity estimates for nonlinear mathematical models. *Mathematical Modelling and Computational Experiments*, 1(4):407–414.

Spear, R. and G. Hornberger, 1980. Eutrophication in Peel InletII. Identification of critical uncertainties via generalized sensitivity analysis. *Water Research*, 14(1):43–49.

Sproles, E., A. Nolin, K. Rittger, and T. Painter, 2013. Climate change impacts on maritime mountain snowpack in the Oregon Cascades. *Hydrology and Earth System Sciences*, 17(7):2581–2597.

St Jacques, J.-M. and D. J. Sauchyn, 2009. Increasing winter baseflow and mean annual streamflow from possible permafrost thawing in the Northwest Territories, Canada. *Geophysical Research Letters*, 36(1). doi:10.1029/2008GL035822.

Staniforth, A. and N. Wood, 2008. Aspects of the dynamical core of a nonhydrostatic, deep-atmosphere, unified weather and climate-prediction model. *Journal of Computational Physics*, 227(7):3445–3464.

Stanton, M., M. Rejmanek, and C. Galen, 1994. Changes in vegetation and soil fertility along a predictable snowmelt gradient in the Mosquito Range, Colorado, USA. *Arctic and Alpine Research*, Pp. 364–374.

Stewart, I. T., D. R. Cayan, and M. D. Dettinger, 2004. Changes in snowmelt runoff timing in western North America under a 'business as usual' climate change scenario. *Climatic Change*, 62(1-3):217–232.

Stockton, C. W. and W. R. Boggess, 1979. Geohydrological implications of climate change on water resource development. Technical report, DTIC Document. pp. 206.

Stow, D. A., A. Hope, D. McGuire, D. Verbyla, J. Gamon, F. Huemmrich, S. Houston, C. Racine, M. Sturm, K. Tape, et al., 2004. Remote sensing of vegetation and land-cover change in Arctic Tundra Ecosystems. *Remote Sensing of Environment*, 89(3):281–308.

Sturm, M., J. Schimel, G. Michaelson, J. M. Welker, S. F. Oberbauer, G. E. Liston, J. Fahnestock, and V. E. Romanovsky, 2005. Winter biological processes could help convert arctic tundra to shrubland. *Bioscience*, 55(1):17–26.

Sunyer, M., H. Madsen, and P. Ang, 2012. A comparison of different regional climate models and statistical downscaling methods for extreme rainfall estimation under climate change. *Atmospheric Research*, 103:119–128.

Tape, K., M. Sturm, and C. Racine, 2006. The evidence for shrub expansion in northern Alaska and the Pan-Arctic. *Global Change Biology*, 12(4):686–702.

Taylor, S. W., A. L. Carroll, R. I. Alfaro, and L. Safranyik, 2006. Forest, climate and mountain pine beetle outbreak dynamics in western Canada. In *The Mountain Pine Beetle: A synthesis of biology, management, and impacts on lodgepole pine*, Pp. 67–94. Natural Resources Canada, Canadian Forest Service, Pacific Forestry Centre, Victoria, British Columbia.

Tebaldi, C., R. L. Smith, D. Nychka, and L. O. Mearns, 2005. Quantifying uncertainty in projections of regional climate change: A Bayesian approach to the analysis of multimodel ensembles. *Journal of Climate*, 18(10):1524–1540.

Thompson, D. W. and J. M. Wallace, 1998. The Arctic Oscillation signature in the wintertime geopotential height and temperature fields. *Geophysical Research Letters*, 25(9):1297–1300.

Thorne, R., 2011. Uncertainty in the impacts of projected climate change on the hydrology of a subarctic environment: Liard river basin. *Hydrology and Earth System Sciences*, 15(5):1483–1492.

Thornthwaite, C. and J. Mather, 1957. Instructions and tables for computing potential evapotranspiration and the water balance, 5th printing. *CW Thornthwaite Associates, Laboratory of Climatology, Elmer, NJ, USA*, 10(3). pp. 254.

Timmermann, A., J. Oberhuber, A. Bacher, M. Esch, M. Latif, and E. Roeckner, 1999. Increased El Niño frequency in a climate model forced by future greenhouse warming. *Nature*, 398(6729):694–697.

Tolson, B. A. and C. A. Shoemaker, 2007. Dynamically dimensioned search algorithm for computationally efficient watershed model calibration. *Water Resources Research*, 43(1). doi: 10.1029/2005WR004723.

Troendle, C., 1983. The potential for water yield augmentation from forest management in the Rocky Mountain region. *Journal of the American Water Resources Association*, 19:359–373.

Uppala, S. M., P. Kållberg, A. Simmons, U. Andrae, V. d. Bechtold, M. Fiorino, J. Gibson, J. Haseler, A. Hernandez, G. Kelly, et al., 2005. The ERA-40 re-analysis. *Quarterly Journal of the Royal Meteorological Society*, 131(612):2961–3012.

Varhola, A., N. C. Coops, M. Weiler, and R. D. Moore, 2010. Forest canopy effects on snow accumulation and ablation: An integrative review of empirical results. *Journal of Hydrology*, 392(3):219–233.

Verseghy, D. L., 1991. Class–a Canadian land surface scheme for GCMs. I. Soil model. *International Journal of Climatology*, 11(2):111–133.

Vihma, T., 2014. Effects of Arctic sea ice decline on weather and climate: A review. *Surveys in Geophysics*, 35(5):1175–1214.

Viviroli, D., D. R. Archer, W. Buytaert, H. J. Fowler, G. Greenwood, A. F. Hamlet, Y. Huang, G. Koboltschnig, I. Litaor, J. I. López-Moreno, et al., 2011. Climate change and mountain water resources: Overview and recommendations for research, management and policy. *Hydrology and Earth System Sciences*, 15(2):471–504.

Viviroli, D. and R. Weingartner, 2004. The hydrological significance of mountains: from regional to global scale. *Hydrology and Earth System Sciences Discussions*, 8(6):1017–1030.

Vrac, M. and P. Friederichs, 2015. Multivariateintervariable, spatial, and temporalbias correction. *Journal of Climate*, 28(1):218–237.

Walker, D., J. C. Halfpenny, M. D. Walker, and C. A. Wessman, 1993. Long-term studies of snow-vegetation interactions. *BioScience*, 43(5):287–301.

Walvoord, M. A. and B. L. Kurylyk, 2016. Hydrologic impacts of thawing permafrost–A review. *Vadose Zone Journal*, 15(6). doi:10.2136/vzj2016.01.0010.

Walvoord, M. A. and R. G. Striegl, 2007. Increased groundwater to stream discharge from permafrost thawing in the Yukon River Basin: Potential impacts on lateral export of carbon and nitrogen. *Geophysical Research Letters*, 34(12). doi:10.1029/2007GL030216.

Wang, T., A. Hamann, D. L. Spittlehouse, and T. Q. Murdock, 2012. ClimateWNA-high-resolution spatial climate data for western North America. *Journal of Applied Meteorology and Climatology*, 51(1):16–29.

Weber, M., M. Bernhardt, J. Pomeroy, X. Fang, S. Härer, and K. Schulz, 2016. Description of current and future snow processes in a small basin in the Bavarian Alps. *Environmental Earth Sciences*, 75(17):1223. doi: 10.1007/s12665-016-6027-1.

Wilbanks, T. J. and R. W. Kates, 1999. Global change in local places: how scale matters. *Climatic Change*, 43(3):601–628.

Wilby, R. L., 2005. Uncertainty in water resource model parameters used for climate change impact assessment. *Hydrological Processes*, 19(16):3201–3219.

Wilby, R. L. and I. Harris, 2006. A framework for assessing uncertainties in climate change impacts: Low-flow scenarios for the River Thames, UK. *Water Resources Research*, 42(2). doi:10.1029/2005WR004065.

Wilby, R. L. and T. Wigley, 1997. Downscaling general circulation model output: a review of methods and limitations. *Progress in Physical Geography*, 21(4):530–548.

Wilcoxon, F., 1945. Individual comparisons by ranking methods. *Biometrics Bulletin*, 1(6):80–83.

Wilks, D. S. and R. L. Wilby, 1999. The weather generation game: a review of stochastic weather models. *Progress in Physical Geography*, 23(3):329–357.

Williams, A. P., C. D. Allen, A. K. Macalady, D. Griffin, C. A. Woodhouse, D. M. Meko, T. W. Swetnam, S. A. Rauscher, R. Seager, H. D. Grissino-Mayer, et al., 2013. Temperature as a potent driver of regional forest drought stress and tree mortality. *Nature Climate Change*, 3(3):292–297.

Williams, T. J., J. W. Pomeroy, J. R. Janowicz, S. K. Carey, K. Rasouli, and W. L. Quinton, 2015. A radiative–conductive–convective approach to calculate thaw season ground surface temperatures for modelling frost table dynamics. *Hydrological Processes*, 29(18):3954–3965.

Willmott, C. and K. Matsuura, 2005. Advantages of the mean absolute error (MAE) over the root mean square error (RMSE) in assessing average model performance. *Climate Research*, 30(1):79–82.

Winstral, A. and D. Marks, 2002. Simulating wind fields and snow redistribution using terrain-based parameters to model snow accumulation and melt over a semi-arid mountain catchment. *Hydrological Processes*, 16(18):3585–3603.

Winstral, A. and D. Marks, 2014. Long-term snow distribution observations in a mountain catchment: Assessing variability, time stability, and the representativeness of an index site. *Water Resources Research*, 50(1):293–305.

Winstral, A., D. Marks, and R. Gurney, 2013. Simulating wind-affected snow accumulations at catchment to basin scales. *Advances in Water Resources*, 55:64–79.

Woo, M.-k. and S. K. Carey, 1998. Permafrost, seasonal frost and slope hydrology, central Wolf Creek Basin, Yukon. In *Wolf Creek Research Basin–Hydrology, Ecology, Environment–Proceedings of a workshop held in Whitehorse, Yukon, edited by: Pomeroy, J. W. and Granger R. J.*, Pp. 45–53. Citeseer.

Woo, M.-k. and R. Heron, 1987. Breakup of small rivers in the subarctic. *Canadian Journal of Earth Sciences*, 24(4):784–795.

Woo, M.-K. and R. Thorne, 2006. Snowmelt contribution to discharge from a large mountainous catchment in subarctic Canada. *Hydrological Processes*, 20(10):2129–2139.

Xie, C. and W. A. Gough, 2013. A simple thaw–freeze algorithm for a multi–layered soil using the Stefan equation. *Permafrost and Periglacial Processes*, 24(3):252–260.

Zhang, Y., S. K. Carey, and W. L. Quinton, 2008. Evaluation of the algorithms and parameterizations for ground thawing and freezing simulation in permafrost regions. *Journal of Geophysical Research: Atmospheres*, 113(D17). doi: 10.1029/2007JD009343.

Zheng, F.-L., 2006. Effect of vegetation changes on soil erosion on the Loess Plateau. *Pedosphere*, 16(4):420–427.

Zhou, J., J. W. Pomeroy, W. Zhang, G. Cheng, G. Wang, and C. Chen, 2014. Simulating cold regions hydrological processes using a modular model in the west of China. *Journal of Hydrology*, 509:13–24.

Zuazo, V. D., J. F. Martínez, C. R. Pleguezuelo, A. M. Raya, and B. C. Rodríguez, 2006. Soil-erosion and runoff prevention by plant covers in a mountainous area (SE Spain): implications for sustainable agriculture. *Environmentalist*, 26(4):309–319.

Appendix A

Further Analysis for Wolf Creek Research Basin

A spatially distributed modeling structure (Figure A.1) is developed with five subbasins and 29 HRUs in Wolf Creek Research Basin (WCRB), based on three elevation bands, four groupings of slope and aspect and three biomes (Figure A.2). A set of physically based modules are assembled for a number of HRUs and the structure is replicated for each subbasin. Each subbasin then possesses the same module configuration but is permitted varying parameter sets and varying numbers of HRUs. Streamflow from each subbasin is routed along the main channel of WCRB.

Sensitivity of snow regimes in different biomes in WCRB over the simulation period (1993–2011) to warming reveals that dry years are more sensitive to warming that wet years (Figure A.3). Figure A.4 illustrates the sensitivity of evapotranspiration, snow intercepted on the canopy, and snow transport by wind in WCRB to warming.

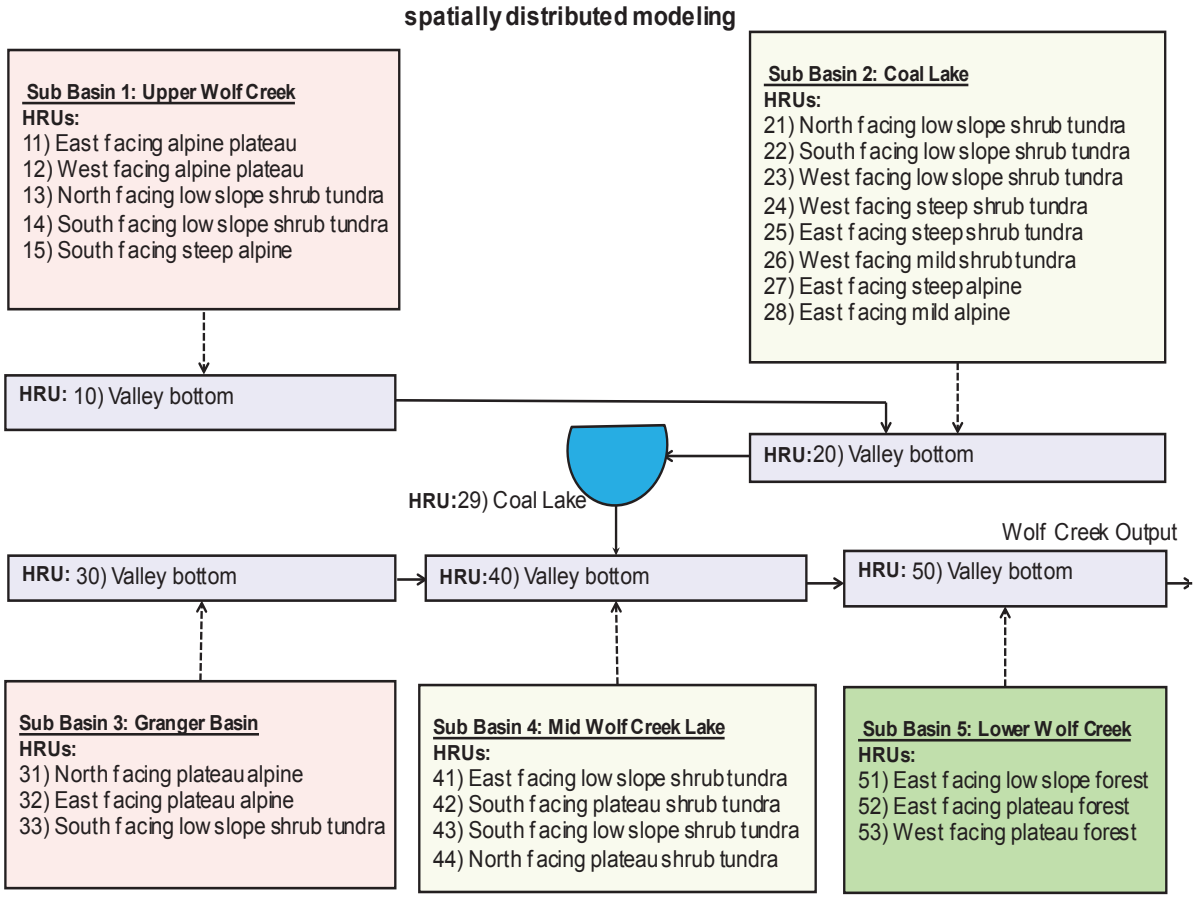

Figure A.1: The spatially distributed modeling structure for WCRB model. The five subbasins are composed of various HRUs and each HRU contains a set of physically based hydrological modules as its internal structure. Clark routing (shown by the dashed line) routes flow from non-channel HRUs to valley bottom HRU in each subbasin and then from all five subbasins (solid lines) to the basin output.

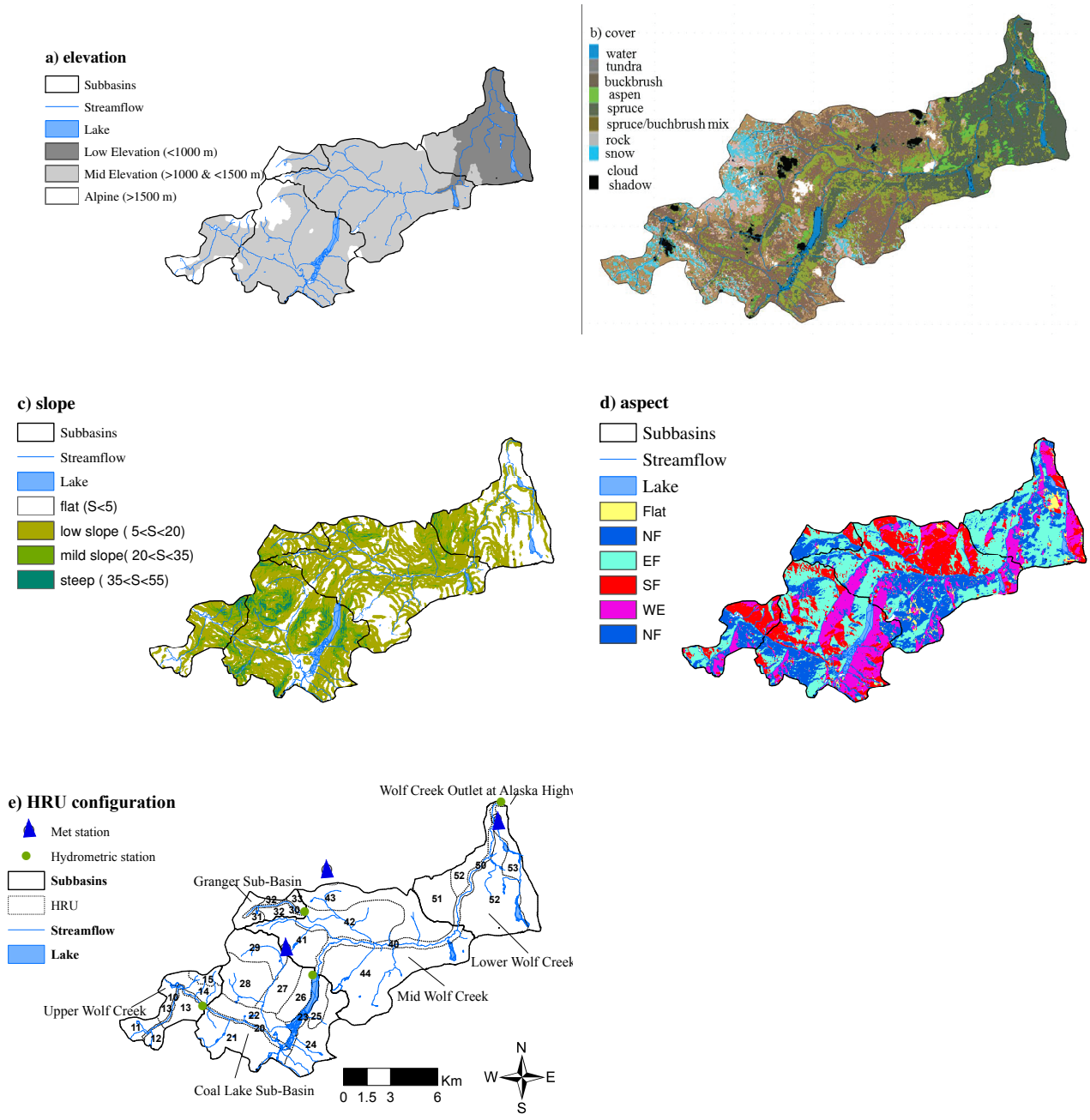

Figure A.2: Wolf Creek Research Basin, Yukon, showing (a) elevation bands, (b) land-cover, (c) slope, and (d) aspect representations used for defining (e) hydrological response units, HRUs in different subbasins (numbered). Green circles denote streamflow gauging stations and triangles denote the location of the meteorological stations. The basin drains to the north.

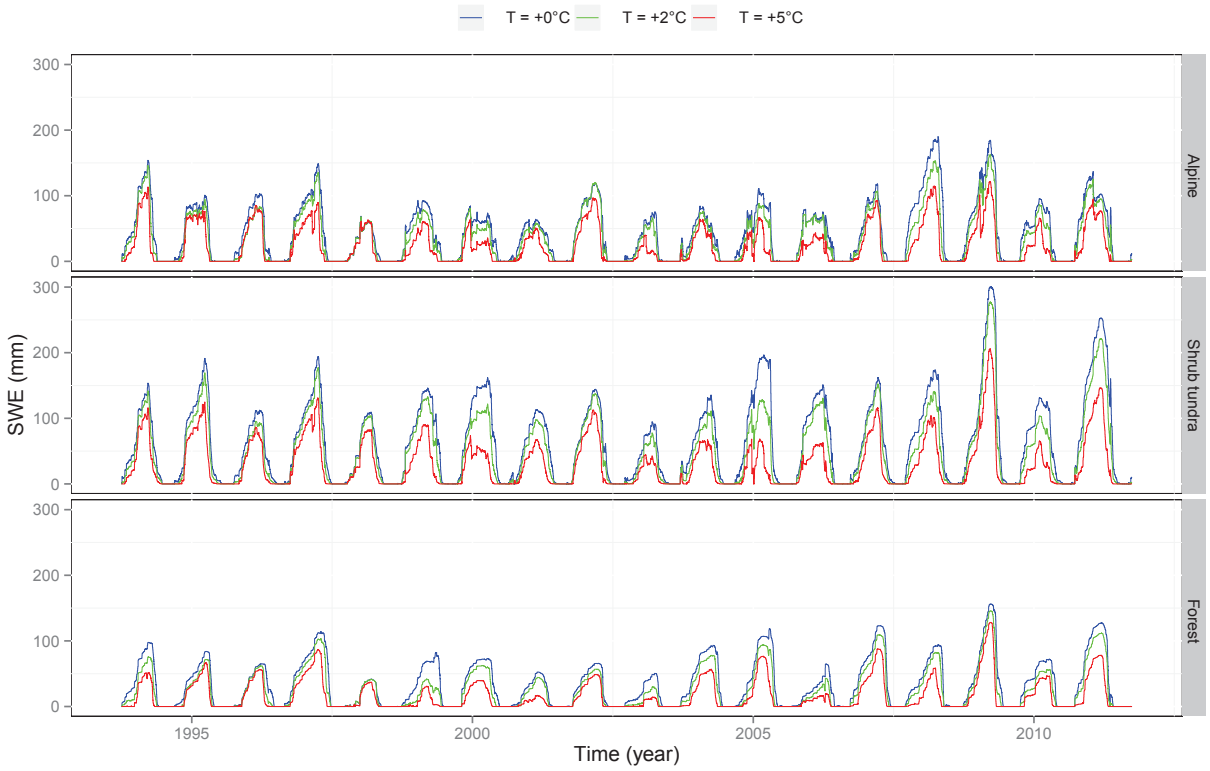

Figure A.3: Snow water equivalent (SWE) regimes for alpine, shrub tundra and forest biomes in Wolf Creek Research Basin, under the current climate and incremental warming of hourly air temperatures by up to 5°C.

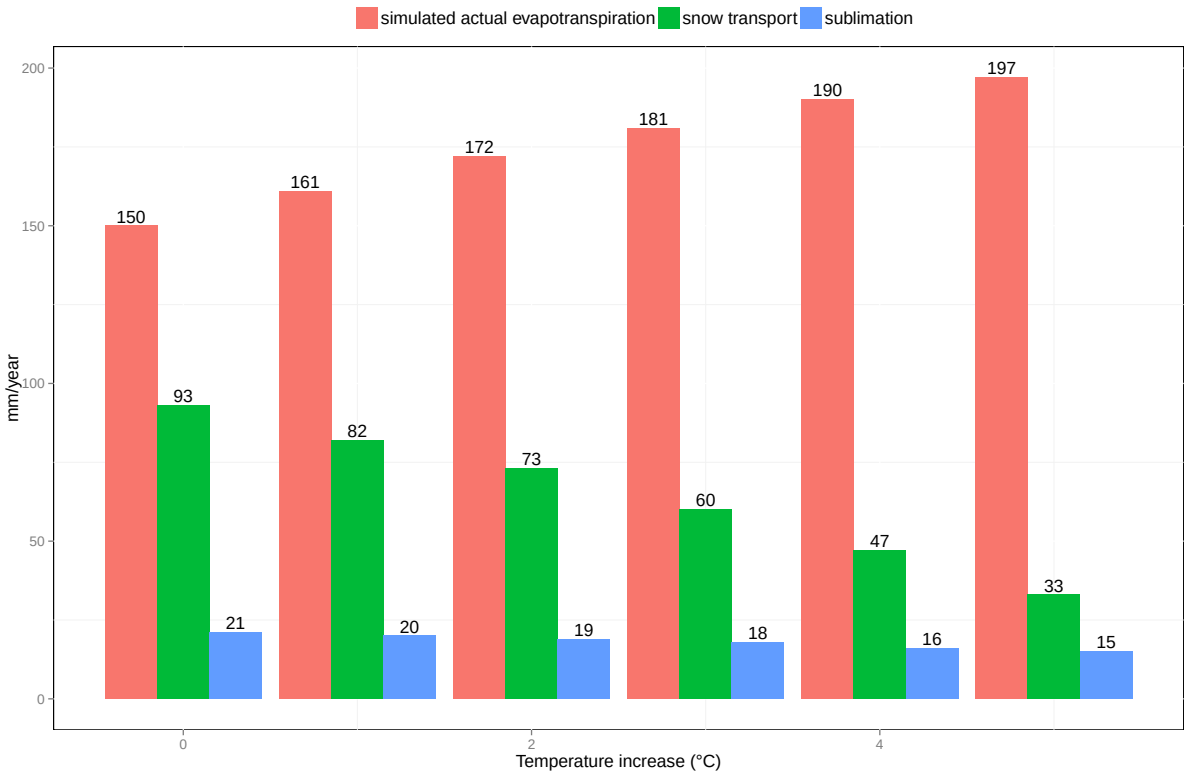

Figure A.4: Changes in the simulated evapotranspiration, intercepted snow sublimation in forest HRUs and blowing snow transport from alpine to shrub tundra biome with warming in Wolf Creek Research Basin. Intercepted snow sublimation decreases with warming from 21 to 15 mm/year.

Appendix B

Further Analysis of Snow Processes in Reynolds Mountain East

The energy and mass balance snowmelt model (Snobal) developed by Marks et al. (1999) is employed in the CRHM modelling system. Figure B.1 illustrates all energy and mass fluxes defined in Snobal. This module conceptually divides the snowpack into two layers: surface-active layer and lower layer, and solves for the temperature and equivalent water depth per unit area in both layers. Snowmelt from each layer is estimated when the input energy exceeds the energy required to warm the snowcover temperature to freezing (0°C).

Because snowpack in RME shows a higher sensitivity to air temperature and precipitation changes, variability of the snowpack is explored with more details in this part of the dissertation. Snowpack seasonal and inter-annual variability in RME from early accumulation in October to complete ablation in summer is illustrated in Figure B.2 for the recent climate (1984–2008) and for warming and precipitation change. Model outputs for low sage, aspen drift, fir, and gap HRUs represent snowpack variability in blowing snow source and sink areas, within tall trees that intercept and sublimate snow, and in forest gaps, which are sheltered from snow redistribution. Snow ablation starts at different times of the year in different HRUs: on March 1st for the sage HRU, in mid-March for forest gap HRU and on April 1st for aspen drift and the fir HRUs. The response of snow ablation to warming of 2°C with and without change precipitation in RME is relatively similar amongst the different HRUs; the start of snow ablation advances to early March everywhere except for the source HRU (low sage) and advances up to two months for 5°C of warming for all types of vegetation. The snow-free date is sensitive to concomitant warming and precipitation change and advances to before April 1st for warming of 5°C and a 20% increase in precipitation. Aspen drift and sage drift HRUs in RME are deep, cold, and north-facing and therefore, latest to melt in most years. During colder years, melt water from drifted snow is available to supply streamflow even as late as July (Figure B.2), and is hydrologically important for this catchment (Winstral and Marks, 2002). The inter-annual coefficient of variation (CV) of SWE, defined as the ratio of standard deviation to average of the SWE values over 25 years, shows greater variability in fall and spring seasons (CV $>$ 1) and lesser variability in midwinter. Warming increases the snowpack inter-annual variability even in winter months, while a precipitation increase slightly decreases the variability in winter and significantly decreases it in spring (Figure B.2 left panels). The small CV in the gap and sink HRUs from December to May, especially in ablation period relative to other sites shows how snow regimes in small forest clearings are not representative of the natural temporal variability of snow regimes in source or forest zones that dominate land-cover in a mountain basin.

Figure B.3 shows the spatial variability of mean annual peak SWE in RME calculated

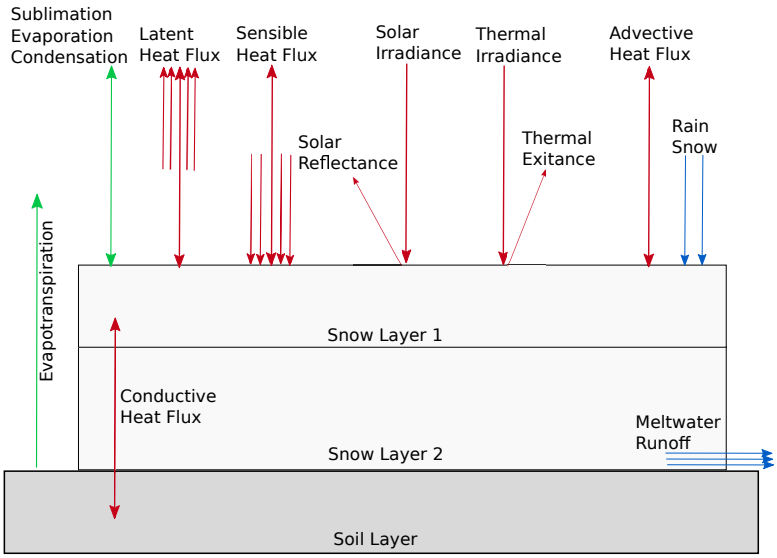

Figure B.1: Schematic view of the energy and mass balance snowmelt model (Snobal) with all input and output fluxes after Marks et al. (1999). Arrow colours denote flux types; red is energy exchange with snow, green is energy exchange with water, blue is mass exchange.

using the recent climate (Figure B.3a) and different scenarios of warming and change in precipitation. Note that the timing of peak SWE is not synchronised across the basin and differs from HRU to HRU. With warming and change in precipitation, spatial variability of peak snowpack decreases and the response of shallow snowpack under severe climate conditions in different regimes becomes more similar. With warming of 2°C, mean annual peak SWE slightly drops in riparian willow, aspen, low sage, and tall sage HRUs with a precipitation increase of 20% (Figure B.3b), and largely declines across the basin with a 20% decrease in precipitation (Figure B.3c). Severe warming (5°C) causes mean annual peak SWE to drop below 200 mm across the basin with a 20% increase in precipitation (Figure B.3d) and to below 100 mm (Figure B.3e) with a 20% decrease in precipitation.

B.1 Snow Sensitivity to Climatic Changes

Because of the higher sensitivity of hydrological variables to air temperature and precipitation changes in RME, this basin is selected for a more detailed sensitivity analysis. Snow processes such as precipitation phase change, snow transport, snowmelt, and sublimation from three sources of blowing snow and snow intercepted on the canopy, and snow surface are discussed. The sensitivity of hydrological processes such as evapotranspiration to climate changes in summer and spring months are also analysed. The spatial variability of precipitation, snow transport, snowmelt, and sublimation from various snow sources in RME catchment is illustrated in Figure B.4. Positive bars in this figure represent the input to the HRUs and negative bars show the loss sources from the HRUs. In general, snow inputs from snowfall and blowing snow are greatest to HRUs that have tall vegetation such as willow, tall sage and

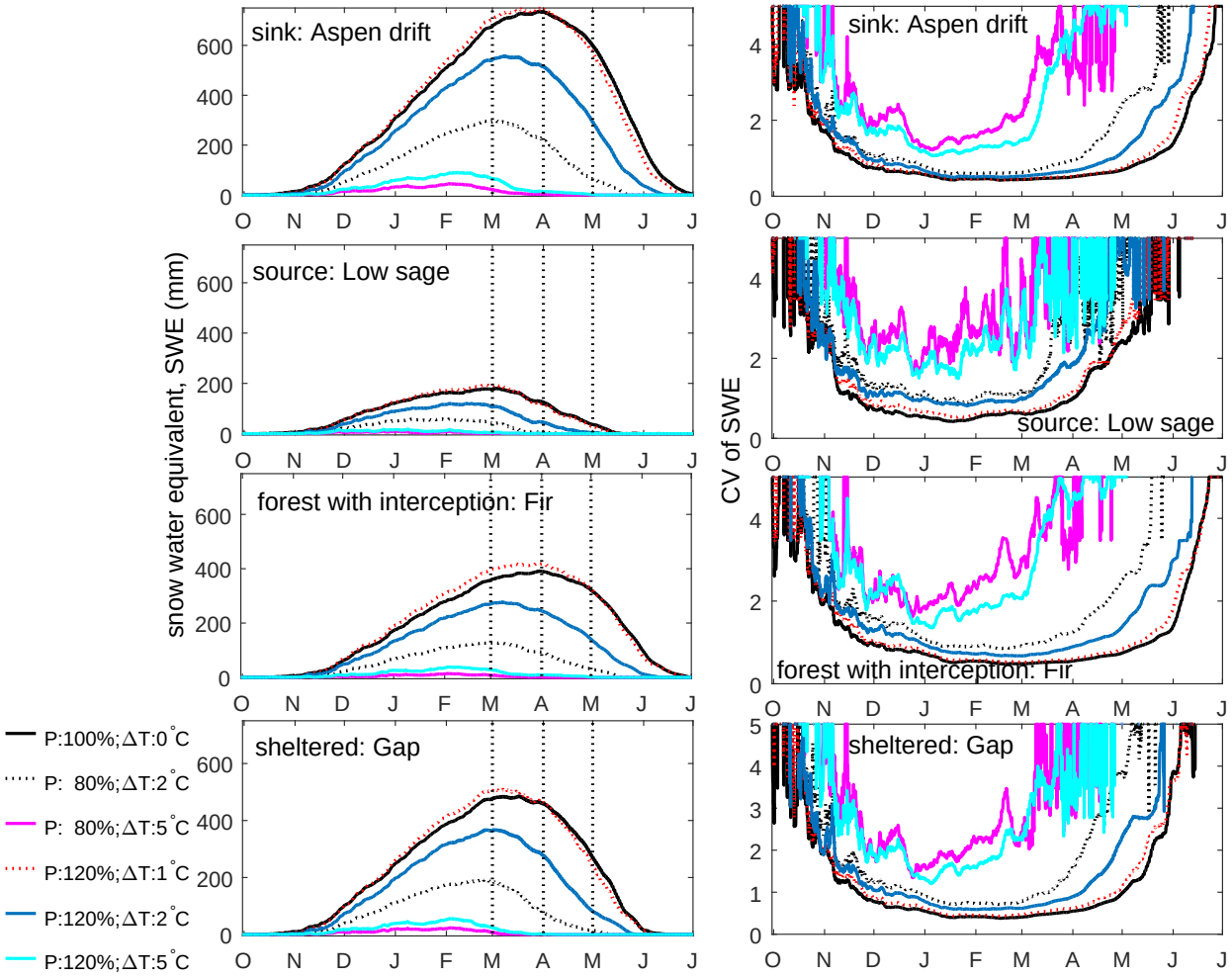

Figure B.2: Sensitivity of snow accumulation and ablation (mean SWE) to warming and changes in precipitation during snowcover season over 25 years of simulation (left panels) and associated coefficient of variability (right panels) for blowing snow sink (aspen drift) and source (low sage), forest (fir), and sheltered (forest gap) HRUs in Reynolds Mountain East catchment. Vertical dashed lines represent March 1st, April 1st, and May 1st SWE values.

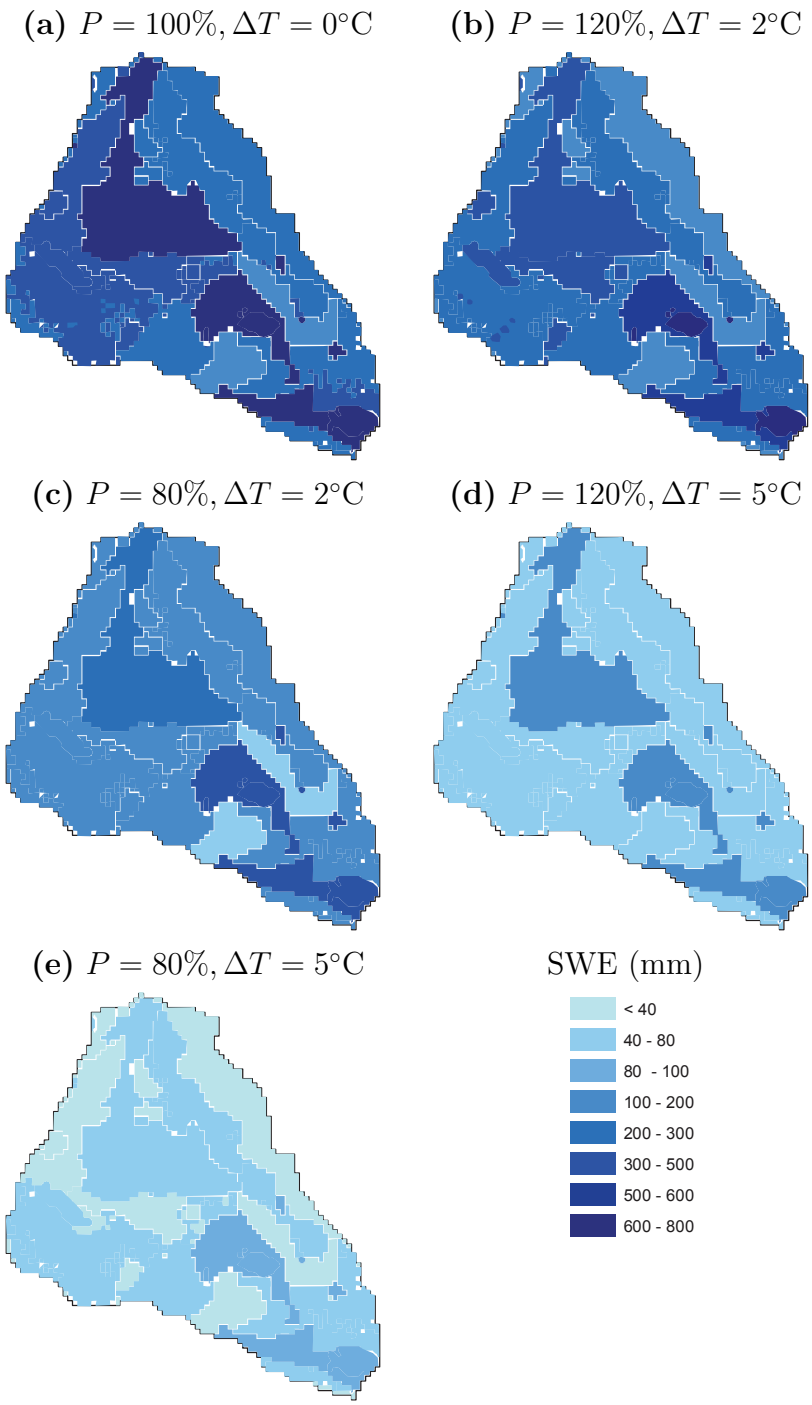

Figure B.3: Spatial variability of mean annual peak SWE (mm) in Reynolds Mountain East catchment a) during control period of 1984–2008 and under b) an increase in precipitation and moderate warming, c) a decrease in precipitation and moderate warming, d) an increase in precipitation and severe warming, and e) a decrease in precipitation and severe warming scenarios

sites in topographic depressions leading to snow drifts; in contrast, accumulation is less than cumulative snowfall in topographically exposed, short vegetation HRUs such as grass and short mountain sagebrush shrubs and where an evergreen canopy permits snow interception and subsequent sublimation losses. Annual sublimation loss from some HRUs is large and reaches 178 mm (in grass HRU) or 20% of total annual precipitation in the catchment over the period of 1984–2008 – it is primarily from blowing snow in sparsely vegetated sites and snow intercepted on fir canopies. Changes in the various mass budget terms are discussed below.

B.1.1 Precipitation

Simulated basin averaged snowfall over 25 years is 602 mm, which under 5°C of warming drops to 224 mm with a 20% increase in precipitation and to 149 mm with a 20% decrease in precipitation (Figure B.4). Precipitation phase is strongly affected by air temperature, which varies with elevation and shows high variability, from 26% rainfall in aspen HRUs to 33% in tall sage HRU with an average of 30% over the basin (Figure B.4). With warming of 5°C, the rain to total precipitation ratio raises to 78% in the catchment (Figure B.5) and is unaffected by precipitation change. Note that RME is a mountain basin and this ratio is expected to be even more for regions with mid- and low-elevation (Nayak et al., 2010). A snow-dominated basin becomes a rain-dominated one under warming of 5°C (Figure B.4).

B.1.2 Snow Transport

Blowing snow is transported from short vegetation HRUs such as grass and sagebrush to tall vegetation and valley bottom HRUs, where snowdrifts may form. Vegetation density and height, which determine the aerodynamic roughness play the key role in snow transport. HRUs with shorter vegetation such as grass show the greatest snow erosion and transport out. Blowing snow transport into and out of an HRU can be up to 196 mm and 71 mm respectively, equivalent to 23% and 8.4% of the average annual precipitation. With 5°C warming blowing snow transport drops to $\leq$8 mm (Figure B.4). This sensitivity to warming is because of the increasing bond strength and cohesion of snow as it warms, which raises the threshold wind speed required to initiate saltation (Li and Pomeroy, 1997). This shows that the occurrence of blowing snow transport in RME is sensitive to warming and almost disappears completely when the basin temperature warms by 5°C and mean annual temperature reaches 10°C.

B.1.3 Snowmelt

Annual snowmelt varies amongst different HRUs depending on the snow transport to or from the HRU and sublimation from surface and intercepted snow. Therefore, it has a non-linear relationship with snowfall. For the same amount of snowfall, aspen drift has the highest depth of snowmelt due to strong snow transport to this HRU. In general, sink HRUs release the greatest snowmelt depth, then sheltered HRUs and the smallest depth

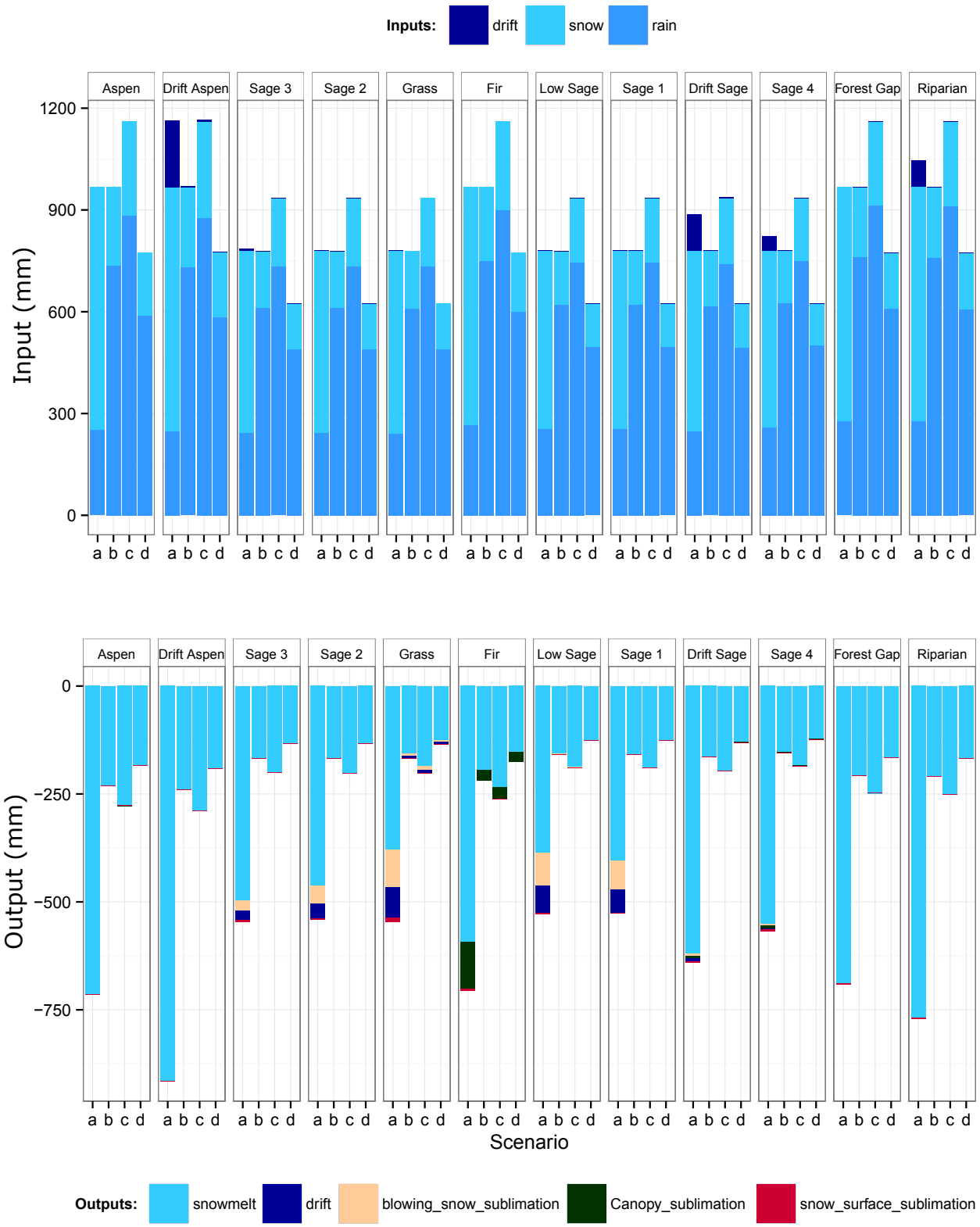

Figure B.4: Vertical snow flux inputs (upper panel) and outputs (lower panel) in winter in Reynolds Mountain East catchment for different HRUs under the following scenarios: (a) averaged over the control period of 1984–2008, (b) only warming: P = 100 %, ΔT = 5°C; (c) increased precipitation and warming: P = 120 %, ΔT = 5°C, and (d) decreased precipitation and warming: P = 80 %, ΔT = 5°C.

from the source HRU, especially grasslands. Under a 5°C warming, snowmelt is reduced 51–79% across the basin depending on the direction of precipitation change. Without precipitation change and under the same warming condition, it drops from 915 mm to 240 mm in aspen drift (Figure B.4). Under different warming scenarios the snowmelt rate drops with greater decline in the sink HRUs including aspen drift, sage drift, willow, and tall sage and lesser decline in the source HRUs (e.g., grass and short sages). This shows that the spatial variability of the response of snowmelt to climate change is high and depends on the combined impacts of snow transport and sublimation processes and melt induced by processes such as rain-on-snow, which increases as the rainfall ratio increases under climate warming. Scenario (c) in Figure B.4 illustrates the impact of a 20% increase in precipitation under warming of 5°C and shows a substantial increase in snowmelt. The increased incidence of warm precipitation would increase the rain-on-snow contribution to melt in such situations.

B.1.4 Sublimation from Blowing Snow

The spatial variability of sublimation from blowing snow is relatively high in RME, ranging from zero in the sink HRUs to 87 mm in a short grass HRU (Figure B.4). This indicates that up to 10% of the total precipitation in short vegetated HRUs such as grass can be sublimated from blowing snow in RME under the recent climate. Because sublimation of blowing snow requires snow transport, with warming of 5°C and a 20% increase in precipitation, sublimation from blowing snow declines to no more than 9 mm in grass HRU and is negligible in other HRUs and as a basin average (Figure B.4).

B.1.5 Sublimation from Intercepted Snow

Mean annual sublimation from snow intercepted by vegetation canopies varies from 8 mm in the tall sage HRU to 110 mm in the fir HRU (Figure B.4). There is a high inter-annual variability in sublimation especially from the fir HRU where annual loss ranges between 75 mm and 140 mm, or on average 11.3% of the total precipitation in this HRU (Figure B.5). Under warming of 5°C, annual intercepted snow sublimation from fir drops to 22 mm or less when precipitation decreases 20% and 28 mm or less when precipitation increases 20%. For this warming scenario, sublimation from intercepted snow in other HRUs is negligible ($\leq$2 mm) irrespective of precipitation change (Figure B.4). This sensitivity to warming is a result of unloading or melt rather than sublimation of intercepted snow during midwinter thaws (Gelfan et al., 2004; Ellis et al., 2010). This shows that similar to the blowing snow transport, sublimation from intercepted snow is sensitive to warming, much more so than to precipitation change. However, intercepted snow sublimation is less sensitive to warming than blowing snow transport and sublimation. Intercepted snow sublimation becomes significant by early December and ceases by the end of April. With 5°C of warming, the period with sublimation from intercepted snow ends in mid-March, 45 days earlier than under the recent climate. This is because of the earlier precipitation phase transition from snowfall to rainfall under warming and greater unloading and drip of intercepted snow from the canopy. Sublimation declines linearly with warming up to 5°C while the rainfall to total precipitation ratio increases from

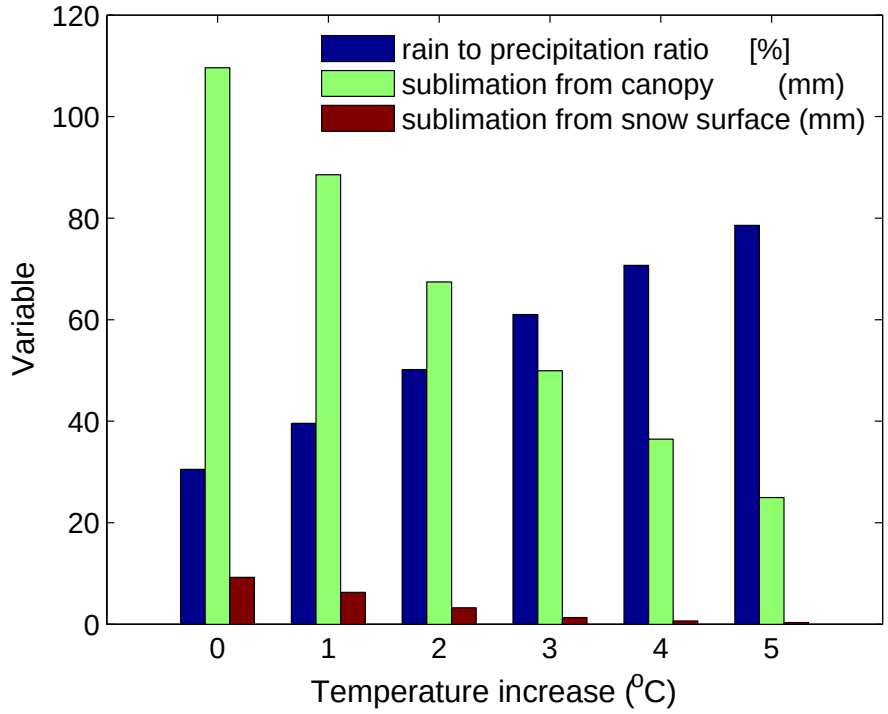

Figure B.5: Sensitivity to an increase in the air temperature for: rainfall to total precipitation ratio, sublimation from intercepted snow in the fir forest HRU and from the snow surface in the grass HRU in Reynolds Mountain East catchment.

30% to 78% (Figure B.5). Change in precipitation does not affect the cumulative seasonal intercepted snow sublimation under warming.

B.1.6 Sublimation from/Condensation to Snow Surface

In comparison to other sublimation terms, sublimation from snow surface is small and rarely reaches 1% of the total precipitation. The sensitivity of sublimation from snow surface in warm conditions and condensation in cold and wet conditions (Marks et al., 1999) is investigated. As shown in Figure B.4 and Figure B.5, up to 9 mm (≈1% of total precipitation) in different HRUs is lost due to net sublimation from snow surface. The sensitivity of sublimation from snow surface to warming is relatively high. Under concomitant change in precipitation (20%) and warming (5°C) sublimation is reversed and up to 1 mm of water vapour condenses onto some HRUs.

Appendix C

Regional Climate Model Outputs versus Observations

This section compares the regional climate model outputs (current and future periods) with the site measurements (high elevation and low elevation observation sites) in the three headwater basins across the North American Cordillera (Figure C.1 to C.10). It also shows the change factors of monthly (30-day) climatological values obtained from the subtraction of the future climate from the current climate (Figure 6.2 to C.13).

Changes in seasonal climatology, which are obtained from the mean of three months for each season, are shown in Figure C.11. The climatological change of precipitation varies with season between –41% and +42%. Similarly, the climatological change of air temperature varies between –1.2°C and +5.7°C in different seasons.

The average warming by 2070, obtained from all 11 RCM–GCM combinations (Mean–AllRCMs in Figure C.11), is expected to reach 2.8°C in spring (March to May, MAM), 1.8°C in summer (June to August, JJA), and 2.2°C in fall (September to November, SON) in WCRB; 2.0°C in spring, 2.2°C in summer, and 1.95°C in fall in MCRB; and 2.3°C in spring, 2.9°C in summer, and 1.95°C in fall in RME. Figures C.12 and C.13 show monthly changes in climatological values of the relative humidity and wind speed, respectively. Figure C.14 shows 10-daily changes in climatological values of precipitation and air temperature in the study basins.

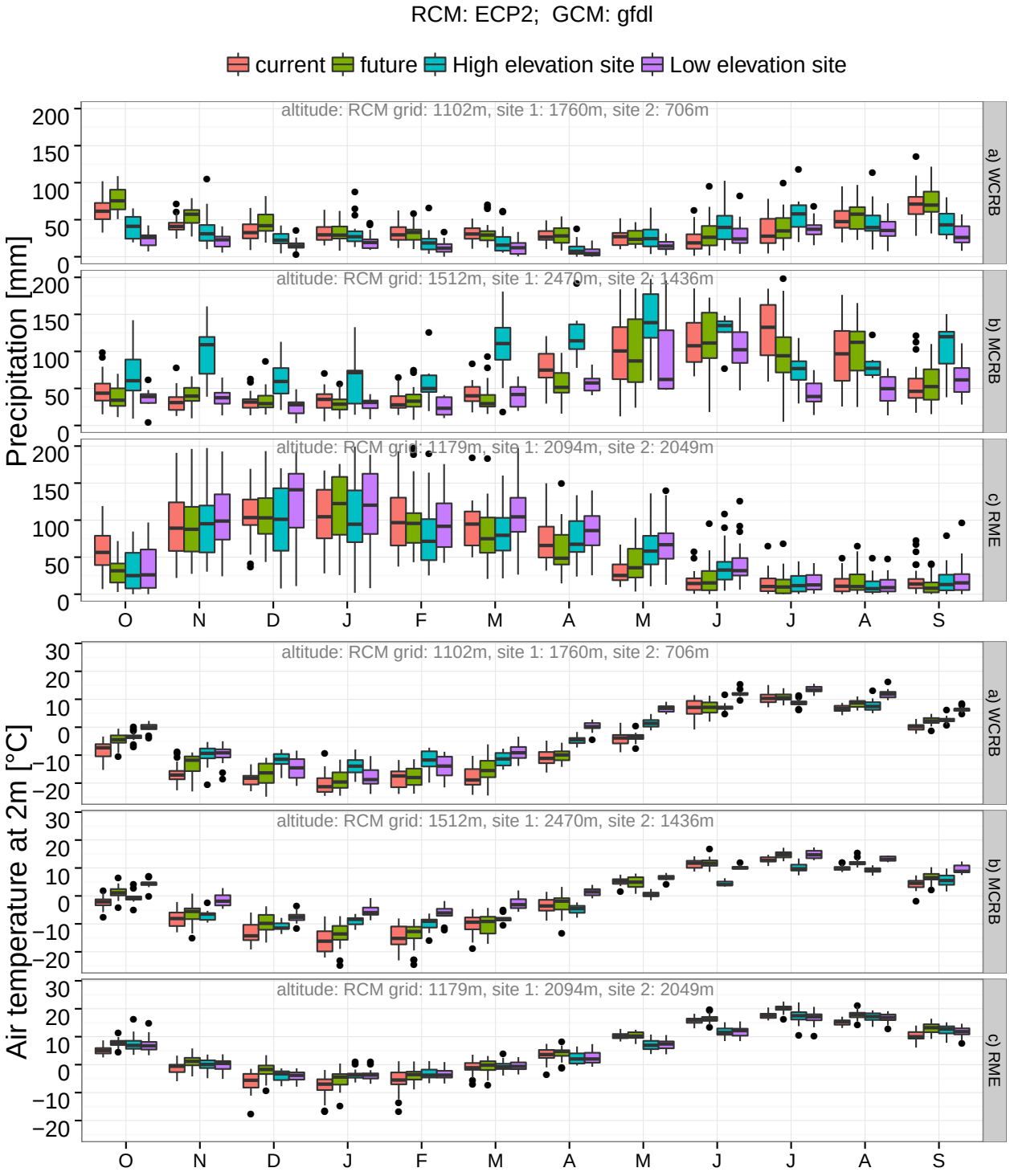

Figure C.1: Comparison of precipitation and air temperature observed in two high elevation and low elevation stations in each basin and simulated by ECP2 regional climate model driven by GFDL GCM. The elevation difference between sites in RME is not large, so two sites represent HRUs that have different wind sheltering but small elevation differences. Black dots denote outliers (outliers were not statistically tested).

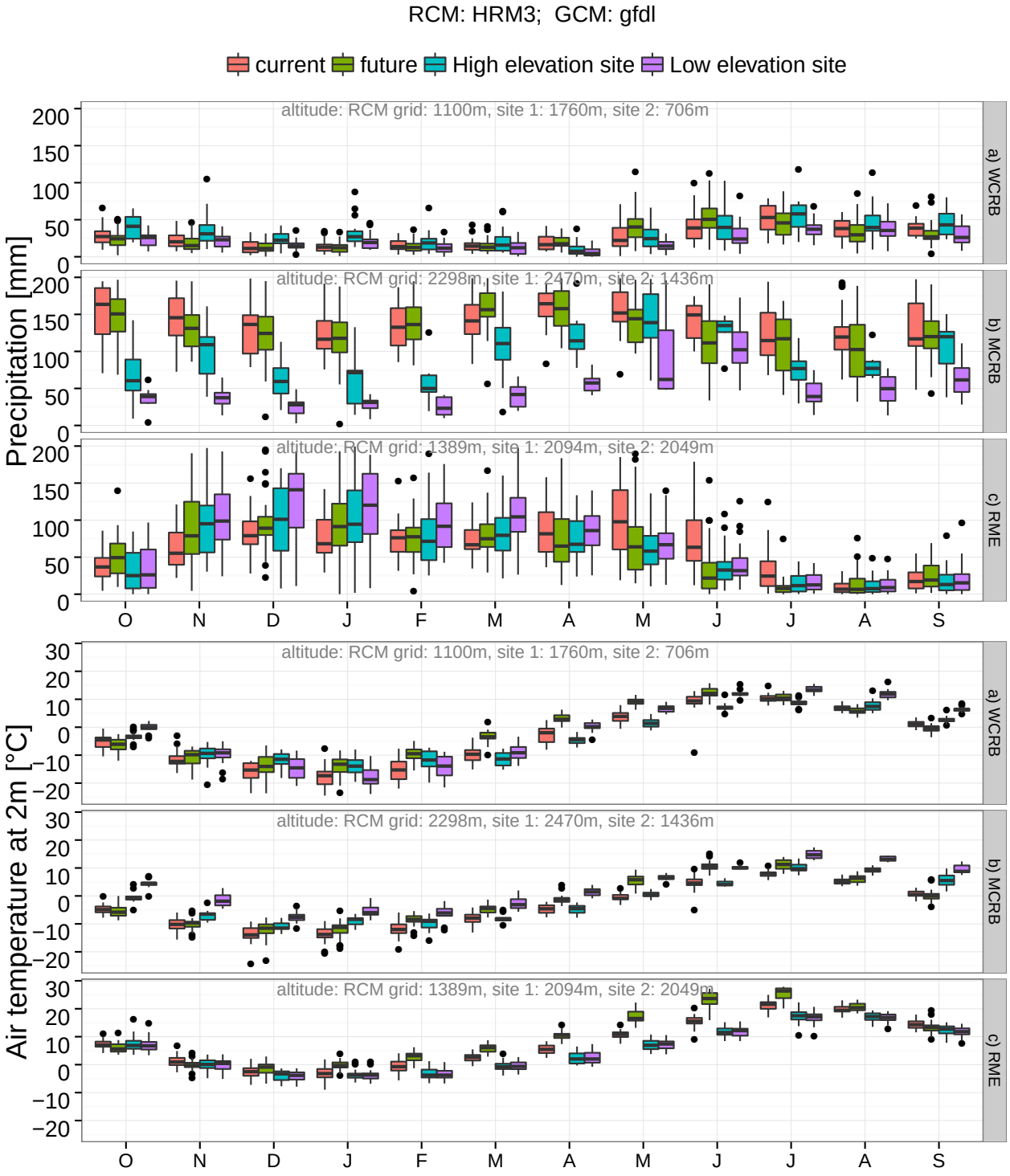

Figure C.2: Comparison of precipitation and air temperature observed in two high elevation and low elevation stations in each basin and simulated by HRM3 regional climate model driven by GFDL GCM. The elevation difference between sites in RME is not large, so two sites represent HRUs that have different wind sheltering but small elevation differences. Black dots denote outliers (outliers were not statistically tested).

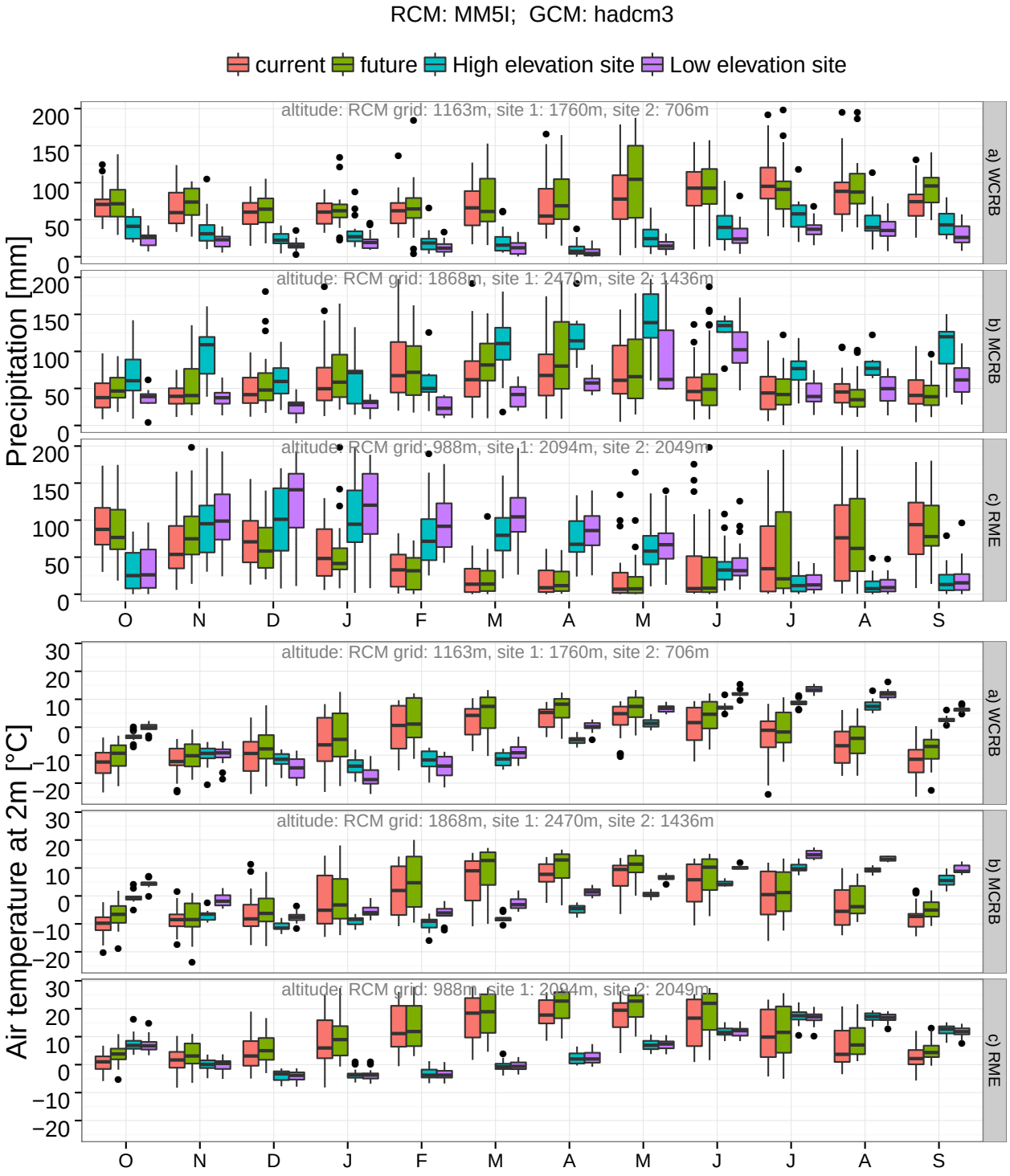

Figure C.3: Comparison of precipitation and air temperature observed in two high elevation and low elevation stations in each basin and simulated by MM5I regional climate model driven by HadCM3 GCM. The elevation difference between sites in RME is not large, so two sites represent HRUs that have different wind sheltering but small elevation differences. Black dots denote outliers (outliers were not statistically tested).

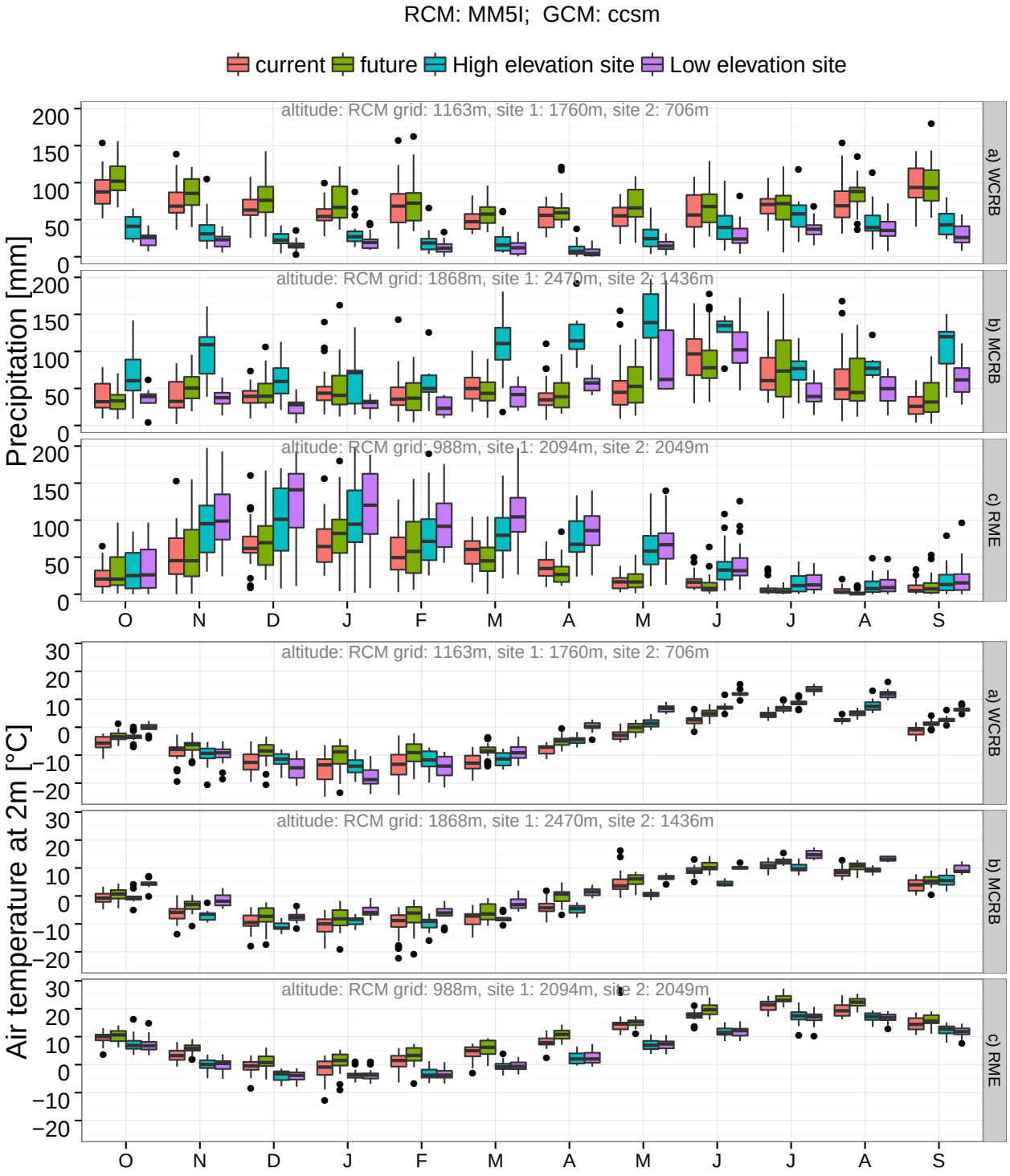

Figure C.4: Comparison of precipitation and air temperature observed in two high elevation and low elevation stations in each basin and simulated by MM5I regional climate model driven by CCSM GCM. The elevation difference between sites in RME is not large, so two sites represent HRUs that have different wind sheltering but small elevation differences. Black dots denote outliers (outliers were not statistically tested).

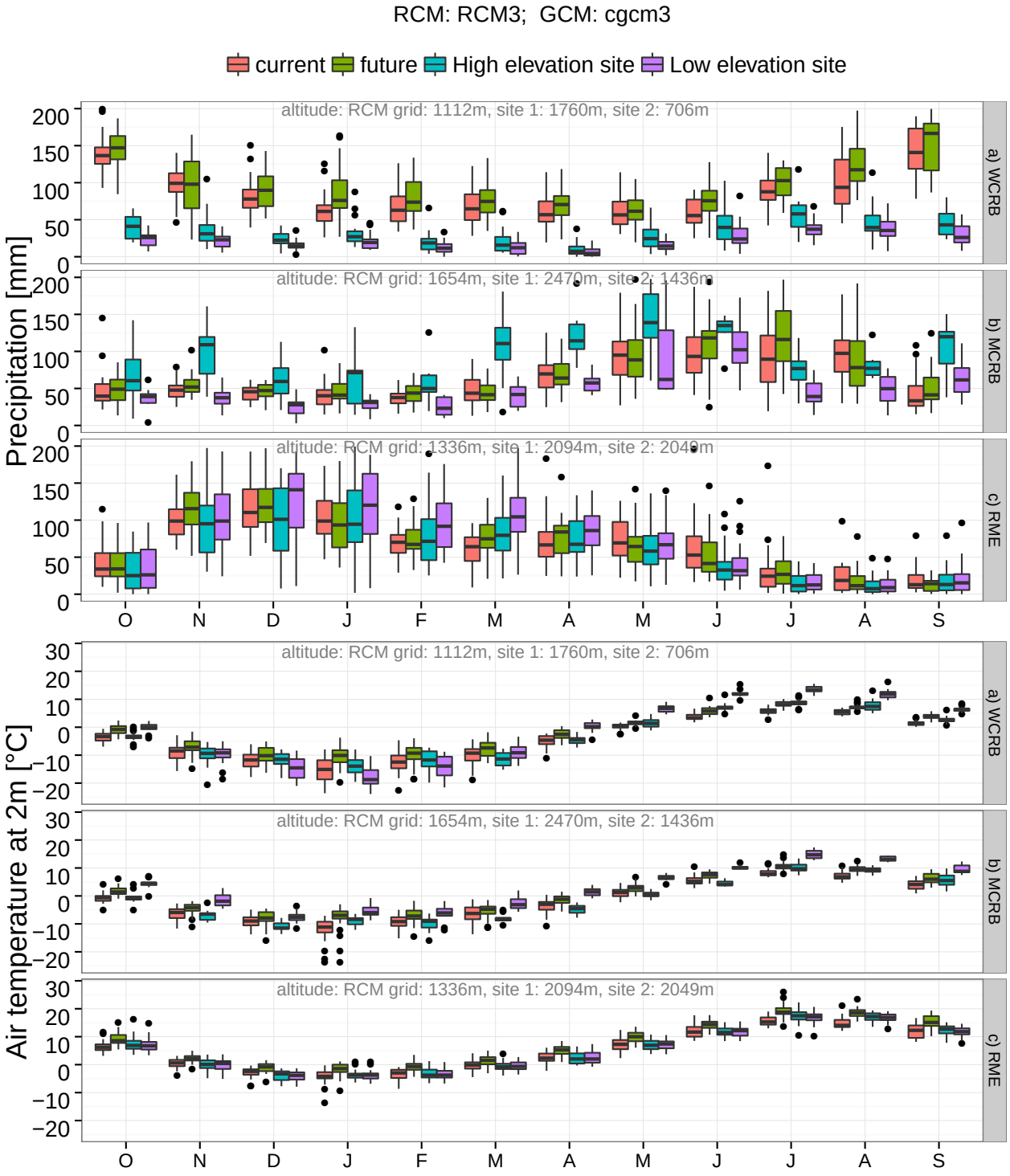

Figure C.5: Comparison of precipitation and air temperature observed in two high elevation and low elevation stations in each basin and simulated by RCM3 regional climate model driven by CGCM3. The elevation difference between sites in RME is not large, so two sites represent HRUs that have different wind sheltering but small elevation differences. Black dots denote outliers (outliers were not statistically tested).

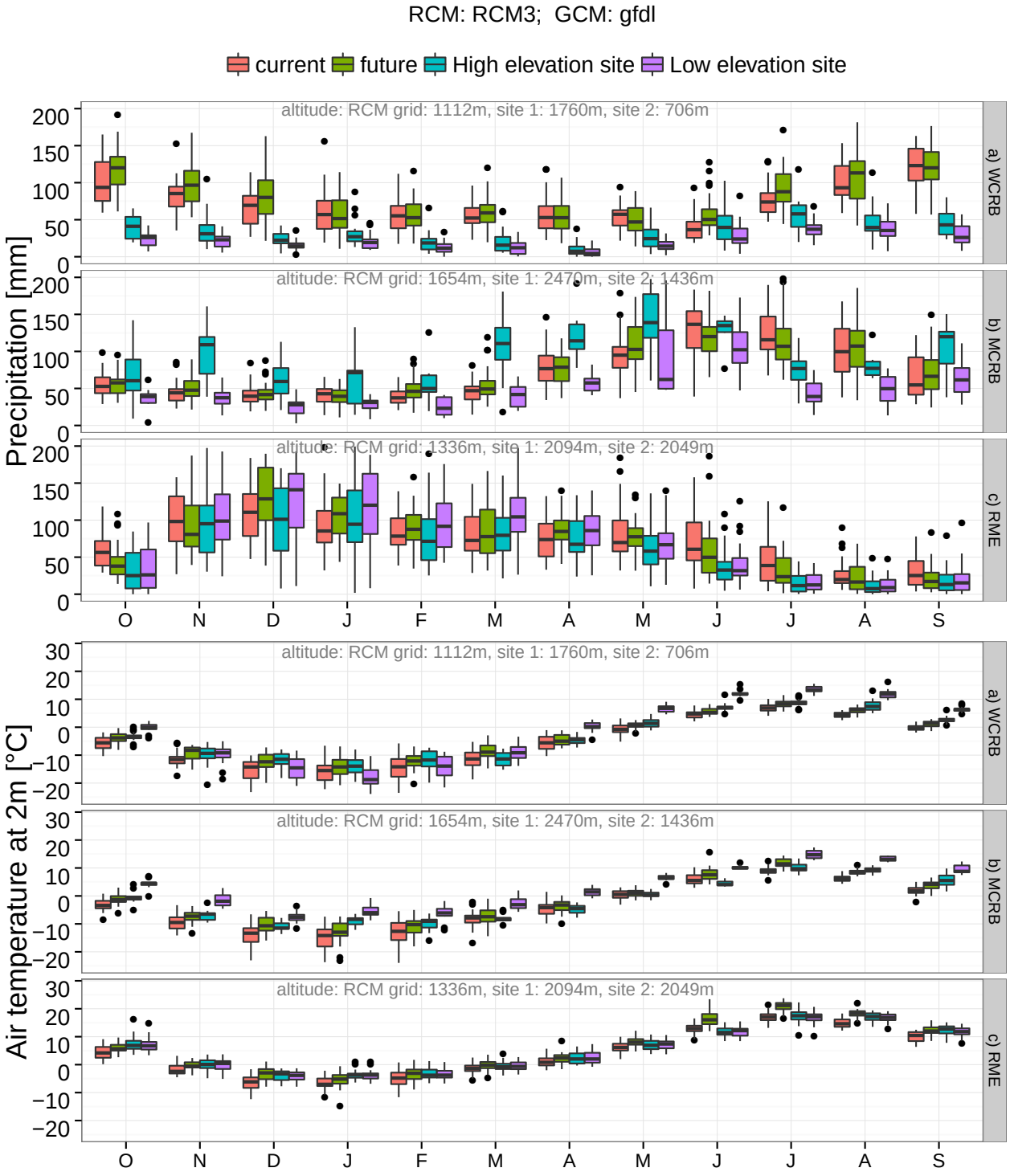

Figure C.6: Comparison of precipitation and air temperature observed in two high elevation and low elevation stations in each basin and simulated by RCM3 regional climate model driven by GFDL GCM. The elevation difference between sites in RME is not large, so two sites represent HRUs that have different wind sheltering but small elevation differences. Black dots denote outliers (outliers were not statistically tested).

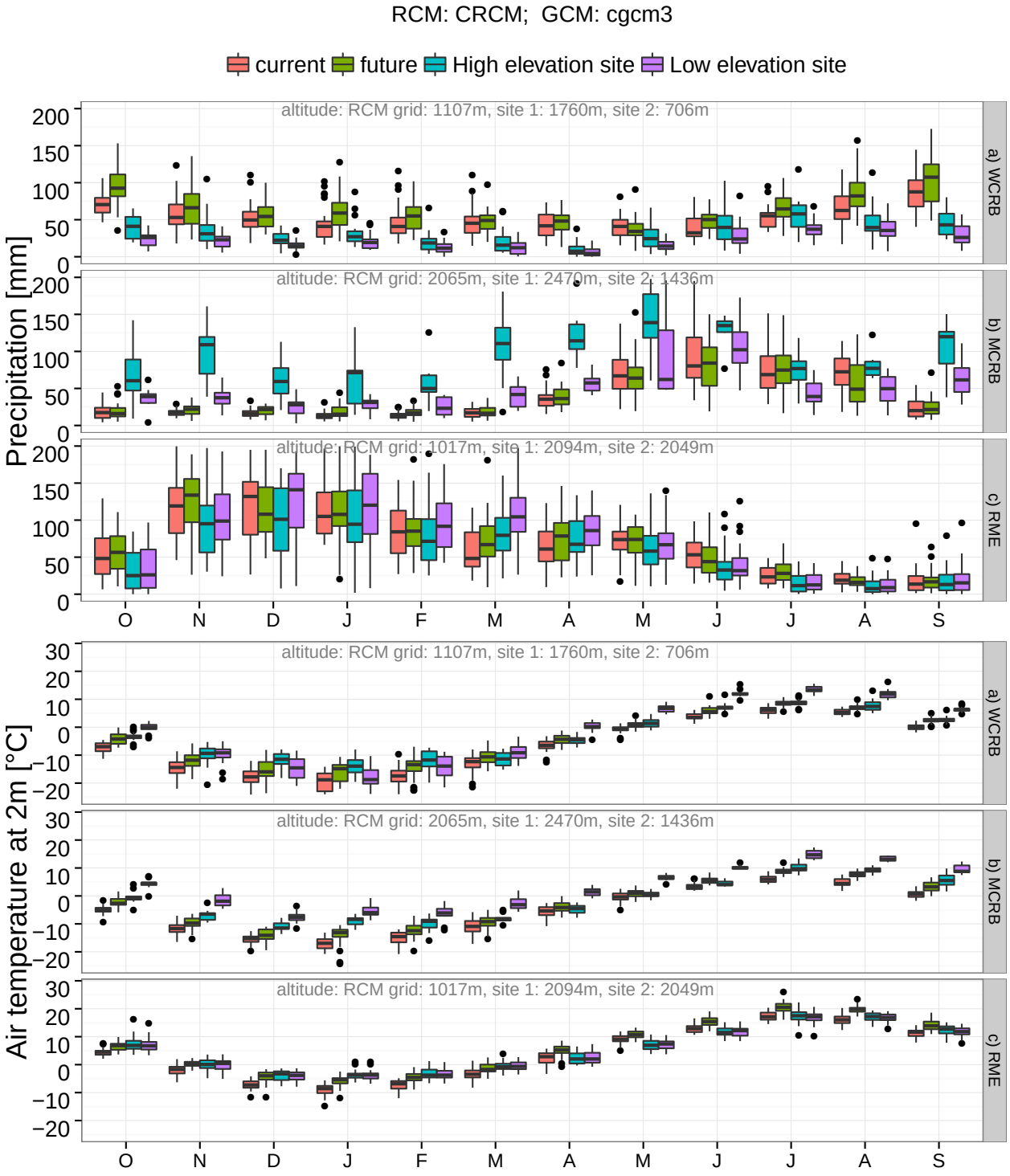

Figure C.7: Comparison of precipitation and air temperature observed in two high elevation and low elevation stations in each basin and simulated by CRCM regional climate model driven by CGCM3. The elevation difference between sites in RME is not large, so two sites represent HRUs that have different wind sheltering but small elevation differences. Black dots denote outliers (outliers were not statistically tested).

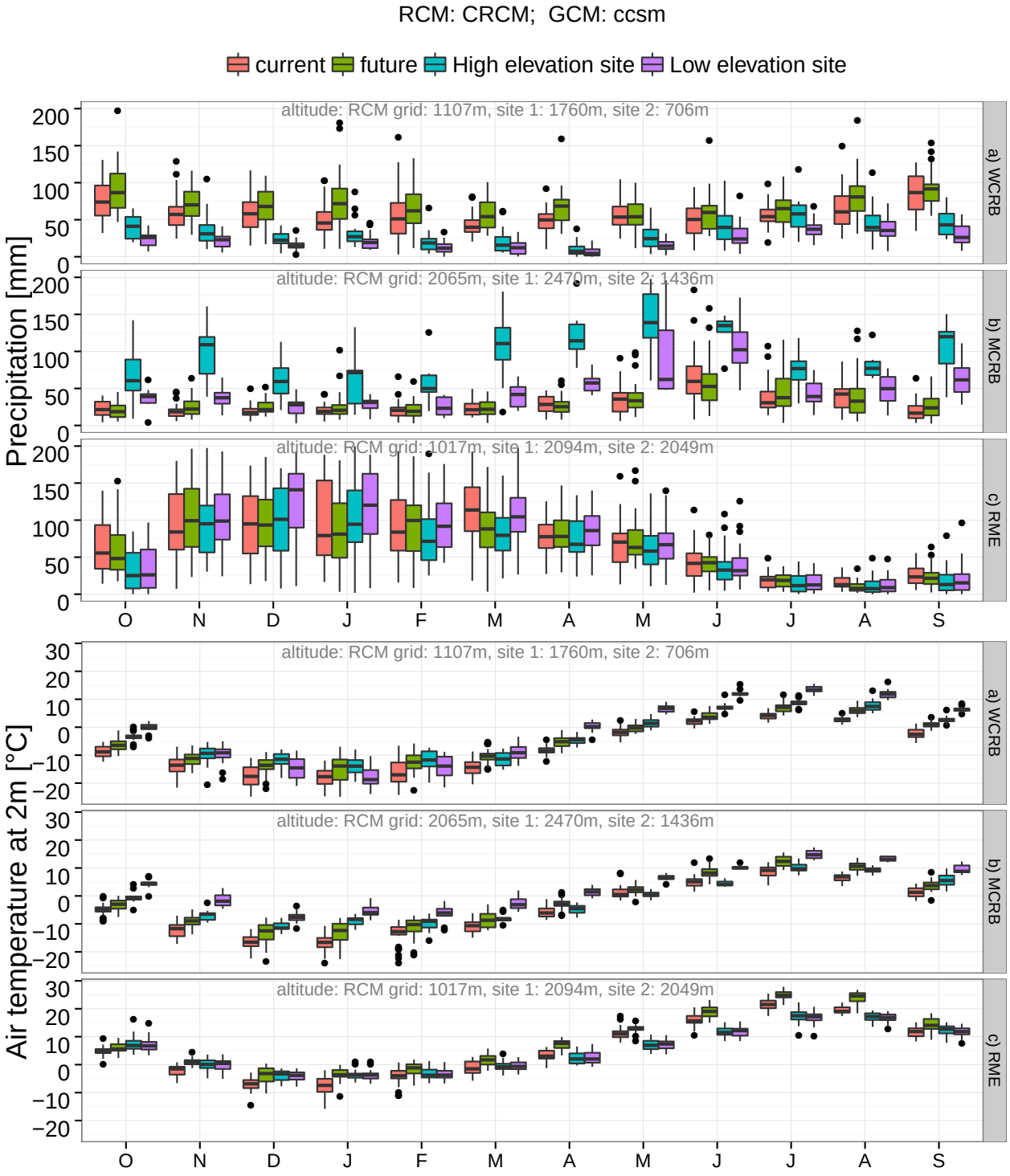

Figure C.8: Comparison of precipitation and air temperature observed in two high elevation and low elevation stations in each basin and simulated by CRCM regional climate model driven by CCSM GCM. The elevation difference between sites in RME is not large, so two sites represent HRUs that have different wind sheltering but small elevation differences. Black dots denote outliers (outliers were not statistically tested).

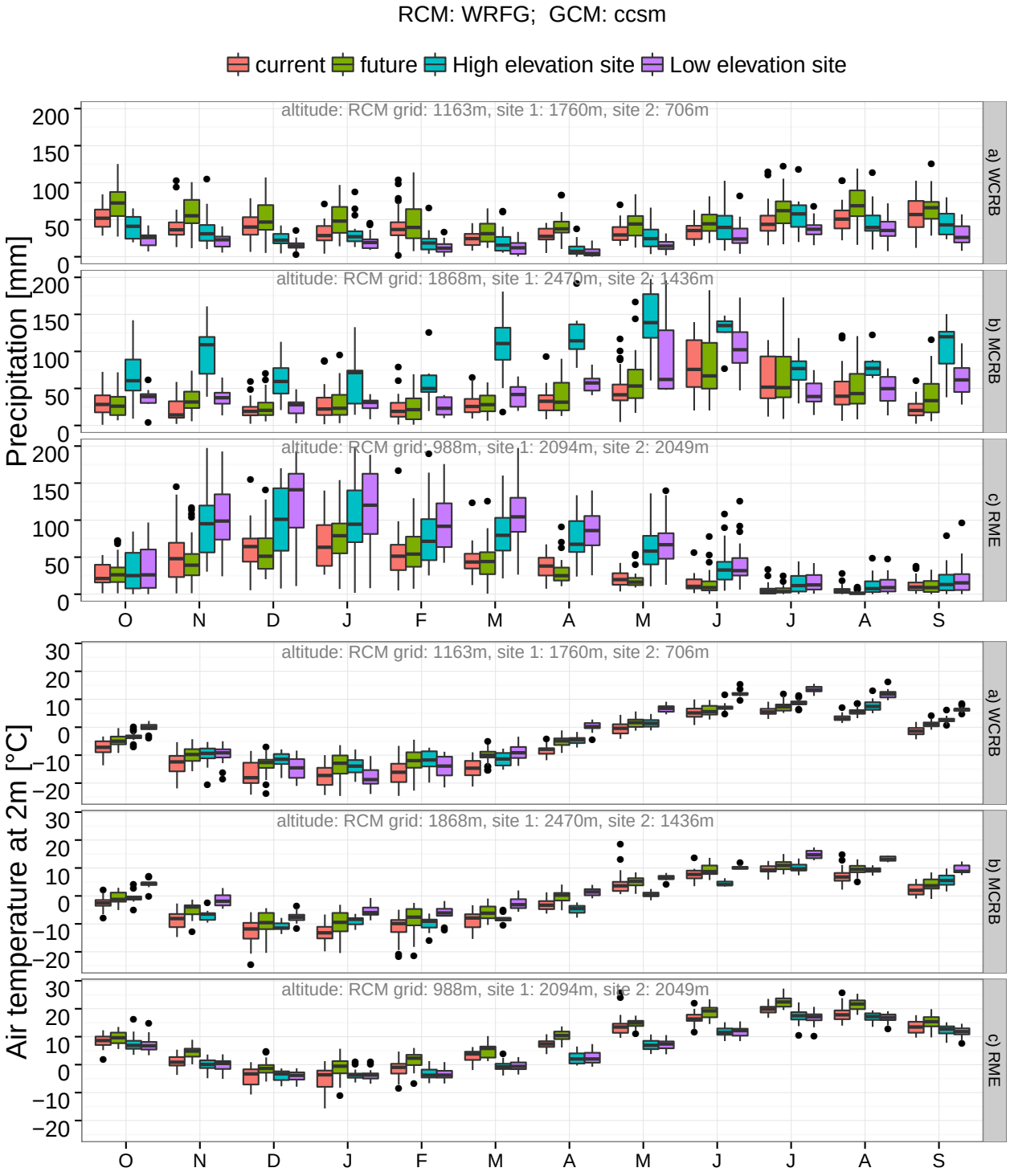

Figure C.9: Comparison of precipitation and air temperature observed in two high elevation and low elevation stations in each basin and simulated by WRFG regional climate model driven by CCSM GCM. The elevation difference between sites in RME is not large, so two sites represent HRUs that have different wind sheltering but small elevation differences. Black dots denote outliers (outliers were not statistically tested).

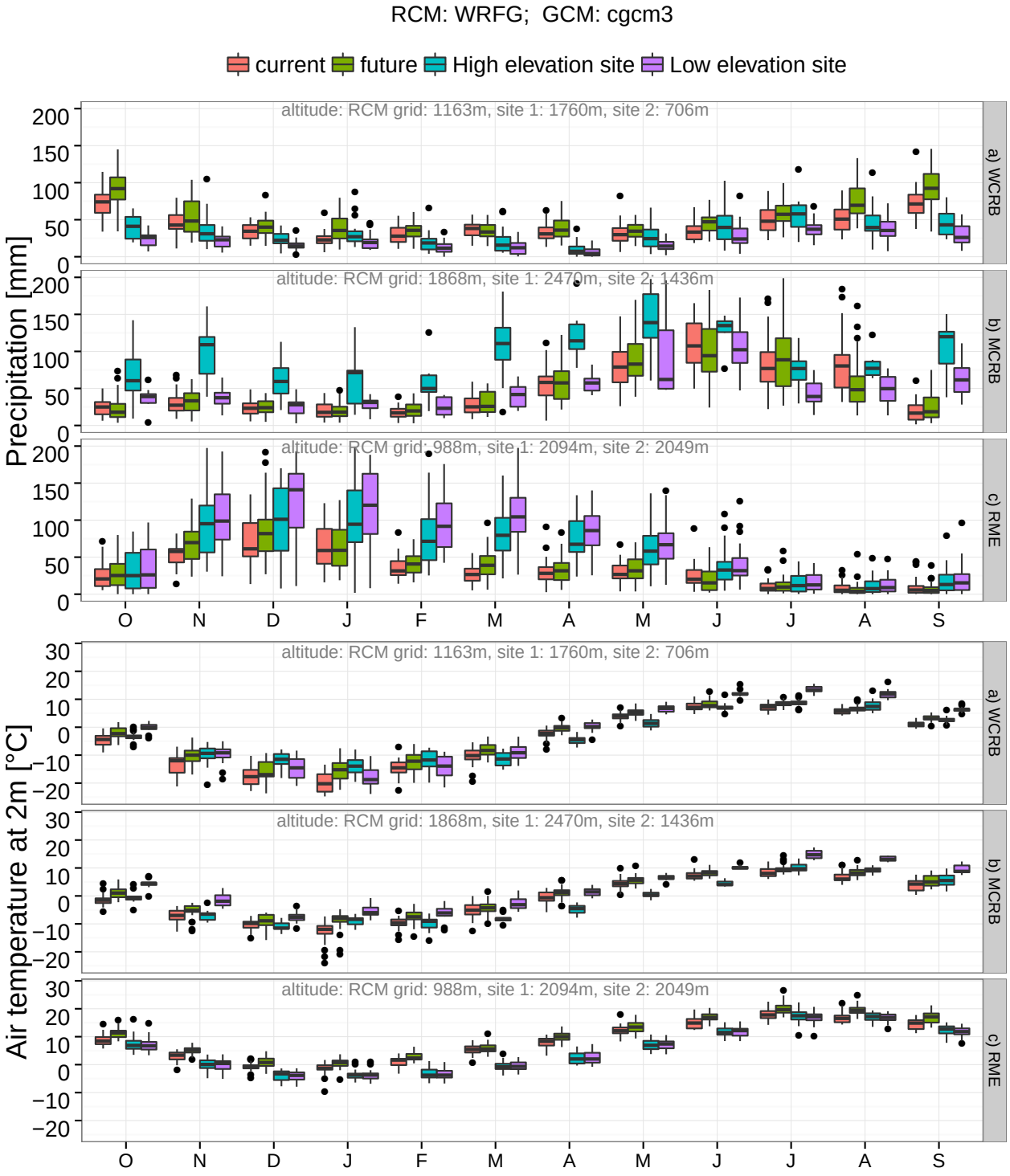

Figure C.10: Comparison of precipitation and air temperature observed in two high elevation and low elevation stations in each basin and simulated by WRFG regional climate model driven by CGCM3. The elevation difference between sites in RME is not large, so two sites represent HRUs that have different wind sheltering but small elevation differences. Black dots denote outliers (outliers were not statistically tested).

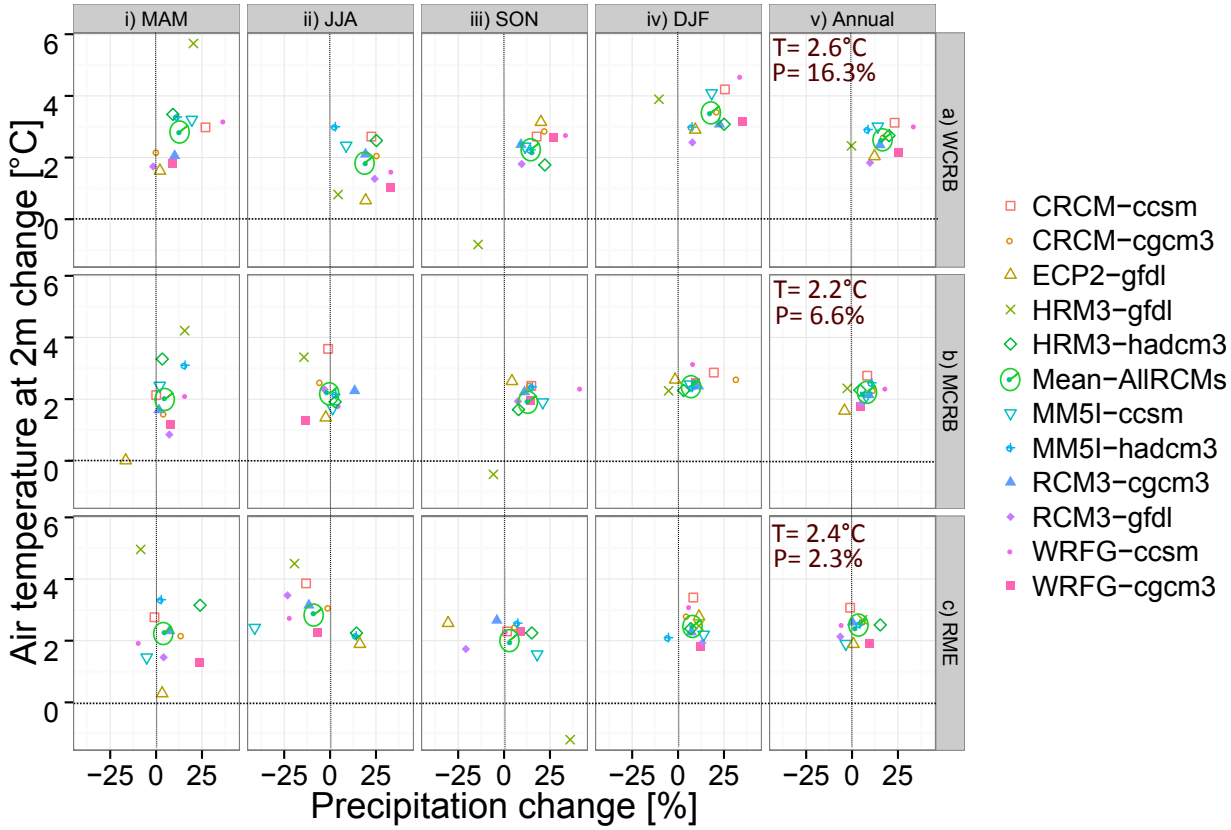

Figure C.11: Changes in the seasonal and annual climatology of air temperature and precipitation from current climate (1971–2000) to future climate (2041–2070) determined for average (Mean–AllRCMs) and 11 combinations of NARCCAP regional and global climate models. Annual changes in air temperature (T) and precipitation (P) for each basin is shown.

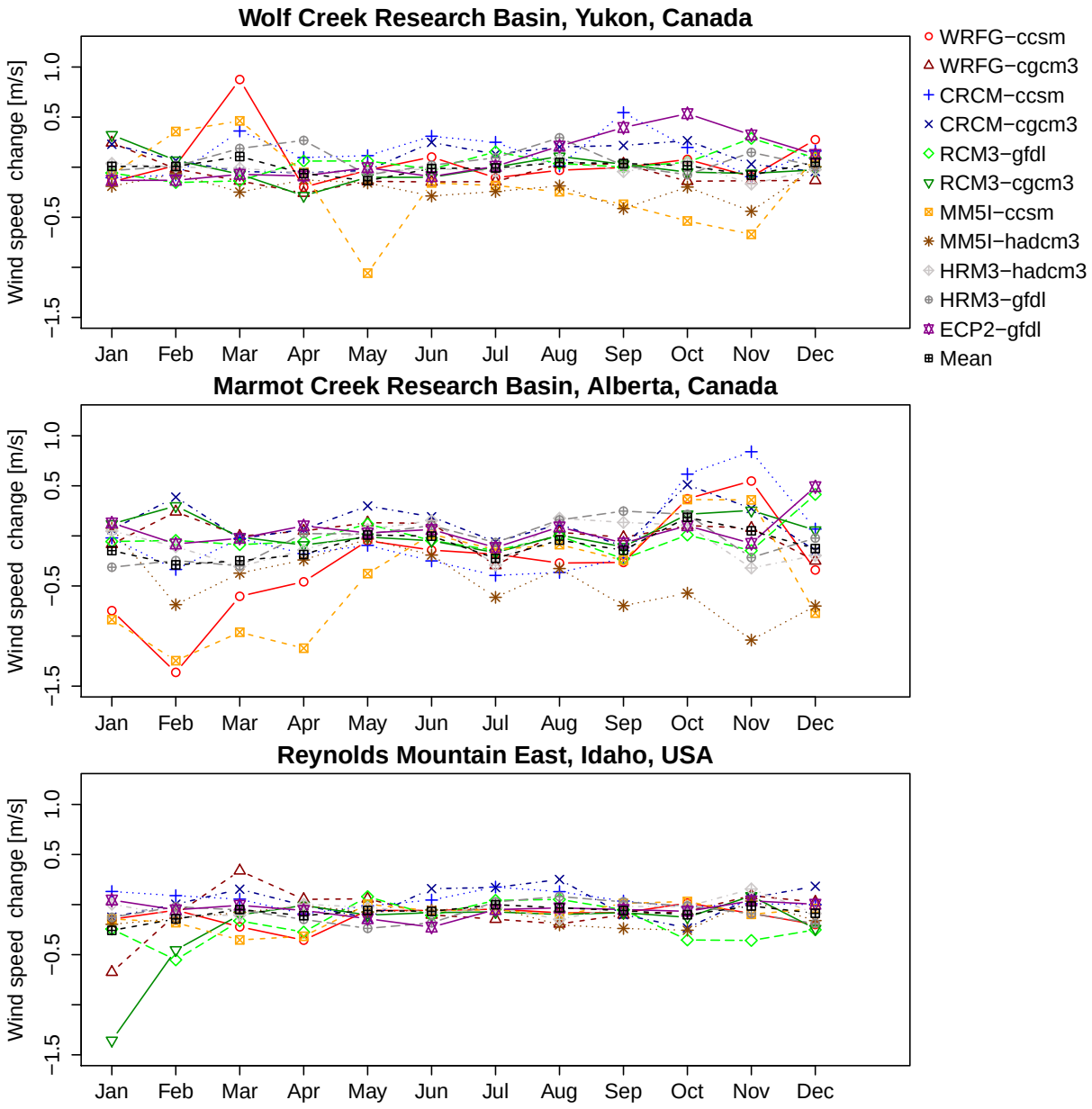

Figure C.12: Monthly (30-daily) changes (deltas) in climatological wind speed for all RCM–GCM combinations for three basins across the North American Cordillera

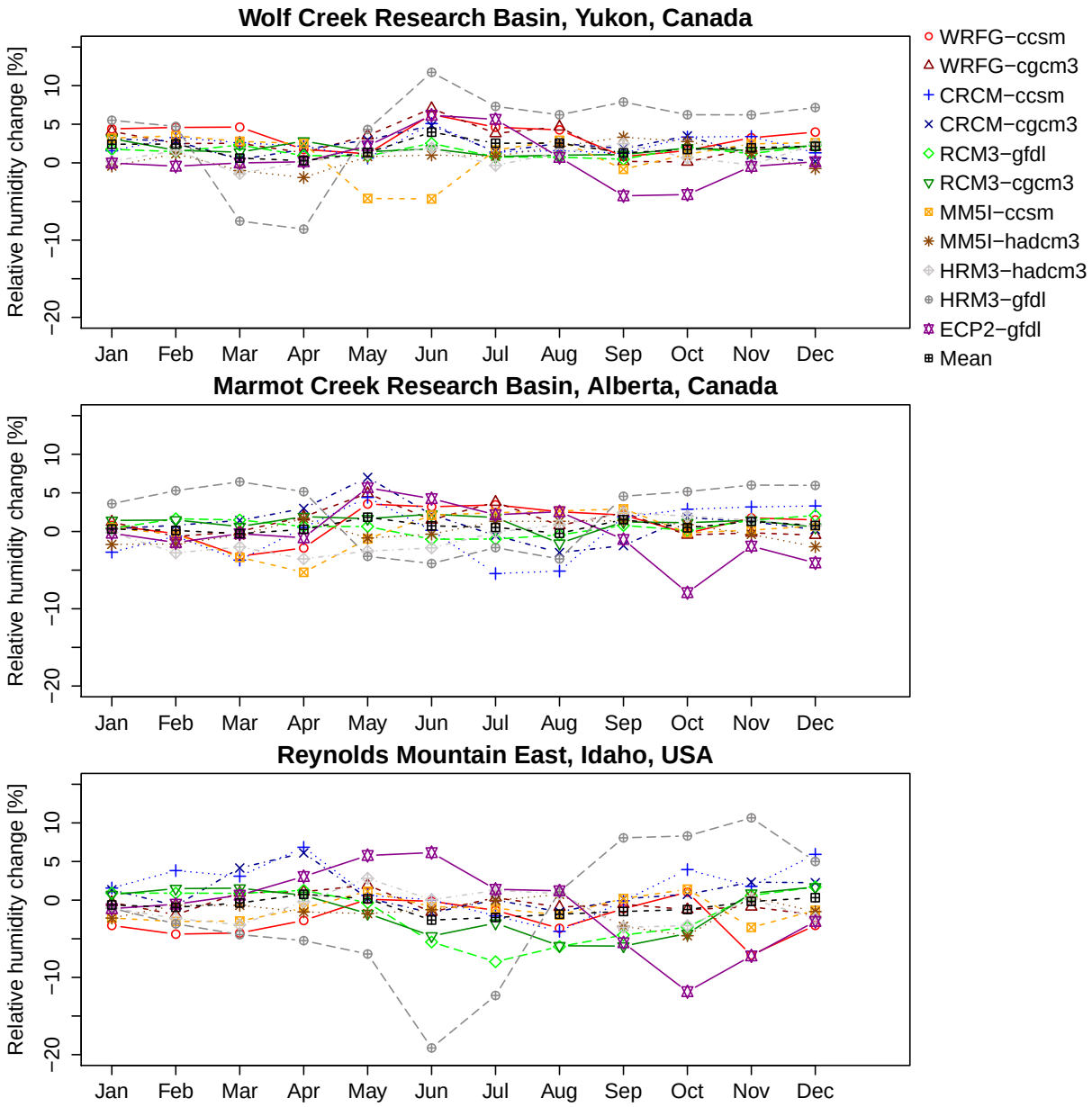

Figure C.13: Monthly (30-daily) changes (deltas) in climatological relative humidity for all RCM–GCM combinations for three basins across the North American Cordillera

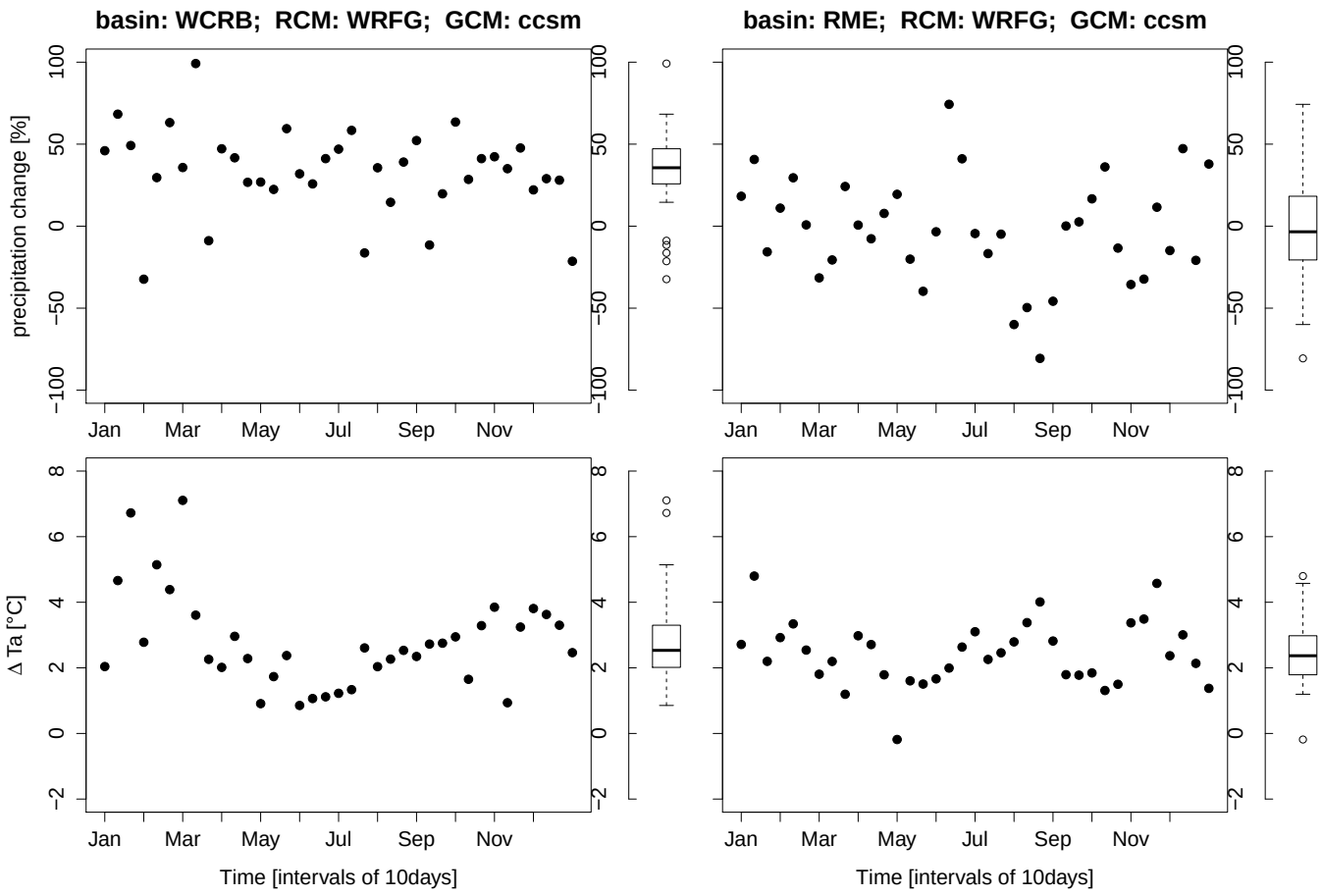

Figure C.14: Ten day changes (deltas) in climatological precipitation and air temperature projected by WRFG regional climate model driven by CCSM GCM for Wolf Creek Research Basin and Reynolds Mountain East.